

Functional and Molecular Characterization of the Vascular Endothelial Response to Fluid Shear Stress

by

Adel Moussa Malek

B.S. Electrical Engineering & Computer Science
M.I.T., 1988

M.S. Electrical Engineering & Computer Science
M.I.T., 1988

Submitted to the Department of Health Sciences and Technology
in Partial Fulfillment of the Requirements for the Degree of

Doctor of Philosophy in Medical Engineering

at the

Massachusetts Institute of Technology

May 1994

MIT LIBRARIES

JUL 18 1994

SCHERING

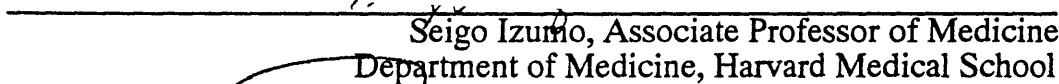
© Adel M. Malek, 1994. All rights reserved

The author hereby grants to M.I.T. permission to reproduce and to distribute publicly copies of this thesis document in whole or in part.

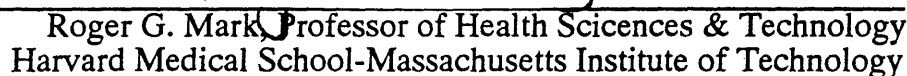
Signature of Author



Certified by


Seigo Izumo, Associate Professor of Medicine
Department of Medicine, Harvard Medical School

Certified by


Roger G. Mark, Professor of Health Sciences & Technology
Harvard Medical School-Massachusetts Institute of Technology

SCHER-PLOUGH

MASSACHUSETTS INSTITUTE

JUN 03 1994

LIBRARIES

Table of Contents

Abstract	3
Acknowledgment	5
Abbreviations	6
 CHAPTER 1	 7
Introduction	7
 CHAPTER 2	 12
Review of Experimental Work and Hypotheses	12
2.1 Relationship between blood flow and vessel structure	12
2.2 Further interpretations of Murray's law	15
2.3 Unitary hypothesis based on Murray's law	17
2.4 Vascular remodeling resulting from surgically-induced blood flow changes	18
2.5 Relationship between atherosclerosis and fluid shear stress	20
 CHAPTER 3	 29
Vascular Wall Structure and Biology	29
3.1 Vessel wall structure	29
3.2 Hemodynamic forces	29
3.3 Biology of the endothelial cell	31
3.3.1 Tone control	31
3.3.2 Coagulation and fibrinolysis control	31
3.3.3 Growth control	32
3.4 Effects of flow and shear stress on endothelial function	33
3.4.2 Cell shape change and alignment	33
3.4.3 Actin stress fiber rearrangement	33
3.4.4 Mechanosensitive channels, potassium current and internal calcium transients	34
3.4.5 Effects on cell function	35
3.4.6 Endothelial cell cycle control	35
3.4.7 Release of prostacyclin and histamine	36
3.4.8 Endothelial-derived relaxing factor	36
3.4.9 Tissue-type plasminogen activator	3
3.5 Summary and plan of action	37
 CHAPTER 4	 44
Design, Construction, and Testing of Shear Stress Apparatus	44
4.1. Background on devices for subjecting endothelium to shear stress	44
4.2. Design requirements	44
4.2.1 Fluid mechanics of cone-plate viscometer	46
4.2.2 Technical description of the device	47
4.3 Experimental validation of device properties	49
4.3.1 Control of cone rotation velocity and step-response to external velocity command	50
4.4 Experimental results	51
4.4.1 Shear induces cell shape change and alignment in a time- and magnitude-dependent manner	52

4.4.2 Long-term fluid shear stress induces cell shape change and alignment in endothelial but not in smooth muscle cells	53
4.4.3 Elevated shear stress induces actin stress fibers and, at high magnitude, b-actin mRNA	53
4.4.4 Shear stress of physiological magnitude decreased rate of DNA but not RNA synthesis	54
CHAPTER 5	77
Regulation of Endothelin-1 by Fluid Shear Stress in Vitro	77
5.1 Endothelin-1, a potent vasoconstrictor and paracrine growth factor	77
5.2 Regulation of endothelin-1 by fluid shear stress	78
5.2.1 Fluid shear stress of physiological magnitude downregulates ET-1 mRNA prior to cell shape change	78
5.2.2 ET-1 mRNA downregulation appears to be the result of shear stress, not flow	79
5.2.3 Shear-induced ET-1 mRNA decrease is independent of serum content in culture medium.....	80
5.2.4 Physiological fluid shear stress reduces ET-1 peptide secretion ...	80
5.2.5 ET-1 downregulation by shear stress is a reversible process	81
5.2.6 ET-1 downregulation is dependent on fluid shear stress magnitude	81
5.3 Importance of the dynamic character of the shear stimulus on the downregulation of ET-1	82
5.3.1 Turbulent flow.....	82
5.3.2 Turbulent shear is indistinguishable from laminar shear in down-regulating ET-1	83
5.3.3 Pulsatile and sinusoidally reversing shear stress.....	84
5.3.4 Regulation of ET-1 mRNA by mechanical stimuli is specific to shear stress but not to low-frequency uniaxial strain	85
5.4 Conclusion	86
CHAPTER 6	99
Regulation of Endothelial-Derived Growth Factors by Fluid Shear Stress in Vitro	99
6.1 Regulation of growth factor expression by fluid shear stress	99
6.2 Platelet-derived growth factor	99
6.2.1 Effect of shear stress on PDGF B-chain expression	100
6.3 Basic fibroblast growth factor	101
6.3.1 Effect of shear stress on basic FGF expression.....	102
6.4 Effect of dynamic character of shear stimulus on PDGF and bFGF mRNA levels	104
6.5 Conclusion and potential implications of findings	105
CHAPTER 7	114
Differential Regulation of Thrombomodulin and Tissue-Type Plasminogen Activator by Fluid Shear Stress	114
7.1 Thrombomodulin and tissue-type plasminogen activator	114
7.2 Effect of shear stress on TM expression	115
7.2.1 Fluid shear stress decreases expression of TM mRNA specifically	116
7.2.2 Shear-induced downregulation of TM mRNA is a completely reversible process	117

7.2.3 Shear stress decreases levels of expressed TM protein.....	117
7.2.4 TM mRNA is regulated similarly by steady, pulsatile, and turbulent shear stress	118
7.3 Differential regulation of TM and t-PA mRNA by fluid shear stress	118
7.4 Discussion	120
7.5 Conclusion	122
CHAPTER 8	132
Molecular Mechanism and Second Messenger Signaling in Response to Fluid Shear Stress	132
8.1 Molecular mechanism of endothelin regulation by fluid shear stress	132
8.1.1 Background on ET-1 gene expression regulation	132
8.1.2 Shear stress induces downregulation of ET-1 by a protein synthesis dependent mechanism	133
8.1.3 Fluid shear stress-induced ET-1 downregulation occurs at the transcriptional level without change in ET-1 mRNA stability	134
8.1.4 Transfection studies	135
8.1.5 Conclusion	136
8.2 Second Messenger involvement.....	136
8.2.1 Protein kinase C	137
8.2.1.1 PMA-induced ET-1 regulation in presence of CHX	138
8.2.1.3 Immunoblotting with anti-PKC antibodies	139
8.2.1.4 PKC inhibitors.....	139
8.2.2 Cyclic AMP	141
8.2.3 Cyclic GMP	142
8.2.4 Cyclooxygenase	143
8.2.5 Intracellular calcium	143
8.2.6 Tyrosine phosphorylation	144
8.3 Discussion	146
CHAPTER 9	173
Role of Cytoskeleton and Mechanosensitive Channels in Shear Stress Transduction ...	173
9.1 Mechanosensitive channels	173
9.1.1 Stretch-activated cation channel	174
9.1.2 Shear stress-activated potassium channel	174
9.2 Cytoskeleton.....	176
9.2.1 Actin microfilament network	177
9.2.2 Microtubule network	178
9.3 Cell shape	180
CHAPTER 10	199
Theoretical Models for Vascular Structure Regulation and for Endothelial Cell Transduction Process	199
10.1 The meaning of the gene regulatory changes with respect to previous work	199
10.2 Present model of endothelial response to shear stress	200
10.3 Future directions	201
APPENDIX	206
Cell culture	206
Dynamic stretch apparatus	206

RNA Isolation and Northern analysis	207
Densitometry	208
Radioimmunoassay for endothelin-1 peptide	208
Isolation of nuclei & runoff transcription	208
Transcription and protein synthesis inhibition	209
Transfection experiments with ET-1 promoter constructs	209
Cell lysis and immunoblotting of protein kinase C.....	210
Protein kinase C activity assay.....	210
Determination of intracellular cAMP & cGMP content	211
Image analysis	211
Construction of apparatus	211
Mode of operation of cone-plate apparatus.....	213
DNA and RNA synthesis rate measurement	214
Immunostaining	214
Western blotting with anti-Phosphotyrosine antibody	215
Western blotting with anti-thrombomodulin antibody.....	216
REFERENCES	217
PUBLICATION REPRINTS	236

List of Figures

Figure 1.1 Sequential steps of thesis project (A).	10
Figure 1.2 Sequential steps of thesis project (B).	11
Figure 2.1 Diagram of blood vessel undergoing Poiseuille-Hågen flow.	22
Figure 2.2 Diagram of vessel bifurcation.	23
Figure 2.3 Illustration of carotid artery-jugular vein shunt experiment.	24
Figure 2.4 Summary figure of Kamiya's result.	25
Figure 2.5 Illustration of carotid artery flow reduction experiment.	26
Figure 2.6 Diagram of sites undergoing disturbed flow.	27
Figure 2.7 Figure from Zarins' work on carotid atherosclerosis.	28
Figure 3.1 Schematic representation of the vessel wall.	39
Figure 3.2 Expression of tensile stress and shear stress.	40
Figure 3.3 Summary of multiple interactions at the vessel wall interface.	41
Figure 3.4 Multiple endothelial responses to fluid shear stress.	42
Figure 3.5 Negative feedback control loop of vessel wall structure.	43
Figure 4.1 Three types of viscometers used to apply shear stress.	56
Figure 4.2 Flow line analysis at the level of the baseplate in a cone-plate device.	57
Figure 4.3 Parts description of cone-plate apparatus.	58
Figure 4.4 Perspective view of cone-plate apparatus.	59
Figure 4.5 Cross-sectional view of the cone-plate apparatus.	60
Figure 4.6 Individual part description of cone-plate device.	61
Figure 4.7 Detailed view of the cone-shaft.	62
Figure 4.8 Illustration of gap between cone and plate.	63
Figure 4.9 Ink flow-line analysis of cone-plate device.	64
Figure 4.10 Typical Reynolds number and shear stress magnitude profiles.	65
Figure 4.11 Step response analysis of cone-plate apparatus.	66
Figure 4.12 Sinusoidal and arbitrary cone velocity profiles.	67
Figure 4.13 Lack of increase of intracellular LDH release.	68
Figure 4.14 Phase-contrast micrographs of BAE monolayers under shear.	69
Figure 4.15 Increased cellular elongation in response to shear stress.	70
Figure 4.16 Change in distribution of angle of orientation in BAE cells under shear.	71
Figure 4.17 Lack of morphological response in BSM cells under shear.	72
Figure 4.18 Induction of actin stress fibers under shear stress.	73
Figure 4.19 Induction of b-actin mRNA increase in response to shear.	74
Figure 4.20 Densitometric analysis of β -actin mRNA increase.	75
Figure 4.21 Alteration in DNA and RNA synthetic rates in response to shear stress.	76
Figure 5.1 Endothelin-1, a potent vasoconstrictor peptide.	87
Figure 5.2 Fluid shear stress decreases ET-1 mRNA levels.	88
Figure 5.3 Densitometric analysis of ET-1 mRNA under shear stress.	89
Figure 5.4 ET-1 mRNA is downregulated by shear stress not flow.	90
Figure 5.5 ET-1 peptide secretion is also decreased by shear stress.	91
Figure 5.6 Shear-induced ET-1 mRNA decrease is a reversible process.	92
Figure 5.7 Decrease of ET-1 mRNA is dependent on shear magnitude.	93

Figure 5.8 Phase contrast micrographs of BAEC under laminar and turbulent shear.	94
Figure 5.9 ET-1 mRNA decrease is similar under laminar and turbulent shear.	95
Figure 5.10 Schematic temporal profiles of shear stress under pulsatile, reversing, turbulent and steady regimes.	96
Figure 5.11 Time course of ET-1 mRNA under pulsatile and reversing shear.	97
Figure 5.12 Time course of ET-1 mRNA under cyclical stretch and steady shear.	98
Figure 6.1 Northern blot analysis of BAE under shear using PDGF-B chain cDNA.	108
Figure 6.2 Normalized densitometric analysis of PDGF-B chain mRNA.	109
Figure 6.3 Northern blot analysis of BAE under shear using bFGF cDNA.	110
Figure 6.4 Normalized densitometric analysis of bFGF mRNA.	111
Figure 6.5 Northern blot analysis using PDGF-B chain cDNA under steady, pulsatile and turbulent shear.	112
Figure 6.6 Northern blot analysis using bFGF cDNA under steady, pulsatile and turbulent shear.	113
Figure 7.1 Northern blot analysis using thrombomodulin (TM) cDNA of BAE cells under shear.	123
Figure 7.2 Normalized densitometric analysis of TM mRNA under shear.	124
Figure 7.3 Northern blot analysis using TM cDNA illustrating recovery.	125
Figure 7.4 Normalized densitometric analysis illustrating recovery.	126
Figure 7.5 Western blot using anti-TM antibody under shear.	127
Figure 7.6 Densitometric analysis of TM Western blot of BAE under shear.	128
Figure 7.7 Northern blot analysis using TM cDNA under steady, pulsatile and turbulent shear.	129
Figure 7.8 Densitometric analysis using t-PA cDNA.	130
Figure 7.9 Schematic diagram of thrombotic/fibrinolytic phenotype of BAE cells under shear.	131
Figure 8.1 Schematic representation of ET-1 gene.	149
Figure 8.2 ET-1 downregulation by shear is dependent on protein synthesis.	150
Figure 8.3 PDGF-B mRNA downregulation by shear is dependent on protein synthesis.	151
Figure 8.4 BAE cell alignment is dependent on protein synthesis.	152
Figure 8.5 Nuclear runoff of BAE cells to measure ET-1 transcription under shear stress.	153
Figure 8.6 ET-1 mRNA stability analysis under shear stress.	154
Figure 8.7 Transfection analysis of ET-1 gene promoter reporter constructs under shear stress.	155
Figure 8.8 ET-1 mRNA decreases in response to forskolin and PMA.	156
Figure 8.9 ET-1 mRNA downregulation by shear is dependent on protein synthesis.	157
Figure 8.10 Shear stress does not significantly induce translocation of PKC activity.	158
Figure 8.11 Shear stress does not induce PKC translocation.	159
Figure 8.12 Staurosporine decreases ET-1 mRNA expression.	160
Figure 8.13 Calphostin C does not affect shear-induced ET-1 mRNA downregulation.	161
Figure 8.14 Northern blot analysis of BAE cells exposed to forskolin.	162

Figure 8.15 Phase-contrast micrographs of BAE cells exposed to Cyt D, forskolin, and PMA.	163
Figure 8.16 Radioimmunoassay of cAMP in BAE under shear and in response to forskolin.	164
Figure 8.17 Radioimmunoassay of cGMP in BAE under shear and in response to ANP.	165
Figure 8.18 L-NMMA does not inhibit shear-induced ET-1 mRNA decrease.	166
Figure 8.19 Inhibition of cyclooxygenase with Ibuprofen does not affect shear-induced ET-1 mRNA decrease.	167
Figure 8.20 Chelation of intracellular calcium and inhibition of tyrosine kinase activity abolish shear-induced ET-1 downregulation.	168
Figure 8.21 Quin2-AM and herbimycin A inhibit BAE cell shape change and alignment.	169
Figure 8.22 Quin2-AM and herbimycin A inhibit actin stress fiber induction under shear	170
Figure 8.23 Shear stress induces increased protein phosphorylation at tyrosine residues.	171
Figure 8.24 Shear-induced tyrosine phosphorylation is inhibited by Quin2-AM and Herbimycin A	172
Figure 9.1 Model of potential cellular mechanotransducers of shear stress.	183
Figure 9.2 Effect of mechanosensor channel inhibitors on ET-1 mRNA downregulation by shear stress.	184
Figure 9.3 Effect of elevated extracellular potassium on ET-1 mRNA downregulation by shear stress.	185
Figure 9.4 Effect of Cytochalasin D treatment on ET-1 mRNA level.	186
Figure 9.5 Effect of Cytochalasin D on projected cell surface.	187
Figure 9.6 Effect of phalloidin pretreatment on ET-1 mRNA down-regulation by shear stress.	188
Figure 9.7 Hoffman phase-modulation micrographs of BAE cells treated with nocodazole and taxol under shear stress.	189
Figure 9.8 Cell shape analysis of BAEC treated with nocodazole and taxol.	190
Figure 9.9 Nocodazole pretreatment inhibits shear-induced ET-1 mRNA downregulation.	191
Figure 9.10 Tubulin staining of BAE cells exposed to shear stress.	192
Figure 9.11 F-actin staining of BAE cells exposed to shear stress.	193
Figure 9.12 Taxol does not affect shear-induced ET-1 mRNA down-regulation.	194
Figure 9.13 Hoffman phase modulation micrographs of BAE cells plated on Petri dish surfaces pre-coated with increasing concentrations of Pronectin F.	195
Figure 9.14 Morphologic analysis of BAE cells plated on Petri dish surfaces pre-coated with increasing concentrations of Pronectin F.	196
Figure 9.15 Northern blot analysis of BAE cells plated on increasing concentrations of Pronectin F.	197
Figure 9.16 Normalized densitometric analysis of ET-1 mRNA from BAE monolayers plated on increasing concentrations of Pronectin F.	198
Figure 10.1 Hypothetical model of gene regulation by shear stress.	204
Figure 10.2 Hypothetical model of cellular transduction of shear stress.	205

Thesis Committee Members

Seigo Izumo M.D.

Associate Professor of Medicine

Harvard Medical School

Professor of Internal Medicine and Chief, Division of Cardiology

University of Michigan

Alan Grodzinsky Sc.D.

Professor of Electrical, Mechanical, and Biomechanical Engineering

Departments of Electrical Engineering and Computer Science, Mechanical Engineering,
and Health Sciences and Technology

Massachusetts Institute of Technology

Roger Kamm Ph.D.

Professor of Mechanical Engineering

Department of Mechanical Engineering

Massachusetts Institute of Technology

Donald Ingber M.D., Ph.D.

Associate Professor of Pathology

Departments of Surgery and Pathology,

Children's Hospital, Harvard Medical School

Lee Gehrke M.D.

Professor of Health Sciences & Technology

Department of Health Sciences & Technology

Harvard Medical School-Massachusetts Institute of Technology

Abstract

Mechanical forces of hemodynamic origin have been shown to play a crucial role in determining the structure and function of living tissue both in development and pathophysiological states. Specifically, fluid shear stress, the tractive force per unit area resulting from blood flow and acting on the luminal surface of the vessel wall at the endothelial cell surface, has been recognized to be an important parameter. Theoretical and experimental studies have proposed that an energetically optimal branching arterial network is characterized by a constant wall shear stress. Furthermore shear stress of low and fluctuating magnitude has been correlated spatially with foci of atherosclerosis initiation and progression. Despite the above observations and well-defined functional and morphological modulation of endothelium by shear stress, the process of transduction at the cellular level has remained poorly understood.

The present thesis is concerned with the *in vitro* study of the effect of fluid shear stress on vascular endothelial function. A review of the field is presented ranging from whole animal to single cell experiments. The design, method of construction, and testing are outlined for a purpose-built cone-plate viscometer which employs standard tissue for high experimental throughput and large sample surface.

The first part of the thesis describes, using a system-identification approach, the regulation of gene expression by shear stress of three classes of endothelial products: a) Vasoactive modulators using endothelin-1 (ET-1) as a prototype, b) Growth regulators using platelet-derived and fibroblast growth factors (PDGF A- & B-chains, bFGF) and c) Mediators of thrombosis and fibrinolysis using thrombomodulin (TM) and tissue-type plasminogen activator (t-PA). The effect of shear stress magnitude and dynamic character (laminar steady, pulsatile and reversing, and turbulent) are evaluated with appropriate control experiments to rule out non-specific mechanical disturbance and confirm endothelial specificity.

The second part of the thesis focuses on the mechanism of ET-1 gene expression regulation by fluid shear stress on three fronts. The first involves the molecular characterization of ET-1 downregulation by shear stress using nuclear runoff analysis, mRNA stability assays, and promoter region analysis. The second examines the involvement of a panel of putative intracellular second messenger including protein kinase C, cAMP, cGMP, cyclooxygenase activity, intracellular calcium and tyrosine kinase activity. The third determines the role of possible transducing structures including mechanosensitive channels (both shear-stress activated $I_{K,S}$ and stretch-activated $I_{S,A}$), the importance of the microfilament- and microtubule-based components of the cytoskeleton, and the contribution of cell shape and spreading. Further experiments are presented to define the relationship between the mechanism of shear stress gene expression regulation and the longer-term shear-induced cell shape change and cytoskeletal remodeling. The results allow the proposal of an improved flow-responsive model of endothelial cell function to explain flow-dependent vessel structural remodeling and the focal nature of atherosclerosis development. Finally, the findings are used to present a new model of shear stress transduction.

To my family.

Acknowledgment

A number of people were important in providing support and guidance. I thank my faculty advisor, Dr. Roger Mark, for his foresight in suggesting cellular mechanotransduction and cell biology, and for his steadfast support during difficult times. I also thank my thesis advisor, Dr. Seigo Izumo, for offering me a position in his lab and being receptive and supportive throughout; he was available to answer questions and was a staunch advocate of the project even during difficult times. I have learned much from him on all fronts. I am grateful to Profs. Alan Grodzinsky, Roger Kamm, Lee Gehrke and Donald Ingber for serving on thesis committee, and for their precious advice and support. I would also like to thank Dr. Robert Rosenberg for his support, and Drs. Victor Dzau and Gary Gibbons for their guidance in the early phases of the project prior to moving to Stanford University. Dick Ahlquist was an indispensable source of help and taught me the art of machining; the work would not have been possible without his generous help and patience. I would also like to thank the members of Molecular Medicine Unit, including Drs. Seth Alper, Lothar Jahn, Junishi Sadoshima, and Issei Komuro, who were both friends and provided generous advice.

The work presented here is the result of work spanning five years as part of the NIH-sponsored Medical Scientist Training Program (MSTP), a combined MD-PhD at Harvard Medical School and M.I.T. The work was also supported by the Johnson & Johnson foundation and the Whitaker foundation.

Abbreviations

A-V:	arterio-venous
bFGF:	basic fibroblast growth factor
BAE:	bovine aortic endothelium
BSM:	bovine smooth muscle
cAMP:	cyclic adenosine monophosphate
cGMP:	cyclic guanosine monophosphate
CHX:	cycloheximide
DME:	Dulbecco's modified Eagle's medium
EC:	endothelial cell
EDRF:	endothelium-derived relaxing factor
ET-1:	endothelin-1
HUVE:	human umbilical vein endothelium
IBMX:	3-isobutyl-1-methylxanthine
ICAM-1:	intracellular adhesion molecule-1
LDL:	low-density lipoprotein
MCP-1:	monocyte chemotactic protein-1
NO:	nitric oxide
NOS:	nitric oxide synthase
PAI-1:	plasminogen activator inhibitor-1
PDGF:	platelet-derived growth factor
PGI ₂ :	prostaglandin I ₂
PKC:	protein kinase C
p-tyr:	phosphotyrosine
SSRE:	shear stress response element
SA:	stretch activated
TGFβ:	transforming growth factor β
t-PA:	tissue-type plasminogen activator
TM:	thrombomodulin
VCAM:	vascular cell adhesion molecule

CHAPTER 1

Introduction

One of the central questions in biology concerns the mechanism by which external mechanical stimuli affect the structure and function of living matter. There exists sufficient evidence to suggest that living organisms operate, within a certain range, as adaptive control systems, varying their characteristics according to external inputs.

Although the ability of living tissue to adapt to external changes in mechanical stimuli is, in most cases, beneficial, it can, in some cases, lead to pathological situations such as cardiac hypertrophy, pulmonary hypertension, and atherosclerosis.

One of the organs in which mechanical forces seem to play a central role in determining tissue structure and function is the blood vessel (Thoma R., 1893; Murray C.D., 1926; Rodbard S., 1975; Kamiya et al., 1980). The vascular network is critical for providing nutrients and gas exchange to, and removing harmful byproducts from, all tissues in the human body. It has evolved to overcome the basic physical constraint of diffusion, thus enabling the existence of increasingly large and complex living organisms (LaBarbera M., 1990).

The blood vessel wall is an active organ system consisting of populations of endothelial, smooth muscle, and fibroblast cells coupled to each other in a set of complex autocrine/paracrine interactions. The net result is a vessel with specific internal and external radii, with corresponding active and passive mechanical properties. It has been shown that hemodynamic forces, namely fluid shear stress

and pressure/strain acting on the wall of the blood vessel play a critical role in determining vessel structure and function (Murray C.D., 1926; Rodbard S., 1975; Kamiya A. et al., 1980; Langille L. et al., 1986; LaBarbera M., 1990) and may contribute to some types of disease such as atherosclerosis (Fry D.L., 1968; Caro, 1977; Goldsmith H.L. et al., 1986; Glagov S. et al., 1988), the leading cause of death in the United States other parts of the Western world.

The endothelial cell forming a monolayer covering the luminal side of the blood vessel is the only type of cell normally exposed to fluid shear stress and could, therefore, be the sensor and, potentially, the transducer of fluid shear forces into altered vascular wall biology. In recent years, the endothelial cell has grown in importance from being considered a simple passive non-thrombogenic surface to a pluripotent cell intimately involved in the regulation of vessel tone, structure and function.

This thesis is concerned with the *in vitro* study of the effect of fluid shear stress on the molecular and functional regulation of the endothelial cell. The work described here was undertaken to address two central issues:

A- the first concerns the need to determine the effect that fluid forces have on endothelial cell function and gene expression. Such understanding would allow the proposal of a flow-responsive model of the vessel wall that could explain observed vessel behavior in response to changes in flow, or the local pattern of intimal thickening seen in atherosclerosis.

B- the second stems naturally from the first and involves, once a suitable shear stress-sensitive functional marker or gene has been identified, the study, using fluid mechanical, molecular, and pharmacological tools, of the multiple steps involved in the transduction of shear stress into altered gene expression.

The various steps in the thesis work are described schematically in figures 1.1 and 1.2. The second chapter is a review of the literature on the relationship between flow and vessel structure as described by Murray (Murray C.D., 1926) and elaborated further by others, and on its implication on and requirements from vascular biology. Chapter 3 is a review of endothelial cell biology as it relates to vessel structure and includes a description of known endothelial responses to fluid shear stress. Chapter 4 describes the construction and design of the experimental apparatus, a cone-plate viscometer that permits the application of fluid shear stress to endothelial cells grown *in vitro*. Chapter 5 describes in a system-identification fashion the effect of fluid shear stress on the expression of the endothelin-1 gene, which is later used as a functional marker in mechanotransduction studies. Chapter 6 and chapter 7 examine, respectively, the effect of fluid shear stress on endothelial-derived growth factors and thrombomodulators. Chapter 8 explores the molecular mechanism and the second messengers involved in mediating the change in endothelin-1 gene expression by fluid shear stress. Chapter 9 describes the role of a number of candidate endothelial sensory structures, including the actin- and tubulin-based cytoskeleton and mechanosensitive channels, in the transduction process.

The results obtained during the early course of this work are used to propose a new model of flow-induced vascular remodeling and the localization pattern of atherosclerosis. Finally, the findings from the second phase of the project, summarized in the last chapter, bring forth an improved picture of the critical sensing and signaling structures in the endothelial response to shear stress.

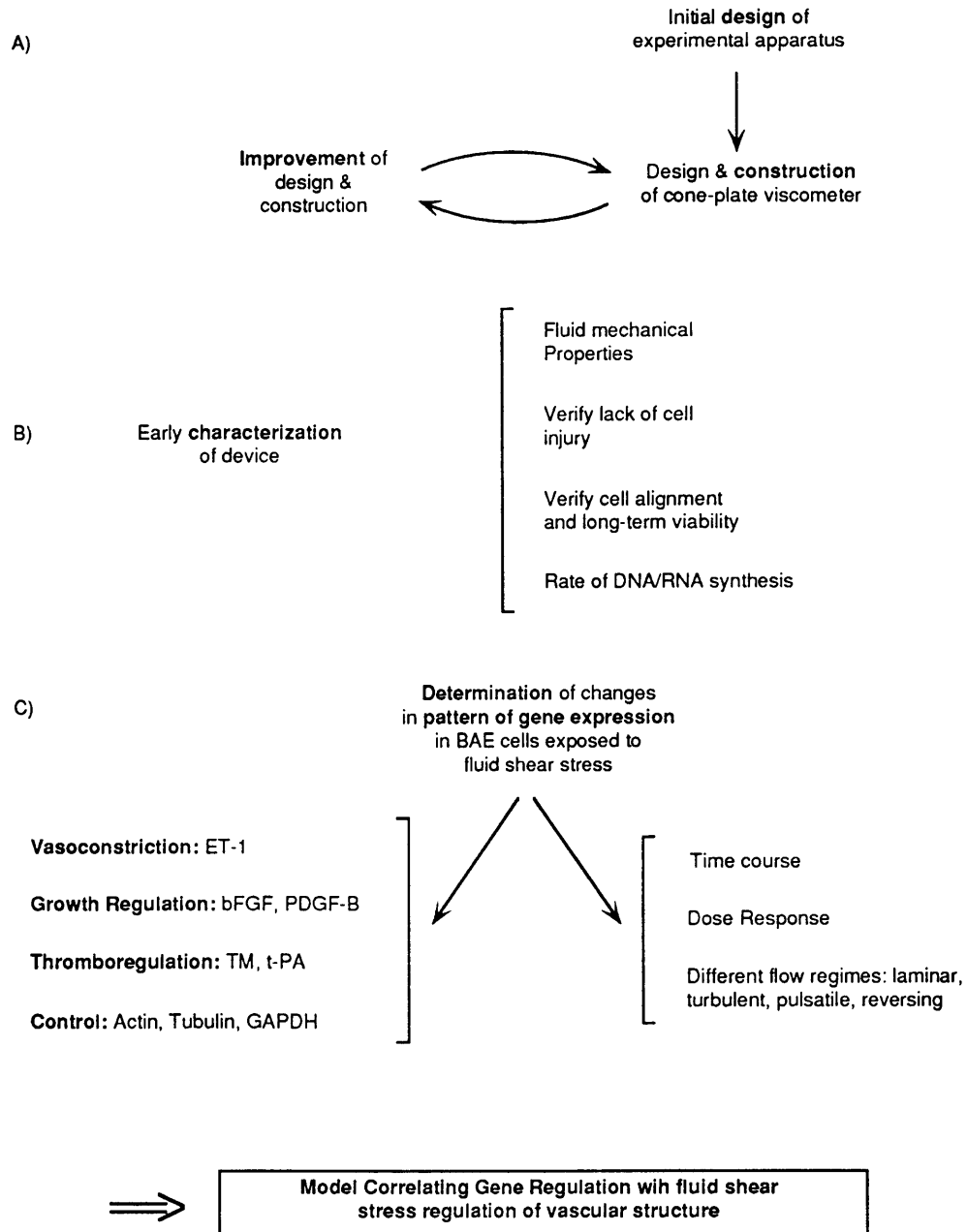


Figure 1.1 Sequential steps of thesis project (A).

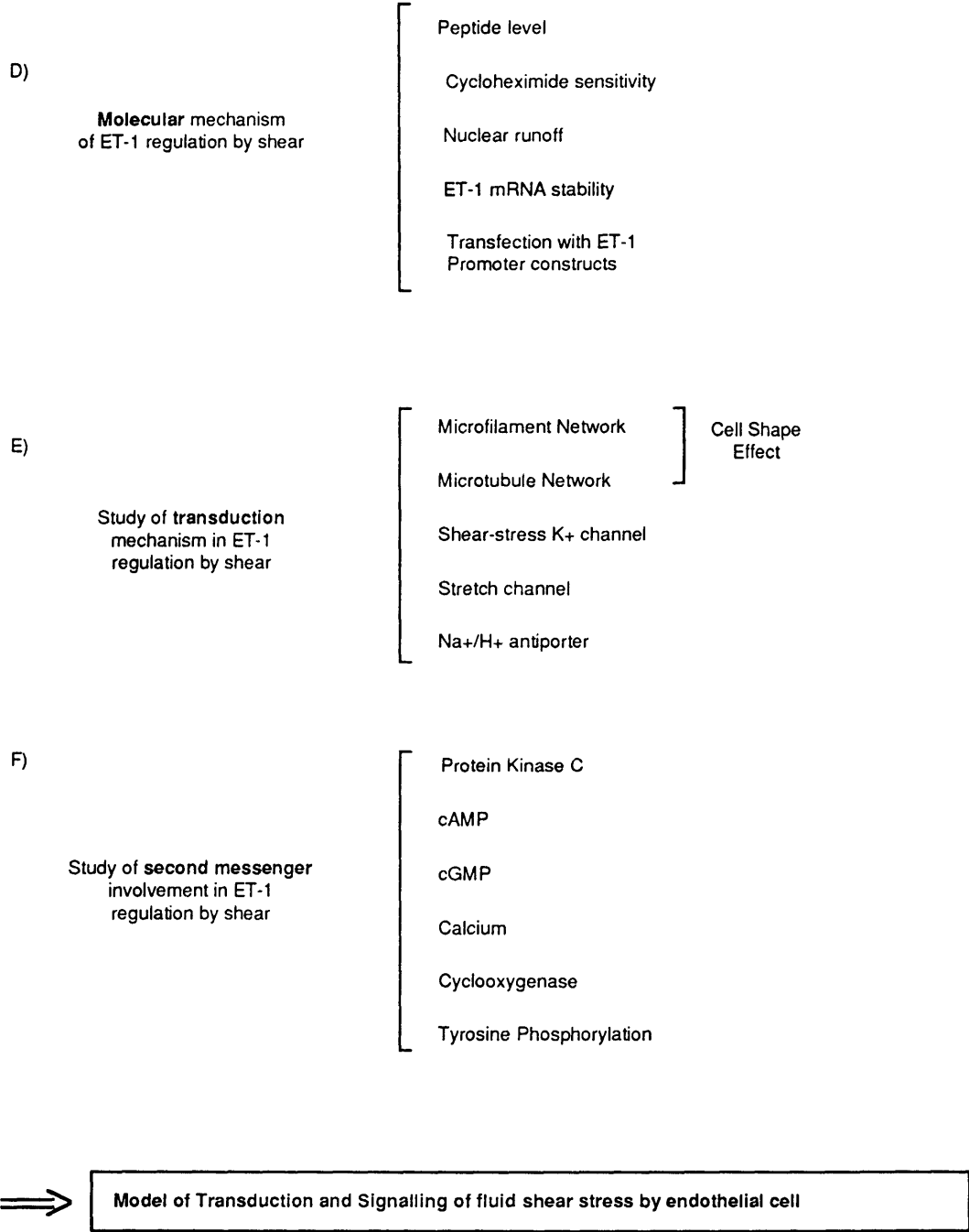


Figure 1.2 Sequential steps of thesis project (B).

CHAPTER 2

Review of Experimental Work and Hypotheses

2.1 Relationship between blood flow and vessel structure

In 1893, Thoma (Thoma R., 1893) proposed the existence of a relationship between blood flow through a vessel and its caliber, arguing that an increase in flow would result in growth and dilation of the vessel. He pointed out that, in the chicken embryo, arteries through which blood velocity was relatively high stayed patent and became the main arteries, while the ones that had a slower blood velocity atrophied. Evidence from arterio-venous shunt and collateral circulation studies also suggested that increased blood flow velocity induced vessel dilatation.

Although workers had assumed some type of relation between vessel size and the amount of blood flowing through it, the exact relationship between these two factors was not known. A related question concerned vessel branching, the process by which a mother vessel is divided into two or more daughter vessels having smaller diameter, and the relationship between the internal radius of the mother and daughter vessels. In 1809, Young proposed a ratio of parent:daughter internal radius ratio of $2^{1/3}:1$ without exactly justifying his choice, a relationship that became known as Young's rule (Young T., 1809; Sherman T., 1981). It was not until Murray's paper in 1926 (Murray C.D., 1926) that a scientific analysis was put forward. Basing his hypothesis on the premise that natural evolution would unfailingly lead to an optimal solution to

any given biological problem, Murray proposed that the structure of the vascular network was designed so as to minimize energy expenditure.

Assuming Poiseuille-Hågen flow through cylindrical blood vessels (Goldsmith H.L. et al., 1986), he proposed the idea of two “antagonistic factors”: the first one concerns the increasing energy required to pump a viscous Newtonian fluid through a vessel of decreasing internal radius, and the other concerning the increasing “metabolic cost” of maintaining the higher volume of blood in vessels of larger internal radius. A brief summary of Murray’s paper is presented below.

Consider a cylindrical vessel of internal radius r , length l , through which exists a flow Q of a Newtonian fluid of viscosity μ (figure 2.1). The flow Q , is related to the pressure drop p , by the hydraulic conductance:

$$Q = cp$$

Assuming Poiseuille flow, the conductance is found to be:

$$c = \frac{\pi r^4}{8\mu l}$$

Defining a for simplicity:

$$a = 8\mu l$$

The pressure drop is then inversely related to the fourth power of the internal vessel radius:

$$p = aQr^{-4}$$

Murray then defines a “metabolic cost” which is related to the volume of the blood contained within the vessel:

$$P_m = mr^2l$$

The power required to pump a Newtonian fluid of viscosity μ through a vessel of unit length is then:

$$P_f = pQ = \frac{aQ^2}{r^4}$$

The total power is the sum of the hydrodynamic and metabolic components:

$$P_t = P_f + P_m = \frac{aQ^2}{r^4} + mr^2l$$

Setting the derivative with respect to r to 0 in order to find the point of minimum power (the second derivative is shown to always be positive):

$$\frac{dP}{dr} = -\frac{4aQ^2}{r^5} + 2br = 0$$

which yields the relationship between flow and the internal radius of the vessel:

$$Q^2 = \frac{b}{2a}r^6$$

Defining a constant k for simplicity:

$$k = \left(\frac{b}{2a}\right)^{1/2}$$

which yields the important relationship that flow is proportional to the third power of the radius:

$$Q = kr^3$$

or alternatively:

$$\frac{Q}{r^3} = k = \text{constant}$$

which can be taken as Murray's law.

Since wall shear stress according to the Poiseuille-Hågen relationship (figure 2.1) is:

$$\tau_w = \left(\frac{4\mu Q}{\pi r^3}\right)$$

which is simply proportional to the constant k , then Murray's law entails that the wall shear stress is everywhere constant, regardless of the value of flow.

The analysis can be further carried to the case of a vessel branching where a mother vessel of internal radius R is divided into two branches of radii r_1 and r_2 (figure 2.2).

Using mass conservation:

$$Q = q_1 + q_2$$

then

$$kR^3 = kr_1^3 + kr_2^3$$

which yield the important relationship:

$$R^3 = r_1^3 + r_2^3$$

This can be generalized to multiple branchings:

$$\sum Q = \sum kr^3 = k \sum r^3$$

yielding the general relationship:

$$R^3 = \sum r_i^3$$

The two important conclusions from Murray's work shown above is that for an "energetically optimal" system governed by Poiseuille flow, minimizing the cost with respect to the radius results in a one-to-one relationship between the flow through a vessel and its internal radius. This is equivalent to saying that the value of shear stress on the wall of the blood vessel needs to be maintained at a constant value, regardless of the magnitude of blood flow; this has become known as Murray's law. When applied to the problem of vessel branching, whether symmetrical or not, this law yields a relationship between the internal radii of branching vessels which is equivalent to Young's rule.

2.2 Further interpretations of Murray's law

Sherman (Sherman et al., 1981) went on to further elucidate the power and implications of Murray's law. One of the weak points of Murray's analysis

was the so-called metabolic cost of maintaining blood. Sherman relaxed this constraint by arguing that attaching a cost function to any power of r^2 such as the cost of maintaining the vessel wall, regardless of the outer radius r_0 , or a combination of the vessel wall and the enclosed volume of blood would also lead to Murray's result. More importantly, using a different approach to the same problem, he considered the question of vessel branching in a system of closed volume characterized by Poiseuille flow, without any restrictions on its symmetry. He showed that minimizing the resistance through such a system would entail a relationship between the R and r_1 and r_2 that was exactly $R^3 = r_1^3 + r_2^3$. He further showed that the analysis could be carried on for 3, 4, or more daughter vessels. Sherman thus showed that Murray's Law "holds for any branching vascular system that, within a given volume, requires minimum flow resistance", without the restriction of assigning metabolic costs of blood or tissue maintenance. Thomas Sherman summarized the importance of Murray's work by writing "Murray's law for connecting large vessels to small is as memorable as Pythagoras' edict on right triangles".

Various measurements of blood flow and vessel internal diameter confirmed Murray's theoretical result. Groat, Suwa (Suwa N. et al., 1963) and others found a relationship between the internal radius of a mother vessel and the internal diameters of its daughter vessels which was consistent with the maintenance of wall shear stress and Murray's Law.

It is also important to state the limitations of Murray's law, namely that it relies on the premise that bulk flow is the principal function of the network. The assumption of blood as a Newtonian fluid is valid in most cases except in some parts of the microvasculature. The most important consequence of Murray's law is that the velocity profile through any vessel of the network has

the same shape, by virtue of the relationship between the flow and the internal radius, and by the assumption of Poiseuille flow: this implies that the shear stress at the wall of the vessel lumen is the same everywhere in the circulatory network.

2.3 Unitary hypothesis based on Murray's law

In 1975, Rodbard (Rodbard S., 1975) rediscovered Murray's Law and suggested that a "unitary hypothesis" should be used to "account for variations in vascular caliber". He advanced the hypothesis that it was the wall shear stress acting on the vessel wall which was the crucial factor in determining the vessel internal radius. Increases or decreases in tissue function called on for an increased or decreased blood flow supply, which was followed by an increase or a decrease in the caliber of the vessels supplying the particular tissue. He also proposed the concept of "set-point shear stress" as being the optimal magnitude of wall shear stress that vessels would either enlarge or shrink their internal radius in order to maintain at any given blood flow. Rodbard also singled out the endothelial surface as the only potential surface that could sense the "hydrodynamic drag" or shear stress, and therefore may be the key sensor and regulator of shear stress. Basing his analysis on this hypothesis, Rodbard was able to justify certain pathological findings that were consistent with this hypothesis such as the post-stenotic enlargement observed in the high shear beyond the stenosis and the occlusion of vein grafts having low blood flow. Zamir (Zamir M., 1977) presented further evidence and measurements to support the constant-shear theory and postulated that, although wall shear stress in many parts of the circulation was pulsatile and time-varying, the endothelial

cell may be perhaps “not sensitive to small or temporary changes in shear, but rather to large and/or prolonged changes only”.

2.4 Vascular remodeling resulting from surgically-induced blood flow changes

Although the analysis provided by Murray, the confirmatory studies by Groat and Suwa, and later the analyses by Rodbard and Zamir all underlined the importance of the “constant-shear” theory and the potential role of the endothelial cell in the regulatory mechanism, their work was based mostly on hypothesis, measurement and observation. It did not directly test whether shear stress was actually the critical factor. These experiments came from the work of Kamiya and Togawa (Kamiya A. et al., 1980) .

Using a canine model, Kamiya et al. surgically constructed an arterial-venous shunt between the common carotid artery and the external jugular vein (figure 2.3). This shunt resulted in an increase in blood flow through the carotid artery whose relative magnitude could be controlled from 1 to 5-fold, without an appreciable change in blood pressure. Using implanted sphygmomanometers, external Doppler flow measurement, and X-ray determination of internal vessel caliber, they were able to follow the main hemodynamic variables. They observed no changes in vessel caliber during an initial period of approximately 40 days, although some endothelial cell changes were detected (Masuda H. et al., 1985; Masuda H. et al., 1989). This period of no change was followed by an increase in the internal diameter of the carotid artery as it continued to expand over a period of several weeks to a new steady state value by 6-8 months. The critical finding came when the wall shear stress was computed in the final result and found to be approximately 15 dyn/cm^2 , the

same value present before surgical intervention. By plotting the fold-increase in blood flow and the final internal diameter of the vessel they found that the internal vessel caliber was adaptively regulated to remain at approximately 15 dyn/cm² despite changes in blood flow of up to 4-5 fold (figure 2.4). This experiment was crucial and presented key findings but did not point out the mechanism of sensing or effecting structural change by the blood vessel. A similar experiment was later carried out by Zarins and Glagov (Zarins C.K. et al., 1987) in a different animal model using the iliac artery.

Langille et al. (Langille L. et al., 1986) attempted the opposite experiment where blood flow through the main carotid artery was reduced by using metal clips in rabbits and blood flow measured (figure 2.5). Local blood pressure was measured and found not to change significantly. Langille observed that the internal radius of the vessel through which blood flow, and consequently wall shear stress, was decreased became reduced when compared to the sham-operated control. Measurement of blood flow and internal diameters allowed the approximate computation of wall shear stress using Poiseuille's equation and yielded again a value of approximately 15 dyn/cm² on both sides. The narrowing of the coarcted vessel was found to be structural and not simply vasomotor, since the use of papaverine to relax smooth muscle contraction did not significantly change the internal radius of the blood vessel. Langille went one step further to confirm the hypothesis put forth by Rodbard and Zamir by showing that the endothelial cell lining the lumen of the blood vessel played a crucial role in the process since its removal abolished the structural change in response to the blood flow decrease (Langille L. et al., 1986).

LaBarbera (LaBarbera M., 1990) has recently expanded these findings to show that, not only mammals, but also sponges and stromatoporoids appear to sense and exploit local fluid shear stress to optimize the structure of their fluid vessels. This finding suggests that the regulation of shear stress by a sensing endothelial-type cell may be a phylogenetically well-conserved mechanism.

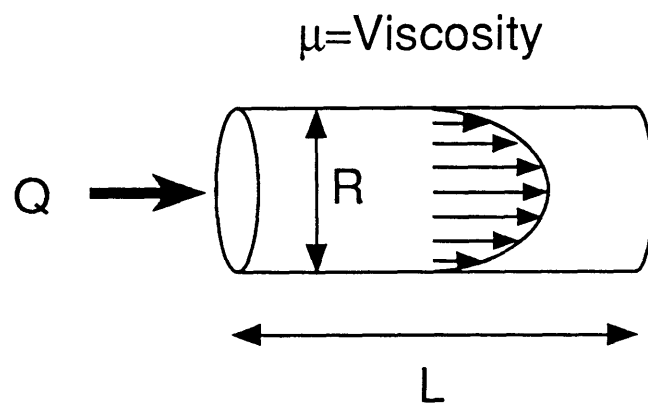
2.5 Relationship between atherosclerosis and fluid shear stress

One of the major health threats is atherosclerosis. Although genetic factors, diet, smoking and life-style play a very important role in the development of the disease, these generalized factors cannot explain the localized and focal nature of the disease (Glagov S. et al., 1988; Asakura T. et al., 1990) (figure 2.6). For years, workers have hypothesized that local hemodynamic factors, namely shear stress, played a pivotal role. Fry (Fry D.L., 1968) and Caro (Caro C.G., 1977) have postulated that it is high and low levels of shear stress, respectively, that may be responsible for the development of the disease. The recent evidence points in favor of the low-shear hypothesis. Zarins and Glagov (Ku D.N. et al., 1985) showed, using the carotid bifurcation atherosclerosis model, that the lesions are localized on the outer side of the branching where vessel wall shear stress levels are low and reversing in direction, while the inner side, where shear stress is of higher magnitude, constant, and non-reversing, is spared. Figure 2.7 shows the measurements of shear stress on both sides demonstrating wall shear stress values greater or equal to 15 dyn/cm^2 on the inner, lesion-free side, and lower magnitude of $\pm 4 \text{ dyn/cm}^2$ with direction-reversal on the outer lesion-prone side of the carotid bifurcation.

Asakura and Karino (Asakura T. et al., 1990), using coronary arteries rendered transparent, found a correlation between areas of low shear stress magnitude and intimal thickening in a number of bifurcations such as the left main coronary artery dividing into the left anterior descending, left circumflex and intermediate branches or the right coronary artery. These results suggest strongly that the temporal and spatial pattern of shear stress might influence endothelial cell function in such a way as to eventually lead to precipitating factors for atherosclerosis.

Other important effects of shear stress include the abnormal hypertrophy and hyperplasia found in vein grafts, A-V shunts and near jet lesions (Rodbard S., 1975). Other workers have shown that low levels of shear stress in arterially-transplanted autogenous vein grafts correlate strongly with intimal proliferation (Kraiss L.W. et al., 1991).

The above observations all seem to implicate fluid shear stress in a role of functional modulation; such regulatory physiological function can be detected by the presence of pathophysiological processes in cases of flow disturbances.



$$\Delta P/Q = \text{Resistance} = \left(\frac{8\mu L}{\pi R^4} \right)$$

$$\text{Wall Shear Stress} = \tau = \left(\frac{4\mu Q}{\pi R^3} \right)$$

Figure 2.1 Diagram of blood vessel undergoing Poiseuille-Hagen flow.

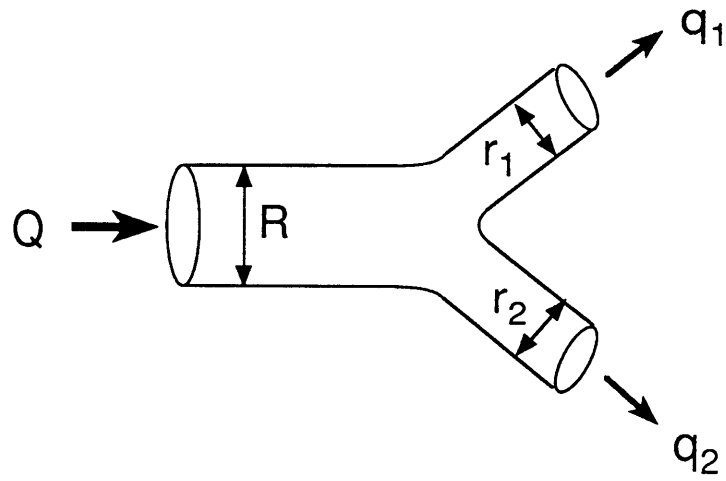


Figure 2.2 Diagram of vessel bifurcation.

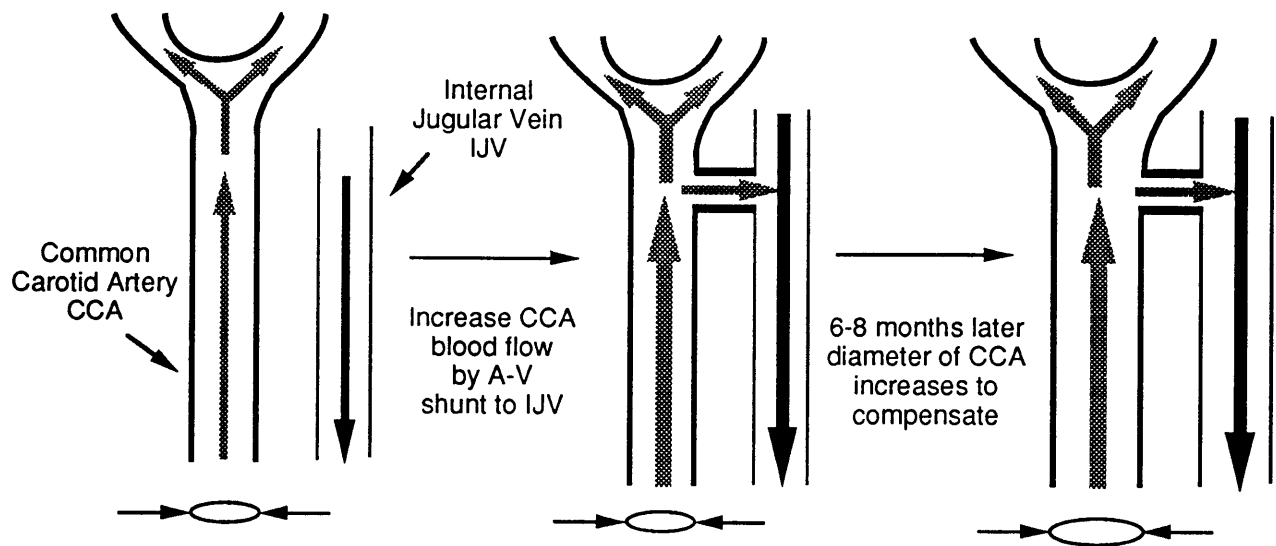
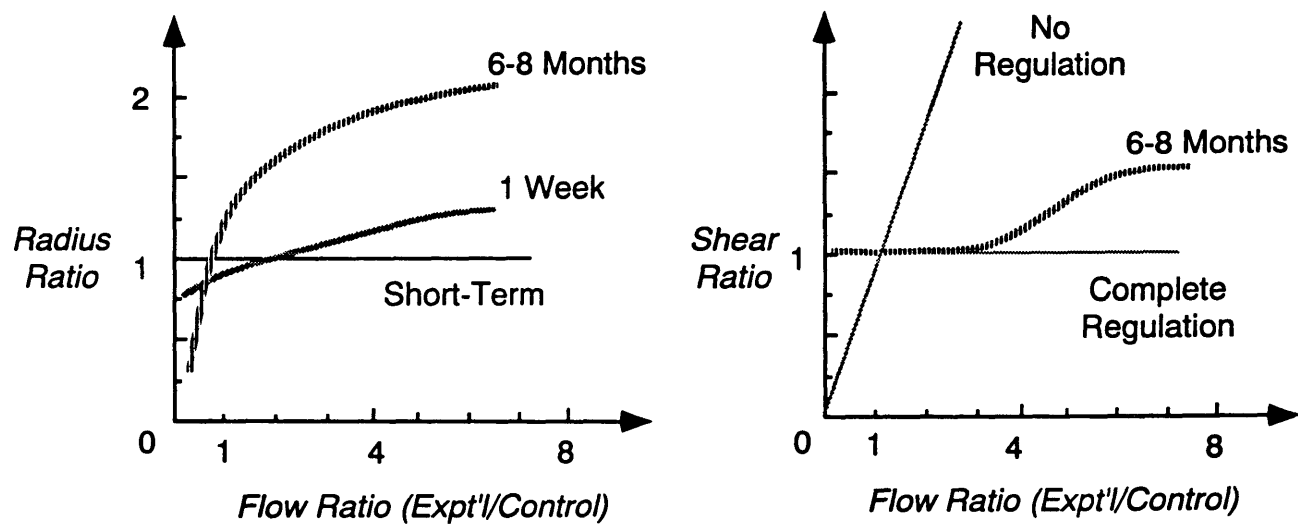


Figure 2.3 Illustration of carotid artery-jugular vein shunt experiment.



(Adapted from Kamiya et al.)

Figure 2.4 Summary figure of Kamiya's result.

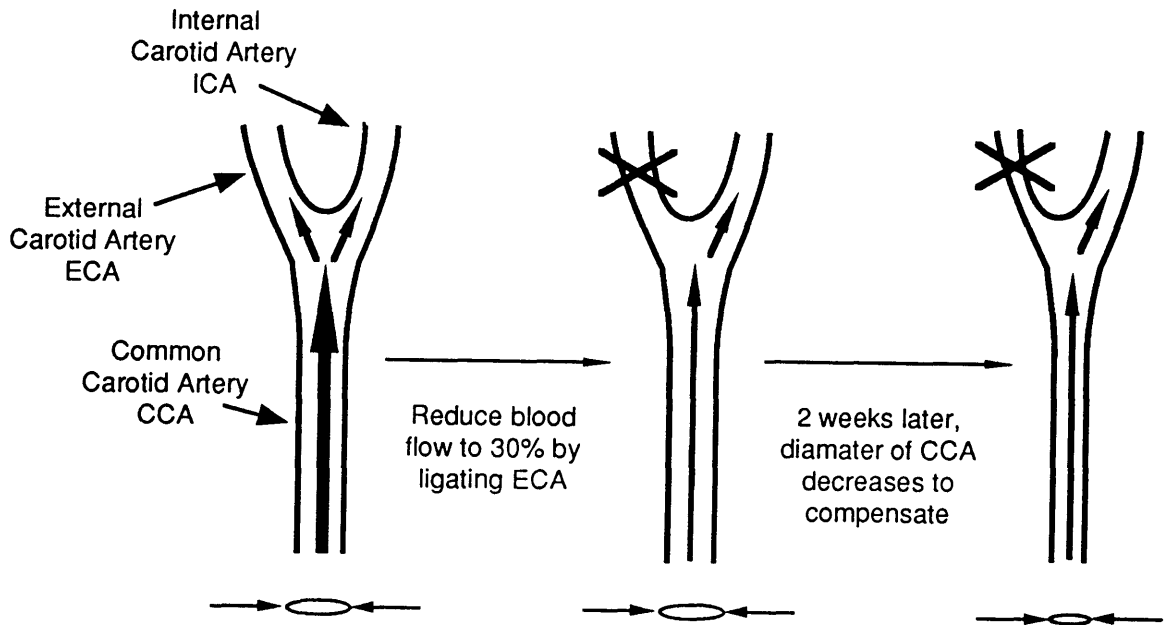


Figure 2.5 Illustration of carotid artery flow reduction experiment.

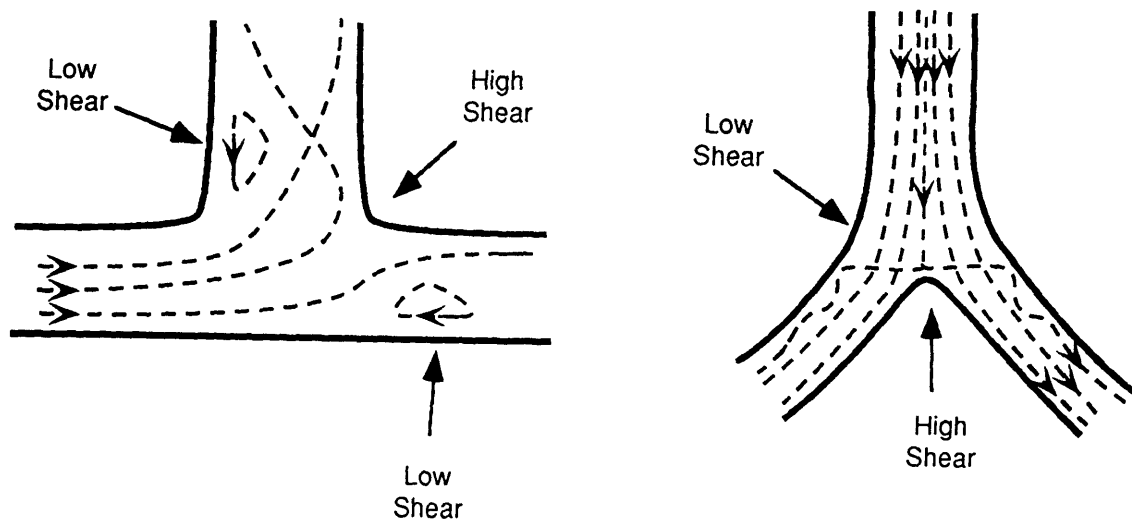
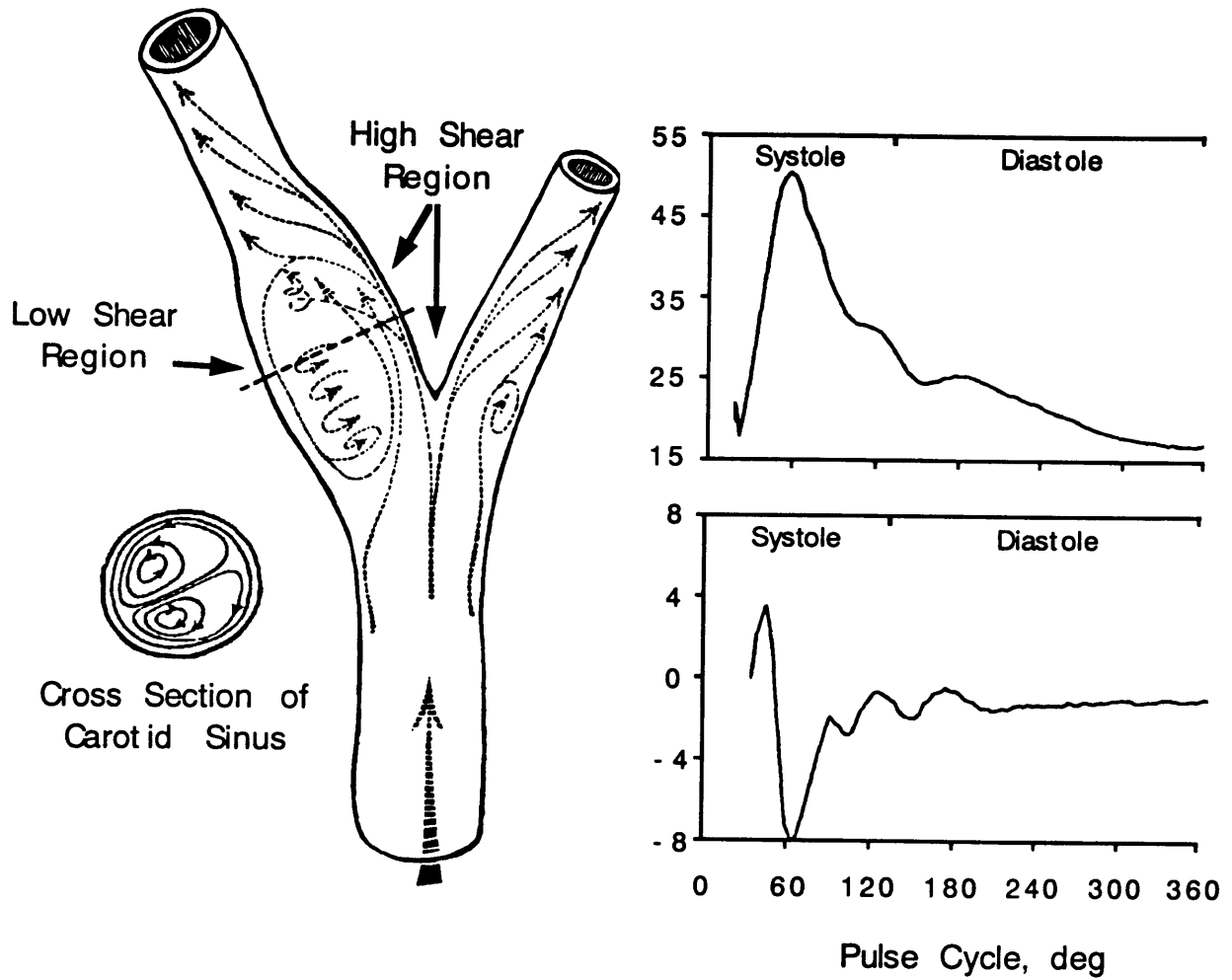


Figure 2.6 Diagram of sites undergoing disturbed flow.



(Adapted from Zarins et al.)

Figure 2.7 Figure from Zarins' work on carotid atherosclerosis.

CHAPTER 3

Vascular Wall Structure and Biology

3.1 Vessel wall structure

The vessel wall is an active organ system consisting of populations of endothelial, smooth muscle and fibroblast cells coupled to each other in a complex autocrine/paracrine set of interactions (figure 3.1). The net result of these interactions is a vessel with specific luminal and outer diameter, and mechanical properties. The vessel wall consists of three layers: the tunica intima made of a single layer of endothelium overlying a thin layer of collagenous and elastic connective tissue inter-mixed with fibroblast and smooth muscle-like cells known as myointimal cells. The tunica media is usually broad and elastic, and consists mainly of elastin, collagenous connective tissue and smooth muscle cells. In muscular arteries, the media contains a preponderance of smooth muscle cells and a smaller elastic and collagenous component than in elastic arteries. The tunica adventitia is made of collagenous connective tissue and provides the rich blood vessel supply to the vessel itself (*Vasa vasorum*) which has been shown in some cases to perfuse up to 75% of the mass of the tunica media.

3.2 Hemodynamic forces

The forces that are exerted on the vessel wall are of dual nature (figure 3.2). A transmural pressure, P , is required to drive blood flow past the downstream resistance and a flow, Q , is generated as a consequence of the pressure gradient.

The endothelial cell is unique because of its position in the vessel which exposes it to at least two types of mechanical force:

- 1) the fluid shear stress resulting from blood flow,
- 2) the tensile strain resulting from transmural pressure.

Although cells in the media and adventitia are also exposed to shear forces, these are not as significant nor as directly-linked to blood flow as in the case of endothelium. The transmural pressure is translated into a circumferential vessel wall tension which can be approximated by Laplace's Law and is shown in figure 3.2 on the left. This is a simplified expression that does not take into account the anisotropy of the vessel wall and the moduli of elasticity of its different layers and constituents. It does, however, show that the smooth muscle and endothelial cells of the wall perceive a level of strain which is approximately proportional to the transmural pressure and inversely proportional to the wall thickness. Conversely, it also indicates that the smooth muscle cells, through their level of tension, can affect transmural pressure.

The flow of blood inside tubular vessels, by virtue of the boundary conditions at the vessel wall, engenders a shear stress on the luminal surface, which is the result of viscous drag. This force is felt in the healthy vessel wall by the endothelial cells which form a uniform monolayer on the luminal surface. The magnitude of the shear stress, in the case of Poiseuille flow, is shown in figure 3.2 on the right. The important features of the equation are the strong inverse dependence on the 3rd degree of the vessel's internal radius and the proportionality to blood velocity.

3.3 Biology of the endothelial cell

The endothelial cell has long been considered to serve as an anti-coagulatory barrier which separates blood from the vessel wall contents and, through the control of its permeability, regulates the traffic of blood borne elements. In recent years, it has become clear that, by synthesizing and secreting a number of potent substances, the endothelium plays a key role in controlling the tone, coagulation state, and structure of the blood vessel. The following is a review of some of the endothelial cell's central functions (figure 3.3)

3.3.1 Tone control

The endothelium has been shown to synthesize and secrete endothelin-1 (ET-1), a 21-amino acid peptide which is the most potent vasoconstrictor known to date both *in vivo* and *in vitro* (Yanagisawa M. et al., 1988). By expressing angiotensin converting enzyme (ACE), the endothelium plays a role in the control of angiotensin II (AII) action, another potent vasoconstrictor (Dzau V.J., 1989). Through its secretion of prostacyclin (PGI₂) (Frangos J.A. et al., 1984) and endothelial-derived relaxing factor-nitric oxide (EDRF, NO) (Rubanyi G.M. et al., 1986; Palmer R.M. et al., 1987) the endothelial cell can cause smooth muscle cell relaxation.

3.3.2 Coagulation and fibrinolysis control

The endothelium plays an important role in mediating the balance between platelet aggregation, and thrombus formation and dissolution (Esmon C.T., 1987). It synthesizes prostacyclin PGI₂ and EDRF which prevent, and tissue factor (TF) and thromboxane (TXA₂) which induce, platelet aggregation. Two anti-coagulant mechanisms are controlled by the endothelial cell (Esmon C.T., 1989): the first

consists of heparin-like molecules expressed on the cell surface which increase the inactivation of coagulation proteases by antithrombin III, and the second involves the surface expression of thrombomodulin (TM) which increases the activation of the protein C anticoagulation pathway. In addition, by secreting tissue- and urokinase-type plasminogen activators (t-PA and u-PA), the endothelial cell can dissolve existing clots and potentially participate in remodeling vascular wall matrix through the activation of plasmin-type enzymes (Mignatti P. et al., 1993; Clowes A.W. et al., 1990).

3.3.3 Growth control

The endothelium synthesizes a number of polypeptide autocrine and paracrine growth factors including platelet-derived growth factor (PDGF) A- and B-chains, basic fibroblast growth factor (bFGF) and transforming growth factor- β (TGF- β) (Rifkin D.B. et al., 1989). PDGF is presumed to act in a mainly paracrine route since the endothelium does not express PDGF receptors; it is a potent positive growth regulator of smooth muscle cells *in vitro*, as well as potent vasoconstrictor *in vivo*. TGF- β can act in both an autocrine and paracrine fashion, and has been shown to be a positive growth regulator at low doses but a negative growth regulator at high doses *in vitro* (Battegay E.J. et al., 1990). Basic FGF is a positive growth factor which can act on both the endothelial and smooth muscle cells *in vitro*, although it does not contain a peptide signal sequence and its secretion mechanism is poorly understood (Vlodavsky I. et al., 1987a & b). ET-1 and AII are both mitogens to smooth muscle cells (Simonson M.S. et al., 1991; Dzau V.J., 1989), while PGI₂ and EDRF have been shown to decrease smooth muscle cell proliferation *in vitro* (Garg U.C. et al., 1989; Moncada S. et al., 1980).

3.4 Effects of flow and shear stress on endothelial function

A summary of the effects of fluid shear stress on endothelial cell function are shown schematically in figure 3.4.

3.4.2 Cell shape change and alignment

It has been observed that endothelium, which grows to form a polygonal cobble-stone like pattern in culture dishes, aligns itself with the flow within 24 to 48 hr, provided that the level of shear stress is above the threshold value of approximately 8-10 dyn/cm² (Remuzzi A., 1984). The orientation process occurs more rapidly in subconfluent than in postconfluent cultures. The rate of alignment is proportional to the level of shear stress and is also dependent on the extra-cellular matrix on which the cells are plated (Ives C.L. et al., 1983). Once the cells are aligned and fluid flow is halted, a relaxation process occurs (Remuzzi A., 1984) whereby the endothelial cells lose their fusiform aligned shape and revert back to their previous polygonal shape within 72 hr.

3.4.3 Actin stress fiber rearrangement

One of the features of the endothelial response to shear stress is a redistribution of its actin filament network into axially-oriented stress fiber actin microfilament bundles that increase in prominence with shear stress application (Franke R. et al., 1984). This presence of stress fibers with myosin co-localization has been shown both *in vivo* (Herman I.M. et al., 1987) and *in vitro* (Wechezak A.R. et al., 1985) and is thought to prevent the sloughing off of the cell as result of shear stress (Wechezak A.R. et al., 1989).

3.4.4 Mechanosensitive channels, potassium current and internal calcium transients

Shear stress on the endothelium has been documented by Olesen et al. (Olesen S. et al., 1988) to result in a hyperpolarization of the cell which is mediated by a potassium current, $I_{K.S}$. This inwardly-rectifying K^+ current is mediated via a barium-sensitive channel that is different from the acetylcholine-activated potassium channel ($I_{K.Ach}$) previously found in endothelium by the same team. The resulting hyperpolarizing current increases asymptotically with shear stress, has a 1/2 maximal effect at 0.7 dyn/cm^2 , and saturates at 15 dyn/cm^2 . It also downregulates slowly but is reactivated quickly as soon as the flow stimulus is removed. Another non-specific ionic channel was described by Lansman & al. (Lansman J.B. et al., 1987) to be opened by membrane strain, although the sensitivity of this channel to fluid shear stress has not been documented. It is thought to be of the same type as described by Sachs & Guharay (Guharay F. et al., 1984) in skeletal muscle cells.

Ando and colleagues (Ando J. et al., 1988) have demonstrated that applying flow on endothelial cells results in a transiently elevated and sustained increase in internal calcium concentration. This increase in internal calcium concentration was shown to be derived from intracellular stores, and not solely from calcium entry through channels in the plasma membrane since Ca^{2+} depletion from the external medium did not abolish the response. More recent studies have shown that flow and shear stress can induce transient increases in intracellular calcium $[Ca^{2+}]_i$ by both an ATP-dependent (Mo M. et al., 1991) ($\Delta[Ca^{2+}]_i = 100\text{-}400\text{nM}$) and ATP-independent ($\Delta[Ca^{2+}]_i = 75\text{nM}$) (Shen J. et al., 1992) mechanism in BAEC.

3.4.5 Effects on cell function

Davies and colleagues (Davies P.F. et al., 1983) have demonstrated an increase in the pinocytotic rate of endothelium with shear stress. They found that the increased pinocytosis occurred earlier than the alignment process and at lower shear stress values than those required to affect cell shape. The increased pinocytosis, which is related to shear stress level, is transient and returns to control values after 4 hr; it is also found with time-varying oscillatory flow as well as with step decreases of shear stress. The pinocytosis was measured by horseradish peroxidase (HRP) which was found to be localized in membrane-bound vesicles and lysosomes, but not in the cytoplasm.

3.4.6 Endothelial cell cycle control

Davies and colleagues (Davies P.F. et al., 1986) also showed a critical feature of the endothelial response to shear stress. Although no change was detected with the application of shear in the laminar flow regime, an increased cellular turnover was observed with the application of turbulent shear stress having the same time-averaged value, but a random orientation and time-dependence. In addition to the increased turnover, significant cell loss and retraction were observed even following short periods of shear application. Work by others (Levesque et al., 1990) suggests a decrease in DNA synthesis rate and in rate of entry into the cell cycle in response to steady laminar shear stress of magnitude equal to or greater than 15 dyn/cm².

3.4.7 Release of prostacyclin and histamine

Grabowski et al. (Grabowski E.F. et al., 1985) and Frangos et al. (Frangos J.A. et al., 1984) showed that fluid shear stress induced the secretion of prostacyclin (PGI₂) by bovine aortic and human vein umbilical endothelial cells respectively. Both groups showed that the response was characterized by an elevated transient release which decayed to a non-zero value with time. This entails that the production of PGI₂ was higher, on average, in pulsatile or time-varying flow than in steady-state flow. The rate of production was also found to be related to the magnitude of the shear and saturated above 15 dyn/cm². Both of these studies were conducted on cell cultures that had not been previously subjected to shear, and were unaligned. It is not clear whether this phenomenon is simply a transient phenomenon during the activation process that results in the cell alignment, or whether it is expected to be present in cultures already physiologically adapted to flow.

In 1978, DeForrest (DeForrest et al., 1978) showed, by perfusing rabbit aortas with platelet-free blood at various levels of flow, that shear stress was positively correlated to the histamine forming capacity of endothelium, as assayed by measuring the activity of the aortic histidine decarboxylase system.

3.4.8 Endothelial-derived relaxing factor

In 1980, Furchgott and Zawadzki (Furchgott R.F. et al., 1980) described that endothelium was critical in the acetylcholine-induced relaxation in the vessel wall that had been previously contracted with epinephrine. They identified the mediator as being EDRF which was later identified as nitric oxide (NO) (Palmer et al.,

1987), a metabolic product of arginine metabolism. Later work showed that flow also induced EDRF-mediated vessel dilatation (Rubanyi G.M. et al., 1986).

3.4.9 Tissue-type plasminogen activator

Diamond and colleagues (Diamond S. et al., 1989) showed that subjecting endothelium to laminar flow resulted in an increase in the secretion of tissue-type plasminogen activator (t-PA), after a delay of about six hours, in a linear kinetic fashion. This increase in secretion was not seen at 4 dyn/cm² but was observed at 15 dyn/cm², and was even higher at 25 dyn/cm². The effect of flow was not found not to be mediated by a transferable factor in the media conditioned by exposure to shear. Secretion of plasminogen activator inhibitor (PAI) was found to remain constant throughout the experiment.

3.5 Summary and plan of action

It is clear that blood flow, and more specifically shear stress, plays a critical role in determining the structure of the vascular system so as to maintain it at an optimal level, consistent with Murray's law (figure 3.5). In addition, fluid shear stress appears to play an important role in atherosclerosis, providing a protective role when its magnitude is equal to or greater than 15 dyn/cm². The endothelial cell is the obvious candidate to be the sensor and effector of fluid shear stress in the blood vessel. Its central role in the adaptive regulation of wall shear stress has been clearly demonstrated. Furthermore, the endothelium produces and secretes a host of active substances that may be responsible for mediating shear-induced vascular remodeling and maintaining vessel structure as discussed above. Recent work has demonstrated that the endothelium possesses structures for the sensing of

mechanical forces such as shear stress and membrane strain. There have been numerous indications of altered endothelial cell functions such as increased PGI₂, EDRF, and t-PA secretion, and effects on cell cycle progression. It is with this background that the present thesis was undertaken.

The first goal of the thesis is to explore the effect of well-controlled *in vitro* shear stress on isolated endothelial cell function described in recent years, on three fronts:

- A- vascular tone control,
- B- growth regulation,
- C- thrombosis/thrombolysis control.

Using a system identification approach to determine the relationship between shear stress and the expression of key factors participating in the above three processes, a study of the mechanism of the transduction of the shear stress stimulus on the expression of candidate mediators will be undertaken ranging from the molecular biological mechanism, the second messenger involvement and the identification of potential mechanosensing structures.

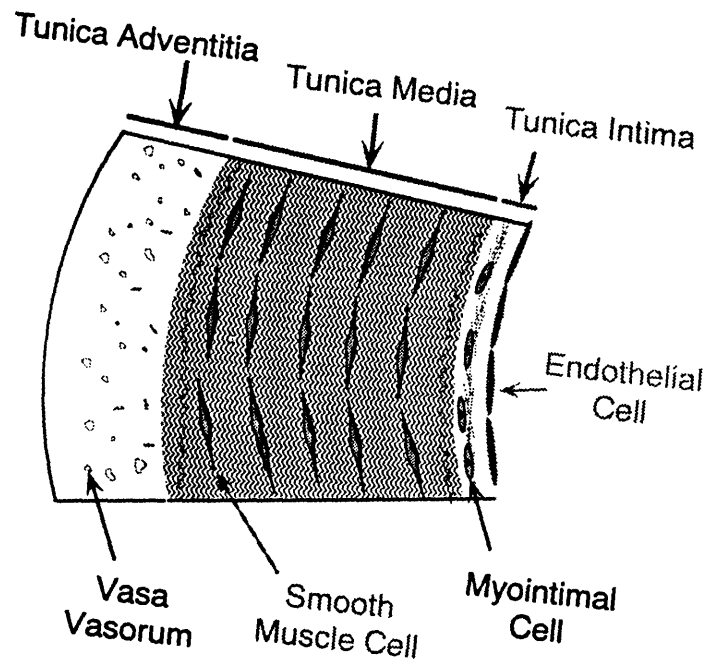


Figure 3.1 Schematic representation of the vessel wall.

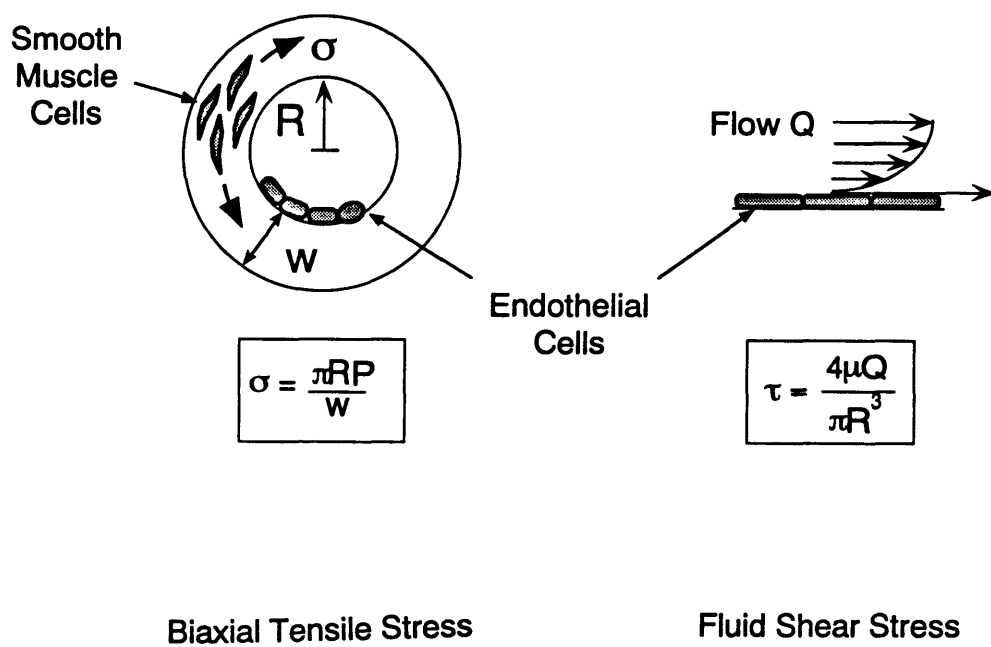


Figure 3.2 Expression of tensile stress and shear stress.

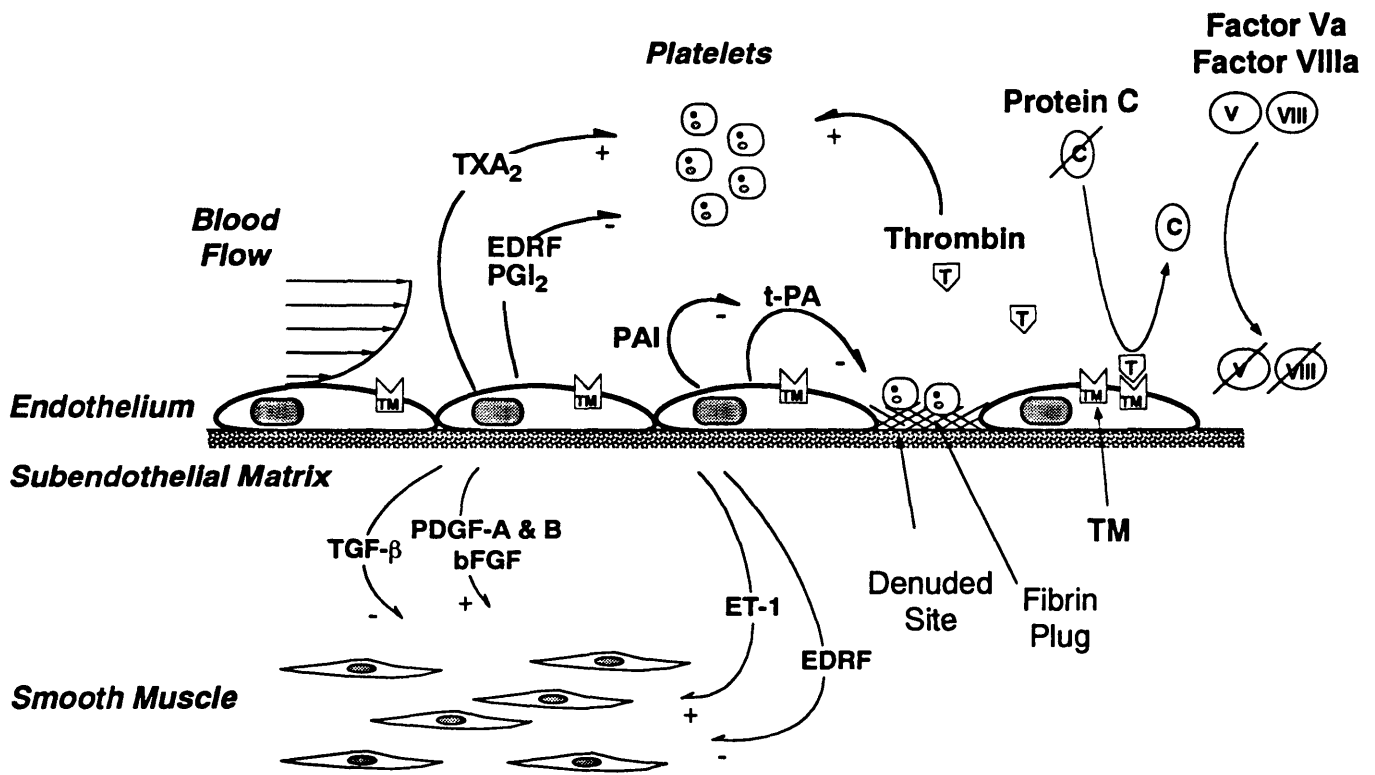


Figure 3.3 Summary of multiple interactions at the vessel wall interface.

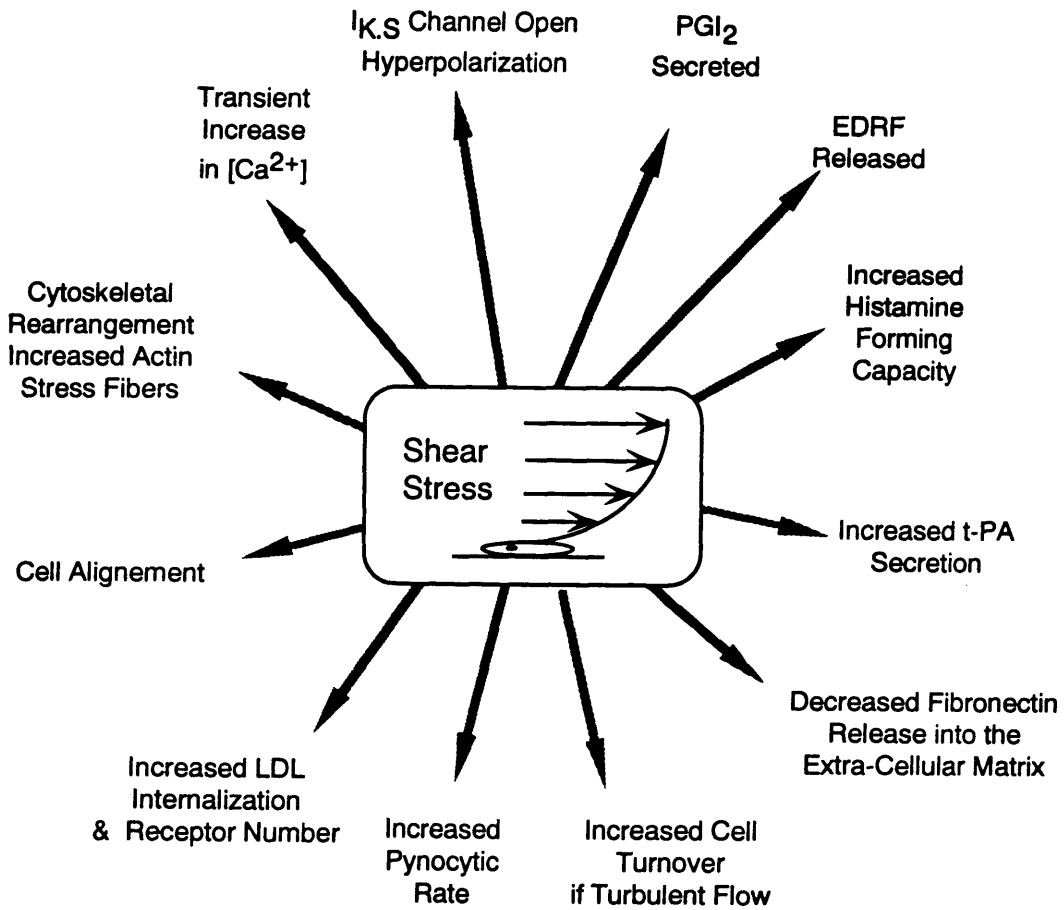


Figure 3.4 Multiple endothelial responses to fluid shear stress.

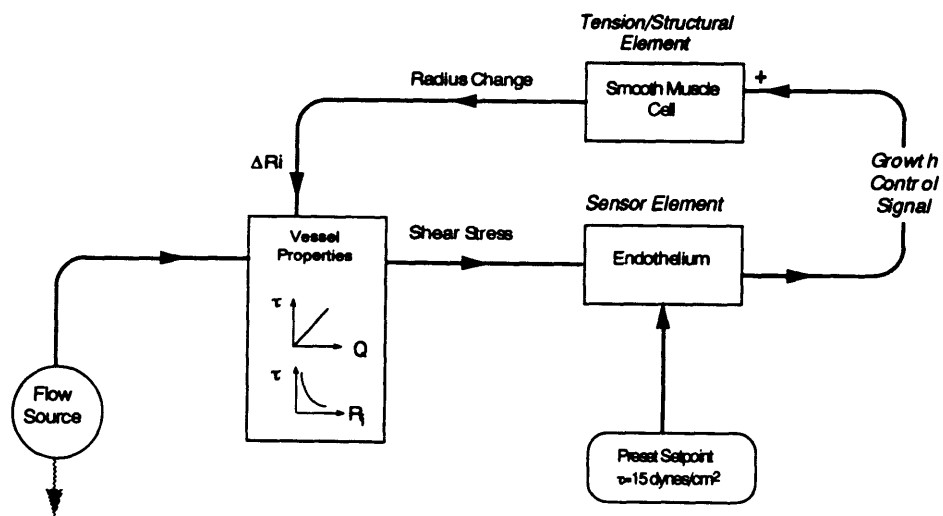


Figure 3.5 Negative feedback control loop of vessel wall structure.

CHAPTER 4

Design, Construction, and Testing of Shear Stress Apparatus

The first part of the work consists of the design, construction, and testing of a molecular biology-compatible experimental apparatus to be used for subjecting endothelial cells *in vitro* to well-controlled levels of shear stress.

4.1. Background on devices for subjecting endothelium to shear stress

Two main classes of devices have been used to date to subject endothelial cells to fluid shear stress. The first includes the cone-plate viscometer and other devices having a rotating structure, such as a disk or cone, moving on top of the growth medium and transmitting shear stress to the endothelial cells (figure 4.1 A). The second type of device includes the parallel-plate (figure 4.1 B) and capillary-tube flow viscometer (figure 4.1 C), and consists of a chamber in which is grown the endothelium and through which fluid is forced by either a pump or a hydrostatic head.

4.2. Design requirements

The design requirements that needed to be met were the following:

a) the ability to subject cells to different magnitudes of shear stress in a number of flow regimes, including laminar, time- and direction-varying laminar, and turbulent,

- b) the compatibility with standard tissue culture techniques and the requirement of minimal additional special-purpose equipment,
- c) the provision of quick isolation of media and cell samples without resorting to complex positioning, disassembly and reassembly procedures,
- d) the provision of high experimental throughput,
- e) the ability to isolate sufficient amounts of cellular material such as protein and mRNA to allow Western and Northern analyses without resorting to amplification procedures, and a sufficiently large cell number to allow transfection studies and nuclear runoff transcription.

These requirements ruled out the use of the parallel-plate viscometer since the available designs using microscope cover slides as growth surfaces do not provide a sufficiently large experimental surface. The parallel-plate flow viscometer also requires a relatively large media volume for the hydraulic circuit which would need to be replaced for every new sample of endothelial cells to avoid introducing confounding cross-contamination. From a fluid mechanical perspective, the parallel-plate viscometer does not easily allow the user to reverse shear stress direction or to provide turbulent flow without further complex peripheral machinery or very high flow rates respectively.

The cone-plate viscometer is commonly used to measure the viscosity of fluids; this type of device was chosen to subject endothelial cells to shear stress because of its flexibility of use and the wide range of shear stress characteristics both in magnitude and in regime that it permits. Its fluid mechanical properties have been well characterized by Sdougos et al. (Sdougos H.P. et al., 1984) at M.I.T. and it has been used by Dr. Michael Gimbrone's group at the Brigham & Women's Hospital (Boston, MA) in a series of pioneering experiments [Davies P.F. et al., 1983; Davies P.F. et al., 1986; Remuzzi A., 1984). The device as described by Sdougos

and used by Gimbrone's group, however, uses a complex positioning mechanism and allows the user to expose endothelial cells grown on microscope slide covers. It is a considerably large unit with a heavy stainless steel cone having a 10-inch diameter and requiring its own incubator. A different design was needed to satisfy the requirements cited above.

4.2.1 Fluid mechanics of cone-plate viscometer

The following is a summary of the fluid mechanical description of the cone-plate viscometer (Sdougos H.P. et al., 1984). Defining the angle of the cone as α ($< 5^\circ$), the rotational velocity ω , medium viscosity μ and kinematic viscosity ν , shear stress τ acting on the plate at a radius r . With a rotating cone, the boundary conditions entail zero flow at the surface of the tissue culture plate, which results in shear stress acting in the tangential direction on the tissue culture plate. At very low rotational velocity or at high kinematic viscosity (i.e. low Reynolds number) the magnitude of the shear stress is uniform across the whole surface and is found to be:

$$\tau = \frac{\mu\omega}{\alpha}$$

which is independent of the radius since both the gap between the cone and the surface of the plate, and the linear velocity at a given point are proportional to r . A Reynolds number R_e can be defined:

$$R_e = \frac{r^2\omega\alpha^2}{12\nu}$$

When $R_e < 1$ the flow is laminar, with the shear stress pointing in the tangential direction. For values of $.1 < R_e < 1 \sim 4$ one observes the onset of secondary flow with the appearance of a radial inward component of shear (figure 4.2). Finally for $R_e > 4$, the flow becomes turbulent. Using asymptotic expansion and fitting of

empirical data, Bussolari (Bussolari S.R. et al., 1982) obtained the following approximation for the magnitude of shear stress for moderate values of R_e :

$$|\tau_{ss}| = \left(\frac{\mu\omega}{\alpha} \right) \left[1 + 2.58 \left(\frac{R_e^{\frac{3}{2}}}{3.5 + R_e} \right) - 0.86 \left(\frac{R_e^{\frac{5}{2}}}{(3.5 + R_e)^2} \right) \right]$$

The shear stress vector can be separated into its tangential τ_t and radial τ_r components, and ϕ is then defined as the angle between the shear stress vector and the tangential direction.

$$\phi = \tan^{-1} \left(\frac{\tau_t}{\tau_r} \right)$$

4.2.2 Technical description of the device

Figure 4.3 lists a legend of the various parts of the device. Figure 4.4 shows an exploded view of the device showing the baseplate made of aluminum and containing a recess and groove to allow the tissue culture plate, on which the adherent cells are grown, to fit exactly flat with respect to the baseplate. The cone, made from transparent plexiglass™, is attached to its shaft which passes through the bearing housing and is connected to the motor drive and gearbox via a flexible coupling. The height of the motor assembly which consists of the block, DC-motor, and reduction gearbox, is adjusted by sliding the assembly vertically on the motor assembly shaft, which is attached at right angle to the baseplate. This feature of the device allows the best adjustment of the motor with respect to the cone shaft so as to minimize loading and transmission of forces (figure 4.4). An important part of this design is the ability of the cone shaft to slide freely through the inner race of the bearings. The bearing housing is made either from plexiglass™ or aluminum alloy and is firmly connected to the cover-plate at a right angle. The

coverplate and cone are made from optically polished plexiglass™ to allow visualization of the cells on the tissue culture dish during operation.

The tip of the cone must constantly be in contact with the center of the tissue culture plate to allow the user to predict the value of shear stress at the surface of the tissue culture plate. The cone in the present device rests at its tip made of low-friction material (ultra-high molecular weight polyethylene) on to the center of the tissue culture plate, thereby insuring flatness of the tissue culture plate surface. The fact that the weight of the cone exerted at its tip helps flatten the surface of commercially available tissue culture plates is a central part of the design. The effect of this feature is shown in figure 4.5 & 4.8. Clamps fixed to the baseplate are tightened to hold down the coverplate on top of the tissue culture plate as shown in figure 4.5; this insures proper pressure on the coverplate, on the tissue culture plate, and onto the recess in the baseplate, while allowing quick and reproducible positioning. The relative positions of the coverplate, bearing housing, cone and tissue culture plate are shown in figure 4.5. A groove is machined into the baseplate to allow the rim of the tissue culture plate to rest into the former (figure 4.6). This is a central feature of the device which maximizes the flatness of the tissue culture plate. To the center of the coverplate is affixed the circular bearing housing at a 90° angle, which contains the ultra-high precision bearings. The coverplate contains a circular slot of rectangular cross-section, which is concentric with the shaft housing and rests on top of the lip of the tissue culture dish. This is a central feature of the device which allows the accurate positioning of the coverplate and the bearing housing attached to it with respect to the baseplate, and allows the cone shaft to be at right angle with respect to the surface of the tissue culture plate. Gas exchange to the cells is achieved in one of two ways: either by drilling holes

that traverse the cover plate or by drilling partial holes, at the diameter of the slot, of greater depth than the slot to allow air flow (figure 4.6).

An additional feature of the cone assembly is the presence of a set screw in the circular base of the cone shaft to allow the setting of a preset wobble in the cone. This is achieved as described in figure 4.7. The screws holding the cone to the shaft are loosened, and the right amount of wobble is dialed in by using the set screw 24. The screws holding the cone 22 are then tightened again. Two or more set screws can be used at different positions around the cone base to allow the setting of the duration and the amount of wobble at a given rotational velocity.

The graph in figure 4.8 illustrates the gap between the surface of the cone and the tissue culture plate for a number of different cone angles as well as the difference between a perfectly flat tissue culture dish (straight line) and an actual one (Falcon Labware, Oxnard CA., Tissue Culture Ware # 3003) when the cone weight is applied at its tip (filled circles) and when it is left unrestrained by the cone weight (hollow circles). The force with which the tip of the cone contacts the center of the dish can be controlled by a spring fitting around the cone shaft, and acting between the base of the cone shaft and the inner race of the bearing (figure 4.5).

4.3 Experimental validation of device properties

Flow visualization studies were carried out by passing a fine line of ink through a hole of 0.2 mm diameter in the tissue culture plate. The angle ϕ (figure 4.9 A) was measured experimentally using a 1° cone and increasing rotational velocity ω , and water or water supplemented with 5% dextran in the region of primary and secondary flow ($.04 < Re < 2.5$). The results are shown in figure 4.9B where the experimental values appear as points and the theoretical prediction as a line. The

result indicates very good agreement up to Re of approximately 2, beyond which ϕ remains at approximately 45° , a previously-reported finding (Bussolari S.R. et al., 1982).

The profiles of the shear stress and Reynolds number distribution and average values across the plate were computed using MathCad (MathSoft, MA) and are shown for three sets of values in figure 4.10, to underline the versatility of the design. In A unsupplemented DME medium was used with a 5° cone at $5 \cdot 2\pi$ rad/s, while in B a 1° cone is used at $4 \cdot 2\pi$ rad/s and finally in C, DME medium supplemented with 5% dextran to increase medium viscosity was used with a cone angle of 0.5° at $3 \cdot 2\pi$ rad/s.

4.3.1 Control of cone rotation velocity and step-response to external velocity command

To determine the ability to control cone rotation velocity and to characterize the operation of the DC-motor controller, we analyzed the temporal response of the cone velocity to a unit-step command of either 3 or 6 rev/s (final velocity). Figure 4.11 illustrates the response for both the small-size cone designed for use with 10 cm and the large one for 15 cm tissue culture plates. Both responses exhibited a delay, t_d , during which cone velocity appeared to increase in a linear fashion to its final value. The value of t_d to a step input of 3 and 6/s was measured at 24 and 68 ms for the small cone and 93 and 183 ms for the large cone respectively. Figure 4.12 illustrates the capability to drive the controller with a signal generator, thereby achieving pulsatile and reversing cone velocity waveforms. In addition, the controller accepts inputs from the D/A board of a personal computer, which allows the user to arbitrarily choose a velocity waveform.

When using the device with time-varying stimuli, it is important to insure that the cone acceleration values are kept low enough to permit sufficient flow development and shear transmission to the plate below. This problem can be approximated (for small cone angles) by that of the suddenly-accelerated plate (Sutera S.P. et al., 1988). The solution to this problem suggests that the following condition be satisfied in order for the difference between the velocity profile and its asymptotic value be less than 1%:

$$t_0 > \frac{0.25h(r)^2}{\nu}$$

where t_0 is the time of development, $h(r)$ is the gap between the plate and the cone surface at a given radius and ν is the kinematic viscosity. An illustrative calculation for a cone of 1° and maximum radius r of 4 cm using regular DME with 10% calf serum would yield $t_0 > 4$ ms. This is clearly negligible when using a sinusoidal waveform of frequency 90 Hz (figure 4.12, pulsatile) with a corresponding period of $T=667$ ms.

In turbulent regime ($Re > 4$), it is possible to estimate the order of magnitude of the Eddy currents generated by computing the Kolmogorov scale; this value can be computed in the cone-plate configuration to be approximately equal to $0.1 \cdot h(r)$, or 10% of the local gap between the cone and the plate (Corrsin S., 1959; Davies P.F. et al., 1986).

4.4 Experimental results

The device was verified to be compatible with tissue culture and cell growth, and that gas exchange was not a limiting factor in either static or operational conditions. Temperature measurements were also made to insure no increase in

temperature of the media under operating conditions (data not shown). The absence of injury to the cells under shear was confirmed by measuring lactic dehydrogenase (LDH) release during shear stress, as shown in figure 4.13.

4.4.1 Shear induces cell shape change and alignment in a time- and magnitude-dependent manner

Furthermore, endothelial cells were exposed to steady laminar shear stress to verify alignment in the direction of the flow. Figure 4.14 shows BAE cells that have been subjected to steady laminar shear stress of magnitude 15 dyn/cm^2 in the cone-plate viscometer for 3, 6, 12, 18 and 24 hr. Cells at six hours show little shape change, but progressively begin to appear more aligned by 12 hr and eventually complete their shape change by 18 to 24 hr.

Figure 4.15 shows that when compared to the lower magnitude of shear stress of 15 dyn/cm^2 (moderate), BAE cells exposed to 36 dyn/cm^2 (elevated) appear to be longer and narrower at 24 hr. Morphometric analysis revealed that the cells exposed to 36 dyn/cm^2 were more elongated and spindle-shaped as demonstrated by a significantly lower computed roundness ratio of 0.24 ± 0.001 ($n=238$, $p<0.001$) when compared to cells exposed to 15 dyn/cm^2 whose roundness ratio was 0.43 ± 0.001 ($n=252$, $p<0.001$) and static control cells of roundness 0.58 ± 0.001 ($n=236$) as shown in figure 4.15.

Histogram analysis showed that cells exposed to the 36 dyn/cm^2 also exhibited a more complete and uniform alignment in the direction of flow as shown by a narrower distribution of the angle made between the major axis of a particular cell and the direction of flow. Figure 4.16 A illustrates the random distribution of static control cells having mean angle of -1.7 and a standard deviation $\sigma = 51.9^\circ$ ($n=238$). This is in contrast with cells exposed to 15 dyn/cm^2 characterized by a mean angle

of $9.5^\circ \pm \sigma = 20.6^\circ$ ($n=266$, figure 4.16 B). and cells exposed to 36 dyn/cm^2 with a mean angle of $5.7^\circ \pm \sigma = 10.7^\circ$ ($n=240$, figure 4.16 C). Note that both populations exposed to shear stress exhibit normal distributions centered approximately around the direction of flow but that the BAE monolayers exposed to the moderate shear (15 dyn/cm^2) had a broader distribution with nearly double the standard deviation of those exposed to high shear (36 dyn/cm^2).

4.4.2 Long-term fluid shear stress induces cell shape change and alignment in endothelial but not in smooth muscle cells

Endothelial cell shape is known to be affected by hemodynamic forces in a specific manner including both shear stress τ (Remuzzi A., 1984; Malek A. et al., 1992) and uniaxial strain (Shirinsky V.P. et al., 1989). In response to the former the endothelium aligns in the same direction as the flow, while in response to the latter it becomes spindle-shaped and assumes a direction perpendicular to the strain axis (Shirinsky V.P. et al., 1989). We exposed confluent monolayers of both BAE and BSM cells to steady laminar fluid shear stress of 15 dyn/cm^2 for 24 hr. Figure 4.17 shows that although BAE cells changed shape and alignment as previously reported, BSM cell shape and direction were not affected by shear. This finding suggests that endothelium appears, at least at the morphological level, to be more responsive or sensitive to shear forces than smooth muscle.

4.4.3 Elevated shear stress induces actin stress fibers and, at high magnitude, β -actin mRNA

It has previously been shown that shear stress caused an increase in actin stress fiber number and their coalescence into actin cables in HUVE cells (Franke R. et al., 1984). These changes are thought to be responsible for resisting shear forces

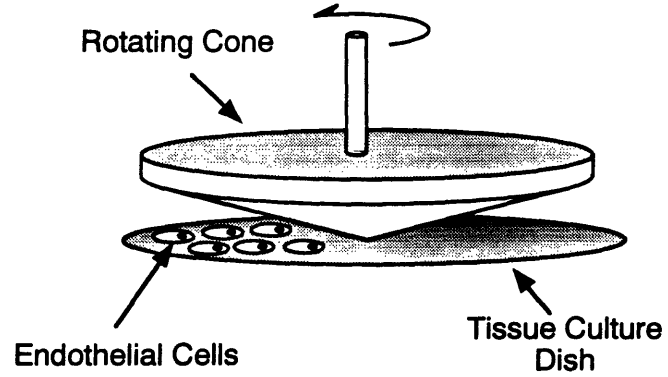
(Wechezak A.R. et al., 1989) and preventing endothelial cells from being sloughed off in response to flow. We were able to visualize the phenomenon in the present device using BAE cells exposed to 24 hr of shear stress at 15 dyn/cm² (figure 4.18). In addition, when exposing confluent BAE monolayers to elevated shear, we observed that part of the increase in actin stress fibers was also accompanied by an increase in the content of β -actin mRNA, particularly in response to elevated magnitude as shown by Northern analysis in figure 4.19 for 25 dyn/cm². Note that mRNA levels of GAPDH remained constant with respect to time as previously described (Malek A. et al., 1992; Malek A.M. et al., 1993a; Malek A.M. et al., 1993b). This finding is the first to link shear stress to β -actin regulation at the mRNA level, and underlines the inadequacy of using β -actin as an internal control for RNA loading in shear studies. Densitometry of Northern blot analysis determined the time course of β -actin mRNA levels normalized with respect to GAPDH at 15, 25 and 36 dyn/cm² (figure 4.20). Note that β -actin mRNA is only elevated at the shear stress magnitudes that are higher than 15 dyn/cm². This response is qualitatively similar to the increase in t-PA (Diamond S.L. et al., 1990) and bFGF (Malek A.M. et al., 1993a) mRNA expression that are markedly induced at higher magnitudes of shear stress (>15 dyn/cm²) (see later chapters).

4.4.4 Shear stress of physiological magnitude decreased rate of DNA but not RNA synthesis

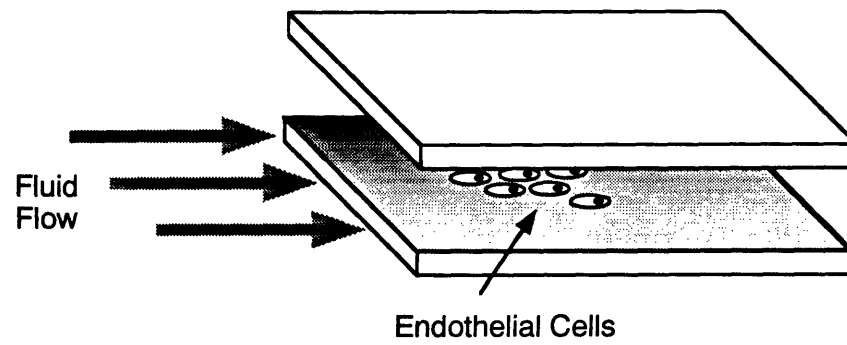
Exposing confluent monolayers to steady laminar fluid shear stress of 15 dyn/cm² (moderate shear) and 36 dyn/cm² (elevated shear) for 6 hr followed by labeling with tritiated thymidine or uridine indicated that shear stress significantly reduced DNA synthesis rates; similar results were obtained by Nerem et al.

(Levesque et al., 1990). RNA synthesis rates were not, however, affected significantly (figure 4.21).

A) Cone-Plate Viscometer



B) Parallel-Plate Viscometer



C) Capillary Tube Viscometer

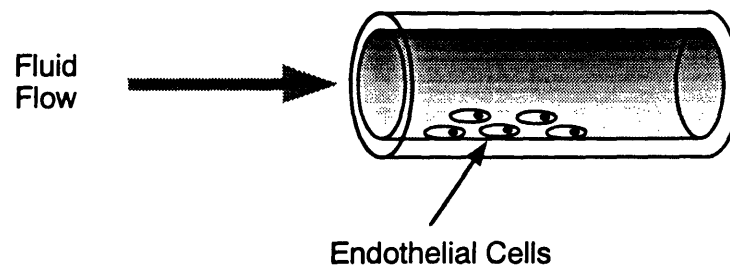


Figure 4.1 Three types of viscometers used to apply shear stress.

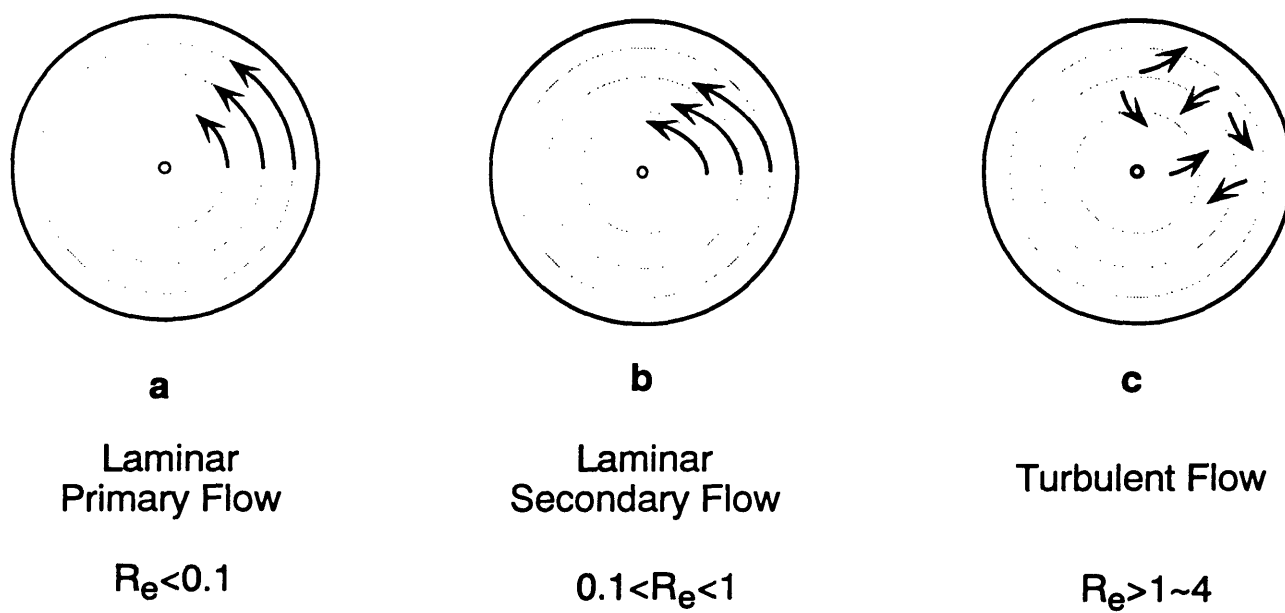


Figure 4.2 Flow line analysis at the level of the baseplate in a cone-plate device.

Parts Description

- | | |
|-----|---|
| 12. | Cone |
| 13. | Cone recess |
| 14. | Tip of Cone made of low friction material |
| | |
| 20. | Shaft that attaches to Cone |
| 21. | Base of shaft which contains screws for connection to cone recess |
| 22. | Screws that attach shaft to cone |
| 24. | Set screw for adjusting the degree of wobble in cone |
| | |
| 30. | Coverplate to which the bearing housing is attached and which fits on top of the tissue culture plate |
| 32. | Circular slot into which the lip of the tissue culture plate fits |
| 34. | Hole through coverplate |
| 36. | Screws for holding bearing housing to coverplate |
| 38. | Drilled depression for aeration |
| | |
| 40. | Housing for Ultra-High precision bearings |
| 42. | Ultra-High Precision Bearings |
| | |
| 50. | Baseplate |
| 52. | Tissue Culture Plate |
| 53. | Groove of tissue culture plate |
| 54. | Recess in baseplate to accept tissue culture plate |
| 55. | Lip of Tissue Culture Plate |
| 56. | Circular slot in Baseplate to accept groove of tissue culture plate |
| 58. | Clamps that press coverplate down |
| | |
| 60. | Shaft for motor assembly |
| 62. | Nut to provide friction for adjusting height of motor assembly |
| 64. | Gearbox |
| 66. | Motor |
| 68. | Flexible coupling that connects the motor drive to the cone shaft |

Figure 4.3 Parts description of cone-plate apparatus.

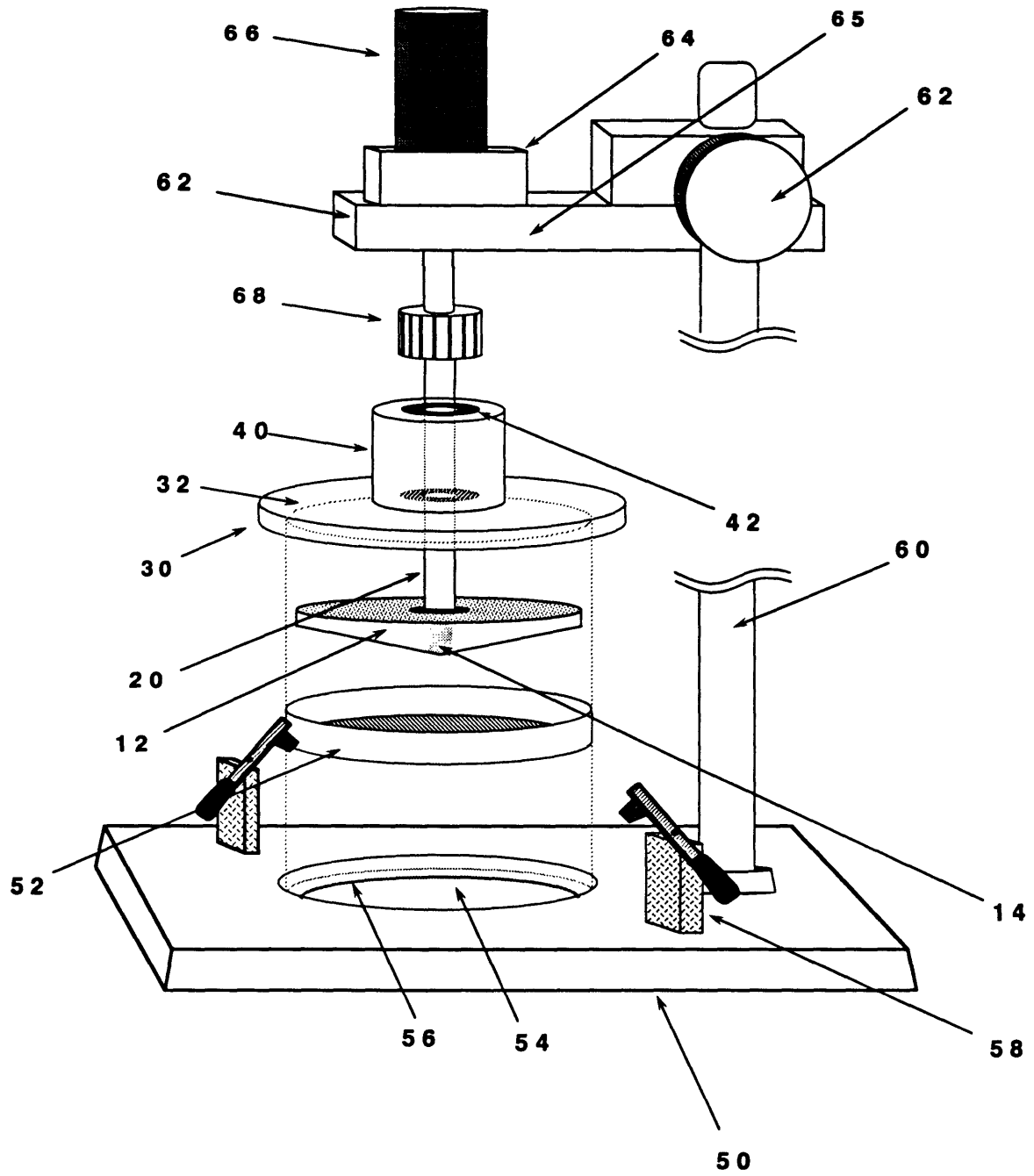


Figure 4.4 Perspective view of cone-plate apparatus.

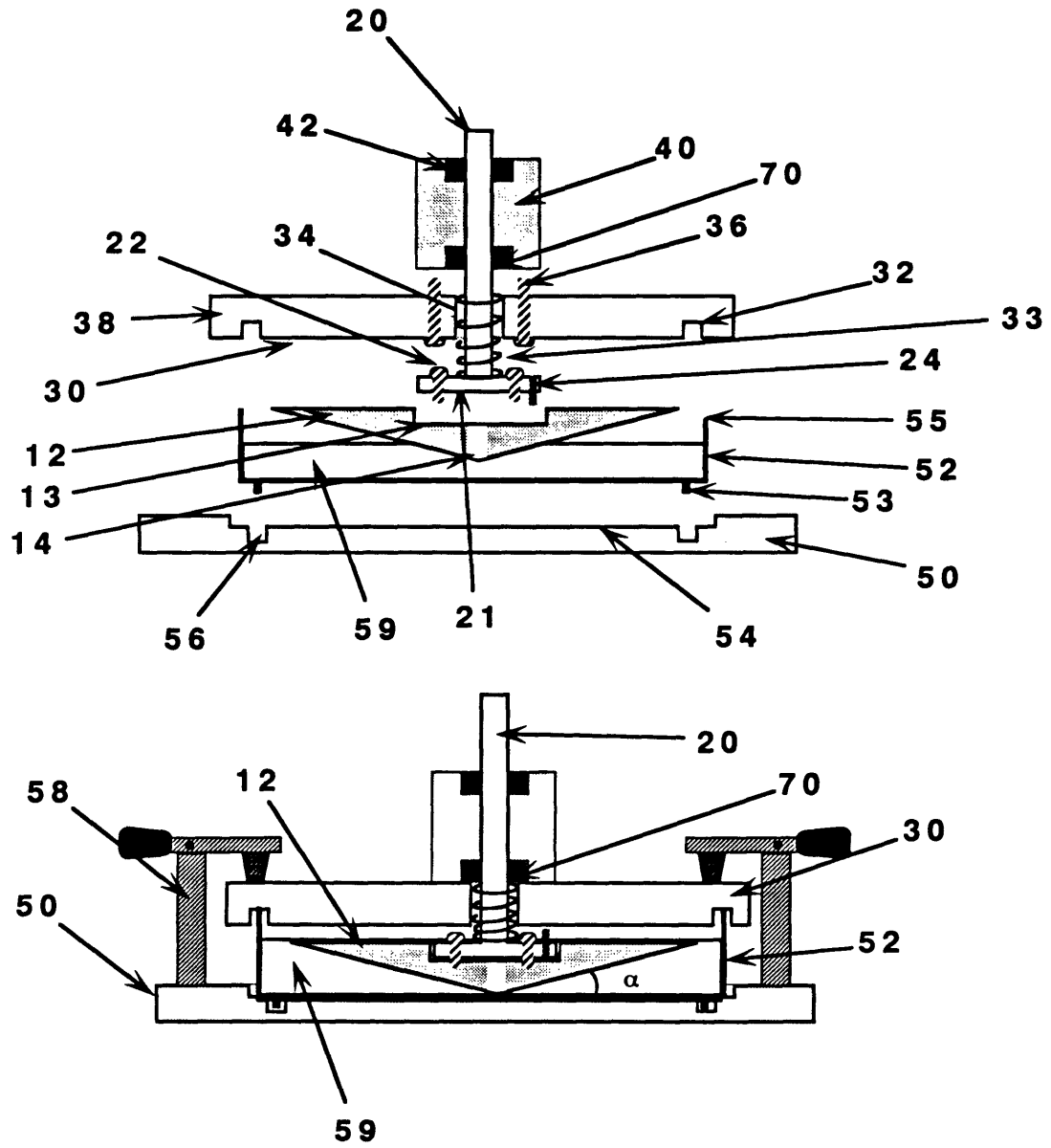


Figure 4.5 Cross-sectional view of the cone-plate apparatus.

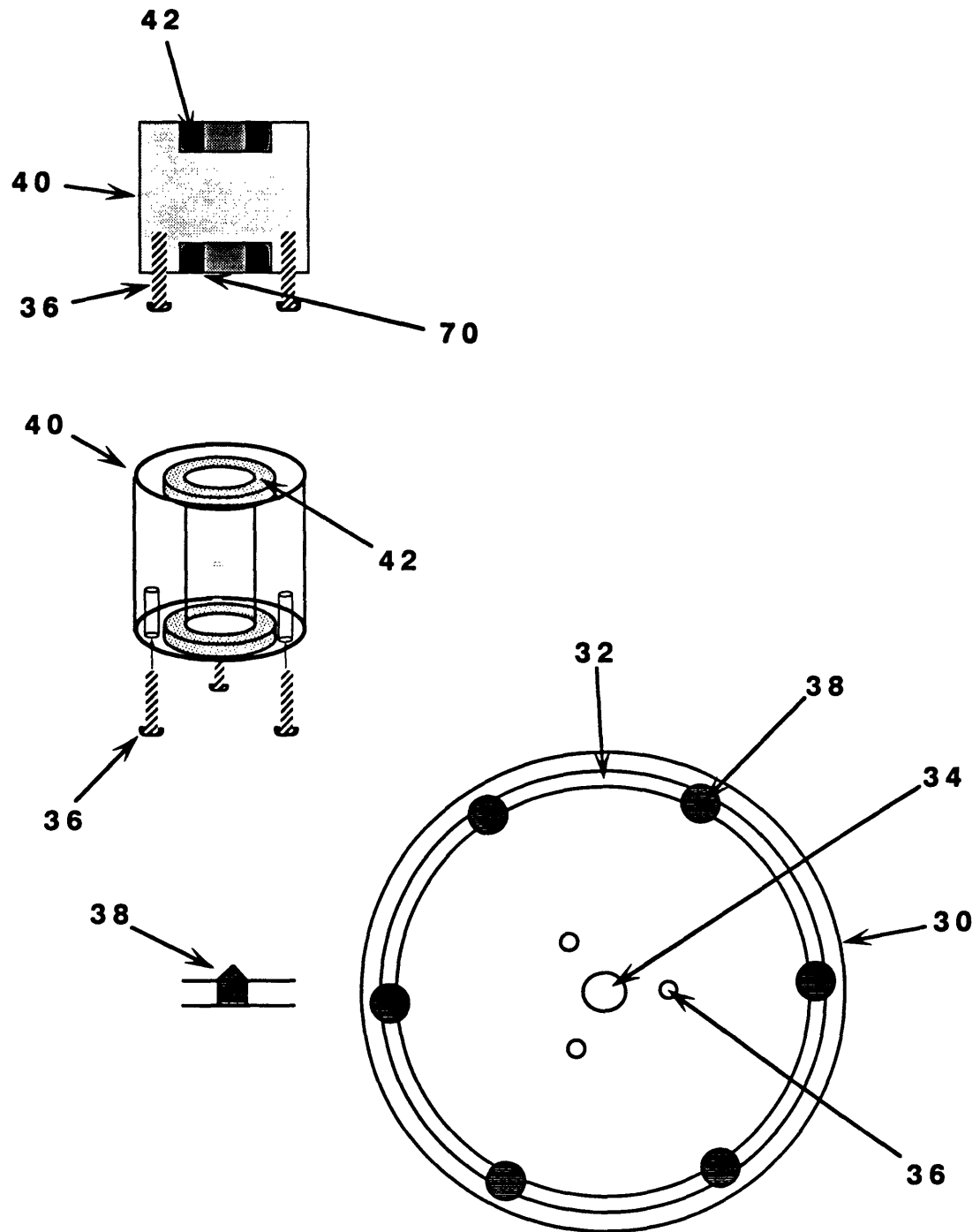


Figure 4.6 Individual part description of cone-plate device.

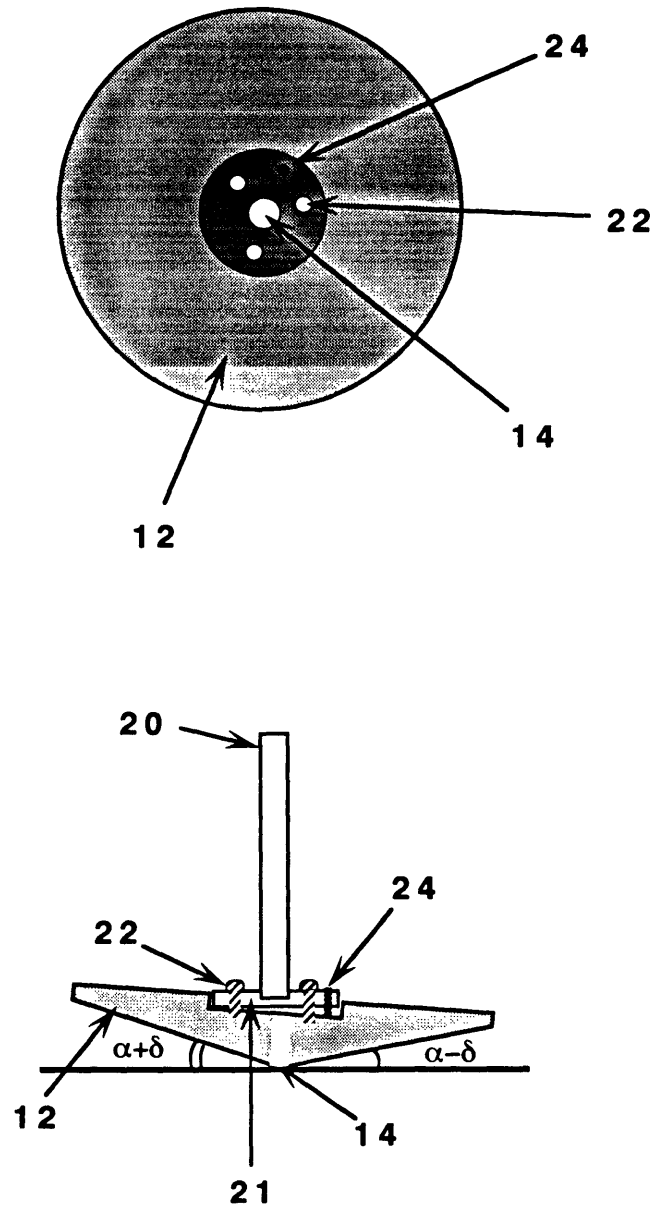


Figure 4.7 Detailed view of the cone-shaft.

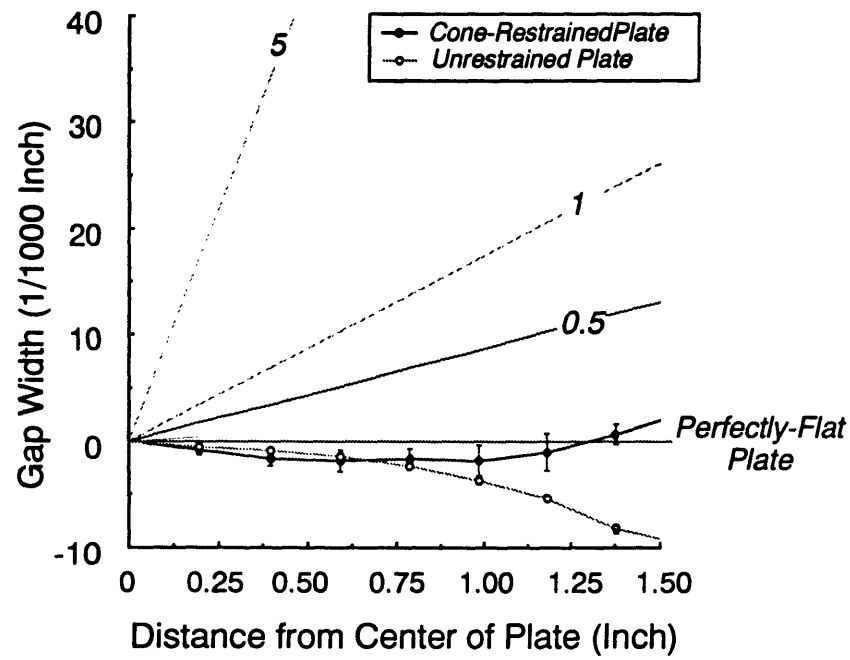
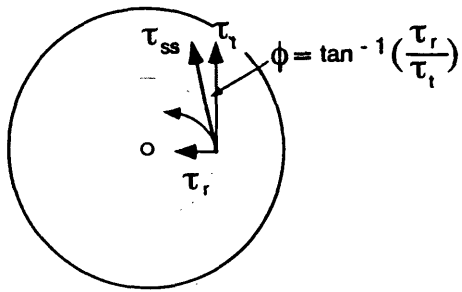


Figure 4.8 Illustration of gap between cone and plate.

A



B

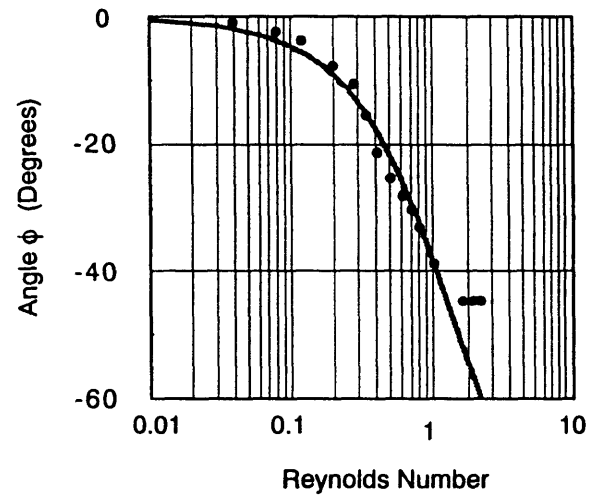


Figure 4.9 Ink flow-line analysis of cone-plate device.

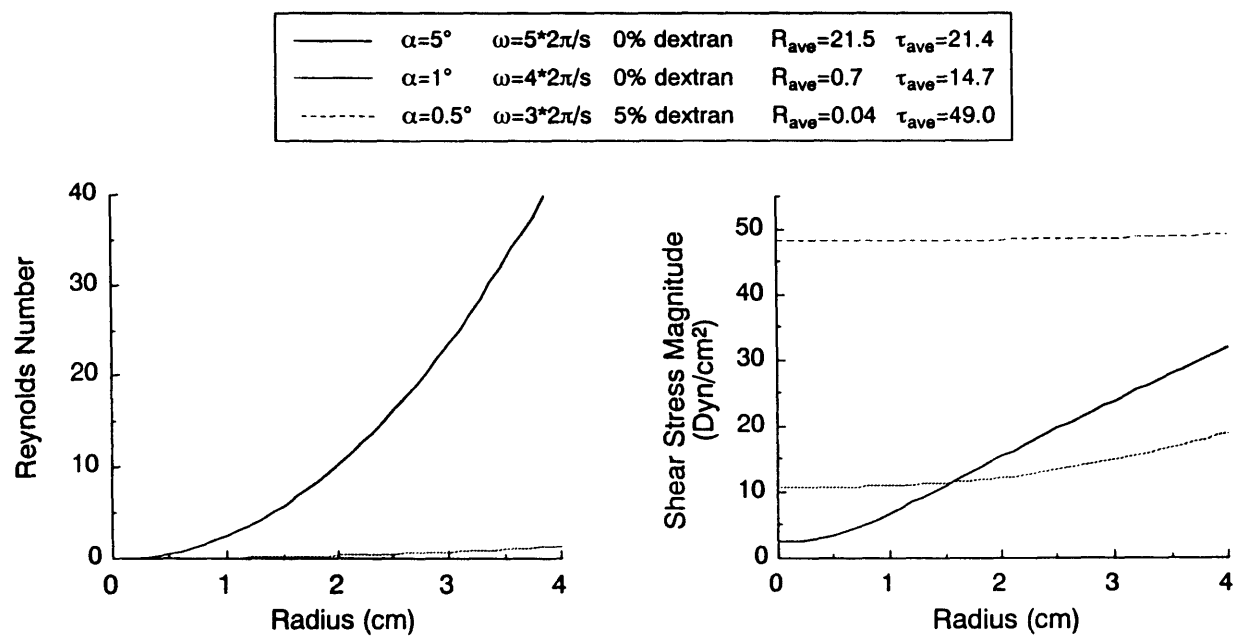


Figure 4.10 Typical Reynolds number and shear stress magnitude profiles.

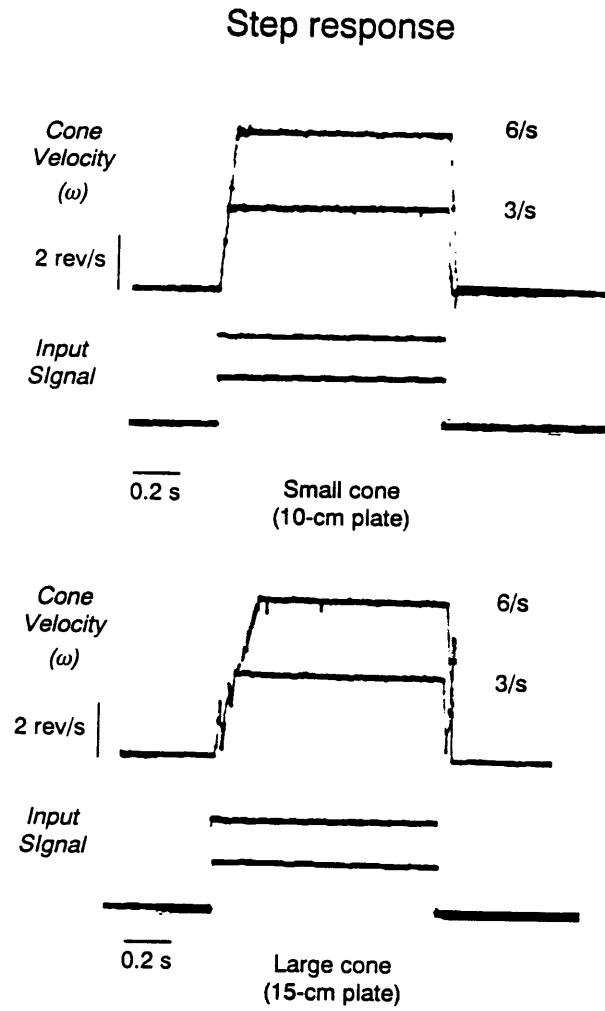


Figure 4.11 Step response analysis of cone-plate apparatus.

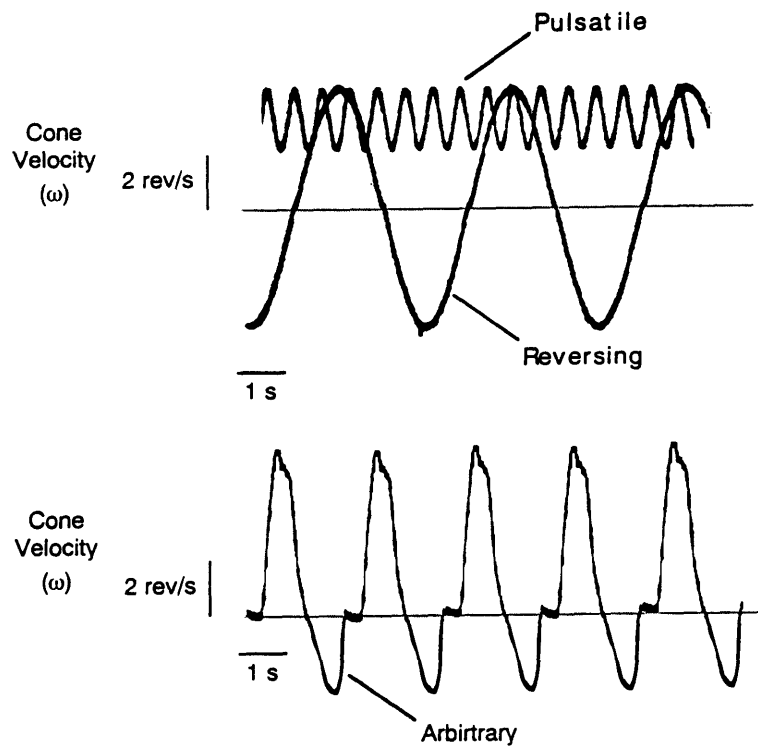


Figure 4.12 Sinusoidal and arbitrary cone velocity profiles.

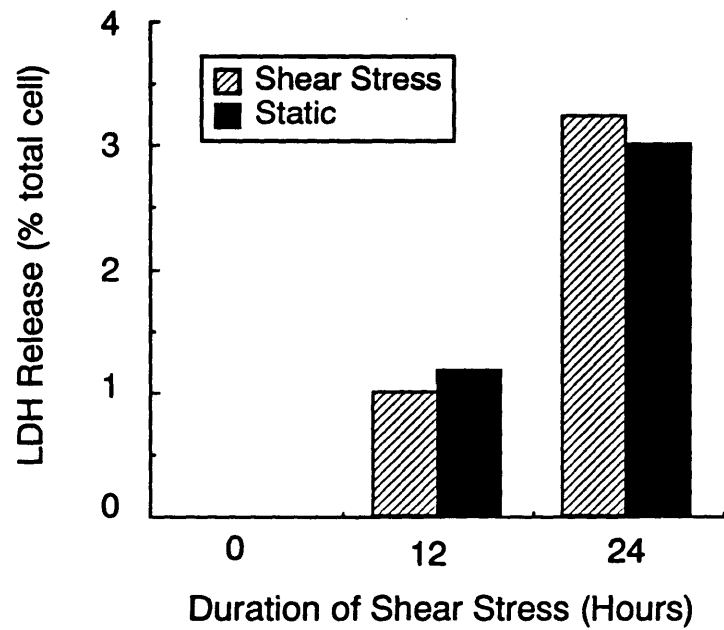
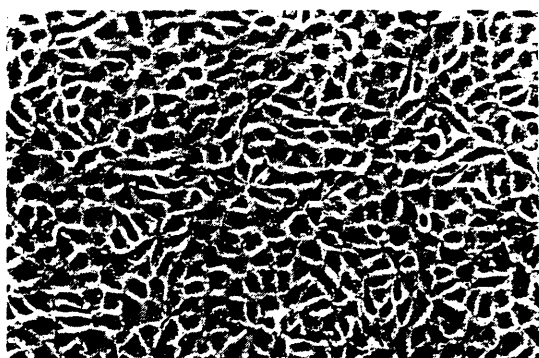
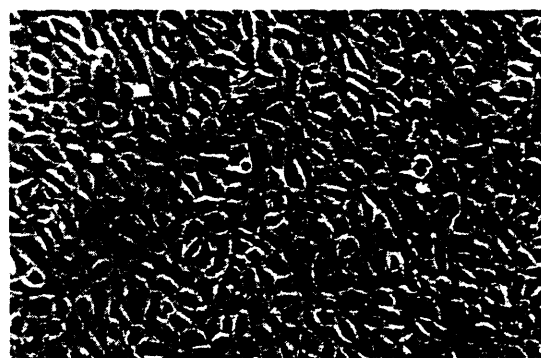


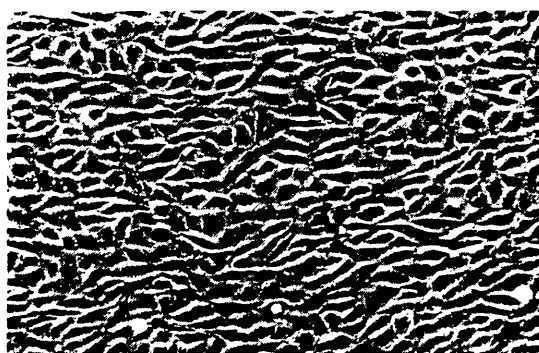
Figure 4.13 Lack of increase of intracellular LDH release.



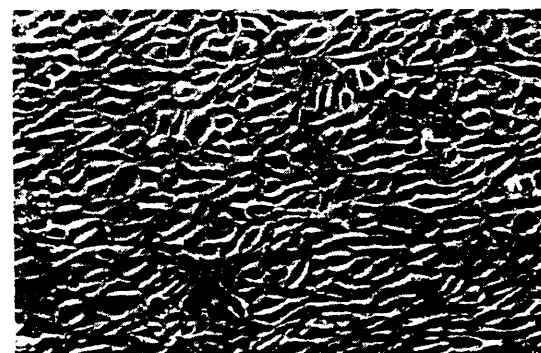
0 Hrs.



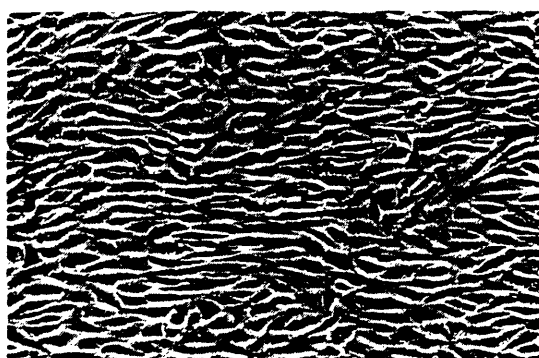
3 Hrs.



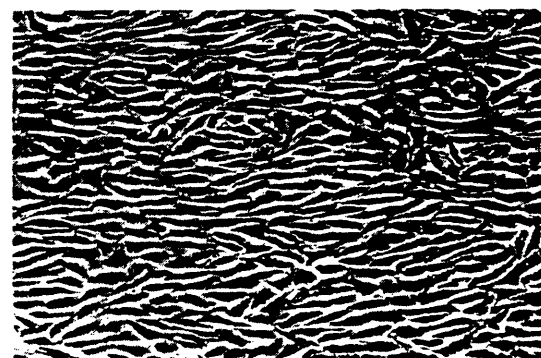
6 Hrs.



12 Hrs.



18 Hrs.



24 Hrs.

Figure 4.14 Phase-contrast micrographs of BAE monolayers under shear.

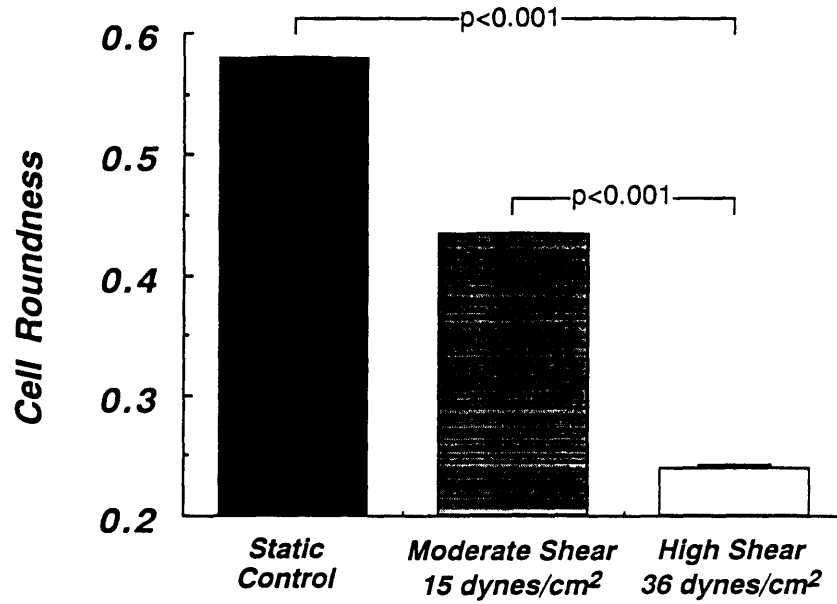


Figure 4.15 Increased cellular elongation in response to shear stress.

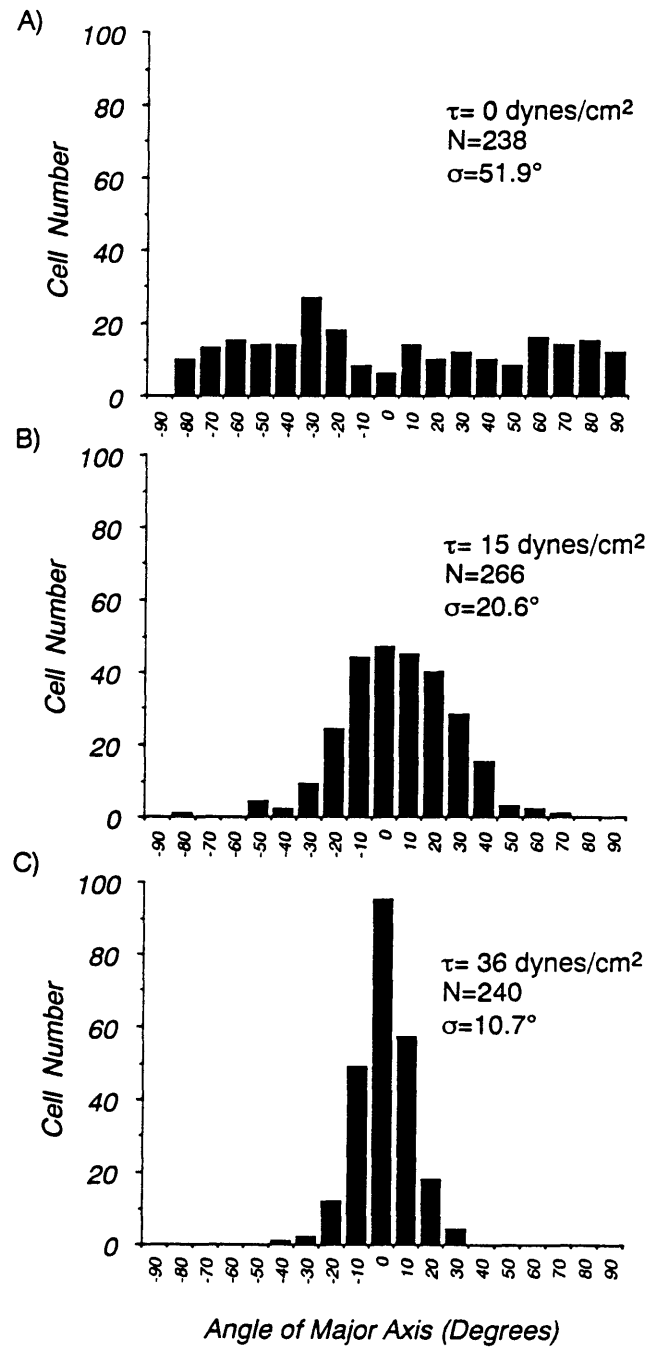


Figure 4.16 Change in distribution of angle of orientation in BAE cells under shear.

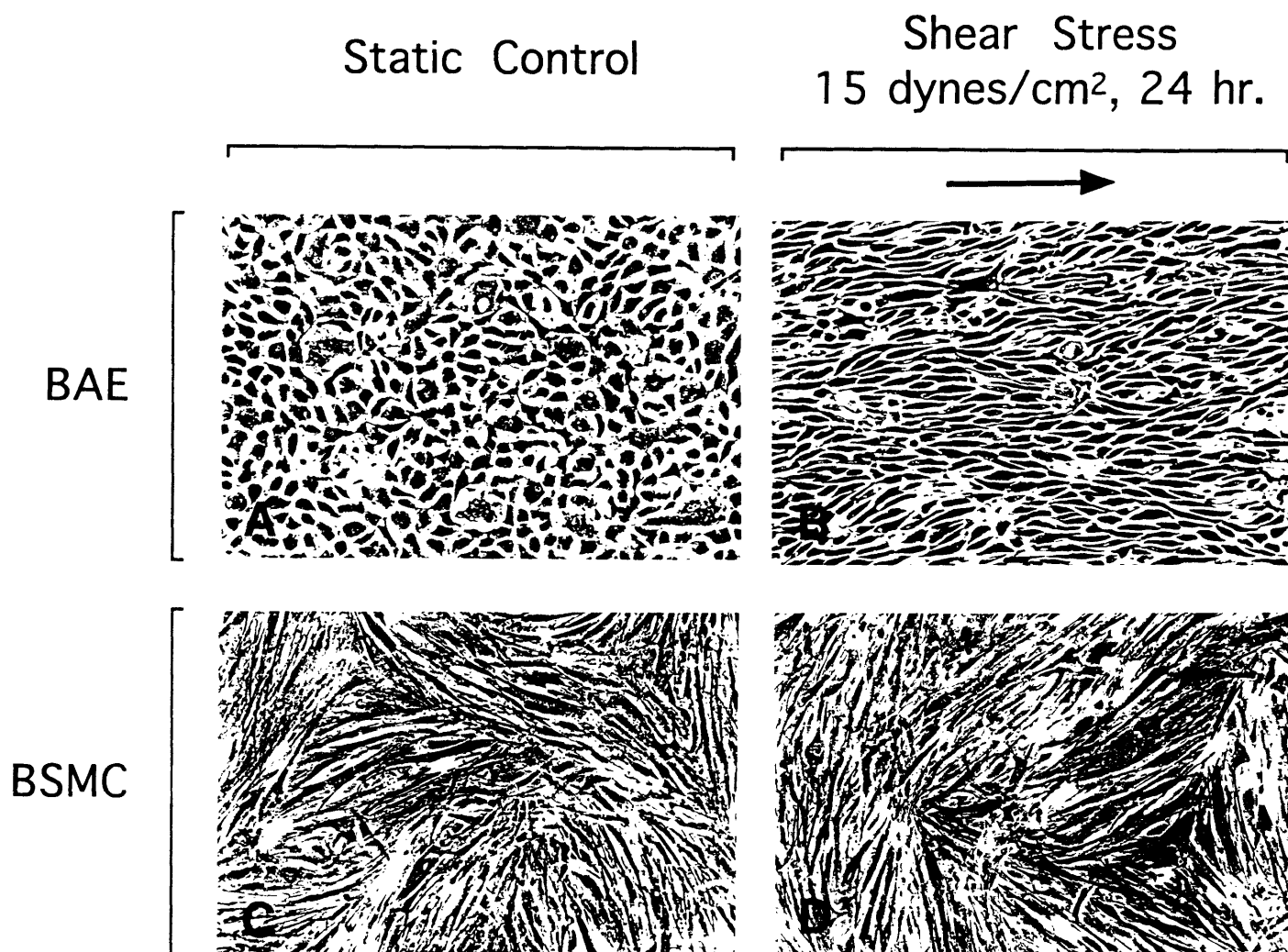
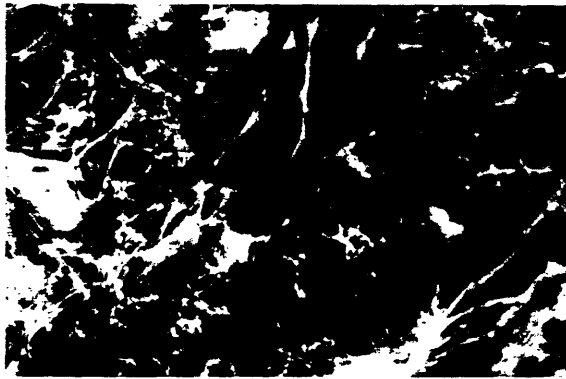


Figure 4.17 Lack of morphological response in BSM cells under shear.

Static
Control



Shear
Stress

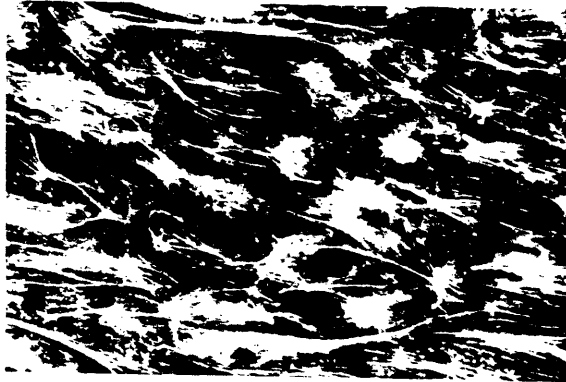


Figure 4.18 Induction of actin stress fibers under shear stress.

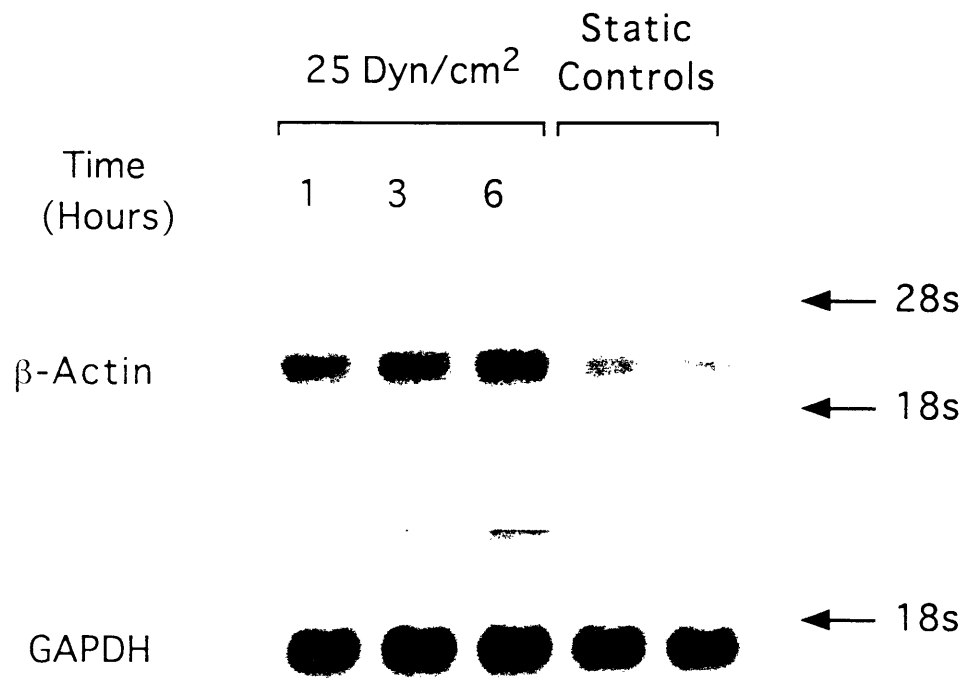


Figure 4.19 Induction of β -actin mRNA increase in response to shear.

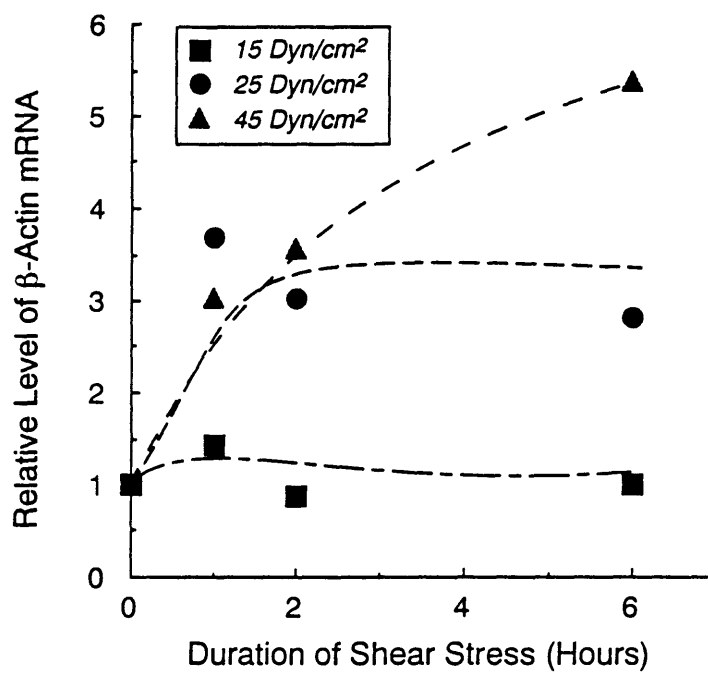


Figure 4.20 Densitometric analysis of β -actin mRNA increase.

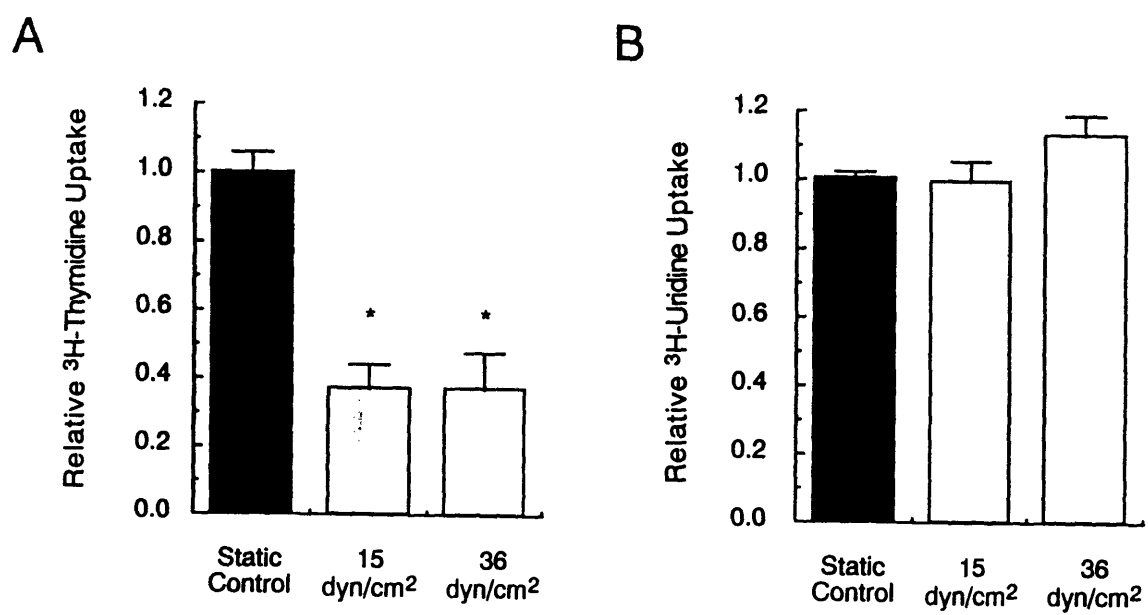


Figure 4.21 Alteration in DNA and RNA synthetic rates in response to shear stress.

CHAPTER 5

Regulation of Endothelin-1 by Fluid Shear Stress *in Vitro*

Given the important role played by the endothelial cell in the regulation of vessel tone (reviewed by Rubanyi G.M. et al., 1991), the previously described effects of flow on PGI₂ and EDRF release, and the potency of the novel vasoconstrictor endothelin-1, a study was undertaken to evaluate the effects of shear stress on ET-1 expression.

5.1 Endothelin-1, a potent vasoconstrictor and paracrine growth factor

Among the potential effectors that may be important in modifying structure in response to external mechanical forces, endothelin-1 (ET-1), a 21-amino acid peptide produced by the endothelium (Yanagisawa M. et al., 1988) (figure 5.1), has been shown to be the most potent vasoconstrictor described to date and can induce *c-fos*, *c-myc*, mitogenesis in smooth muscle cells and fibroblasts (Muldoon L.L. et al., 1989), and hypertrophy in the cardiac myocyte (Shubeita H.E., 1990; Simonson M.S. et al., 1991). ET-1 was originally isolated from the supernatant of endothelial cells maintained in culture, was sequenced and found to contain two disulfide bonds, and to be the member of a new family of peptides that are related to neurotoxins affecting voltage-dependent Na⁺ channels (Yanagisawa M. et al., 1988). Although initially thought to be secreted exclusively by the endothelial cell, it has since been shown to be expressed in other cell types (MacCumber M.W. et

al., 1990) as well as in fetal but not adult tissues of the lung spleen and pancreas (Haegerstrand A. et al., 1989). ET-1 is proteolytically cleaved from a preproendothelin-1 peptide to yield BigET-1 and further cleaved to the 21-residue ET-1 (figure 5.1). Both ET-1 mRNA expression and release have been shown to be induced by thrombin, TGF- β , Angiotensin II, calcium ionophore, and IL-1 (Rubanyi G.M. et al., 1991; Simonson M.S. et al., 1991).

Since few secretory granules are found in endothelium, and since endothelial cell lysates do not possess vasoconstrictor activity (Simonson M.S. et al., 1991), it is thought that ET-1 is constitutively secreted into the exterior. *In situ* hybridization has suggested that ET-1 mRNA is found in close association with its target tissues (MacCumber M.W. et al., 1989). Recent work (Yashimoto S. et al., 1991) has demonstrated that release of ET-1 is preferentially towards the basement membrane side and not the luminal side of the vessel. These findings, taken together, make ET-1 an excellent candidate for the local regulation of vascular tone and structure via its effect on smooth muscle and fibroblast cells of the vessel wall.

5.2 Regulation of endothelin-1 by fluid shear stress

5.2.1 Fluid shear stress of physiological magnitude downregulates ET-1 mRNA prior to cell shape change

In order to explore the effect of fluid shear stress on ET-1 mRNA levels in endothelium, confluent monolayer of BAE cells last fed growth medium containing 10% calf serum 24-48 hr prior to onset of stimulus, were subjected to fluid shear stress in the cone-plate viscometer using a 1° cone at 4 rev/sec (corresponding to $\tau=15 \text{ dyn/cm}^2$ and $R_{ave}=0.69$) for increasing times. The magnitude of 15 dyn/cm^2 was chosen as a starting point since it is the average value in the arterial network

and would be of appropriate and physiological significance. Total RNA was isolated (cf. Appendix) and analyzed by Northern blotting with a radiolabelled cDNA probe for bovine ET-1. Figure 5.2 shows that the physiological shear stimulus induced a quick downregulation in ET-1 mRNA, which was specific since mRNA levels of GAPDH were not affected. Densitometry of multiple Northern blots normalized to GAPDH mRNA revealed a sustained 4-5 fold decrease as shown in figure 5.3. This shear-induced downregulation was evident as soon as 1 hr following the onset of shear-stress application and was complete by 2 to 4 hr. The change in ET-1 mRNA occurred prior to any observable changes in the shape of the endothelium as seen by phase-contrast microscopy (compare figure 5.3 to figure 4.14) and persisted following cell-shape changes.

5.2.2 ET-1 mRNA downregulation appears to be the result of shear stress, not flow

Supplementation of the growth medium with 5% uncharged dextran to induce a 2.5 fold increase in kinematic viscosity allowed the use of a lower rotational velocity of the cone ($\omega = 3$ vs. 4 rev/s) (figure 5.4, left panel), and thus a correspondingly lower fluid velocity on top of the BAE monolayer while achieving a higher level of shear stress (17 vs. 14 dyn/cm²). The results using 5% dextran at the higher level of shear stress but at a lower fluid velocity showed the same ET-1 downregulation phenomenon, occurring with a similar time course and to an even greater extent. This finding strongly suggests that it is the shear stress rather than fluid velocity which is the factor responsible for inducing the downregulation of ET-1 mRNA. This is in contrast to the convective-diffusive effect recently reported by Mo et al. (Mo M. et al., 1991) (Dull R.O. et al., 1991) on changes in free cytoplasmic $[Ca^{2+}]_i$ in response to applied ATP. The finding of endothelial

functional and biochemical changes prior to cellular shape changes is similar to that of Franke et al. (Franke R. et al., 1984) who have documented actin stress fiber changes as soon as 3 hr following onset of low-magnitude shear stress, before the appearance of any cell-shape changes.

5.2.3 Shear-induced ET-1 mRNA decrease is independent of serum content in culture medium

In order to assess the importance of serum concentration in the culture medium on the downregulation of ET-1 by fluid shear stress, cells were fed with low serum (0.5%) and serum-free (0%) media prior to exposure to the onset of the experiment. Shear stress induced strong ET-1 mRNA downregulation in these cells that was similar to the one observed with cells grown in 10% calf serum (data not shown). The occurrence of the phenomenon at 0% calf serum allowed us to make use of this condition for most of the pharmacological experiments described in chapters 8 and 9.

5.2.4 Physiological fluid shear stress reduces ET-1 peptide secretion

To determine whether the decrease in ET-1 mRNA was also accompanied by decreased ET-1 secretion by the endothelial cells, aliquots of supernatant from BAE cells that were fed with fresh media containing 10% calf serum at the onset of shear ($\tau=15$ dyn/cm²) were collected and ET-1 immunoreactive peptide measured using a radioimmunoassay kit (cf. Appendix). Figure 5.5 shows that cells exposed to shear stress secreted significantly lower levels of ET-1 peptide at 24 and 48 hr compared to controls maintained under static conditions.

5.2.5 ET-1 downregulation by shear stress is a reversible process

It is important to determine whether the ET-1 decrease by shear stress is a one-time event or whether it is a reversible process. To address the question, BAE cells were exposed to shear stress for six hours to induce ET-1 mRNA downregulation. Following the 6 hr stimulus period, shear was halted and the cells left under stationary conditions for different times at the end of which total RNA was harvested and analyzed. Densitometric analysis of ET-1 mRNA normalized with respect to GAPDH mRNA showed that the shear-induced downregulation of ET-1 was a reversible process that returned nearly completely to pre-stimulus levels by six hours after the cessation of shear although there was some variability between experiments in the speed of recovery. Some experiments showed complete, while other exhibited only partial, recovery (~50%) by six hours. Figure 5.6 is the average of four separate experiments. The finding of reversibility is important since it lends credence to the hypothesis that ET-1 regulation by shear stress may be a participant in a negative-feedback loop for the control of vessel caliber.

5.2.6 ET-1 downregulation is dependent on fluid shear stress magnitude

Since endothelial cells in the circulation are exposed to a wide spectrum of shear magnitudes, determining the effect of shear stress magnitude on ET-1 downregulation is critical. The level of ET-1 mRNA was determined by Northern analysis and densitometry following the application of 4 hr of shear-stress of increasing magnitude (figure 5.7). The magnitude-response curve showed a slight and non-significant decrease at shear-stress magnitude of 3 dyn/cm² and a steep sigmoidal shape with an asymptote above 15 dyn/cm². This indicates that ET-1 mRNA is downregulated at physiological shear stress levels and that cells exposed to shear stress levels less than 15 dyn/cm² have a higher level of ET-1 mRNA. It

also suggests that the response is not an all-or-none (binary) process or one characterized by a threshold beyond which complete down-regulation is observed, but is rather a graded one. Interestingly, the saturation at shear stress levels above 15 dyn/cm² is similar to the saturation observed by Olesen et al. in the shear-induced outward potassium current (Olesen S. et al., 1988). Perhaps of equal importance is the fact that the magnitude-response curve saturates at magnitudes above the average value of shear in the arterial circulation. Experiments conducted at the higher shear stress of 45 dyn/cm² after 6 hr of shear (using 5% dextran) also showed similar 4-5 fold decrease.

In conclusion, ET-1 mRNA and peptide levels of BAE monolayers are decreased significantly by physiological levels of fluid shear stress in a time- and dose-dependent fashion, exhibiting saturation above 15 dyn/cm² by a process that is reversible and appears not to be linked to cell shape *per se*. The sensitivity of this process to different shear stress regimes will be addressed next, and the putative second messenger and the transduction mechanism in chapters 8 and 9.

5.3 Importance of the dynamic character of the shear stimulus on the downregulation of ET-1

Given the time-varying characteristics of shear stress in the human body, it was deemed important to determine the effect of varying the dynamic content of the shear stress stimulus on the gene expression changes.

5.3.1 Turbulent flow

A number of pathological situations in the vasculature, including atherosclerosis, are commonly justified as being the result of turbulent blood flow and its potential injurious effect on the vessel wall. Frankly turbulent flow, is

however not encountered in the healthy human and is only rarely seen in cases of severe stenosis (Goldsmith H.L. et al., 1986). The pioneering work of Davies et al. (Davies P.F. et al., 1986) showed however that BAE monolayers exposed to turbulent, but not laminar, shear stress entered the cell cycle and exhibited increased DNA synthesis rates. It is with this background of anecdotal *in vivo* data and the definite demonstration of importance of turbulent shear on cell cycle that the effect of non-laminar shear was investigated .

5.3.2 Turbulent shear is indistinguishable from laminar shear in down-regulating ET-1

Turbulent shear stress was achieved by using a 5° cone (cf. Appendix). This resulted in an average shear stress magnitude of 15 dyn/cm² and average Reynolds number of 17 on the BAE monolayer. Figure 5.8 shows BAE cells exposed to fluid shear stress of magnitude 15 dyn/cm² for 18 hr in the laminar and in the turbulent regimen. The shape of the cells exposed to turbulent flow is closer to control cells than to cells exposed to steady laminar shear stress, but it does show a mild alignment in the general direction of the flow. The densitometric analysis of a number of experiments is shown in figure 5.9. The data indicates that both laminar and turbulent shear stress of magnitude 15 dyn/cm² result in ET-1 mRNA of indistinguishable magnitude. This finding implies, that unlike Davies' data, ET-1 responsiveness to shear is not sensitive to the high frequency time and direction variations of shear as long as an average shear force is of sufficient magnitude. This result is in accordance with Zamir's hypothesis of endothelium acting as a sensor of average shear (Zamir M., 1977).

5.3.3 Pulsatile and sinusoidally reversing shear stress

Since a large proportion of arteries are exposed to pulsatile flow at baseline, it is important to determine the effect of pulsatile shear stress on the endothelial regulation of ET-1. Two methods were devised for exposing the BAE cells to cyclical variations in shear stress while maintaining the same magnitude of shear stress of 15 dyn/cm^2 in order to avoid confounding the effects of average magnitude and the dynamic content of the shear stimulus. Sinusoidally-varying shear stress was obtained in two ways:

a- Pulsatile fluid shear stress of frequency 2.5 Hz and magnitude 12-18 dyn/cm^2 was obtained by introducing a wobble effect at the level of the 1° cone as previously described (Davies P.F. et al., 1983).

b- Reversing sinusoidal fluid shear stress of magnitude $\pm 21 \text{ dyn/cm}^2$ and frequency 0.25 Hz was obtained by varying the angular velocity of the 1° cone, while maintaining the rates of cone rotational acceleration low enough to insure transmission of the shear forces to the tissue culture plate as described by Suter et al. (Sutera S.P. et al., 1988). Notice that the parameters for the two above conditions were chosen so as to maintain the same mean value of the absolute shear stress magnitude as for the laminar and turbulent conditions (15 dyn/cm^2). The time profiles for the various flow regimens used in this chapter are shown schematically in figure 5.10 (the time profile for turbulent shear is simply shown for illustration and is not exact).

The results in figure 5.11 show that pulsatile shear stress of physiological level induces a time-dependent downregulation of ET-1 mRNA that is similar that in response to steady shear stress of same average magnitude. This indicates that the mechanism of shear-induced ET-1 is not sensitive to small variations of physiological frequency in the presence of a mean shear amplitude that is sufficient

to induce downregulation, a result that is comparable to that observed in response to turbulent shear stress.

In contrast, when BAE monolayers were subjected to shear stress of sinusoidally-reversing direction (frequency 0.25 Hz) and magnitude having an absolute square root mean value of 15 dyn/cm² but a total time average value of 0 dyn/cm², ET-1 mRNA expression was not affected. This indicates that the absolute mean magnitude of shear is not the only important determinant of shear stress-induced downregulation, and raises the possibility that the endothelial cell responds only to the time-average value of the shear stimulus beyond a certain frequency. In other words, the process of shear-induced ET-1 mRNA decrease behaves like a low-pass filter structure; such a hypothesis is not unreasonable considering the viscoelastic properties of living cells and tissues (Herman I.M. et al., 1987; Adams D.S., 1992) and is again consistent with Zamir's hypothesis (Zamir M., 1977). This result further argues against the possibility that shear-induced ET-1 downregulation is simply the result of culture media disturbance.

5.3.4 Regulation of ET-1 mRNA by mechanical stimuli is specific to shear stress but not to low-frequency uniaxial strain

To verify that the observed ET-1 mRNA downregulation is not due to some other mechanical stimuli not directly related to shear stress, such as uniaxial strain, BAE cells were subjected to cyclical uniaxial (linear) strain. BAE cells were grown to confluence on Silicone sheet pre-coated with rat-tail type I collagen (cf. Appendix). 36-48 hr following the last feeding with media containing 10% calf serum, confluent cells were mounted on a dynamic stretch apparatus (courtesy of Dr. Thomas Kulik, cf. Appendix) and their substratum linearly stretched by 20% cyclically at a rate of 20/min for varying times followed by lysis for RNA

isolation.. This mechanical stimulus, failed however, to induce a change in ET-1 mRNA (figure 5.12). This result does not rule out possible changes in ET-1 expression at other rates of strain and/or frequency.

5.4 Conclusion

The results shown here indicate that the EC's ET-1 response to shear stress is similar to that of a low-pass filter since small variations in magnitude and direction in the input signal, such as the random variations seen with the turbulent shear or the superimposed sinusoidal signal in the case of the pulatile shear, did not result in a distinguishably different signal when compared to steady laminar shear stress of magnitude 15 dyn/cm². Using reversing shear stress of zero average magnitude and 15 dyn/cm² absolute root mean square values failed however to affect ET-1 mRNA. This is what would be expected from a low-pass structure, since it would simply return the time-average values, in this case the ET-1 response to zero shear. Finally, the ET-1 downregulation response was shown to be specific to shear stress and could not be elicited by membrane strain despite the fact that uniaxial cyclical strain resulted in a very quick re-orientation and spindle-like alignment of the stretched BAE cells perpendicular to the strain direction within 9 hr of the stimulus.

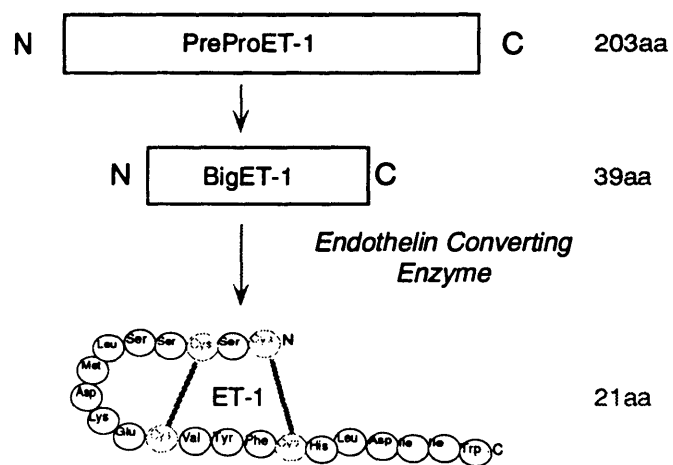


Figure 5.1 Endothelin-1, a potent vasoconstrictor peptide.

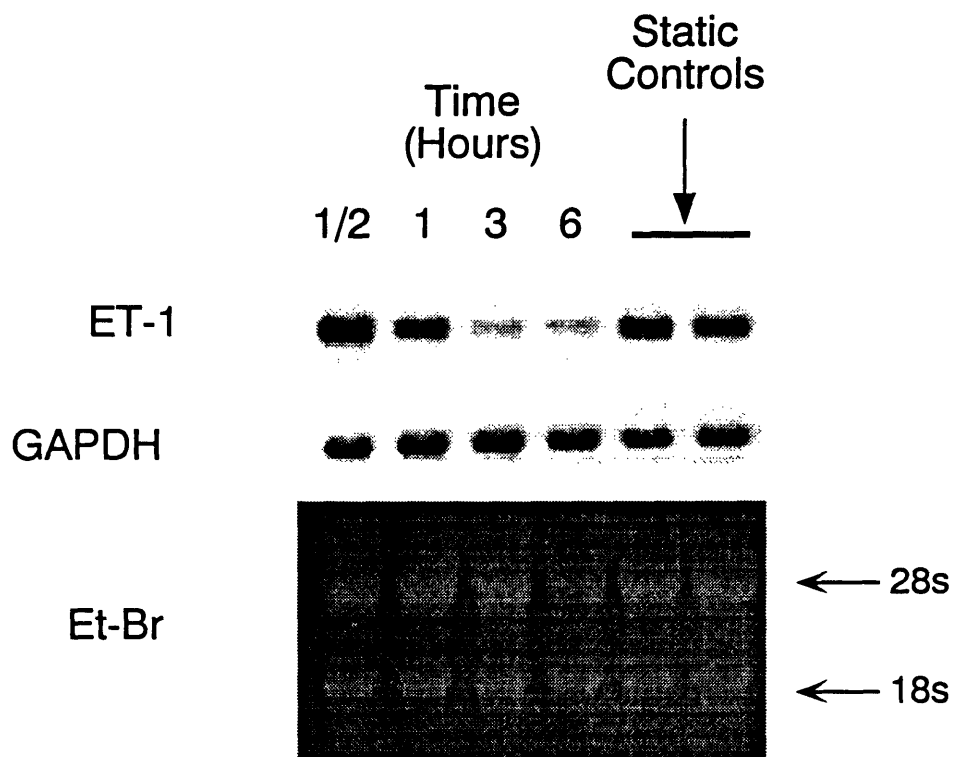


Figure 5.2 Fluid shear stress decreases ET-1 mRNA levels.

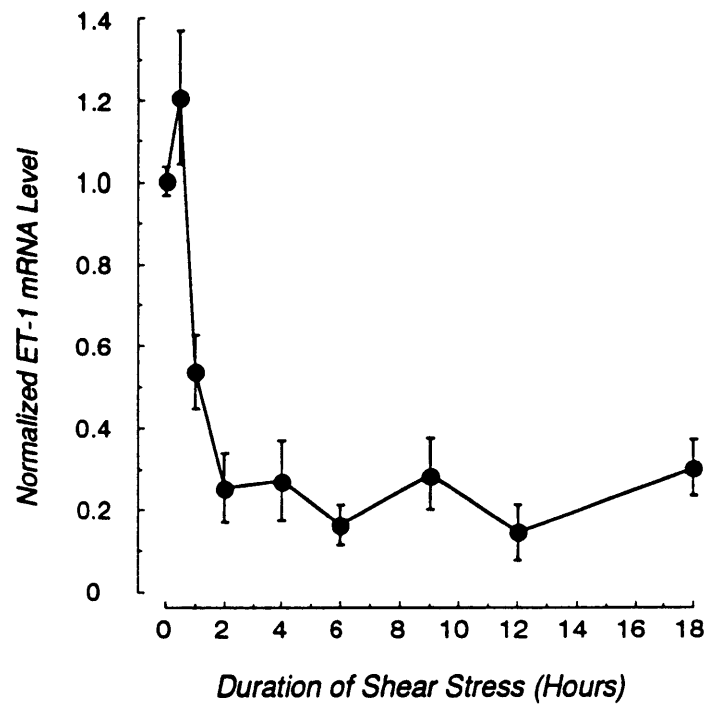


Figure 5.3 Densitometric analysis of ET-1 mRNA under shear stress.

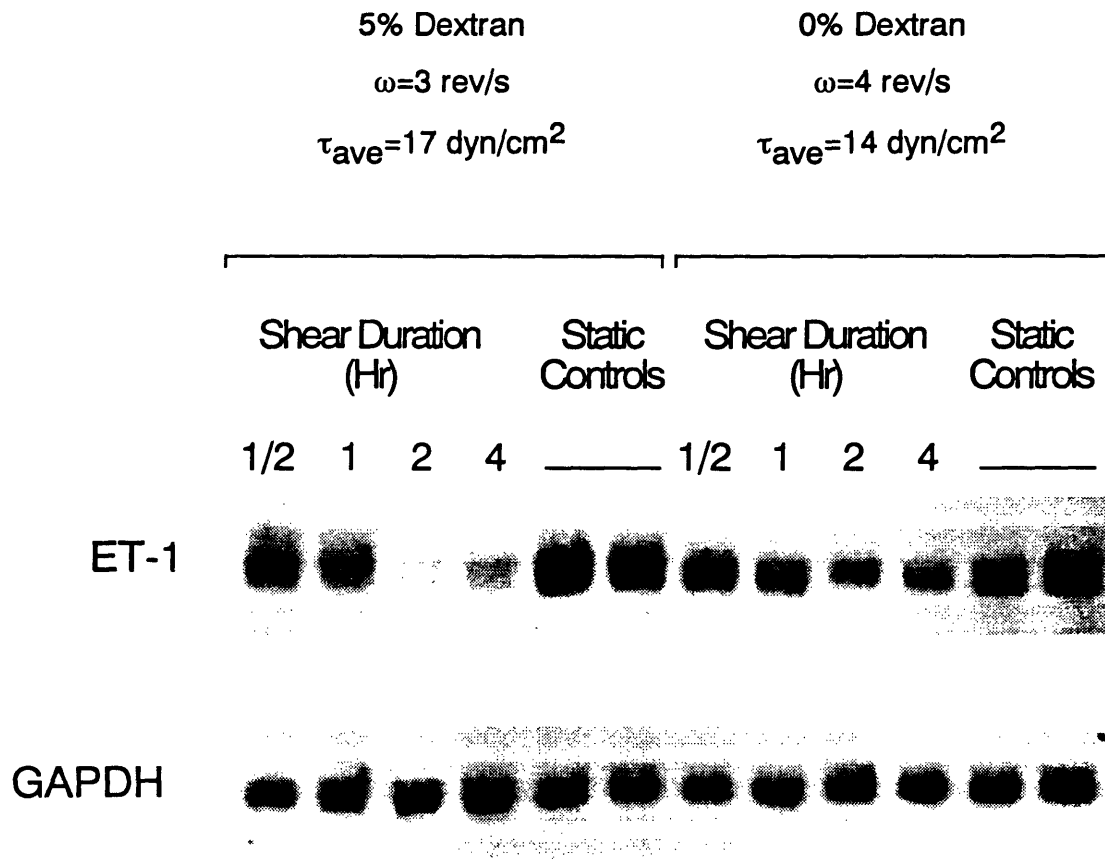


Figure 5.4 ET-1 mRNA is downregulated by shear stress not flow.

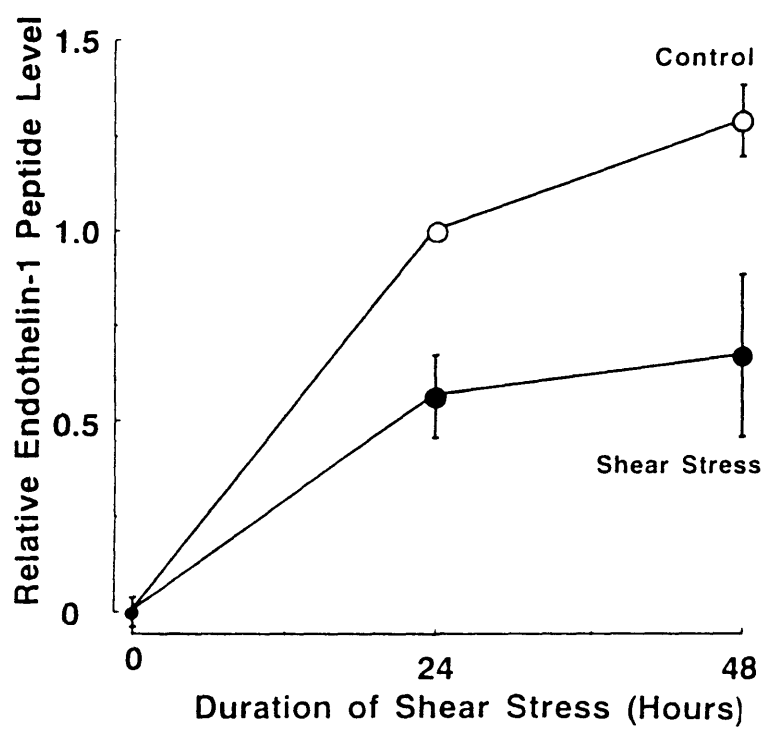


Figure 5.5 ET-1 peptide secretion is also decreased by shear stress.

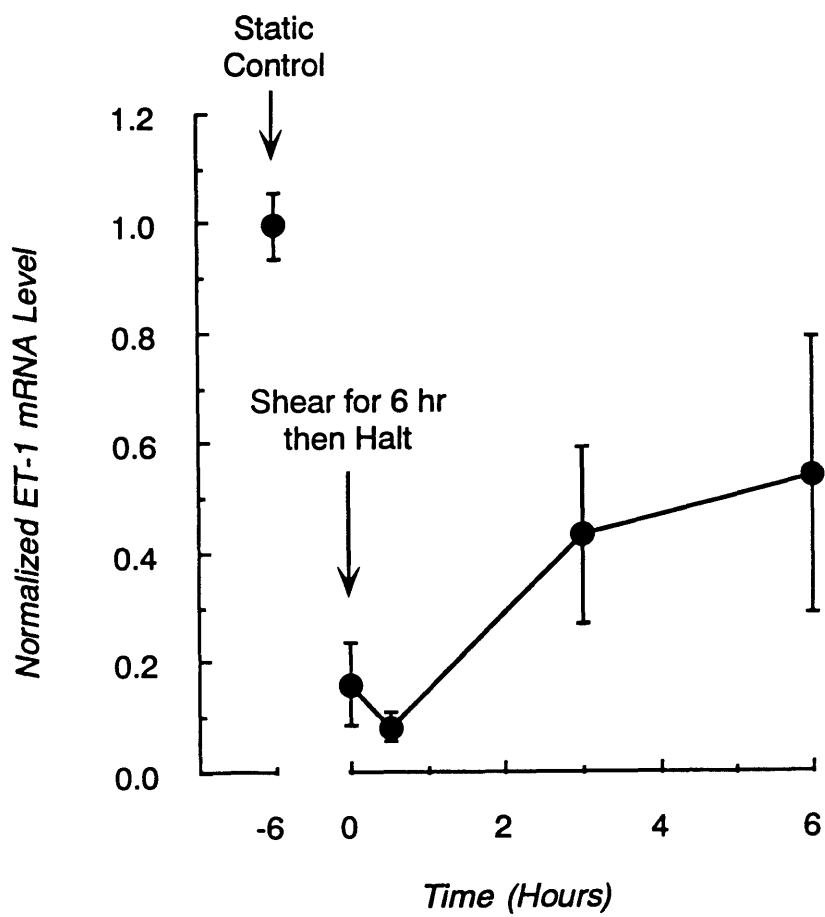


Figure 5.6 Shear-induced ET-1 mRNA decrease is a reversible process.

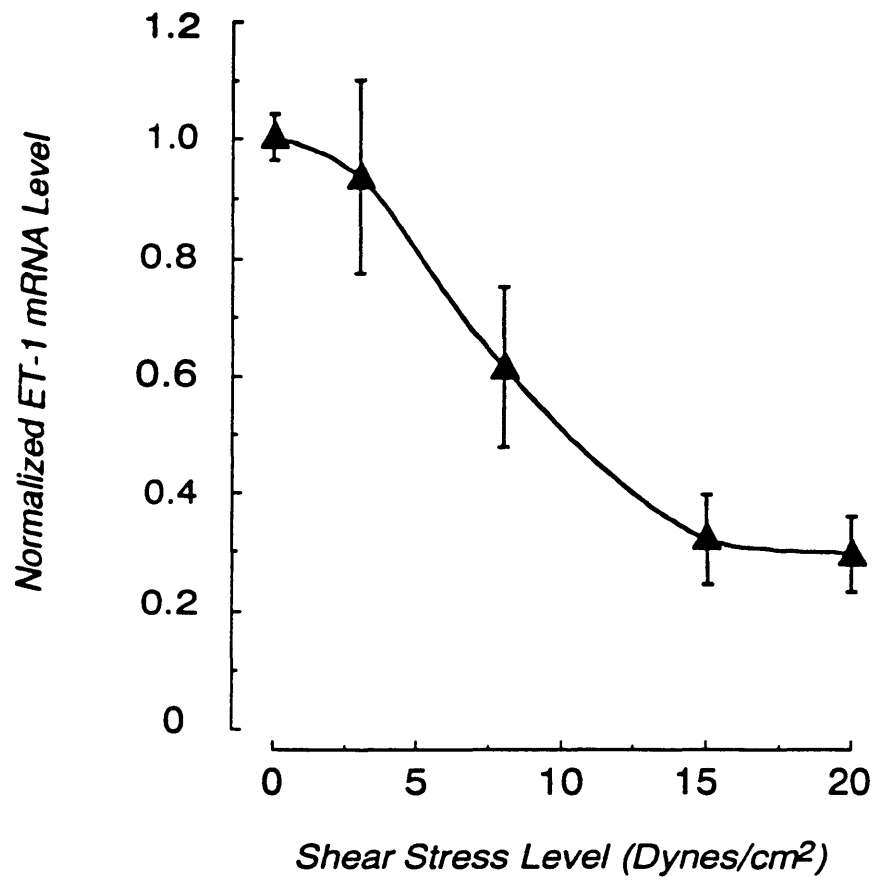


Figure 5.7 Decrease of ET-1 mRNA is dependent on shear magnitude.

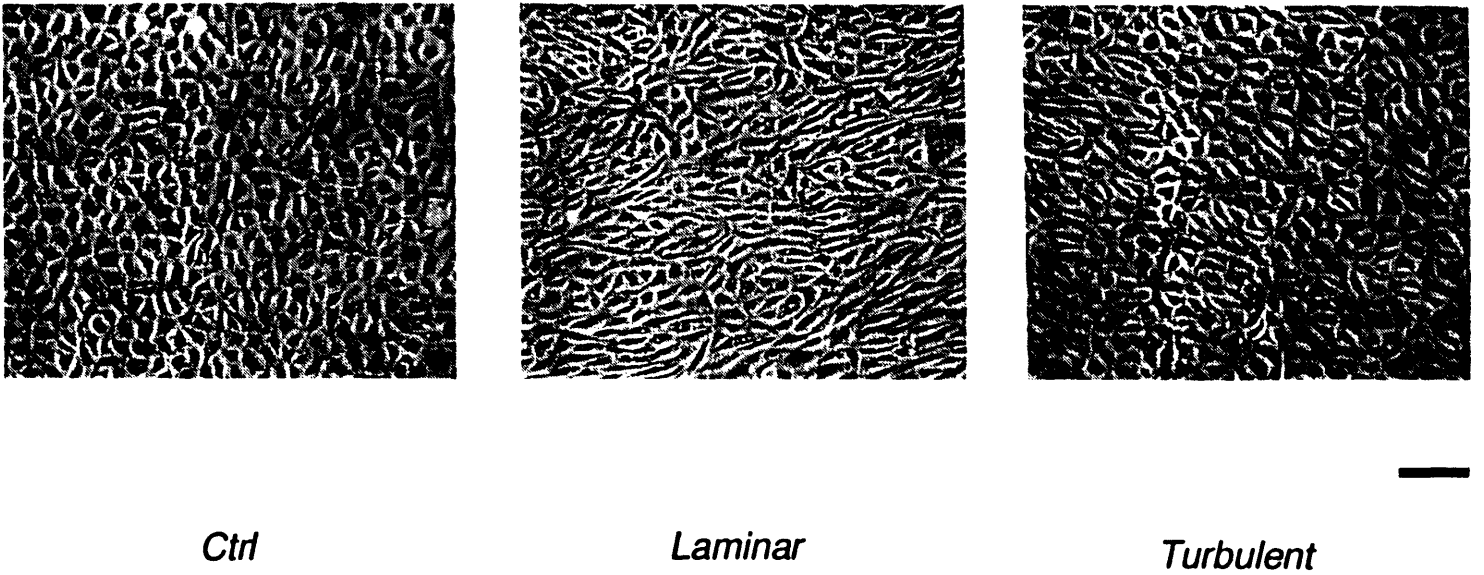


Figure 5.8 Phase contrast micrographs of BAEC under laminar and turbulent shear.

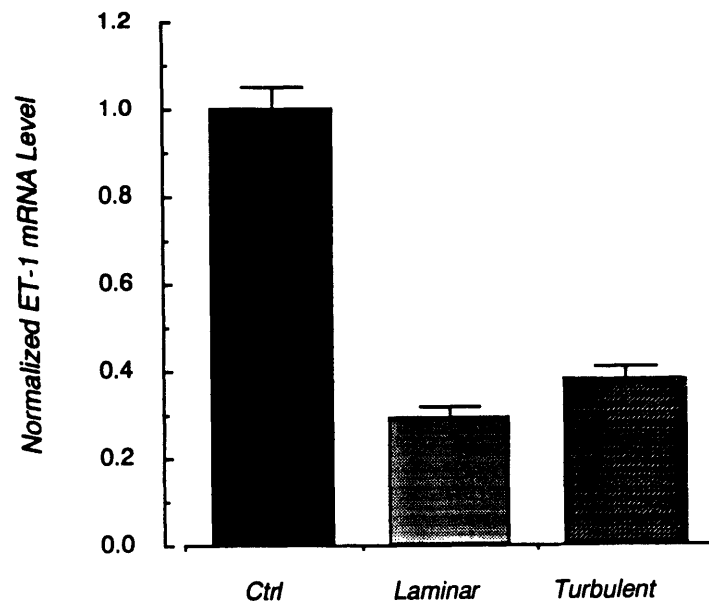


Figure 5.9 ET-1 mRNA decrease is similar under laminar and turbulent shear.

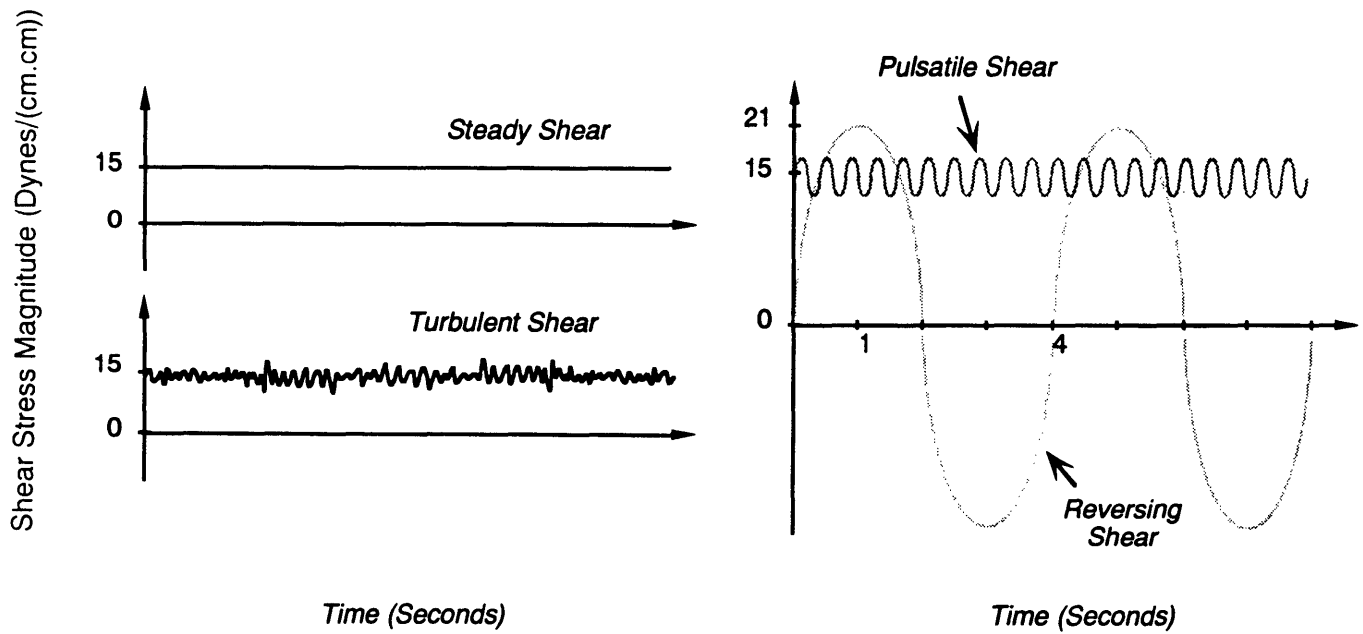


Figure 5.10 Schematic temporal profiles of shear stress under pulsatile, reversing, turbulent and steady regimes.

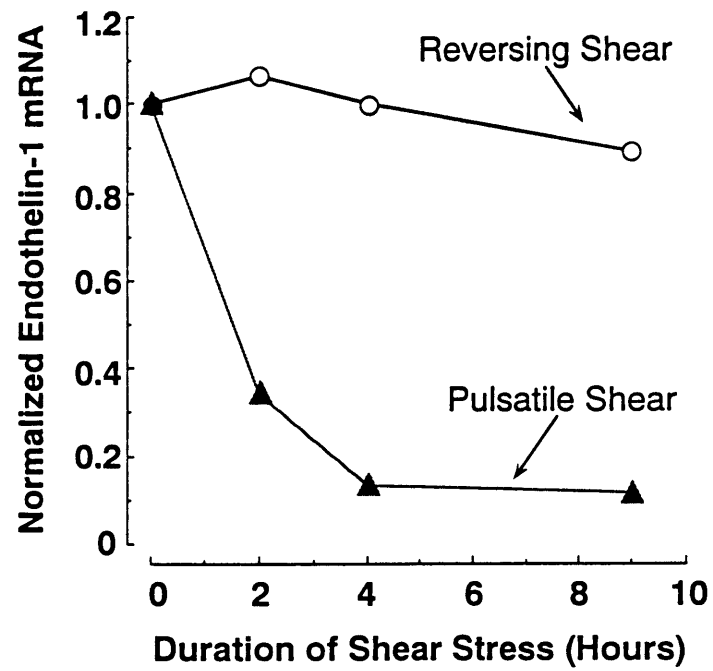


Figure 5.11 Time course of ET-1 mRNA under pulsatile and reversing shear.

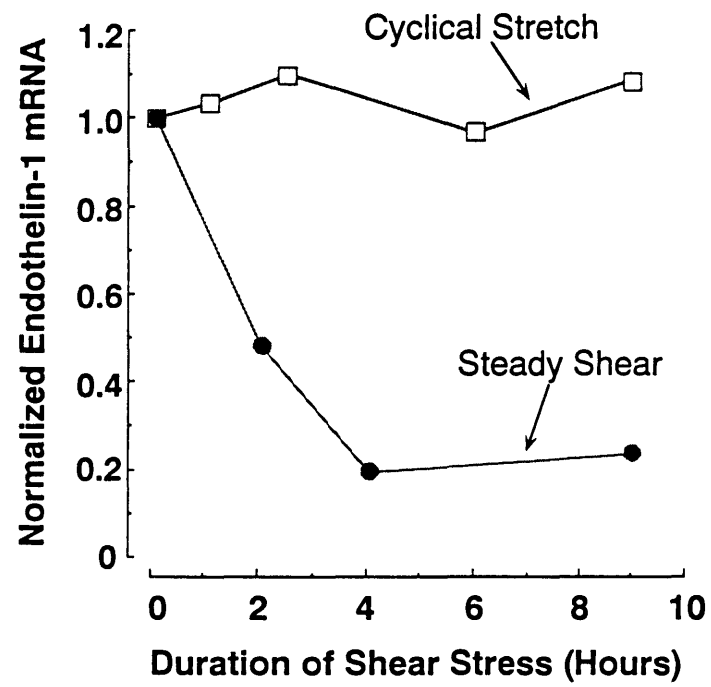


Figure 5.12 Time course of ET-1 mRNA under cyclical stretch and steady shear.

CHAPTER 6

Regulation of Endothelial-Derived Growth Factors by Fluid Shear Stress *in Vitro*

6.1 Regulation of growth factor expression by fluid shear stress

In this chapter the effect of shear stress was evaluated for the two potent heparin-binding polypeptide growth factors platelet-derived growth factor A- and B-chain, (PDGF A- and B-chain) and basic fibroblast growth factor (bFGF). Both basic FGF and PDGF-B are potent heparin-binding polypeptide growth factors (Vlodavsky I. et al., 1987) with important chemotactic and mitogenic properties, which have been proposed as potential key players in determining vascular structural response in models of injury (Jawien A. et al., 1992) and atherosclerosis (Barrett T.B. et al., 1988; Libby P. et al., 1988).

6.2 Platelet-derived growth factor

Platelet-derived growth factor is a glycoprotein of 30,000 kd which was found to be responsible for the mitogenic activity to mesenchymal cells found in serum (Ross R. et al., 1986). It is a dimer of the A and B chains which are coded for by distinct transcripts, resulting in three possible combinations, the AA and BB homodimers and the AB heterodimer. It is a potent growth factor to smooth muscle cells and fibroblasts in which it induces phosphatidylinositol turnover and phospholipase A₂ activation. PDGF is synthesized and secreted by endothelial cells as a paracrine growth factor since they do not themselves express the PDGF

receptor (in large vessel endothelium). Endothelium of venous origin expresses both the A- and B-chain mRNA while endothelium of aortic origin expresses only the B-chain of PDGF. In addition to its effect on mesenchymal cell growth (smooth muscle and fibroblast), PDGF is a very potent chemoattractant to these cells as well as to monocytes and neutrophils, which do not respond in a mitogenic fashion to PDGF. In addition, PDGF is a powerful vasoconstrictor (Berk B.C. et al., 1986) which is more potent on a molar basis than angiotensin II, acting by increasing free intracytoplasmic $[Ca^{2+}]$. It is interesting that endothelial cells isolated from fresh tissue express only a small fraction of the amount they express *in vitro* (Barrett T.B. et al., 1984). The level of endothelial-synthesized PDGF is increased by treatment with thrombin, phorbol esters, and endotoxin. In many respects, PDGF is similar to endothelin in that both are mitogenic substances to smooth muscle and fibroblast cells, and both are potent vasoconstrictors. They, like angiotensin II, belong to the class of mitogen-vasoconstrictors. The interest in relating the effect of fluid shear stress to the expression of PDGF B-chain secreted by endothelium is fundamentally the same as that for ET-1. Both are potent smooth muscle cell vasoconstrictors and growth factors that have the potential of influencing vessel structure and function (Dzau V.J. et al., 1991).

6.2.1 Effect of shear stress on PDGF B-chain expression

We have investigated the effect of fluid shear stress on the mRNA levels of the paracrine vasoconstrictor and growth factor PDGF A- and B-chain. Northern blot analysis of total RNA using a cDNA probe for PDGF-A failed to detect any measurable A-chain mRNA in BAE cells, a finding consistent with previous observations (Collins T. et al., 1987). Northern blot analysis using *c-sis* cDNA probes for PDGF-B chain mRNA revealed that exposure of BAE cells to fluid

shear stress of both 15 and 36 dyn/cm² induced a mild transient increase in PDGF B-chain mRNA, which peaked at 30 min and was followed by a more significant and long-lasting downregulation by 6 hr (figure 6.1). A similar downregulation of PDGF B-chain was also observed at the higher magnitude of 36 dyn/cm². Densitometric analysis (figure 6.2) of three to nine separate experiments revealed a 10-20% statistically non-significant increase in PDGF B-chain mRNA at 30 min followed by a sustained decrease of 2.6-fold ($p < 0.005$) at 6 hr and 3.9-fold at 9 hr ($p < 0.05$) at 15 dyn/cm². At shear stress magnitude of 36 dyn/cm² PDGF-B mRNA decreased 3.6-fold at 6 hr ($p < 0.005$) and 4.2-fold ($p < 0.005$) at 9 hr compared to its level in matched static controls. The extent of PDGF-B mRNA change at moderate shear (15 dyn/cm²) was not significantly different from that observed at high shear (36 dyn/cm²). To confirm specificity of the shear stress stimulus, cyclical stretch elicited a mild increase in PDGF-B mRNA which returned to baseline and was not sustained (figure 6.2).

These results are important for two reasons:

A- They are consistent with the direction of ET-1 change in response to shear stress indicating decreased expression of a vasoconstrictor/mitogen at higher shear. They are consistent with a regulatory negative feedback loop such as the one proposed for ET-1.

B- They suggest the possible existence of a common link between the regulation of ET-1 and PDGF B-chain by shear stress.

6.3 Basic fibroblast growth factor

Basic fibroblast growth factor consists of a single polypeptide chain that binds to a combination of high-affinity specific receptors and lower-affinity

proteoglycans found on the cell surface of the target cell (Klagsbrun M. et al., 1991). Basic FGF is mitogenic to endothelial and smooth muscle cells, and is a powerful angiogenic factor which is associated with the extracellular matrix and basement membrane (Rifkin D.B. et al., 1989). Although it does not possess a signal sequence for export via the classical ER-Golgi pathway, it has been demonstrated to be released by cell injury (McNeil P.L. et al., 1989) in certain tumors (Kandel J. et al., 1991) and by other yet undetermined mechanisms (Mignatti P. et al., 1991). It has been recently suggested to play a role in the balloon angioplasty-induced intimal thickening. Basic FGF is important to consider in the context of shear stress because endothelial as well as smooth muscle and fibroblast cells possess bFGF receptors, making bFGF a potential player in autocrine and paracrine interactions within the vessel wall. It has recently been shown to be induced at the mRNA level by thrombin, phorbol ester, and itself (Weich H.A. et al., 1991).

6.3.1 Effect of shear stress on basic FGF expression

One of the initial aspects of this project was the examination of the effect of fluid shear stress on the expression of bFGF because of its dual potential role as an autocrine and paracrine growth factor. Using an early prototype in which the cone positioning mechanism was not yet perfected, and in which the radius of the cone shaft with respect to cone radius was relatively small, sporadic but significant increases in bFGF were detected. These were particularly obvious when a shallow cone of angle such as 0.5° was used. After design improvement and modification of the device, no changes in bFGF mRNA were detected under either laminar, turbulent, or time varying shear stress of 15 dyn/cm^2 . A stretch experiment using Dr. Thomas Kulik's device failed to elicit similar changes in bFGF expression.

However, later experiments using the improved cone-plate viscometer device at much higher levels of shear stress, achieved either by dextran supplementation or by using a 0.5° cone at high rotational velocities, allowed once again the detection of significant changes in bFGF mRNA.

In order to determine the effect of fluid shear stress on vascular endothelial mRNA levels of bFGF, confluent monolayers of BAE cells last fed growth media 24-48 hr were exposed to steady laminar shear stress at both 15 and 36 dyn/cm^2 , the same magnitudes of shear used for morphometric analysis. Figure 6.3 shows a Northern blot of total RNA isolated from shear-exposed monolayers at increasing durations of exposure showing hybridization to three mRNA species as previously described of approximate size 7.0, 4.0, and 1.9 kb. Northern analysis of BAE monolayers exposed to 15 dyn/cm^2 showed no significant change in bFGF expression, although a mild increase was observed in some experiments. In contrast, exposure to steady laminar shear stress of 36 dyn/cm^2 resulted in a significant increase in bFGF signal of all three mRNA bands by 3 hr which remained elevated at 9 hr. Shear stress of neither 15 nor 36 dyn/cm^2 had any significant effect on GAPDH mRNA levels. Densitometric analysis was performed on Northern blots from three to nine separate experiments (figure 6.4). The results from the shear stress magnitude of 15 dyn/cm^2 revealed a mild and transient increase in relative bFGF mRNA reaching 1.5 fold of static control at six hours ($p < 0.05$). Exposure to the higher shear stress magnitude of 36 dyn/cm^2 resulted in an increase of 4.2-fold at 3 hr ($p < 0.05$), 4.8-fold at 6 hr ($p < 0.005$) and 2.6-fold at 9 hr ($p < 0.05$) compared to static control monolayers. Basic FGF remained elevated at 9 hr although the time course suggested a transient effect. In order to verify whether the change in bFGF mRNA levels was specific to shear stress and not to any mechanical stimulus, BAE monolayers were subjected to cyclical stretch of

20% strain at a rate of 20/min, which showed no significant effect as shown in figure 6.4.

6.4 Effect of dynamic character of shear stimulus on PDGF and bFGF mRNA levels

In an effort to determine the effect of altering the time characteristics of the shear stress stimulus on growth factor mRNA levels, we subjected BAE monolayers to four different conditions which are schematically illustrated in figure 5.10 for a duration of 6 hr:

- a) steady laminar shear stress of 15 dyn/cm² (moderate),
- b) steady laminar shear stress of 36 dyn/cm² (high),
- c) pulsatile laminar shear stress varying between 12 and 18 dyn/cm² (mean magnitude of 15 dyn/cm²) at a frequency of 2.5 Hz, and
- d) turbulent shear stress of time-average magnitude 15 dyn/cm² (Reynolds number R=15.2).

A representative panel of the results for PDGF-B mRNA levels appear in figure 6.5 and indicate that steady laminar of 15 and 36 dyn/cm², and turbulent and pulsatile laminar shear of 15 dyn/cm² all resulted in decreased PDGF-B mRNA levels at 6 hr to a comparable extent. The corresponding result for bFGF appears in figure 6.6 and shows no significant difference in bFGF mRNA level between steady laminar and turbulent, and between steady laminar and pulsatile laminar shear stress, all of magnitude 15 dyn/cm², when compared to static control. In contrast, steady laminar shear stress of 36 dyn/cm² caused a clear increase in bFGF mRNA. This result suggests that the magnitude of the shear stress stimulus is a more important determinant of bFGF and PDGF-B mRNA levels than the dynamic characteristics of the shear stress at a given time-average magnitude, at least for the

four conditions employed in this study. The results presented here do not rule out a different result when a shear stress stimulus of different degree of turbulence or of variation at a different frequency is used.

6.5 Conclusion and potential implications of findings

Since bFGF has been shown to play a role in autocrine growth regulation (Schweigerer L. et al., 1987) and migration (Mignatti P. et al., 1991) of the endothelial cell, this high shear-induced increase may be relevant to the observed long-term increase in endothelial density which is observed following surgically-induced increases in blood flow in the canine carotid artery AV-shunt model (Masuda H. et al., 1989). Recent work has shown that constant bFGF delivery at the adventitia in a rat model of intimal hyperplasia did not affect medial SMC growth when endothelial cells were intact, but did so significantly when endothelium was removed or injured with endotoxin (Edelman E. et al., 1992). In view of this finding, the observed increase in endothelial bFGF mRNA at higher shear could selectively act in an autocrine manner without necessarily influencing the growth of the underlying smooth muscle cells.

Hsieh et al. (Hsieh H. et al., 1991) using HUVE cells reported that fluid shear stress induces a transient increase in both PDGF A- and B-chain mRNA that returns to baseline by 4 hr. In contrast, our study showed that physiological shear stress of both moderate (15 dyn/cm^2) and elevated magnitude (36 dyn/cm^2) induced a marked 4-5 fold decrease in PDGF-B chain mRNA. The BAE cells, unlike HUVE cells, express the B- but not the A-chain of PDGF (Collins T. et al., 1987); the difference in the results may be due to the difference in cell origin, or could alternatively be the result of the compounded effect of hydrostatic pressure, which is expected in the parallel-plate type viscometer used in that report.

Furthermore, changes in RNA levels were not reported for durations of shear greater than 4 hr, the time after which the downregulation reported in the present work is most significant. Some of our experiments have shown occasional increases (~50 %) in PDGF B-chain mRNA at times between 0.5 and 2 hr, but these were transient and not as prominent and as the long-lasting 4-5 fold decrease in PDGF B-chain mRNA observed after 4-6 hr.

It is interesting to note that PDGF mRNA levels behaved in a similar fashion to ET-1 in response to shear stress, exhibiting a significant 4-5 fold decrease in response to shear stress, and a dependence on the time-average magnitude rather than the dynamic aspect of the shear stimulus. Both of these substances are powerful vasoconstrictors and smooth muscle mitogens, and their decrease with shear stress raises the possibility of their involvement in the mechanism of the observed internal diameter decrease in response to decreased blood flow and wall shear stress seen *in vivo* (Langille L. et al., 1986). The decrease of PDGF-B and ET-1 expression may also be relevant to the recent observations of increased smooth muscle ingrowth in rigid PTFE grafts (Kraiss L.W. et al., 1991) in the absence of short-term internal vessel diameter changes at low (11 dyn/cm²) but not high (22 dyn/cm²) shear stress magnitude. Furthermore, the increased PDGF-B and ET-1 levels at physiological shear stress may also be of interest in explaining the correlation of focal atherosclerotic lesions and intimal thickening seen preferentially in areas of low (0-4 dyn/cm²) (Zarins C.K., 1983; Asakura T. et al., 1990) but not higher (15 dyn/cm²) shear stress magnitude. Finally, the decreased expression of PDGF-B chain in response to physiological shear stress reported here may explain the property that freshly-isolated BAE cells express much lower (25-fold) levels of PDGF-B than when cultured *in vitro* under static conditions (Barrett T.B. et al., 1984).

The mechanism of the regulation of bFGF and PDGF-B mRNA levels by fluid shear stress is not at the present well understood. Although the effect of shear stress on bFGF and PDGF B-chain were not characterized as well as for ET-1, it is tempting to speculate that the mechanism of regulation of the ET-1 and PDGF-B chain genes by shear stress may be shared to a certain extent because of their similar behavior in response to shear.

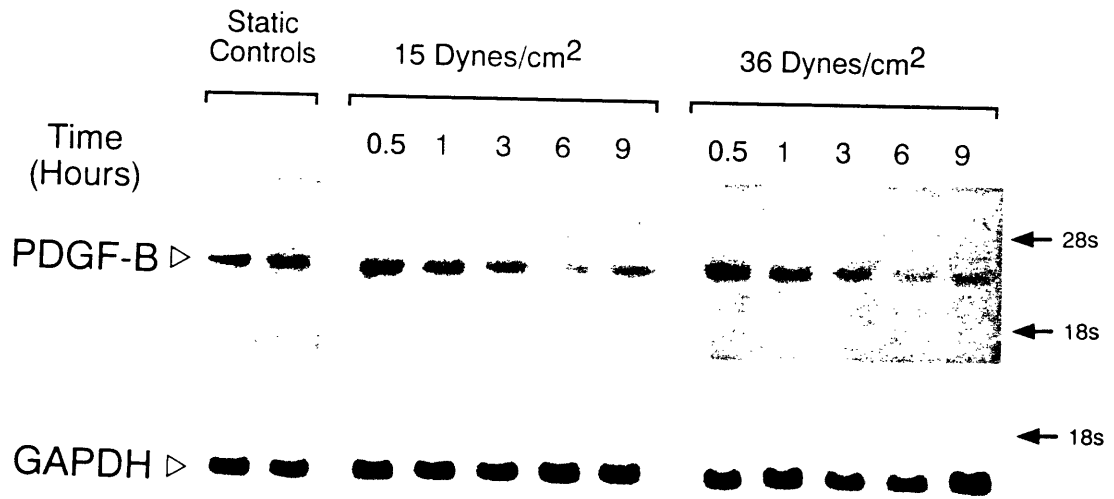


Figure 6.1 Northern blot analysis of BAE under shear using PDGF-B chain cDNA.

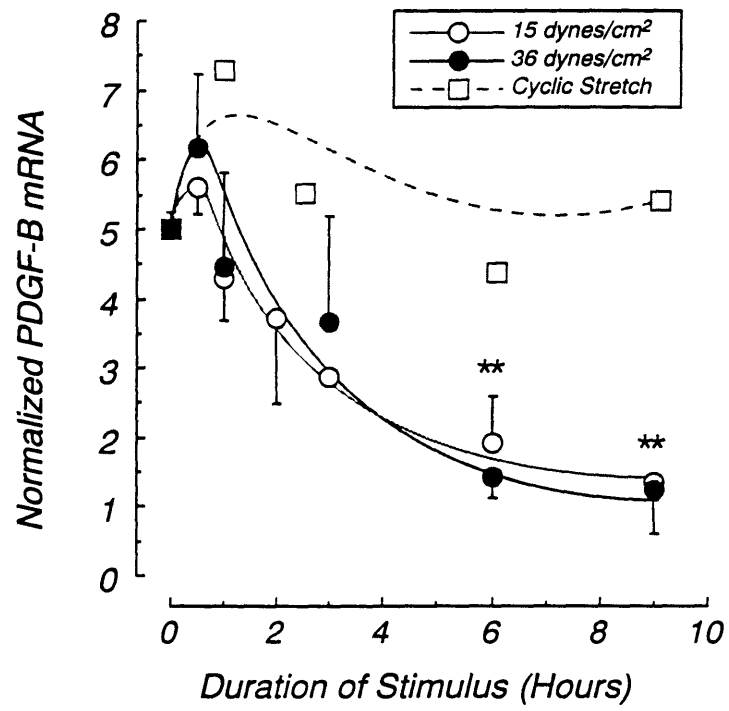


Figure 6.2 Normalized densitometric analysis of PDGF-B chain mRNA.

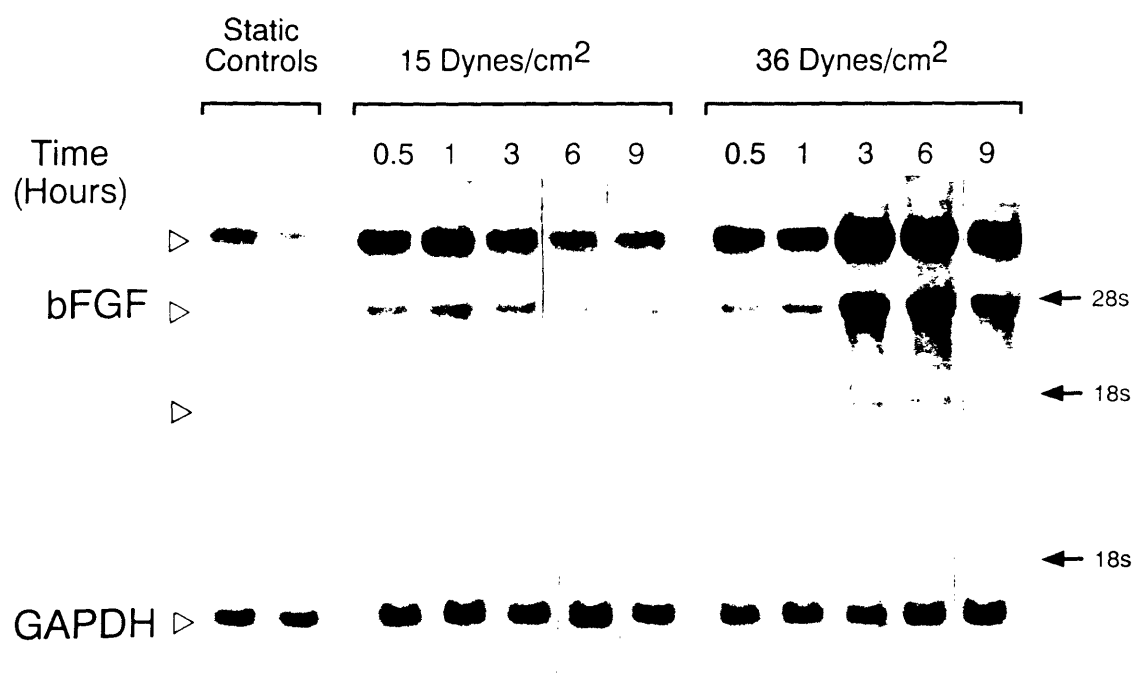


Figure 6.3 Northern blot analysis of BAE under shear using bFGF cDNA.

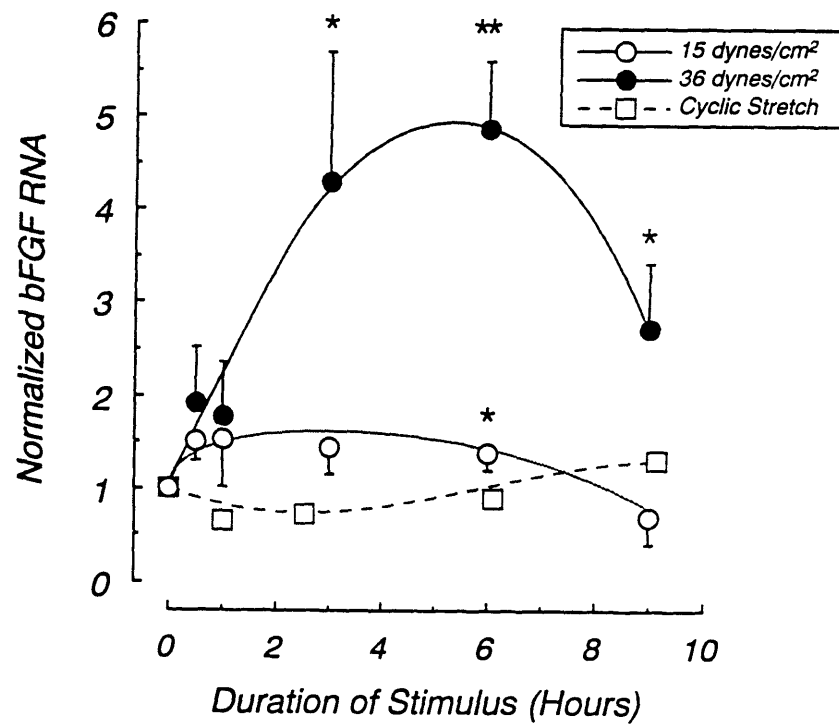


Figure 6.4 Normalized densitometric analysis of bFGF mRNA.

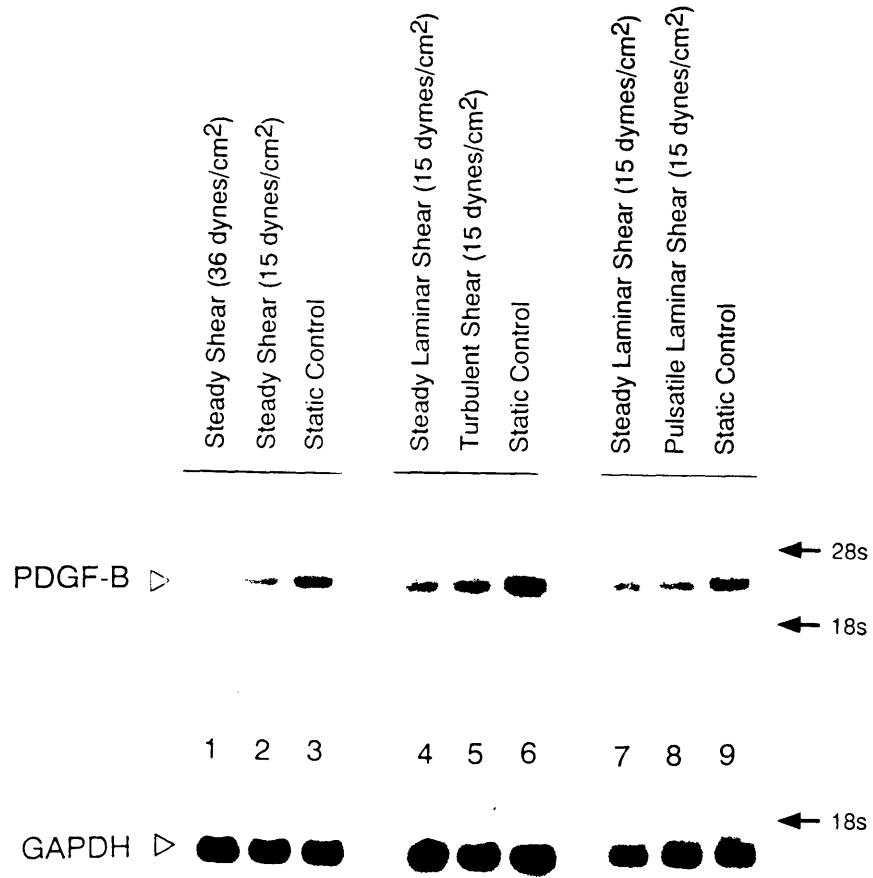


Figure 6.5 Northern blot analysis using PDGF-B chain cDNA under steady, pulsatile and turbulent shear.

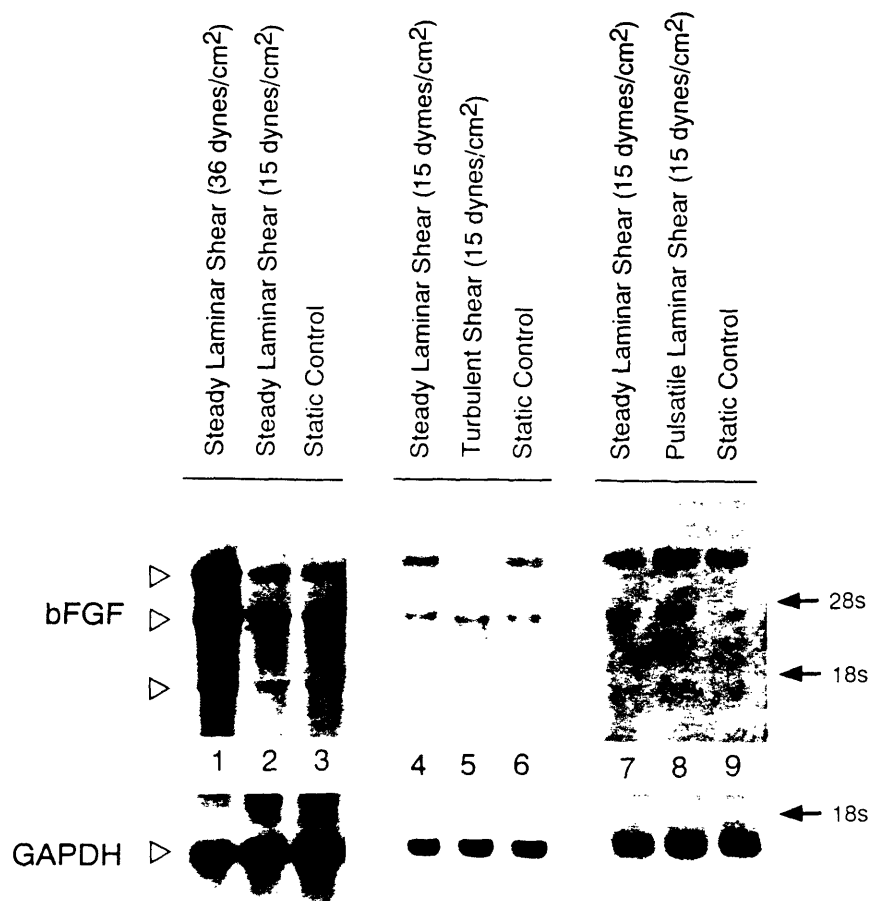


Figure 6.6 Northern blot analysis using bFGF cDNA under steady, pulsatile and turbulent shear.

CHAPTER 7

Differential Regulation of Thrombomodulin and Tissue-Type Plasminogen Activator by Fluid Shear Stress

7.1 Thrombomodulin and tissue-type plasminogen activator

The endothelial cell plays an active role in preventing the occurrence of blood clots in the blood vessel and in maintaining the blood vessel patent by dissolving existing fibrin clots. The endothelial cell's antithrombotic activity is carried out by at least two mechanisms (Esmon C.T., 1987): the first consists of natural endothelial surface heparin-like molecules which catalyze the inactivation of coagulation proteases by antithrombin III, and the second is carried out via thrombomodulin (TM).

TM is an integral membrane glycoprotein expressed on the surface of the endothelial cell that functions as a receptor with a high affinity for thrombin and forms with the latter a 1:1 stoichiometric complex that serves as a potent catalyst of the thrombin-induced activation of protein C. Activated protein C complexes to protein S, and together they catalyze the inactivation of factors Va and VIIIa, thereby serving to inhibit thrombin formation (Esmon C.T., 1989). The relative importance of the protein C system is underscored by increased thromboembolic disorders in individuals with protein C or S deficiencies (Comp P.C., 1986; Moore K. L., 1989), and by the ability of exogenous TM to counteract, and anti-TM antibodies to potentiate, thrombin-induced thromboembolism in mice (Gomi K. et

al., 1990). TM has also been demonstrated to be involved in internalization and clearance of extracellular thrombin (Conway E.M. et al., 1992). TM removes circulating thrombin by endocytosis following binding and subsequent degradation (Maruyama I. et al., 1985). TM cDNA has been isolated from a bovine library, sequenced and found to be very similar in its C-tail region to the LDL receptor. TM is an important regulator of the endothelium's anticoagulant properties. Although TM expression has been shown to increase in response to increased cAMP, retinoic acid (Weiler-Guettler H. et al., 1992) and thrombin (Dittman W.A., 1989), and TM surface activity to decrease in response to endotoxin, IL-1, and TNF- α (Conway E.M. et al., 1988), it is not clear if and how mechanical forces resulting from blood flow may regulate TM levels.

7.2 Effect of shear stress on TM expression

The hemodynamic stimulus is likely to be an important physiological factor since vascular endothelium is constantly exposed to flow and the resulting fluid shear stress acting on the endothelial cell surface. Exposure of endothelium to shear stress has been shown to result in increased secretion of PGI₂ (Frangos J.A. et al., 1984) and EDRF (Cooke J.P. et al., 1991) both of which inhibit platelet aggregation. The endothelial cell's fibrinolytic activity is due mainly to its secretion of tissue-type plasminogen activator which acts to generate plasmin, and leads to dissolution of existing fibrin clots. Shear stress of 25 dyn/cm² has been reported to increase secretion and mRNA levels of tissue-type plasminogen activator (Diamond S.L. et al., 1989 and 1990) which, through activation of plasmin, plays a key role in fibrinolysis. Since areas of low flow, low wall shear stress, or flow recirculation would be characterized by a prolonged particle residence time which may increase the likelihood of interaction between activated

blood-borne elements and the vessel wall (Goldsmith H.L. et al., 1986), hemodynamic forces may be a critical factor in the development of thrombosis. Accordingly, we explored the role of well-controlled fluid shear stress in both laminar and turbulent regimens on the expression of TM mRNA and protein in bovine aortic endothelial and smooth muscle cells.

7.2.1 Fluid shear stress decreases expression of TM mRNA specifically

Application of steady laminar fluid shear stress in the physiological range of either 15 or 36 dyn/cm², resulted in a time-dependent decrease in the content of TM mRNA in confluent BAE cells as seen in Northern blot analysis of total RNA (figure 7.1) (Malek A.M. et al., 1994). Some experiments also exhibited a mild transient increase in TM mRNA at early times between 0.5-2 hr, reaching up to 1.43-fold at 0.5 hr under 36 dyn/cm². The decrease in TM mRNA was specific since steady-state levels of GAPDH mRNA remained unaffected by shear. Densitometric analysis was performed on a number of experiments (n=3 to 8) on the TM mRNA band normalized with respect to the corresponding GAPDH signal (figure 7.2). The analysis revealed that shear induced a decrease in TM mRNA from a basal control static level of unity to 0.34 ± 0.03 (n=17, p<0.0005) at 6 hr and to 0.36 ± 0.29 (n=3, p<0.001) at 9 hr for 15 dyn/cm², and to 0.36 ± 0.17 (n=3, p<0.05) at 6 hr and to 0.16 ± 0.03 (n=3, p<0.0005) at 9 hr for 36 dyn/cm². TM mRNA remained decreased to a similar extent even following 24 hr of continuous flow, indicating that the decrease is not a transient phenomenon. To determine if the shear-induced regulation of TM is a characteristic feature of endothelial cells, BSM cells which have been previously reported to express TM mRNA (Soff G.A. et al., 1991) were subjected to the same steady laminar shear of 15 dyn/cm². Shear stress of that magnitude and regime failed to elicit any significant changes in smooth

muscle cell TM mRNA (figure 7.2), suggesting that the phenomenon is cell-specific. The lack of TM response to shear in BSM cells is in accordance with the lack of cell shape change and alignment of these same cells shown earlier in figure 4.17.

7.2.2 Shear-induced downregulation of TM mRNA is a completely reversible process

To assess whether the decrease in TM mRNA in response to shear is reversible upon return to static no-flow conditions, BAE cells were first subjected to 6 hr of steady laminar shear at 15 dyn/cm², after which point flow was halted and total cellular RNA was isolated at 0.5, 3, and 6 hr. Northern analysis shows a gradual recovery of TM mRNA (figure 7.3) to basal levels. Densitometric analysis (figure 7.4) of TM mRNA normalized with respect to GAPDH mRNA revealed that following 6 hr of shear stress, TM mRNA levels decreased by 2.8-fold (n=4, p<0.01) and by 6 hr following cessation of flow had recovered to 0.98 of static control levels (n=4, p=0.37). Similar results were found following shear stress of 36 dyn/cm² for 6 hr as shown by the smaller oval symbols in figure 7.4. Thus the effect of shear stress on TM mRNA appears to be completely reversible within a time frame of six hours.

7.2.3 Shear stress decreases levels of expressed TM protein

We then explored whether the decrease in TM mRNA was also mirrored by decreases in the expression of TM protein. Western blot analysis of BAE cells exposed to 36 hr of steady laminar shear stress of 15 dyn/cm² using affinity-purified polyclonal antibody against bovine thrombomodulin previously described (Jackman R.W. et al., 1986) revealed a significant decrease. Figure 7.5 shows the

specific band at ~100 kDa. Laser densitometry revealed that BAE cells exposed to shear stress expressed only 0.33 ± 0.07 of the amount of TM ($n=3$, $p < 0.005$) from BAE cells left under stationary conditions (figure 7.6). This finding indicates that the decrease seen in TM mRNA by shear stress is also observed at the protein level. No experiments were, however, carried out to measure changes in TM function in membrane preparations of endothelium, exposed to shear.

7.2.4 TM mRNA is regulated similarly by steady, pulsatile, and turbulent shear stress

Fluid shear forces are inherently time-varying and more complex in the living organism than those resulting from fully-developed laminar flow. To this end, we exposed confluent monolayers of BAE cells to pulsatile shear stress at a frequency of 2.5 Hz varying between 12 and 18 dyn/cm^2 , and to turbulent shear stress having a Reynolds Number of 17.2. The results of Northern analysis shown in figure 7.7 indicate no detectable change in the extent of decreased TM mRNA expression between steady laminar, pulsatile laminar and turbulent shear stress stimuli after 6 hr. All three shear stimuli had the same absolute mean shear stress magnitude of 15 dyn/cm^2 .

7.3 Differential regulation of TM and t-PA mRNA by fluid shear stress

Since t-PA mRNA has previously been reported to be increased by fluid shear stress in human umbilical vein endothelial (HUVE) cells exposed to 25 dyn/cm^2 (Diamond S.L. et al., 1990), it was of interest to determine the relation between the TM and t-PA changes in mRNA expression induced by fluid shear stress. It was also important to determine whether BAE behaved in the same fashion as HUVE cells in response to shear stress. Accordingly, mRNA collected from BAE cells

exposed to either 15 or 36 dyn/cm² was analyzed by Northern blot using a t-PA cDNA probe (cf. Appendix). Densitometry of the normalized signal indicates that at 15 dyn/cm² where TM is downregulated by 2.7-fold (figure 7.2), t-PA is increased by ~3-fold compared to static control levels (figure 7.8). However, t-PA mRNA levels increase very dramatically (~20 fold) at the higher shear magnitude of 36 dyn/cm² while TM mRNA remains downregulated at 36 dyn/cm², somewhat further (at 6.3-fold) than at 15 dyn/cm². The finding of dramatically higher response of t-PA to shear of 36 compared to 15 dyn/cm² is qualitatively similar to the previously reported increase in HUVE t-PA mRNA at 25 but not 4 dyn/cm² reported by Diamond et al. (Diamond S. et al., 1989). These results suggest the existence of two independent mechanisms for regulation of hemostasis and thrombosis. Under static conditions and at low levels of shear stress TM expression of both mRNA and protein is at an elevated level while t-PA expression is very low. At the average physiological shear stress level of 15 dyn/cm² TM expression is decreased while t-PA expression remains relatively low. Under conditions of higher shear stress, such as 36 dyn/cm², t-PA expression becomes significantly greater while TM decreases further. Thus, it appears that t-PA is activated by high shear stress (above the average physiological magnitude) while TM is activated under conditions of stasis and low shear stress. This finding suggests that TM may be regulated in such a way as to provide an added protective role against thrombosis under stationary conditions where increased residence time of platelets and other components of the coagulation cascade at the blood vessel surface may favor thrombosis (Goldsmith H.L. et al., 1986)

The increased t-PA mRNA at high shear presents a model to explain the mechanism by which vascular structure may be altered in response to increased levels of shear, as exemplified by the Kamiya model, in light of t-PA's ability to

activate plasmin which is a pluripotent enzyme that is thought of being capable of dissolving existing matrix and tissue architecture, a process that would be of ultimate importance in structural vessel dilatation (Mignatti P. et al., 1993).

7.4 Discussion

Among richly vascularized tissues, TM mRNA is found at its highest concentration in the lung, and probably in greater quantities in continuous than in fenestrated endothelium (Ford V.A. et al., 1992). Thanks to its potent action in catalyzing the activation of protein C, TM is thought to play an important role in regulating the antithrombotic activity of the endothelial cell by multiple mechanisms including activation of protein C, inactivation of factors Va and VIIIa, and internalization of thrombin (Esmon C.T., 1989). Since the endothelium is constantly exposed to flow and the resulting fluid shear stress *in vivo*, it is important to determine the role of fluid dynamic forces on the expression of TM.

The findings reported here are significant since they suggest that cells constantly exposed to flow and shear stress eventually express lower steady-state levels of TM mRNA and protein than do cells under conditions of low or no-flow. Such a property suggests that TM may serve a protective role in cells under static conditions which may be prone to a higher probability of thrombosis and clot formation (Goldsmith H.L. et al., 1986). The decrease in TM mRNA by shear stress was demonstrated to be entirely reversible within 6 hr following the cessation of shear stress, suggesting that the cells have not undergone an irreversible injurious insult and also pointing to the possibility that such a mechanism would be responsive *in vivo* to changing local hemodynamic conditions. The response of TM to fluid shear stress did not appear to discriminate between laminar, turbulent or pulsatile regimens of equal mean magnitude of 15 dyn/cm², a finding that is similar

to that previously described for ET-1. This result does not mean however that other time-varying fluid conditions of higher frequency or magnitude may not elicit a different result.

The decrease in TM mRNA occurred as soon as 6 hr following the onset of shear stress and also recovered within the same amount of time period back to its previous level. Since the half-life of TM mRNA has been previously estimated at $t_{1/2} \sim 8.9$ hr (Dittman W.A. et al., 1988), it appears unlikely for the shear-induced downregulation to be solely mediated by decreases in TM transcription without alterations in message stability such as has been described for ET-1 (Malek A.M. et al., 1993b). It is important to note however that the measured TM mRNA and protein changes reported here may not entirely reflect changes in TM activity that would be observed *in vivo*.

The decrease of TM mRNA and protein with application of fluid shear stress was observed to be concomitant with an increase in t-PA mRNA, especially at the higher magnitude of 36 dyn/cm^2 . This result suggests that the shear-responsiveness of the t-PA gene originally described in HUVE cells (Diamond S.L. et al., 1990) is also present in BAE cells. Together the TM and t-PA patterns of regulation suggest a switch in the phenotype of the endothelial cell from a predominantly anti-thrombotic role characterized by high TM and low t-PA expression under static conditions to a fibrinolytic phenotype with decreased TM and increased t-PA expression under conditions of flow (figure 7.9). This is further strengthened by reports documenting that TM accelerates the thrombin-mediated inactivation of single-chain u-PA and can thereby play an anti-fibrinolytic in addition to its well-known anti-thrombotic role (Majerus P.W. et al., 1991; Molinari A. et al., 1992).

7.5 Conclusion

The work presented in the last three chapters was a summary of a large set of experiments which were conducted to define the effect of fluid shear stress at different physiological magnitudes on the expression of multiple genes thought to play a role in the regulation of blood vessel tone, growth and anti-thrombosis. The findings made here present an improved picture of the potential role of fluid shear stress on endothelial function, and are helpful in proposing a new model for the role of the endothelial cell that will be further explored in chapter 8. The exquisite physiological sensitivity of the ET-1, PDGF-B, bFGF, and TM to fluid shear stress coupled to their important physiological actions make them ideal candidate markers for the study of the mechanism of transduction and second messenger involvement in the response to shear.

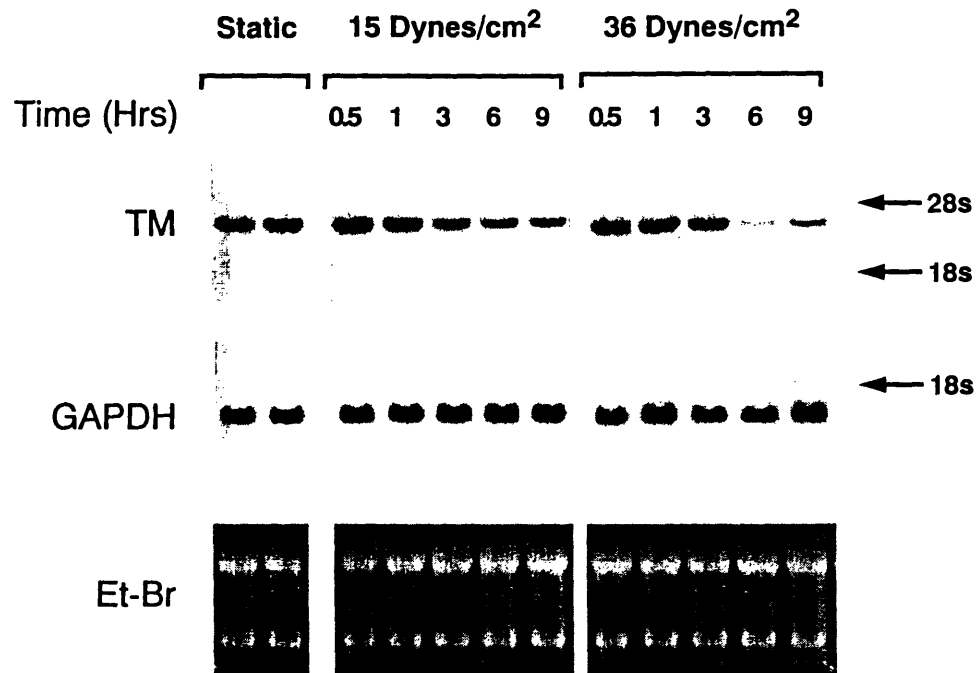


Figure 7.1 Northern blot analysis using thrombomodulin (TM) cDNA of BAE cells under shear.

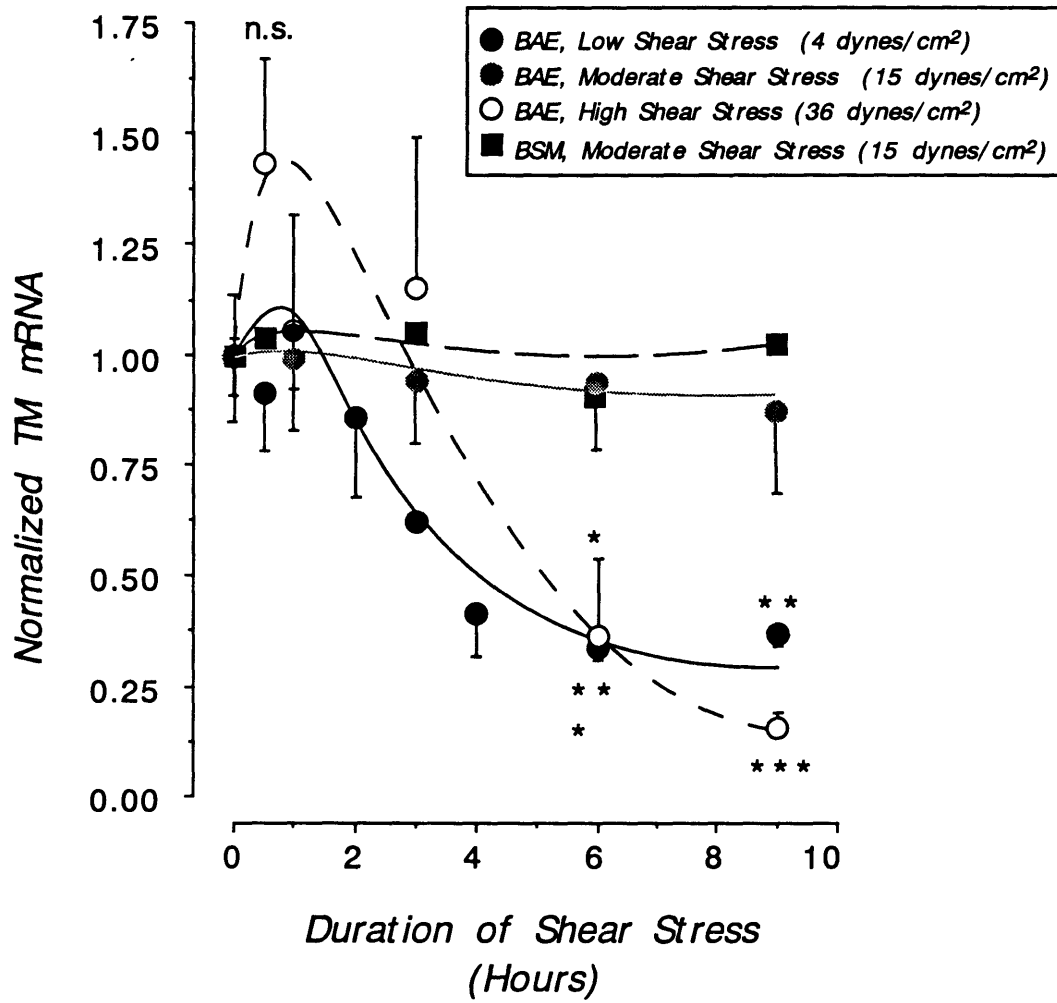


Figure 7.2 Normalized densitometric analysis of TM mRNA under shear.

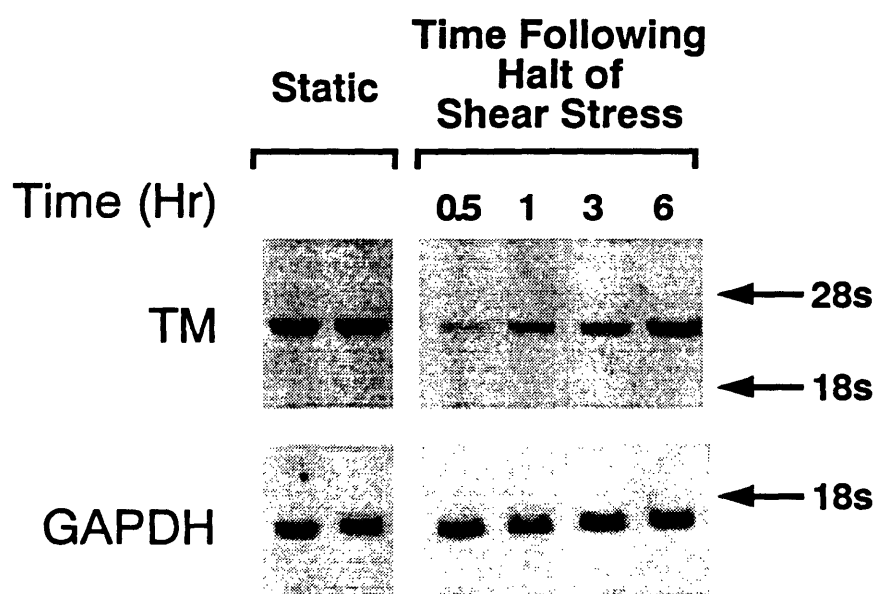


Figure 7.3 Northern blot analysis using TM cDNA illustrating recovery.

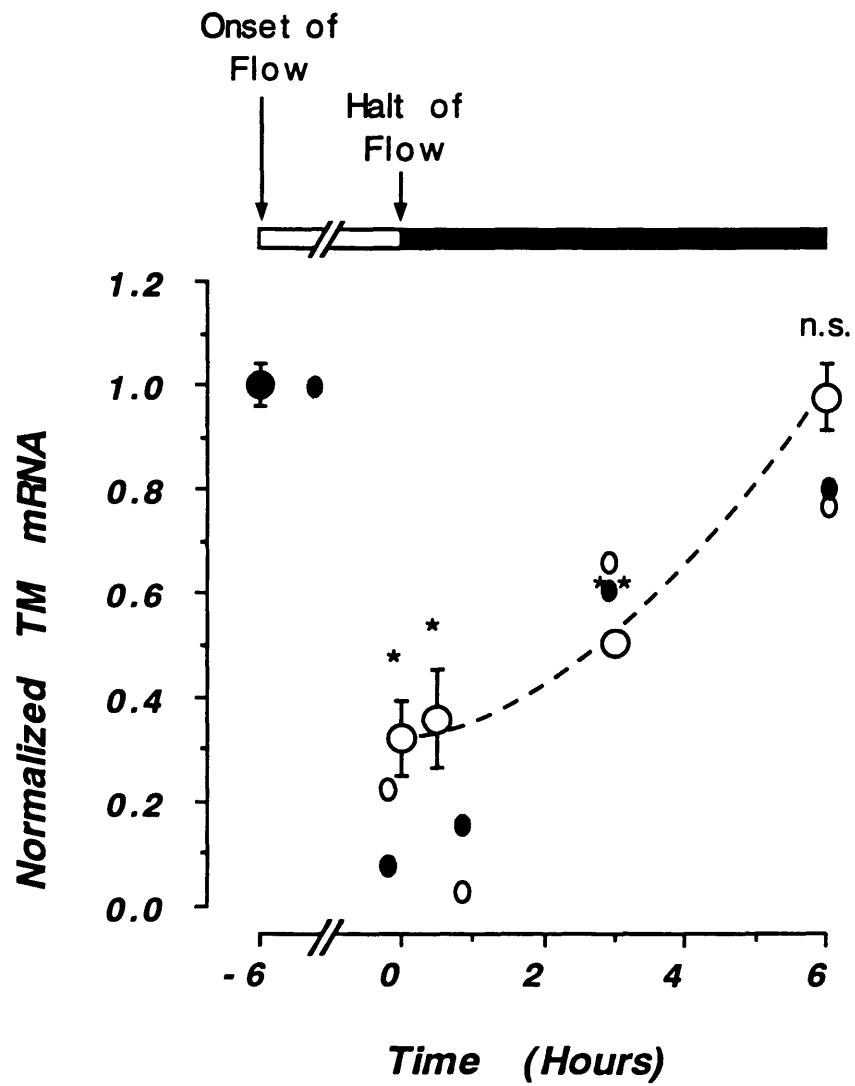


Figure 7.4 Normalized densitometric analysis illustrating recovery.

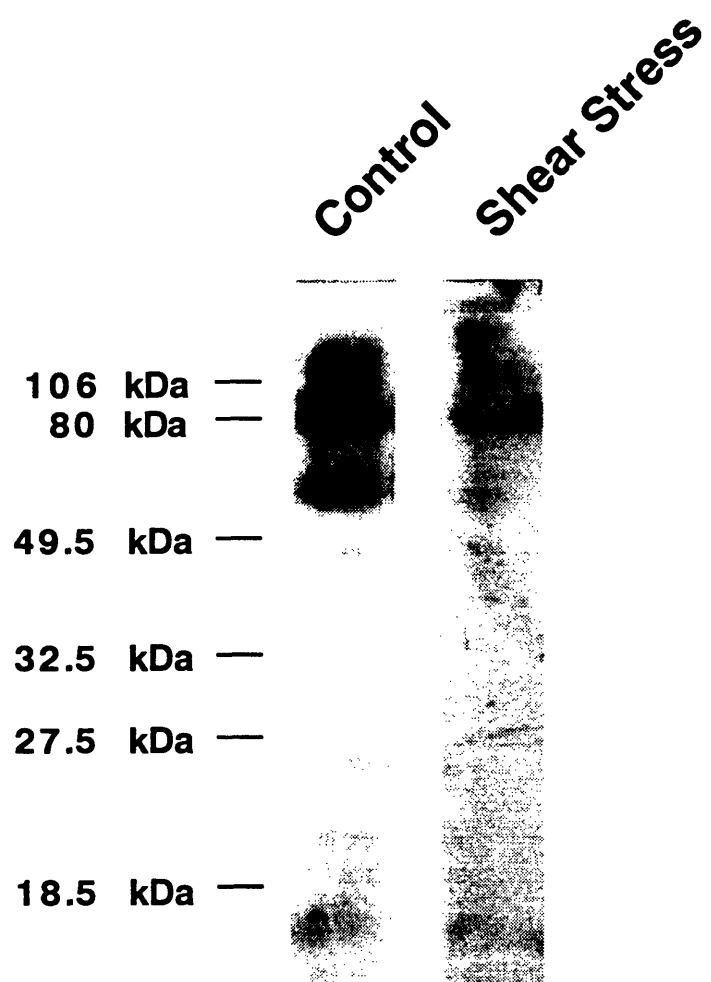


Figure 7.5 Western blot using anti-TM antibody under shear.

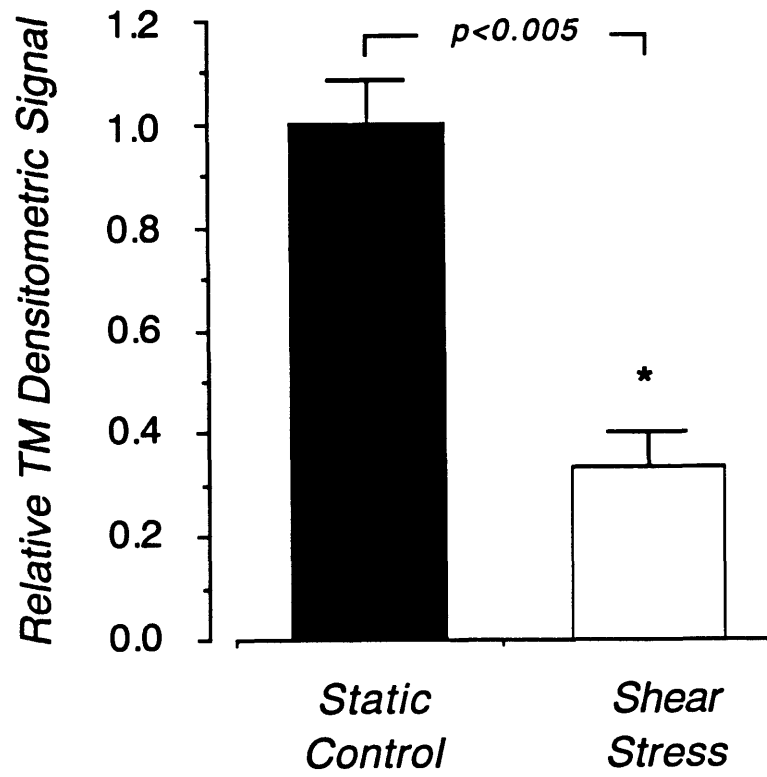


Figure 7.6 Densitometric analysis of TM Western blot of BAE under shear.

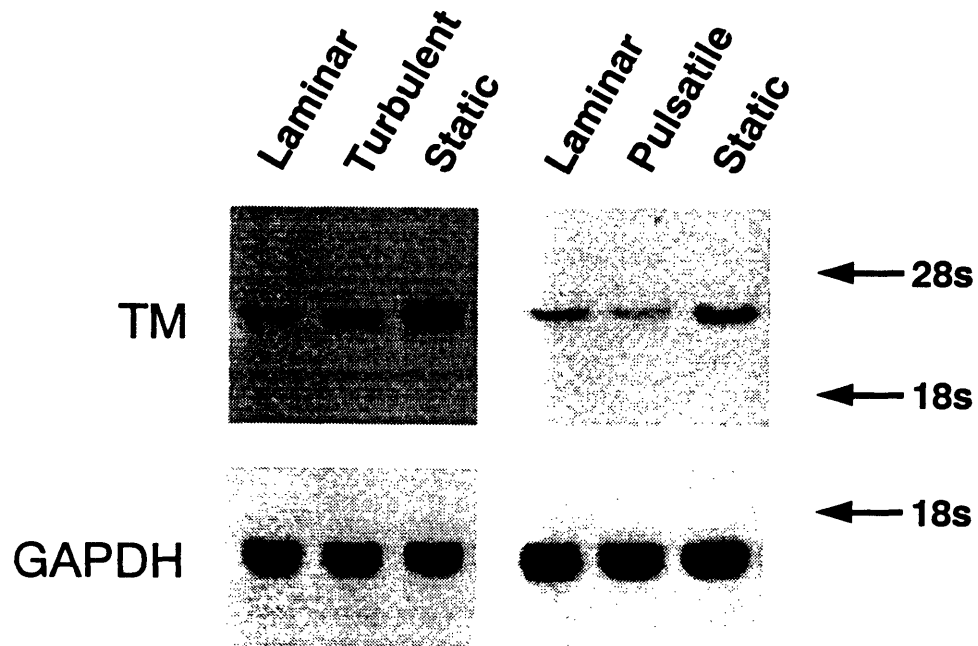


Figure 7.7 Northern blot analysis using TM cDNA under steady, pulsatile and turbulent shear.

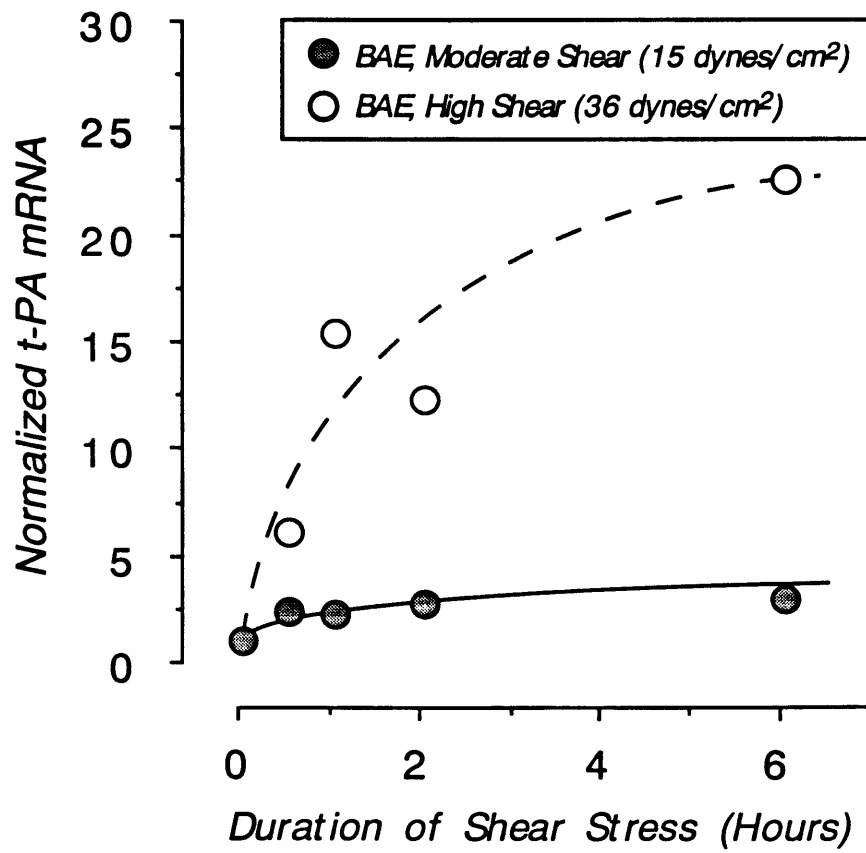


Figure 7.8 Densitometric analysis using t-PA cDNA.

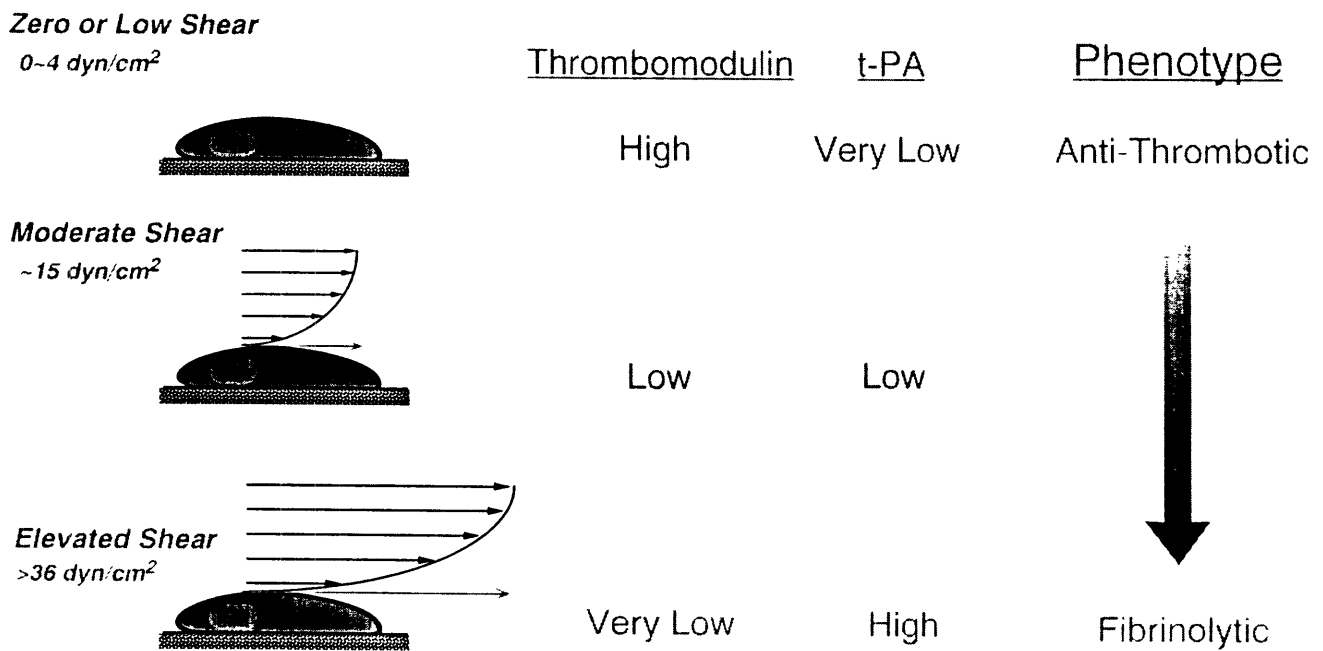


Figure 7.9 Schematic diagram of thrombotic/fibrinolytic phenotype of BAE cells under shear.

CHAPTER 8

Molecular Mechanism and Second Messenger Signaling in Response to Fluid Shear Stress

8.1 Molecular mechanism of endothelin regulation by fluid shear stress

Of the multiple endothelial products that were shown to be regulated by shear stress in the last three chapters, ET-1 was chosen as the functional marker for the study of the signalling and transduction of shear for multiple reasons. First of all, ET-1 is a very potent vasoconstrictor and smooth muscle cell/fibroblast mitogen (Muldoon L.L. et al., 1989), endowing it with the potential to be involved in pathophysiological regulation of the vessel wall. ET-1 mRNA is abundant and thus easily detected on Northern analysis. Finally, ET-1 mRNA levels quickly respond to shear stress because of its low message stability (Malek A. et al., 1992; Inoue A. et al., 1989).

8.1.1 Background on ET-1 gene expression regulation

Basal transcription levels of the ET-1 gene has been shown to be dependent on two critical regions in its promoter (Lee M. et al., 1990; Wilson D.B. et al., 1990), one containing a GATA motif at bp -135 to -132 and the other containing an AP-1 consensus sequence, a target site for PKC activation, between bp -109 and -102. The GATA-binding factor (GATA-2 factor) necessary for basal transcription of ET-1 has been cloned from a human cDNA library and found to contain the zinc-finger motif (Dorfman D.M. et al., 1992). The AP-1 consensus sequence has been demonstrated to bind *c-fos/c-jun* complex and to be critical for basal ET-1

transcription (Lee M. et al., 1991). The ET-1 gene has been reported to be upregulated by both calcium ionophore treatment and phorbol ester-induced PKC stimulation (Inoue A. et al., 1989), while retinoic acid-treatment of endothelium has been shown to result in a down-regulation in ET-1 mRNA probably via the GATA-2 factor (Dorfman D.M. et al., 1992). Figure 8.1 shows a schematic diagram illustrating the structure of the ET-1 gene, its promoter region and its 3'-untranslated region.

The present set of experiments were designed to address the mechanism of ET-1 mRNA downregulation by shear stress.

8.1.2 Shear stress induces downregulation of ET-1 by a protein synthesis dependent mechanism

Incubation of BAE monolayers for 60 min with 10 $\mu\text{g/ml}$ cycloheximide (CHX), an inhibitor of protein synthesis, prior to the exposure to shear stress prevented the down-regulation of ET-1 mRNA in response to the shear stimulus (figure 8.2). This was accompanied by increased basal ET-1 mRNA levels (super-induction) previously described (Inoue A. et al., 1989), thought to be the result of destabilizing AUUUA sequences in the 3'-region of ET-1 mRNA. Thus, on-going protein synthesis appears to be critical for the down-regulation of ET-1 mRNA by shear stress. Similar findings were made for the regulation of PDGF-B chain mRNA by fluid shear stress as shown in figure 8.3. Further it appears that CHX allows to uncover two shear-induced processes (or two steps in the same process) in PDGF-B regulation: a CHX-insensitive shear-induced increase which occurs early on, and a later CHX-sensitive decrease. Equally of interest is the observation that CHX prevented the shape change and alignment of the BAE cells in the direction of shear stress as shown in figure 8.4. Paradoxically, the cell shape relaxation that

occurs following the endothelial alignment (Remuzzi A. et al., 1984) once the shear stress stimulus occurs was found to be independent of protein synthesis (data not shown). Therefore, a factor dependent on on-going protein synthesis appears to be required for the transduction of shear forces into altered cell morphology but not for the relaxation of the cell morphology itself.

8.1.3 Fluid shear stress-induced ET-1 downregulation occurs at the transcriptional level without change in ET-1 mRNA stability

In order to determine whether the decrease in ET-1 mRNA was the result of decreased transcription or decreased stability, nuclear runoff transcription assays were performed using cell nuclei from BAE monolayers that had been exposed to steady laminar shear stress of 20 dyn/cm² for 6 hr. The radiolabelled transcripts, processed as described in the Appendix (Greenberg M.E. et al., 1984), were hybridized with immobilized linearized cDNAs for bovine ET-1, α -tubulin (positive control), and pUC 18 (negative control). Figure 8.5 shows that nuclei isolated from cells exposed to shear stress had a significantly lower transcriptional activity of the ET-1 gene than in static control nuclei. This decrease in ET-1 gene transcription by shear is a specific response because transcription of the α -tubulin gene was not altered by fluid shear stress. ET-1 mRNA is relatively unstable and has been reported to have a half-life of approximately 15 min (Inoue A. et al., 1989). In order to rule out the possibility that the decrease in ET-1 mRNA levels in response to shear was the result of a further increase in ET-1 mRNA instability, mRNA half-life measurements were performed by adding a transcriptional inhibitor, actinomycin D (5 μ g/ml), coincident with the onset of shear. Figure 8.6 shows densitometry of Northern blot analysis of the treated cells and the computation of the half-life by exponential fit, yielding a half-life of 17 min for

static cells and 20 min for cells exposed to shear. These results indicate that the decrease in the rate of transcription is primarily responsible for the decrease of ET-1 mRNA expression in response to fluid shear stress.

8.1.4 Transfection studies

In order to determine whether the decrease in ET-1 gene transcription by shear and PMA is mediated by the 5'-flanking sequence of the ET-1 gene, transfection experiments were performed using reporter constructs containing four portions of the 5'-flanking sequence of the ET-1 gene: -157 bp, -1.5 kb, -2.5 kb, -2.9 kb, and -4.4 kb. The reporter constructs containing 4.4 kb and 2.9 kb of the 5'-flanking region of the ET-1 gene showed that both shear stress and PMA treatment induced a decrease, following 18 hrs of treatment, in the transcriptional activity at the 5'-flanking region of the ET-1 gene (Figure 8.7). These results are consistent with the nuclear runoff transcription experiments and indicate that the downregulation of the ET-1 gene is transcriptionally regulated. In contrast, the reporter constructs containing 157 bp and 1410 bp of the 5'-flanking region failed to show any measurable change with shear stress or PMA treatment. This allows one to conclude that the 400 bp region contained between -2.5 and -2.9 kb is necessary for conferring shear-responsiveness to the ET-1 gene.

Treatment with retinoic acid has been shown to cause ET-1 downregulation along with a decrease in GATA-2 mRNA (Dorfman D.M. et al., 1992). Measurement of GATA-2 mRNA levels did not reveal any change in response to shear stress (data not shown). These results suggest that the two important *cis*-elements required for the basal transcription of the ET-1 gene, the GATA-2 site located at -135 and the AP-1 site at -109 bp, do not seem sufficient to mediate shear-induced ET-1 downregulation.

8.1.5 Conclusion

The results in the first part of this chapter are the first to show that shear stress can induce a change in gene expression via a change in transcription, and not via changes in mRNA stability. The findings imply that shear induces a signal to the nucleus which then acts on the upstream region of the ET-1 gene, probably via the region between somewhere between -2.5 kb and -2.9 kb. The further refining of location and the sequence of this "shear-stress responsive element" (SSRE) is presently being undertaken.

8.2 Second Messenger involvement

The mechanism of transduction of shear forces into altered gene regulation is not well understood. Recent studies have shown that flow and shear stress can induce transient increases in intracellular calcium $[Ca^{2+}]_i$ by both an ATP-dependent (Mo M. et al., 1991) ($\Delta[Ca^{2+}]_i=100-400$ nM) and ATP-independent ($\Delta[Ca^{2+}]_i=75$ nM) (Shen J. et al., 1992) mechanism in BAEC. Earlier experiments have indicated that shear stress can double the levels of inositol tris-phosphate (Nollert M.U. et al., 1990) and increase the incorporation of arachidonic acid into diacylglycerol in human vascular endothelium (Nollert M.U. et al., 1989). Mechanical stimulation of other cell types has also been shown to affect intracellular second messenger systems. In rat neonatal cardiac myocytes, uniaxial stretch increases phosphoinositide turnover and protein kinase C activity, but not cAMP levels (Komuro I. et al., 1990 and 1991), while hypotonic swelling in lymphocytes (Watson P.A., 1990) has been suggested to increase adenylate cyclase activity via a mechanically-induced conformational change, with a resulting increase in intracellular cAMP (Watson P.A., 1991). Furthermore, activators of

protein kinase C and adenylate cyclase are also known to induce morphological alterations of vascular endothelial cells in a synergistic fashion (Antonov A.S. et al., 1986). These findings, along with the observed cell shape change resulting from application of shear stress, suggest a potential role for protein kinase C or adenylate cyclase in mediating changes in gene regulation in response to shear stress.

Although there exists a large body of literature on endothelial biology, little is known about the signalling mechanisms involved in the transduction of shear stress on the endothelial cell into altered cell function. This is at the present a field of intense research. A number of potential mediators of the shear stimulus into altered ET-1 expression were evaluated.

8.2.1 Protein kinase C

Treatment of endothelial cells with phorbol ester, an activator of protein kinase C, has been reported to induce increased ET-1 mRNA (Inoue A. et al., 1989). However when BAE cells were treated with phorbol 12-myristate 13-acetate (PMA, 100 nM), only a mild increase in ET-1 mRNA was observed at short times (20 min) followed by a very dramatic decrease by 2 hr which rendered ET-1 mRNA nearly undetectable (figure 8.8). This observation suggested the possibility of increased PKC activity being responsible for the shear-induced regulation of ET-1. This hypothesis was further strengthened by the observations of Nollert et al. (Nollert M.U. et al, 1989 and 1990) concerning increased arachidonic acid uptake, IP₃, and DAG levels in response to shear stress in HUVE cells. In order to rule this possibility in or out, a number of experiments were carried out.

8.2.1.1 PMA-induced ET-1 regulation in presence of CHX

Another route was used to assess the role of protein kinase C in the shear-induced regulation of ET-1. BAE cells, pre-treated with CHX for 1 hr to inhibit *de novo* protein synthesis, were incubated with PMA for various time durations. Figure 8.9 shows that despite the superinduction effect of CHX on ET-1 mRNA, PMA induced decreases in ET-1 mRNA both in the presence and absence of CHX. This finding, in contrast with the result in figure 8.2 showing the dependence of shear-induced ET-1 downregulation on ongoing protein synthesis, suggests that the PMA- and the shear-induced downregulation of ET-1 are different processes, diverging at least at one step.

8.2.1.2 PKC activity measurement

Protein kinase C has been shown to be mostly in the soluble fraction of the cell lysate under basal conditions and becomes membrane-bound or translocated to the particulate fraction when it is stimulated by phobol ester or other agonists (Thomas T.P. et al., 1987; Nishizuka Y., 1986). Thus, BAE cells subjected to 15 min of shear stress at 20 dyn/cm², were lysed, separated into soluble and particulate fractions, and partially purified by passage through DE-52 columns (cf. Appendix). The activity of PKC was then evaluated by measuring the incorporation of label into histone IIIs in the presence of Ca²⁺ and diolein. The results (figure 8.10) show that although PMA (100 nM) induced a frank translocation from the soluble to the particulate fraction, shear stress of 20 dyn/cm² for 15 min did not result in significant difference when compared to the static control. Although some experiments at the higher shear stress of 36 dyn/cm² showed some translocation, the results at 20 dyn/cm², a magnitude at which ET-1 (and PDGF-B) mRNA is

readily downregulated, argue against the involvement of PKC in the shear-induced down-regulation of ET-1 and PDGF-B.

8.2.1.3 Immunoblotting with anti-PKC antibodies

Immunoblotting of soluble and particulate fractions obtained from BAE cells exposed to shear stress for varying times at 15 dyn/cm² was performed. Antibodies were used against the α and β isozymes of PKC (cf. Appendix) (Mattila P., 1991). The results of figure 8.11 show the absence of translocation of immunodetectible α -PKC in response to shear stress (20 dyn/cm²), in contrast to a significant translocation in response to PMA (100 nM) for 15 min. The β isoform of PKC was not detectable in BAE cell lysate.

8.2.1.4 PKC inhibitors

The first set of experiments consisted of using PKC inhibitors to block PKC function. Staurosporine (10 nM), a potent PKC inhibitor resulted in pronounced ET-1 mRNA decrease by itself in the absence of shear stress (figure 8.12). This phenomenon was accompanied by cell retraction and morphological alterations similar to those seen in response to PMA treatment, as well as a decreased resistance to shear at long time points (>6 hr) (Dlugosz A.A. et al., 1991; Antonov A.S. et al., 1986). Treatment with H-7 (30 μ M), an inhibitor of protein kinases with a high specificity towards PKC, did not interfere with basal ET-1 mRNA levels, and actually resulted in inhibition of the shear-induced down-regulation, reversing it into a slight up-regulation. However, treatment with HA-1004 (30 μ M), a compound structurally related to H-7 but less specific for PKC, also exhibited the same effect, arguing against the involvement of PKC inhibition in the H-7 effect. Sphingosine (10 μ M), another PKC inhibitor, was evaluated but

showed mixed results, in some experiments having no effect on the shear-induced ET-1 decrease and in others inducing decreased ET-1 mRNA under static conditions or sloughing under shear. Finally, Calphostin C (1 μ M), a recently described PKC inhibitor with a K_i \sim 50 μ M which binds to the regulatory portion of PKC (Koyabashi E. et al, 1989), was used. Calphostin C did not cause changes in basal ET-1 mRNA levels and did not affect the shear-induced downregulation of ET-1 mRNA (figure 8.13). Given concerns about calphostin C's activity changes under conditions of low light, experiments were conducted under both dark and light conditions and yielded the same result. Furthermore, Calphostin C did not affect the endothelial alignment in the direction of flow, arguing against the involvement of PKC in the morphological response to flow.

In summary, three lines of evidence argue against the involvement of protein kinase C in the downregulation of ET-1, PDGF-B, and TM in response to shear stress of 20 dyn/cm²:

1- Calphostin C (1 μ M), a potent PKC inhibitor which did not exhibit any unrelated side effects on the BAE cells, failed to affect the shear induced downregulation of ET-1,

2- the phorbol ester PMA (100 nM) caused a dramatic downregulation of ET-1 mRNA both in the presence and in the absence of CHX, while the down-regulation of ET-1 by shear stress was inhibited by CHX,

3- both enzymatic activity assays and immunoblotting experiments against protein kinase C failed to show translocation or activation in response to shear stress of 20 dyn/cm², a magnitude that is sufficient to decrease ET-1 mRNA.

8.2.2 Cyclic AMP

Watson (Watson P.A., 1990) has recently proposed cAMP as a potential second messenger responsible for transduction of intracellular forces, namely the swelling induced by external hypo-osmotic solution in S49 lymphoma cells, into altered cell metabolism. He has suggested that the membrane strain could result in altered adenylate cyclase activity possibly via a force-induced conformational change (Watson P.A., 1991). Furthermore, Reich et al. (Reich K. et al., 1990) has shown that applying flow can result in increased intracellular cAMP levels in osteoblasts and to some degree in some species of endothelial cells. Cyclic AMP has been previously shown to induce decreased DNA synthesis in BAE cells under static conditions, and has also been shown to potentiate the PMA-induced morphological alterations shown by Antonov et al. (Antonov A.S. et al., 1986; Shirinsky V.P. et al., 1989).

Treatment of BAE cells with forskolin, an activator of adenylate cyclase, resulted in sharp reductions in ET-1 mRNA levels within 4-6 hr (figure 8.14) which was also accompanied by mild cell retraction and stellate-like projections (figure 8.15). These findings suggested that cAMP may be mediating the observed effects of shear stress, namely the decreased DNA synthesis rate shown in chapter 4 and the decreased ET-1 gene expression. In order to test this hypothesis, intracellular cAMP was measured in BAE cells exposed to varying durations of shear stress. Figure 8.16 shows the time course of cAMP in response to shear stress as well as short-term (3 min) treatment with forskolin (10 μ M). It is evident that shear did not induce any significant changes in intracellular cAMP content at the various time points while forskolin induced a 10-fold increase, suggesting that the shear-induced down-regulation of ET-1 cannot be accounted for by changes in cAMP.

8.2.3 Cyclic GMP

One of the central roles played by the endothelial cell is the quasi-instantaneous release of EDRF (nitric oxide) in response to acetylcholine (Ach) and blood flow, resulting in smooth muscle cell relaxation and vessel dilation (Rubanyi G.M. et al., 1986). Recent work has demonstrated that agents that increase intracellular $[Ca^{2+}]$ such as ionophore (A23187) and bradykinin result in EDRF release and subsequent increase in intracellular cGMP (Martin W. et al., 1988). Nitric oxide (NO), a labile compound with a short half-life of approximately 10 s increases soluble guanylate cyclase activity, and is responsible for the increased cGMP levels, a finding that has been confirmed by using NO quenchers such as hemoglobin and inhibitors of arginine metabolism such as L-NMMA. cGMP analogues as well as nitric oxide-generating compounds have been shown to decrease endothelial rates of DNA synthesis. Intracellular cGMP content was measured in BAE monolayers exposed to shear stress (20 dyn/cm^2) or to atrial natriuretic peptide (ANP, $10 \text{ }\mu\text{M}$). Figure 8.17 shows that shear stress quickly (within 1 min) results in increased cGMP levels that remain elevated for as long as 1 hr following the stimulus. This increased cGMP has been demonstrated to be the result of increased NO release and is blocked by L-NMMA (Cooke J.P. et al., 1991). In order to evaluate the role of NO-induced cGMP increase in the shear-induced downregulation of ET-1, cells pre-treated with $50 \text{ }\mu\text{M}$ L-NMMA were subjected to shear stress of 20 dyn/cm^2 . Figure 8.18 shows that BAE cells still respond to shear stress by decreasing ET-1 mRNA in the presence of NO synthesis inhibitors, suggesting that the regulation of ET-1 mRNA is not mediated by EDRF and is most likely independent of cGMP. Recently, the Frangos group (Kuchan M.J. et al., 1993) has published data showing that another inhibitor of NO synthase, L-NNA, can effectively block the shear-induced decrease in ET-1 peptide. It is unclear whether this is also mirrored by

decreased ET-1 mRNA or whether it occurs via a later step (i.e. protein processing, stability, export).

8.2.4 Cyclooxygenase

Cyclooxygenase has been previously shown to be important in the shear induced increase in PGI₂ release (Bhagyalakshmi A. et al., 1989). Using 10 μM ibuprofen to inhibit cyclooxygenase function did not interfere with the shear-induced downregulation of ET-1 mRNA. This finding rules out the possibility of autocrine action by any of the prostaglandin products on the transduction of shear into ET-1 gene expression (figure 8.19). Ibuprofen also did not interfere with cell alignment in the direction of shear stress (data not shown).

8.2.5 Intracellular calcium

Ando et al. showed in 1988 (Ando J. et al., 1988) using average FURA-2 quantitative fluorescence microscopy that BAE cells exposed to shear stress underwent transient increases in intracellular Ca²⁺. Although Ando's finding was not initially duplicated by other groups, it became clear that ATP present in the perfusion solution used by Ando was responsible for the large transient Ca²⁺ increase (Mo M. et al., 1991). Hsieh et al. (Hsieh H. et al., 1991) using single-cell calcium measurements showed that BAE cells responded to shear stress of magnitude as low as 0.5 dyn/cm² by increases in intracellular calcium of 50-100 nM in a magnitude-dependent fashion up to 20 dyn/cm² even in the absence of ATP. This finding propose Ca²⁺ as a central second messenger that may be important in the signal transduction of shear stress in endothelial cells.

Quin-2 AM (acetoxymethyl ester, 10 μM), a membrane-permeable chelator of intracellular calcium (Di Virgilio F. et al., 1984), was used to pretreat BAE cells

prior to applying shear stress of 20 dyn/cm². Figure 8.20 shows that calcium chelation by Quin-2 AM prevented the shear stress-induced down-regulation of ET-1 (Quin2-AM pretreatment followed by washout did not; this is to be expected since Quin-2 is broken down with time by intracellular enzymes). Attempts to chelate calcium with another agent, BAPTA-AM, resulted in cell death and sloughing under shear at ~10-12 hr. Quin-2 AM also prevented with the shear-induced cell shape change and alignment (figure 8.21), and interfered with stress fiber induction in the direction of shear (figure 8.22). These results seem to implicate intracellular calcium as a key second messenger in the transduction of shear stress into altered ET-1 expression.

8.2.6 Tyrosine phosphorylation

Phosphorylation of proteins on one or more tyrosine residues has been shown to be a key signalling pathway in the regulation of cell growth and division. Recent work has revealed the existence of a number of cytoskeletal proteins containing SH2 domains which can interact with tyrosine kinases such as paxillin, which is associated with focal adhesion complexes (Turner C.E., 1991), and the actin-binding protein tensin (Davis S. et al., 1991). Since shear stress exerted on the endothelial cell results in cytoskeletal and focal contact rearrangement, it is tempting to postulate that shear stress may act via cytoskeleton-associated proteins resulting in an altered pattern of tyrosine phosphorylation inside the cell, leading to altered cell function. We explored the role of steady laminar shear stress (magnitude 20 dyn/cm²) on the tyrosine phosphorylation (p-tyr) pattern in BAE cell monolayers and have found that several proteins demonstrate increased phosphotyrosine contents including M_r ~90, ~65, ~55 and ~40 kDa (figure 8.23, arrowheads). The increase in tyrosine phosphorylation occurs as soon as 1 min

following onset of flow for pp90, pp55, and pp40, but appeared somewhat later for pp65. The increase in p-tyr of pp65 was most prominent and was observed as soon as 5 min after onset of shear, and remained sustained at 120 min of shear (figure 8.23) and up to 18 hr (not shown). Given the recent reports implicating pp125^{FAK} phosphorylation in response to cell shape changes and spreading (Burrige K. et al., 1992; Lipfert L. et al., 1992), we performed immunoprecipitation of total protein from BAE monolayers with anti-pp125^{FAK} followed by western blot analysis with anti-phosphotyrosine antibody. We found however no change in p-tyr content of pp125^{FAK} at 1, 5, 15, 30 min nor at 6 hr of shear stress suggesting that the identity of the proteins seen in figure 8.23 is different (data not shown).

We then evaluated the importance of $[Ca^{2+}]_i$ in the shear-induced increased p-tyr by loading of BAE cells with Quin2-AM (10 μ M, 30 min), the membrane permeable calcium ion chelator (Di Virgilio F. et al., 1984). Quin2-AM pretreatment prevented the shear-induced increase in phosphotyrosine content (figure 8.24, left). Inhibiting tyrosine kinase activity by pretreatment of BAE monolayers with herbimycin A (875 nM, 24 hr) (Uehara Y. et al., 1991) also prevented the increase in p-tyr content (figure 8.24, right). Together, these findings suggest that the increase in p-tyr in response to shear to be dependent on $[Ca^{2+}]_i$, and likely the result of increased tyrosine kinase activity and not of decreased phosphatase activity.

We then examined the role of TK activity in the regulation of ET-1 gene expression by flow. Herbimycin A inhibited the shear-induced downregulation of ET-1 mRNA (1.0 \pm 0.13 vs. 0.18 \pm 0.03, $p < 0.01$) (figure 8.20) previously described to be transcriptional and independent of protein kinase C and cAMP signaling (Malek A.M. et al., 1993b). These findings extend the importance of both $[Ca^{2+}]_i$ and tyrosine kinase activity in the longer-term responses of the endothelial cell to

shear. Herbimycin A pretreatment also interfered with the long-term cell shape change and alignment as well as the actin stress fiber induction in response to shear stress (figures 8.21 and 8.22).

8.3 Discussion

Our findings point to tyrosine phosphorylation as an early endothelial response to flow which is dependent on $[Ca^{2+}]_i$. Geiger et al. (Geiger R.V. et al., 1992) have demonstrated flow-induced increases in $[Ca^{2+}]_i$ release early following onset of flow from intracellular stores peaking at ~40 s and depending at times greater than 40 s, on influx from extracellular medium. Prasad et al. (Prasad A.R.S. et al., 1993) have recently shown that flow causes a biphasic increase in IP_3 content in BAE cells with a peak at ~15 s followed by a later and greater increase at 5 min. Our results suggest that intracellular calcium is crucial for the shear-induced tyrosine phosphorylation. The precise mechanism of how tyrosine kinase activity and $[Ca^{2+}]_i$ release are linked is, at the present, not known. We were not able to explore the importance of extracellular Ca^{2+} in the longer-term endothelial response to shear because extracellular addition of EGTA resulted in cell rounding by 1 hr and subsequent detachment under flow. Similarly the TK-inhibitor genistein induced BAE cell rounding and basal ET-1 mRNA decrease under static conditions by 2 hr, which precluded its use.

Shear induces cytoskeletal reorganization and induction of actin stress fibers which are thought to originate from focal adhesions (Franke R. et al., 1984; Wechezak A.R. et al., 1985; Kim D.W. et al., 1989). Recently it has been shown that focal adhesions contain cytoskeleton-associated proteins having tyrosine kinase activity such as pp125^{FAK} (Burrige K. et al., 1992; Lipfert L. et al., 1992), and that such activity may be important in focal adhesion and actin stress fiber

formation. The inhibition by herbimycin A of shear-induced endothelial cell shape change and actin stress fiber formation described here is consistent with its observed inhibition of focal adhesion and stress fiber formation during fibroblast spreading on fibronectin-plated substrate (Burrige K. et al., 1992). Wang et al. (Wang N. et al., 1993) have demonstrated that mechanical forces can be transduced through the cytoskeleton via integrin receptors at focal adhesions. Shear stress has been reported to influence focal adhesion formation dynamics (Robotewskyj A. et al., 1991). Taken together, these results suggest a pathway whereby shear forces on the surface of the endothelial cells may be transmitted to the underlying focal adhesions via the cytoskeleton (Ingber D., 1991; Davies P.F. et al., 1993). Although it is tempting to speculate that such force transmission may in turn affect TK activity of focal adhesion-associated proteins such as pp125^{FAK} (Burrige K. et al., 1992; Lipfert L. et al., 1992), our results from anti-pp125^{FAK} immunoprecipitation revealed no shear-induced change in p-tyr content. This result does not however preclude changes of other SH-2 domain-containing cytoskeleton-associated proteins (Davis S. et al., 1991), which could rapidly transduce externally-applied shear into intracellular signalling. We are currently in the process of determining the identity of the proteins demonstrating increased p-tyr content under shear, particularly p55 which consistently showed the greatest increase in p-tyr under shear. Recent work has revealed that tyrosine phosphorylation can play an important role in directly regulating transcription factor activity and nuclear translocation in some systems (such as in response to γ -IFN) (Schindler C. et al., 1992). Given our previous work showing shear stress inducing a decrease in the transcription of the ET-1 gene via a 400 bp sequence at -2.5 kb of the promoter region (Malek A.M. et al., 1993b), the requirement for p-tyr in shear-regulation of the ET-1 demonstrated here raises the possible existence

of a link between tyrosine phosphorylation and the gene regulatory responses to shear.

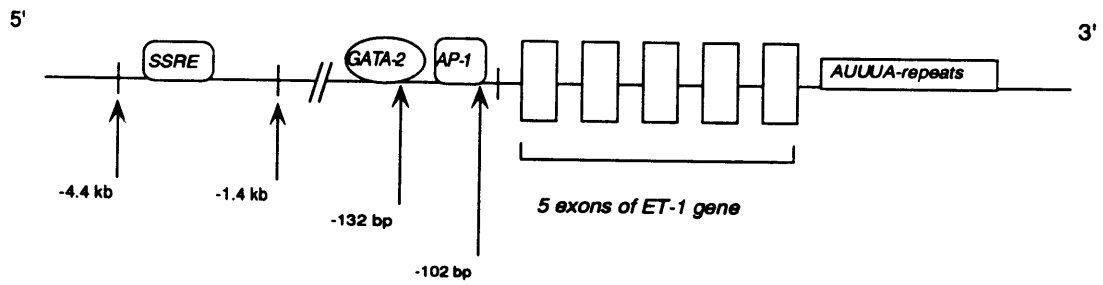


Figure 8.1 Schematic representation of ET-1 gene.

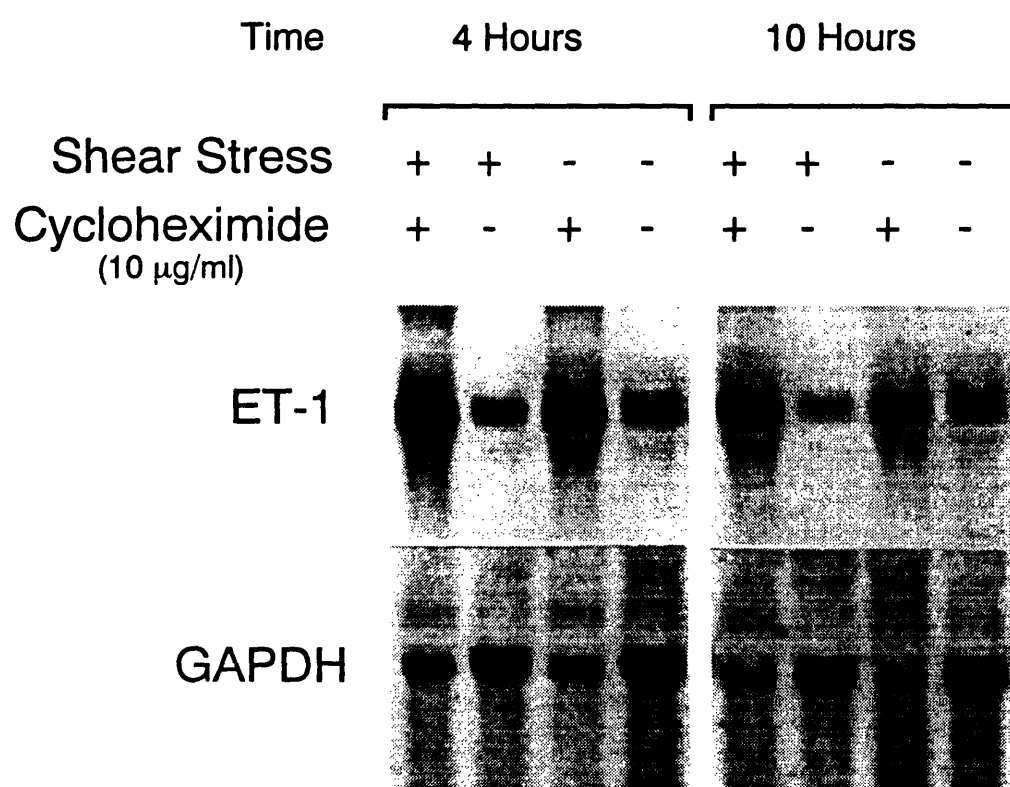


Figure 8.2 ET-1 downregulation by shear is dependent on protein synthesis.

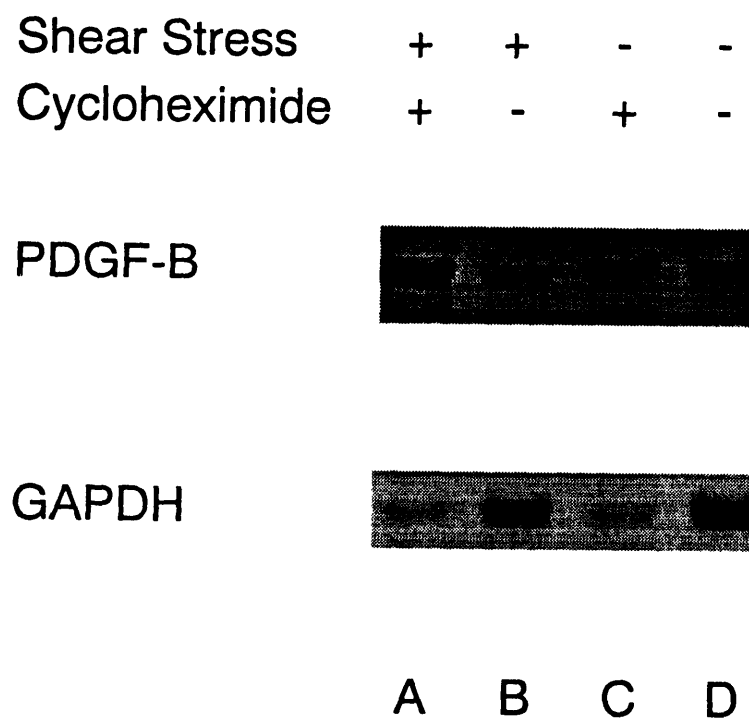


Figure 8.3 PDGF-B mRNA downregulation by shear is dependent on protein synthesis.

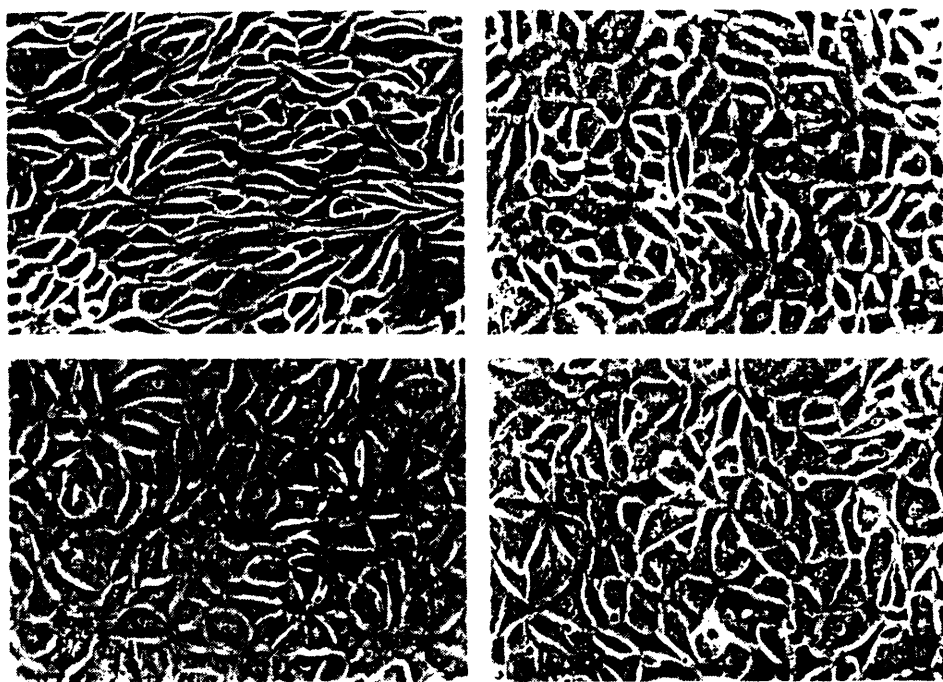


Figure 8.4 BAE cell alignment is dependent on protein synthesis.

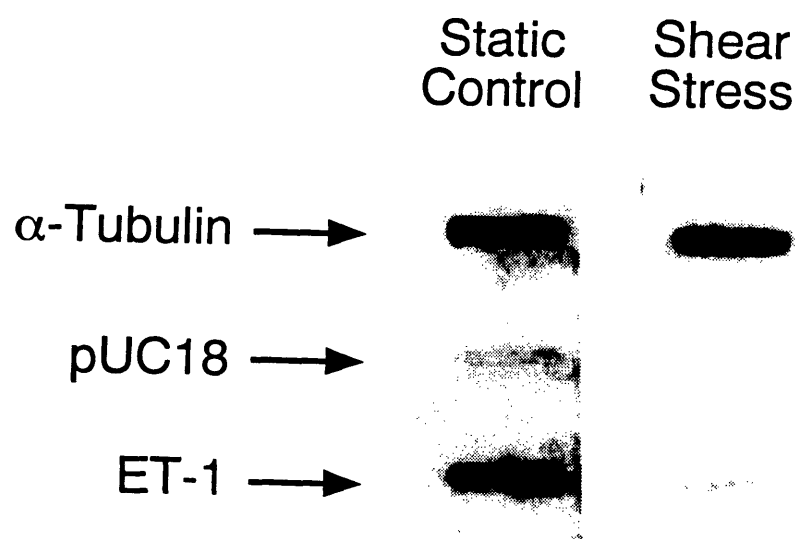


Figure 8.5 Nuclear runoff of BAE cells to measure ET-1 transcription under shear stress.

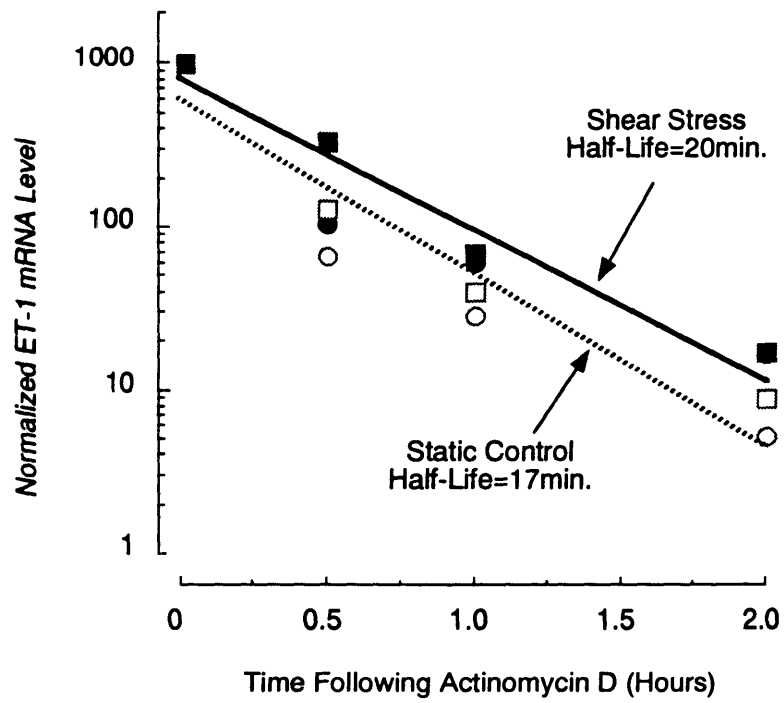


Figure 8.6 ET-1 mRNA stability analysis under shear stress.

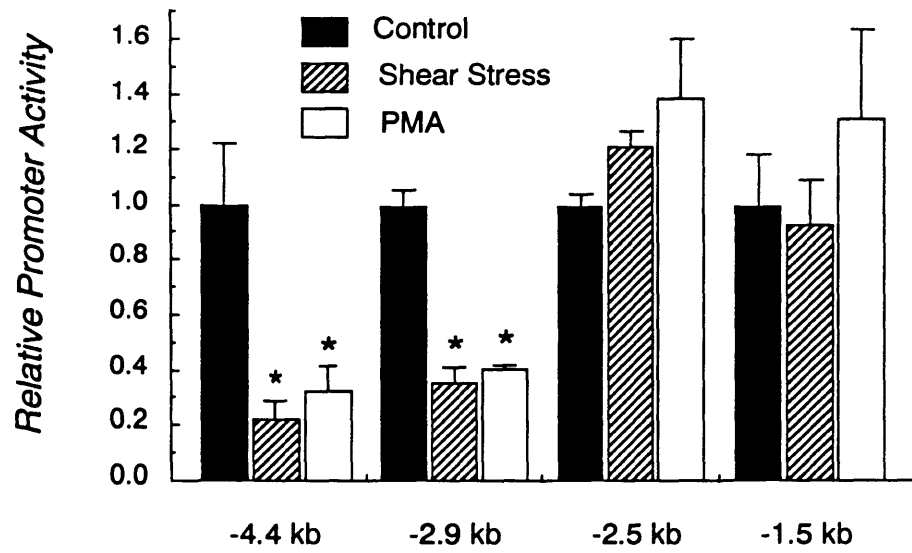


Figure 8.7 Transfection analysis of ET-1 gene promoter reporter constructs under shear stress.

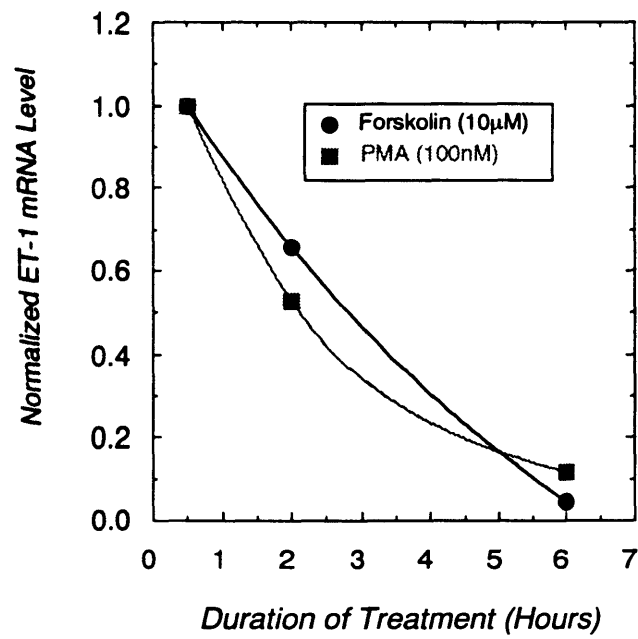


Figure 8.8 ET-1 mRNA decreases in response to forskolin and PMA.

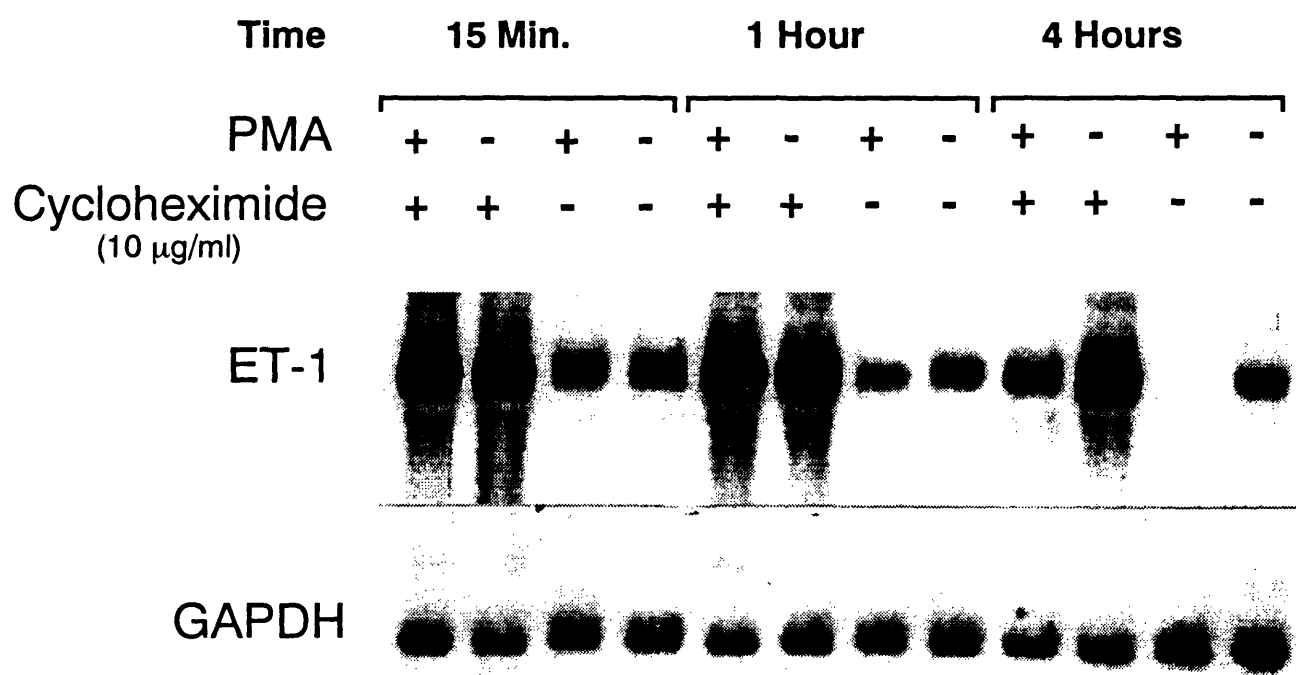


Figure 8.9 ET-1 mRNA downregulation by shear is dependent on protein synthesis.

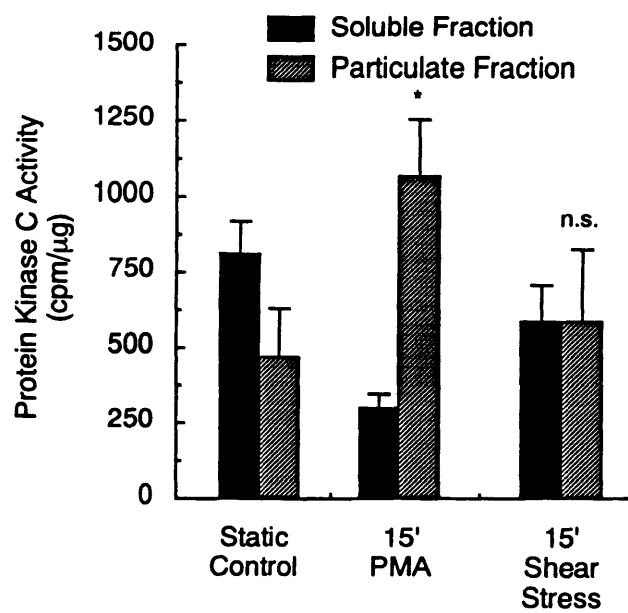


Figure 8.10 Shear stress (20 dyn/cm²) does not significantly induce translocation of PKC activity.

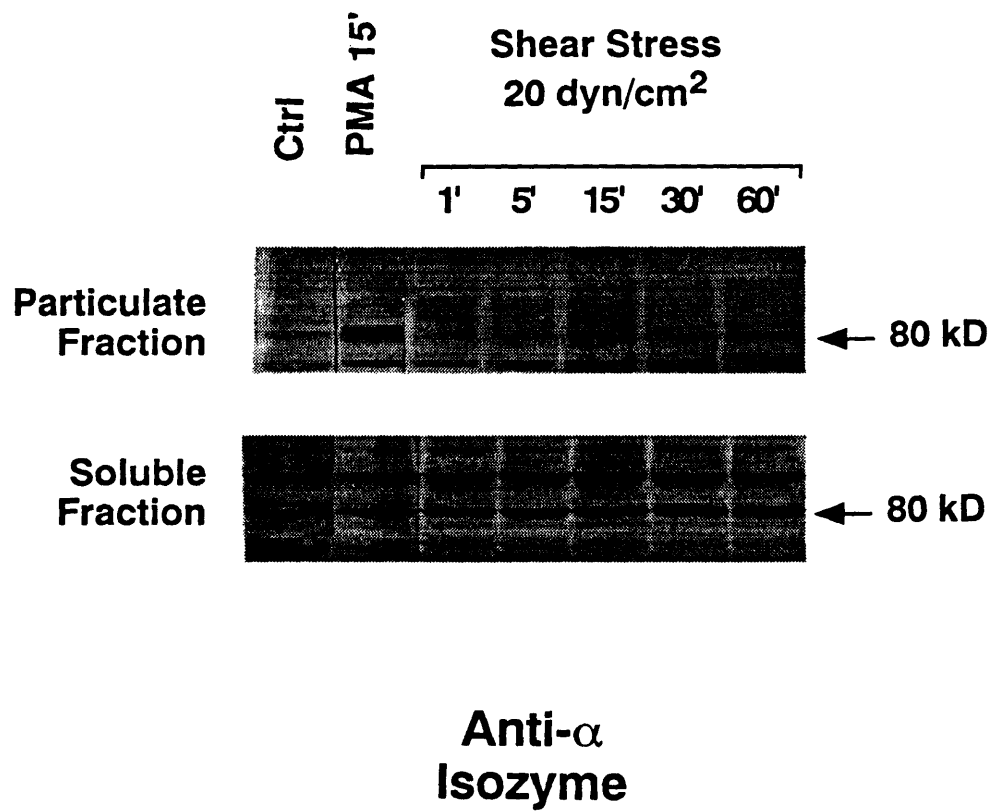


Figure 8.11 Shear stress (20 dyn/cm²) does not induce PKC translocation.

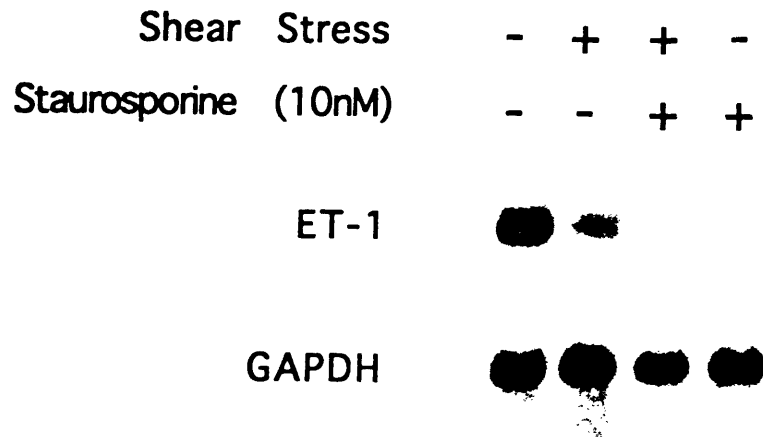


Figure 8.12 Staurosporine decreases ET-1 mRNA expression.

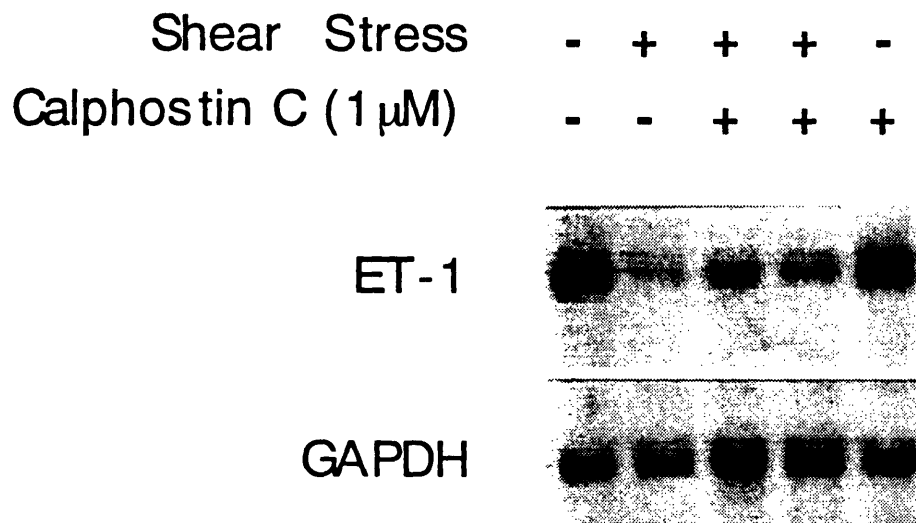


Figure 8.13 Calphostin C does not affect shear-induced ET-1 mRNA downregulation.

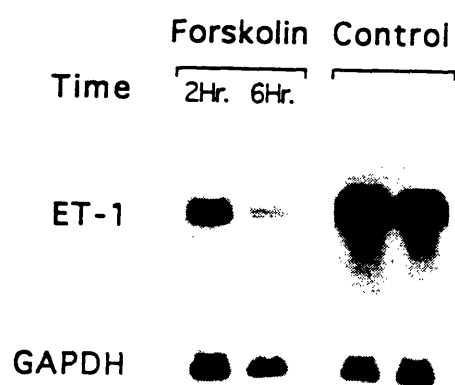
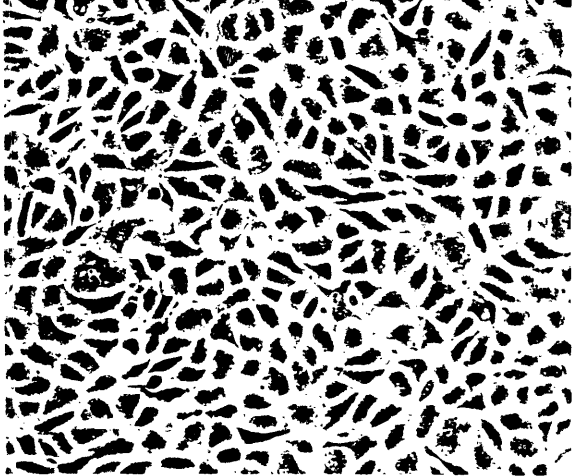
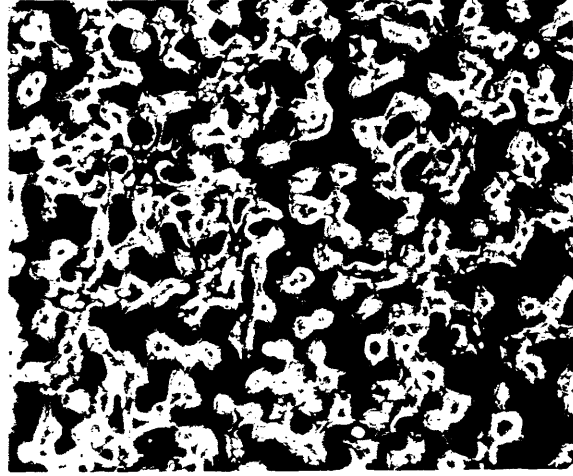


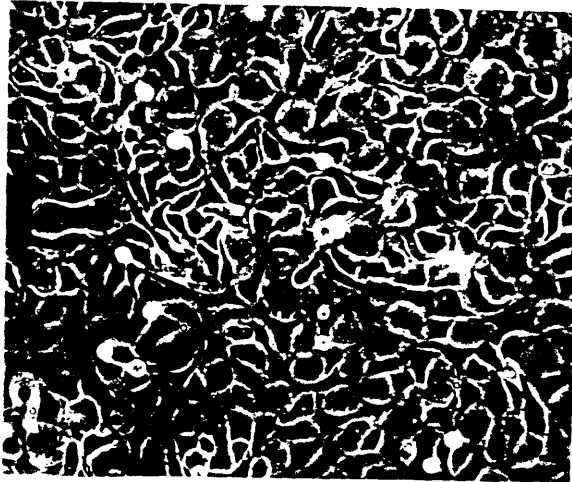
Figure 8.14 Northern blot analysis of BAE cells exposed to forskolin.



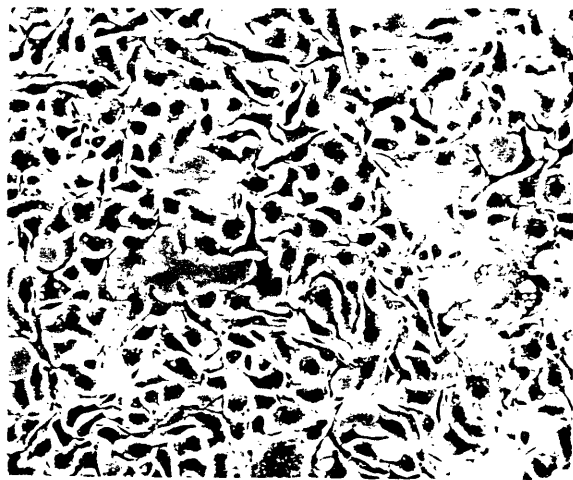
Control



Cytochalasin D



Forskolin



PMA

Figure 8.15 Phase-contrast micrographs of BAE cells exposed to Cyt D, forskolin, and PMA.

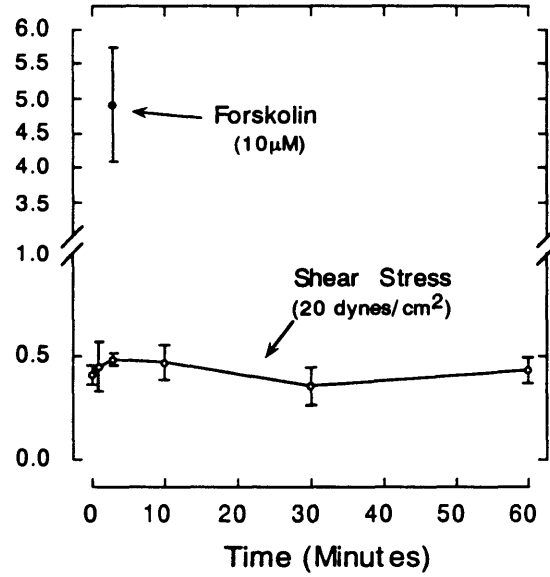


Figure 8.16 Radioimmunoassay of cAMP in BAE under shear and in response to forskolin.

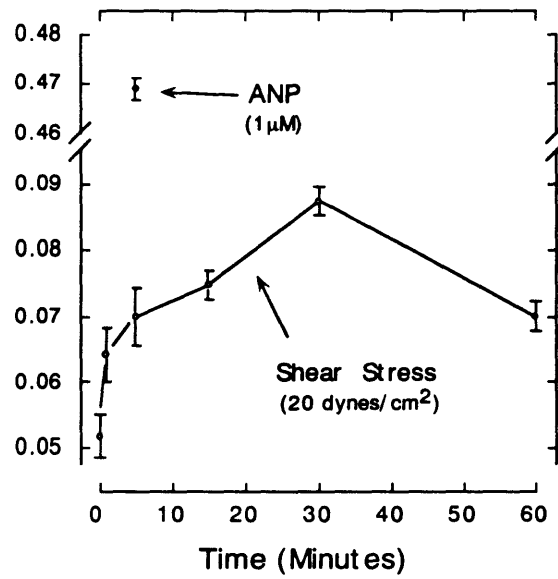


Figure 8.17 Radioimmunoassay of cGMP in BAE under shear and in response to ANP.

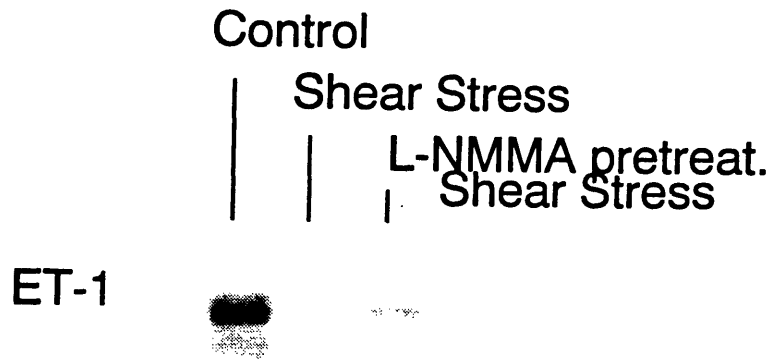


Figure 8.18 L-NMMA does not inhibit shear-induced ET-1 mRNA decrease.

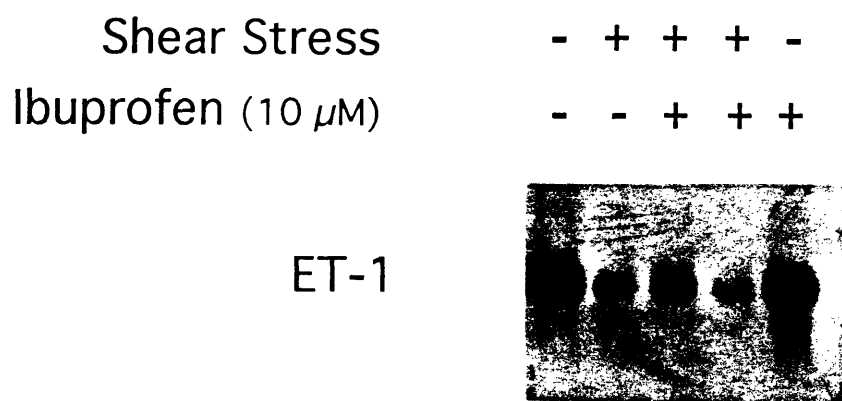


Figure 8.19 Inhibition of cyclooxygenase with Ibuprofen does not affect shear-induced ET-1 mRNA decrease.

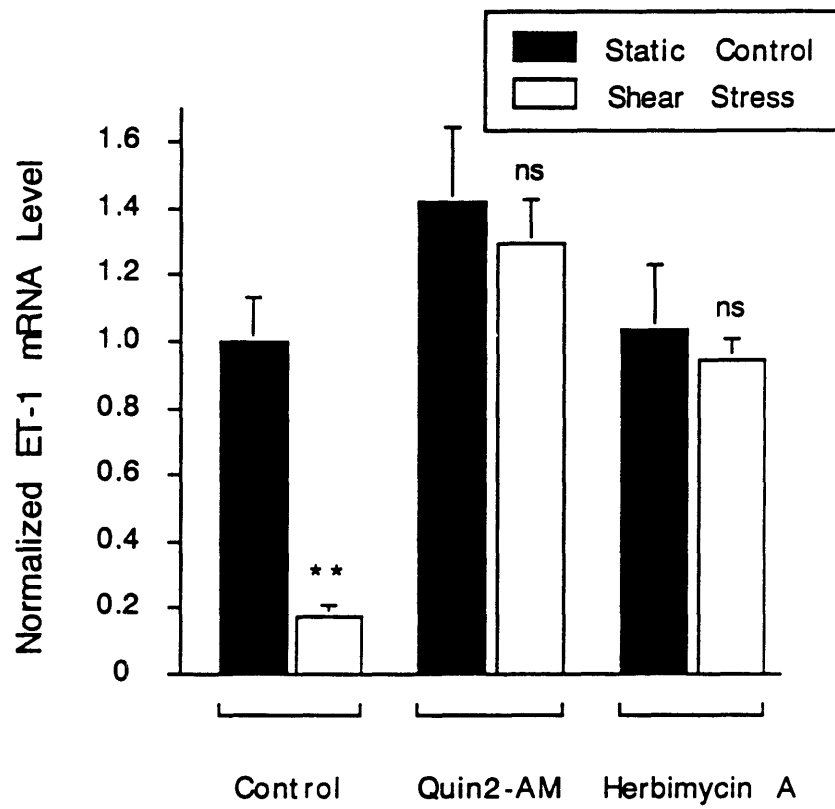


Figure 8.20 Chelation of intracellular calcium and inhibition of tyrosine kinase activity abolish shear-induced ET-1 downregulation.

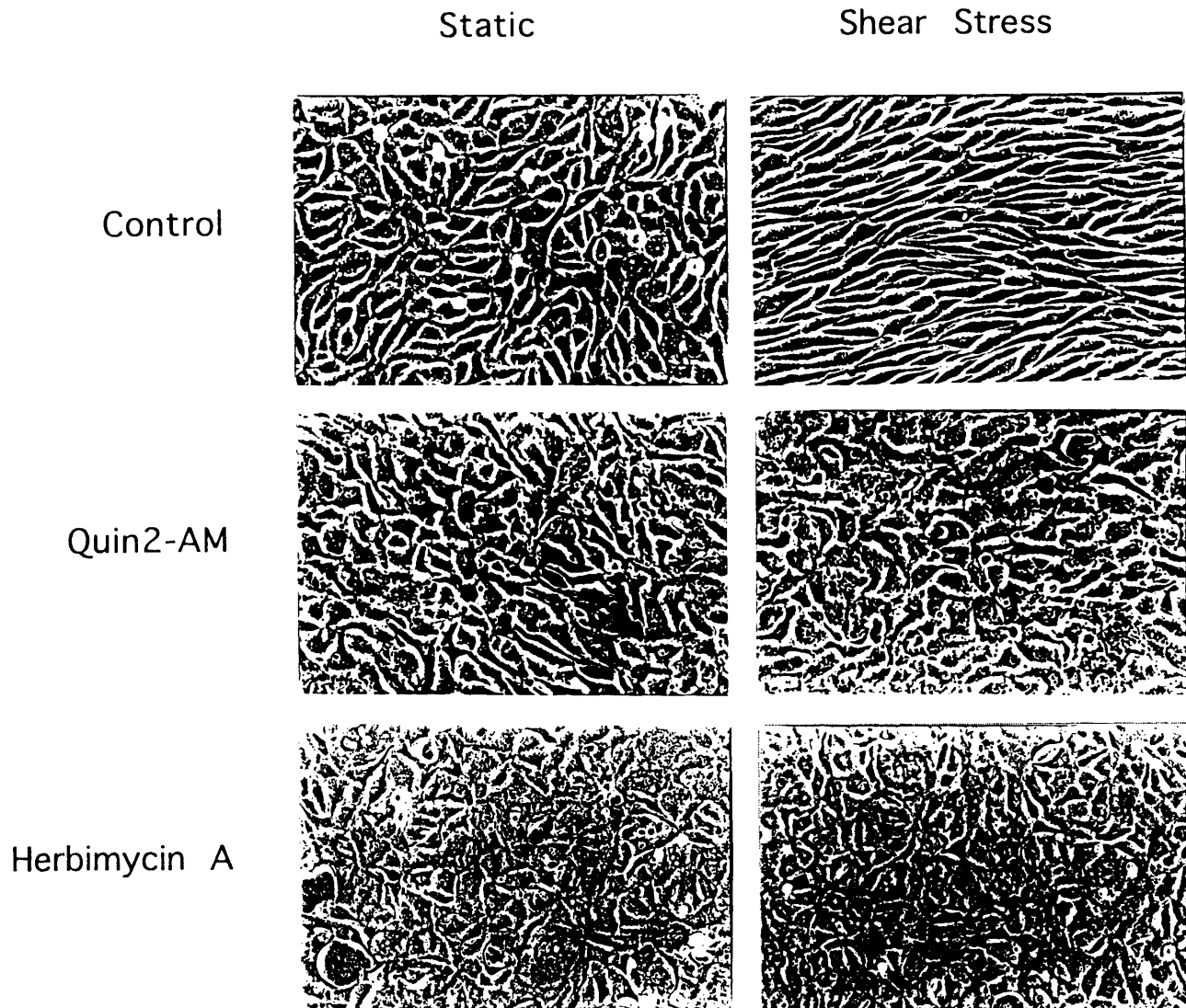


Figure 8.21 Quin2-AM and herbimycin A inhibit BAE cell shape change and alignment.

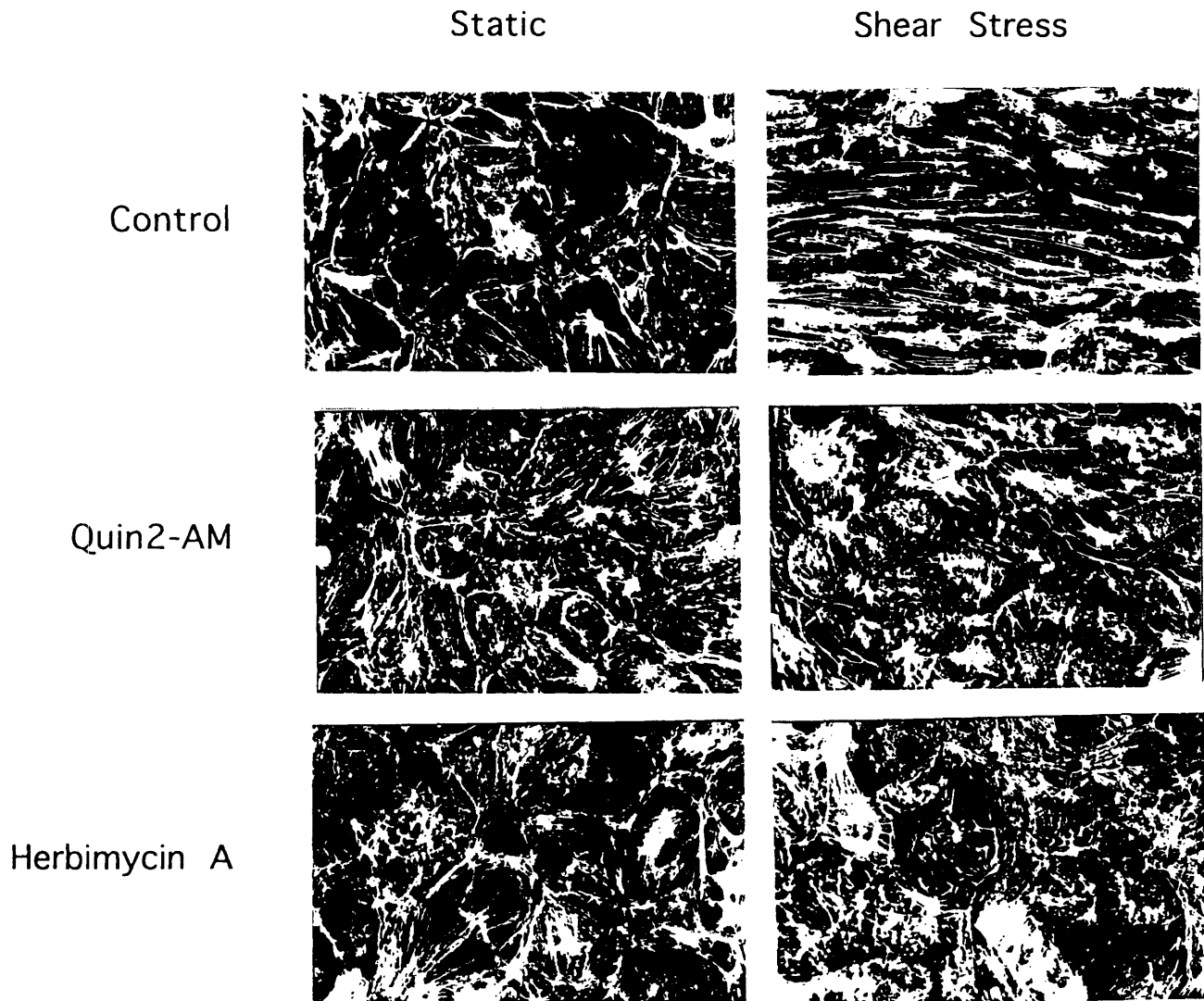


Figure 8.22 Quin2-AM and herbimycin A inhibit actin stress fiber induction under shear

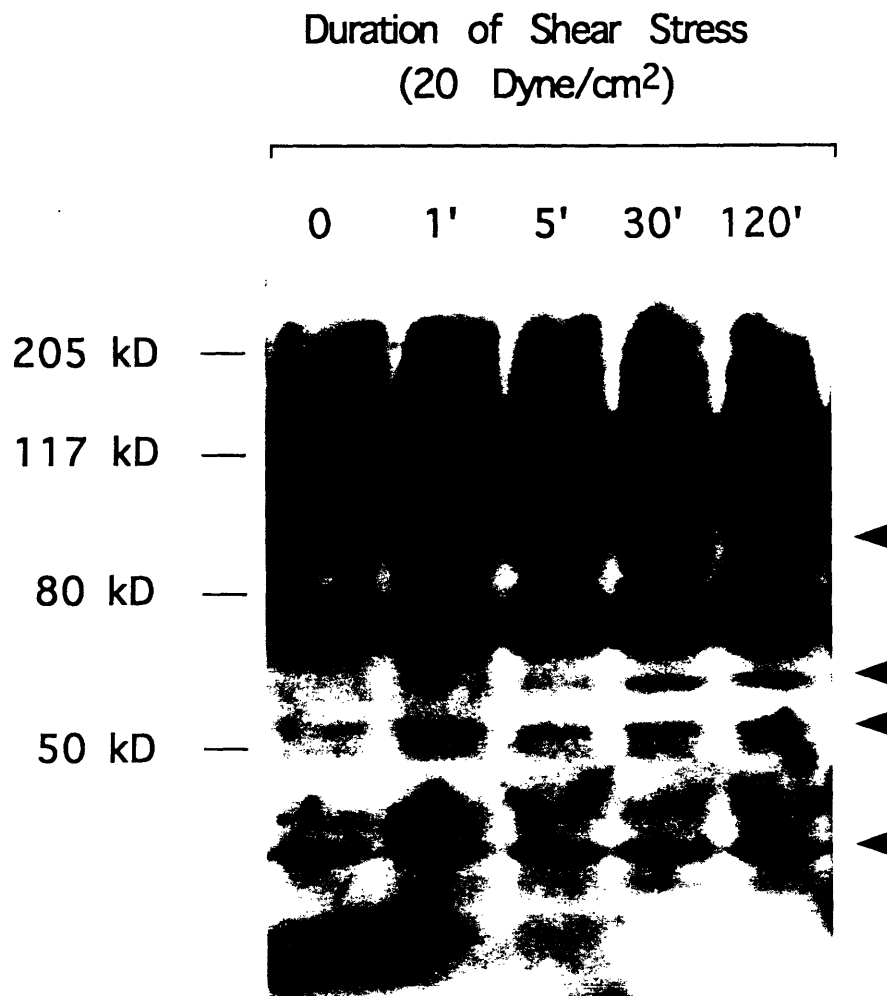


Figure 8.23 Shear stress (20 dyn/cm²) induces increased protein phosphorylation at tyrosine residues.

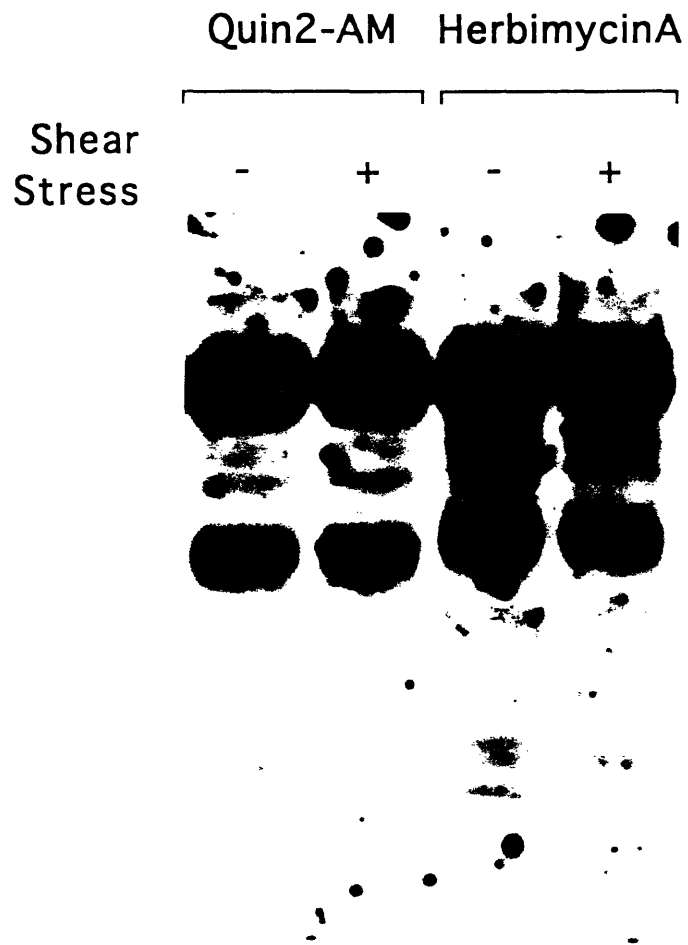


Figure 8.24 Shear-induced tyrosine phosphorylation is inhibited by Quin2-AM and Herbimycin A

CHAPTER 9

Role of Cytoskeleton and Mechanosensitive Channels in Shear Stress Transduction

9.1 Mechanosensitive channels

A number of sensory structures have been proposed as potential transduction entities of shear stress; they are schematically summarized in figure 9.1.

Two types of channels have been demonstrated in endothelial cells of aortic origin whose function is dependent on mechanical stimulation. The first one is the cation-selective channel of conductance ~ 40 pS (in standard saline) which is activated by membrane stretch induced by applying suction on the recording pipette. The channel is permeable to Na^+ and Ca^{2+} , is of the same type described by Guharay & Sachs in skeletal muscle and can be blocked by $10 \mu\text{M}$ gadolinium (Gd^{++}) (Lansman J.B. et al., 1987; Yang X.C. et al., 1989; Sadoshima J. et al., 1992; Naruse K. et al., 1993). The second type of channel is the shear stress-induced potassium hyperpolarizing current, $I_{K,S}$, described by Olesen et al. (Olesen S. et al., 1988). This current was demonstrated in BAE cells subjected to physiological magnitude of shear stress, is blocked by 1 mM barium chloride, BaCl_2 , has half-maximal magnitude at 0.7 dyn/cm^2 and saturates at 1.5 dyn/cm^2 . Jacobs et al. (Jacobs E.R. et al., 1993) have expanded Olesen's findings by demonstrating shear-activated inward-rectifier single K^+ channel recordings in BAE cells. The $I_{K,S}$ channel was found to desensitize within ~ 10 min, and appeared to be highly voltage-dependent and inhibited by tetraethylammonium (TEA). Although K^+ channels have been implicated in the flow-induced nitric

oxide-like vasodilator (EDRF) release (Cooke J.P. et al., 1991; Rubanyi G.M. et al, 1986), their role remains undefined in the longer-term gene regulation induced by shear.

9.1.1 Stretch-activated cation channel

Although this type of stretch-activated (SA) channel has been shown to play a role in some cell types, it is not clear whether it would be active under physiological shear stress conditions (Lansman J.B. et al., 1987). Figure 9.2 shows the normalized densitometric analysis of the Northern blot from two separate experiments where 10 μM gadolinium (in low-sulfate DMEM) was used to block the stretch channel in BAE cells exposed to 20 dyn/cm^2 of shear stress for 6 hr. The results indicate no inhibition of ET-1 downregulation by shear, ruling out the possibility of involvement of a stretch-sensitive cation-permeable channel of the type described by Lansman.

9.1.2 Shear stress-activated potassium channel

The initial experiment was carried out using DME medium supplemented with 10% calf serum. Although addition of 1 mM BaCl_2 did not interfere with the shear-induced downregulation of ET-1 in initial experiments, there appeared microscopic crystals on the BAE monolayer, suggesting that precipitation of barium salts had occurred, making the interpretation of the data difficult. Since barium sulfate has a very low solubility, a modified DME medium was prepared by substituting sulfate salts with their equivalent chloride counterparts (Cooke J.P. et al., 1991). Using this new medium, BAE cells still responded to fluid shear stress magnitude 20 dyn/cm^2 by downregulating ET-1 mRNA. No precipitation of barium crystals was observed upon addition of 1 mM BaCl_2 and the latter treatment

completely blocked the shear-induced decrease in ET-1 mRNA as seen in figure 9.2 without affecting basal levels of ET-1 mRNA in static cells. BAE cells also showed normal alignment in the presence of 1 mM BaCl₂. In order to further explore the role of the shear-sensitive potassium channel, TEA, a rather non-specific blocker of potassium channels was used. Although its effect on the shear channel has only been partially documented (Jacobs E.R. et al., 1993), it is a known blocker of endothelial calcium-activated potassium channels (I_{K,Ca}). Figure 9.2 illustrates the result of using 3 mM TEA, showing only a partial inhibition of the shear-mediated ET-1 decrease. It must be noted that recently Schilling et al. (Schilling W.P. et al., 1992) showed that neither 20 mM tetrabutylammonium (TBA), a TEA-related compound, nor charybdotoxin, a known blocker of I_{K,Ca}, had any effect on the shear-stress induced potassium efflux as measured by rubidium (⁸⁶Rb), a finding which is difficult to reconcile with recent work (Jacobs E.R. et al., 1993). In our system, 3 mM TEA did not have any effect on the endothelial cell shape change and alignment in response to shear. This result and our findings suggest that although I_{K,Ca} may be involved in ET-1 mRNA downregulation, it is not important for the morphological response to shear.

Finally, a reformulated high potassium ([K⁺]_o) DME enabled the evaluation of the role of cell depolarization on the ET-1 response to shear (figure 9.3). Use of [K⁺]_o=70 mM partially inhibited while [K⁺]_o=135 mM abolished ET-1 downregulation completely. These results confirm that I_{K,S} may be playing an important role in the regulation of ET-1 but they also suggest the importance cell membrane voltage, since TEA, BaCl₂ and elevated [K⁺]_o all result in membrane depolarization. Furthermore, both elevated [K⁺]_o and barium chloride may block the entry of calcium into the endothelial cell and thus deplete the intracellular calcium stores of the endothelial cell by decreasing the voltage gradient driving

calcium influx from the extracellular space. Such an effect would explain why barium chloride and very high $[K^+]_o$ ($[K^+]_o=135$ mM) completely block the shear-responsiveness of ET-1 while TEA and intermediately high extracellular potassium ($[K^+]_o=75$ mM) have only partial effects. Another explanation of the result is that $I_{K,S}$ may be crucial in transduction of shear into altered ET-1 mRNA expression not via its hyperpolarization effect of potassium efflux, but perhaps through a mechanism which depends on potassium ion efflux itself. The answer will have to await better electrophysiological characterization of $I_{K,S}$ and the determination of its responsiveness to channel blockers. It is clear however that neither the shear-responsive K-current, $I_{K,S}$, nor the stretch-activated channel, $I_{S,A}$, play any significant role in transducing shear stress into altered cell morphology and alignment (data not shown).

9.2 Cytoskeleton

One of the cell structures that may be important in the transduction of shear stress, either directly or indirectly, is the cytoskeleton framework. It consists of the actin-myosin microfilament network, which has been shown to remodel in response to shear stress, the microtubule network, which is important in cell division but also thought to act as a compression element, and the intermediate filament network, which is thought to be important in stabilizing the nucleus (reviewed in Ingber D, 1993). Recent work has shown that various cytoskeleton-associated proteins may play a role in second messenger signaling, raising the possibility of transmission of shear forces into changes in cytoskeleton tension and potentially into altered activity of these proteins. The other hypothetical possibility entails the transmission of the shear-induced forces through the cytoskeleton and thereby to cytoskeletal-associated sensing structures such as mechanosensitive channels,

intracellular calcium pools, or to focal adhesion contacts containing tyrosine kinase activity.

9.2.1 Actin microfilament network

Cytochalasin D (Cyt D, 2 $\mu\text{g/ml}$) was used to treat confluent monolayer of BAE cells to disrupt the microfilament network. Cyt D treatment resulted in the rounding of BAE cells and retraction of their processes (figure 8.15). This phenomenon was time-dependent. Northern blot analysis of the Cyt D-treated BAE cells revealed significant decreases in ET-1 mRNA as soon as 2 hr and near-complete disappearance by 6 hr in a dose-dependent manner (figure 9.4). Cyt D treatment decreased the ability of the BAE cells to resist shear stress and precluded the study of the combined effect of shear stress and microfilament disruption. It is interesting to note that Cyt D treatment decreased ET-1 mRNA, a phenomenon also observed with phorbol ester and forskolin treatments, both of which result in cell retraction and cell shape change, though by different mechanisms. The projected area of BAE cells treated with 2 $\mu\text{g/ml}$ of Cyt D was computed using cell staining and image analysis program (cf. Appendix), and was found to decrease to less than 50% of control cells as soon as 1 hr following treatment (figure 9.5)

Experiments were then conducted in which BAE cells had been incubated for 24 hr with 10^{-5} M phalloidin to cause cross linking of F-actin then exposed to 6 hr of shear stress and analyzed for ET-1 mRNA content. Figure 9.6 indicates no significant difference in the extent of downregulation between untreated cells and treated cells in the amount of ET-1 mRNA decreased in response to shear stress.

9.2.2 Microtubule network

Microtubules form a network that surrounds the cell nucleus and forms an arboreal network that spreads to the cell perimeter (figure 9.10). It is involved in the transport of organelles and has been shown to contribute in to the force that the endothelial cell exerts on its substrate. Kolodney et al. (Kolodney M.S. et al., 1992) showed that disruption of the microtubule by nocodazole resulted in an increase in the contractile force generated by an endothelial monolayer grown on silicone. Although the microtubule network does not, unlike the actin-myosin microfilament network, generate force, it is thought to act as a relatively rigid scaffolding that may be acting as a compression element.

In order to address the importance of the microtubule system in the transduction of the shear stress effect, drug interference studies were carried out using:

- 1) nocodazole and colchicine, agents which cause depolymerization of the microtubules, and
- 2) taxol, an agent which increases microtubule polymerization.

Disruption of the microtubule network with nocodazole (1 $\mu\text{g/ml}$, 1 hr) resulted in a cell shape change that, unlike the one induced by cytochalasin D did not involve retraction, but rather a remodeling of the cell-cell borders from a heterogeneous one to a homogeneous one, with BAE cells appearing as symmetric polygons (figure 9.7, middle left to right) compared to control static cells (figure 9.7, top left to right) In order to quantitatively assess this phenomenon, phase-contrast micrographs were acquired and digitized using a frame-grabber board and morphometric analysis carried out (cf. Appendix). Following tracing of the cell border, connectivity analysis yielded the best fit ellipse through the contour and enabled the computation for each cell of a roundness ratio, with a ratio of 0 for a perfect line and 1 for a circle. The roundness ratio is shown for the various

treatments in figure 9.8. Upon exposure to shear stress, nocodazole-treated cells failed to align in the direction of shear stress and change cell shape significantly. In fact their roundness ratio increased in response to shear, while control cells had a lower value of roundness indicating cell alignment. More importantly, ET-1 mRNA was not downregulated by application of shear stress, while basal ET-1 mRNA levels in static cells were not measurably affected (figure 9.9). The staining of the microtubule network using α -tubulin antibody shows that the nocodazole-treated cells had a diffuse staining confirming microtubule network dissolution and did not change in conformation significantly upon exposure to shear stress (figure 9.10, middle left to right). The microtubule network of the BAE cells exposed to shear stress (figure 9.10, top left to right), in contrast showed a very clear realignment in the direction of the flow. This result suggests that an intact microtubule network is indispensable for the transduction or transmission of the shear effect into altered ET-1 gene expression as well as cell shape change. In addition, F-actin staining with TRITC-phalloidin revealed that microtubules were also crucial for the induction of actin stress fibers in the direction of shear stress (figure 9.11).

Conversely, taxol treatment was used to enhance tubulin polymerization (figure 9.10, bottom). Tubulin immunostaining showed that taxol treatment resulted in a significant increase in tubulin polymerization, with fine and dense uniform tubulin staining (figure 9.10, bottom left to right). Taxol did not prevent cell shape change and alignment in the direction of flow although it partially inhibited it (figure 9.7, bottom left to right). Taxol did not interfere with, nor inhibit, the down-regulation of ET-1 by fluid shear stress (figure 9.12), nor did it prevent the induction of actin stress fibers in response to shear stress (figure 9.11, bottom left to right).

The drug interference study shown above indicated that the presence of an intact microtubule network is essential for the downregulation of ET-1 mRNA, the cell shape change, and the actin stress fiber induction by fluid shear stress. The exact structure of the microtubule network may not by itself be important since taxol, which induced significant tubulin polymerization, did not interfere with any of these processes. Furthermore, the process of BAE cell alignment and ET-1 mRNA downregulation both share the common requirement of intact microtubules suggesting a potential, at least partially, common pathway.

A further potential explanation might be the need for protein synthesis which was previously shown to be required for both the cell shape change and the ET-1 mRNA downregulation by shear. Alternatively, disruption of microtubules has recently been shown to interfere with tyrosine phosphorylation, which is crucial for all three shear-dependent processes described here (Smallwood J.I. et al., 1993).

9.3 Cell shape

A number of the findings described in this thesis have suggested an intimate role between the shape of the BAE cell and its level of ET-1 mRNA. Downregulation of ET-1 mRNA was seen when any agent was used that causes BAE cell retraction, including phorbol ester (PMA), forskolin, cytochalasin D, and other pharmacological agents such as staurosporine and genistein. These data suggested a possible link, that may or not be related to the shear stress effect on ET-1 mRNA, between cell shape and ET-1 gene expression. Such a relationship between cell spreading and gene expression has been previously postulated (Ben-Ze'ev A., 1991). Previous studies have clearly shown a direct link between cell shape and intracellular pH_i , whereby round cells had a lower pH_i than spread cells (Schwartz M.A. et al., 1989). Ingber has shown that fibronectin cell proliferation

through its effect on cell shape, with cell spreading being a prerequisite for cell division (Ingber D., 1990). These reports and the results presented here suggested the hypothesis that BAE cell shape and spreading has an effect on ET-1 mRNA expression. This possibility was made more interesting since the recent report of decreased pH_i (Ziegelstein R., 1992) and the already established finding of decreased DNA synthesis rate in response to shear (Levesque M.J. et al., 1990 and cf. chapter 4) are both effects observed in round but not spread cells, suggesting that shear may somehow be similar to cell shape control. This could be occurring via a decrease in intracellular tension that could be mediated via the actin microfilaments to tyrosine kinase entities in focal adhesions. Consistent with the hypothesis of decreased intracellular tension in response to shear, BAE alignment in response to shear has been shown to result in decreased shear stress gradients (Barbee K.A. et al., 1994). Furthermore, the effect of varying the dynamic stimulus of shear stress indicated that stimuli which resulted in cell shape change such as pulsatile, turbulent, and steady shear stress all resulted in a decreased ET-1 expression while reversing shear stress which did not induce significant cell shape change also did not result in ET-1 mRNA downregulation (chapter 5).

Figure 9.13 shows BAE cells which were plated on uncharged non-adhesive Petri dishes coated with an increasing concentration of synthetic fibronectin fragments (Pronectin F). The figure shows that low Pronectin F concentrations resulted in weak attachment of BAE cells to the dish, which became stronger with increased pronectin concentration until the cells plated on 0.5 and 2 $\mu\text{g/ml}$ had a spread appearance, which was similar to cells grown on tissue culture plastic. Quantitation of projected cell surface area confirmed the result, and is shown in figure 9.14, where cells plated on 2 $\mu\text{g/ml}$ of pronectin F had the same computed projected surface area as cells grown on tissue culture plastic. Northern blot

analysis of ET-1 mRNA from the same cells indicates that ET-1 mRNA levels are depressed significantly and increase with increased cell spreading (figures 9.15). The normalized densitometric analysis appears in figure 9.16. The ET-1 mRNA increases with cell spreading are specific since GAPDH mRNA levels were constant across all cells. This finding confirms the suspicion raised by the decreased ET-1 mRNA levels seen with PMA, forskolin, Cytochalasin D, staurosporine, genistein, and other cell-retracting or shape-altering treatments. This allows the proposal of a unifying theme: expression of ET-1 mRNA is intimately linked to cell shape and/or cell spreading.

Although the link between cell shape and ET-1 expression may appear difficult to reconcile with the findings of ET-1 mRNA down-regulation occurring before cell shape change, the two findings are not mutually exclusive. It is not inconceivable that shear may alter intracellular tension prior to any detectable changes in cell shape, especially considering the viscoelastic properties of the cell and its cytoskeleton . This hypothesis is also consistent with the finding that a number of essential processes are shared between the two mechanisms: namely the requirement for protein synthesis, intact microtubules, intracellular calcium, and tyrosine kinase activity.

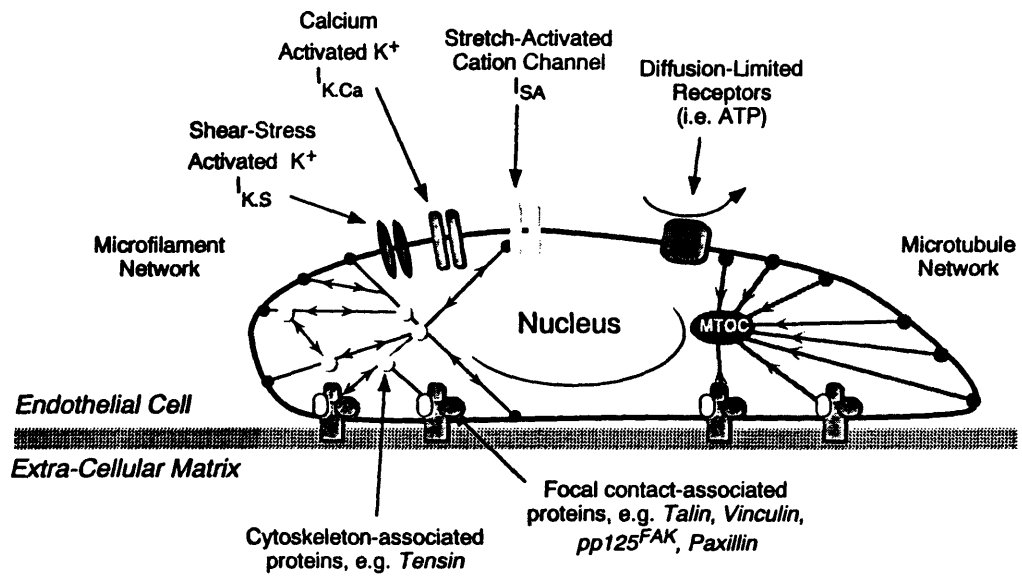


Figure 9.1 Model of potential cellular mechanotransducers of shear stress.

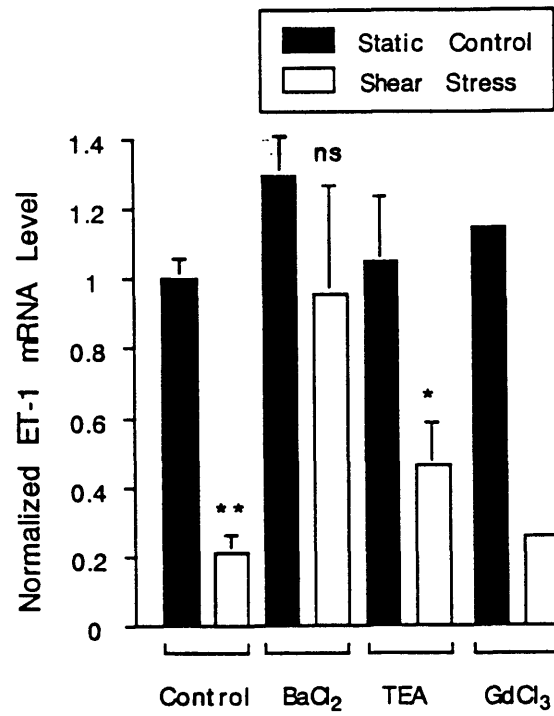


Figure 9.2 Effect of mechanosensor channel inhibitors on ET-1 mRNA downregulation by shear stress.

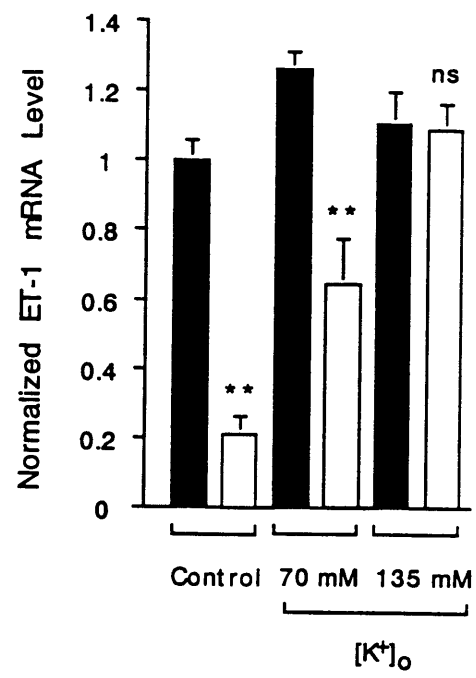


Figure 9.3 Effect of elevated extracellular potassium on ET-1 mRNA downregulation by shear stress.

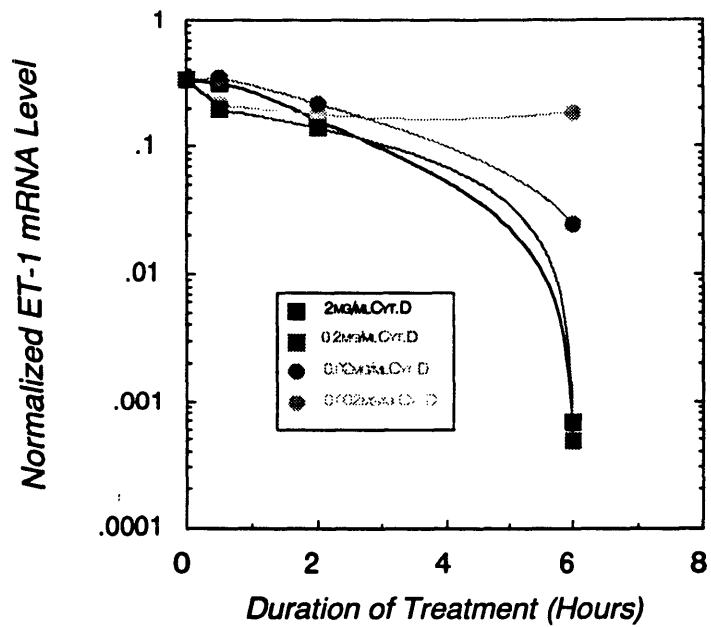


Figure 9.4 Effect of Cytochalasin D treatment on ET-1 mRNA level.

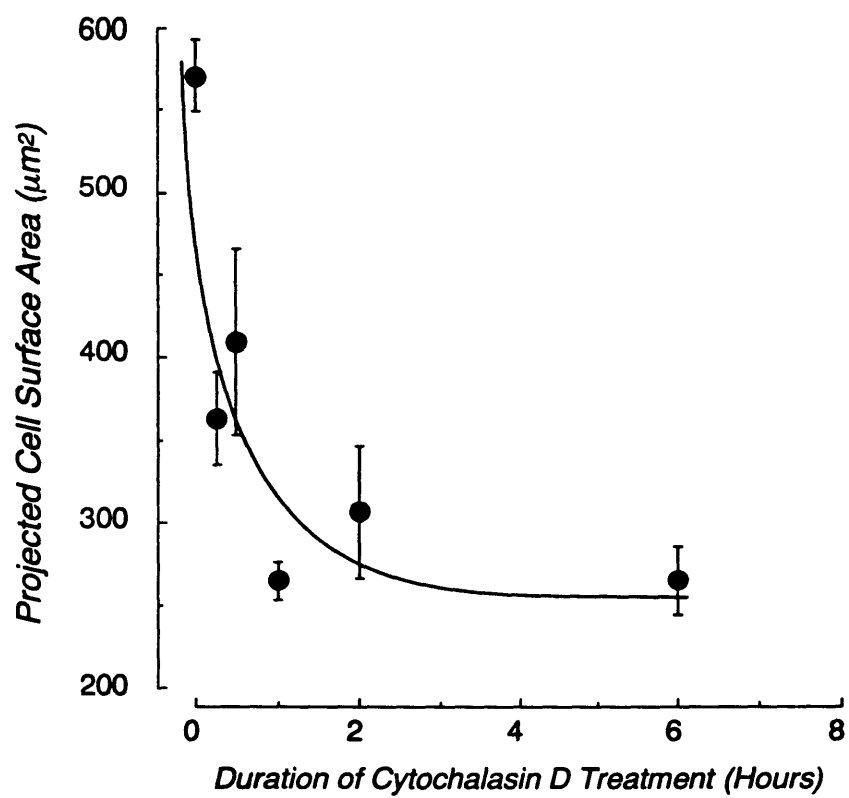


Figure 9.5 Effect of Cytochalasin D on projected cell surface.

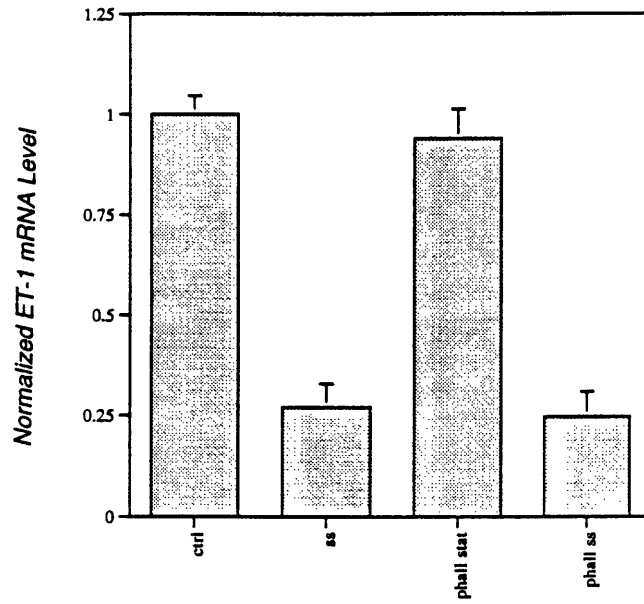


Figure 9.6 Effect of phalloidin pretreatment on ET-1 mRNA down-regulation by shear stress.

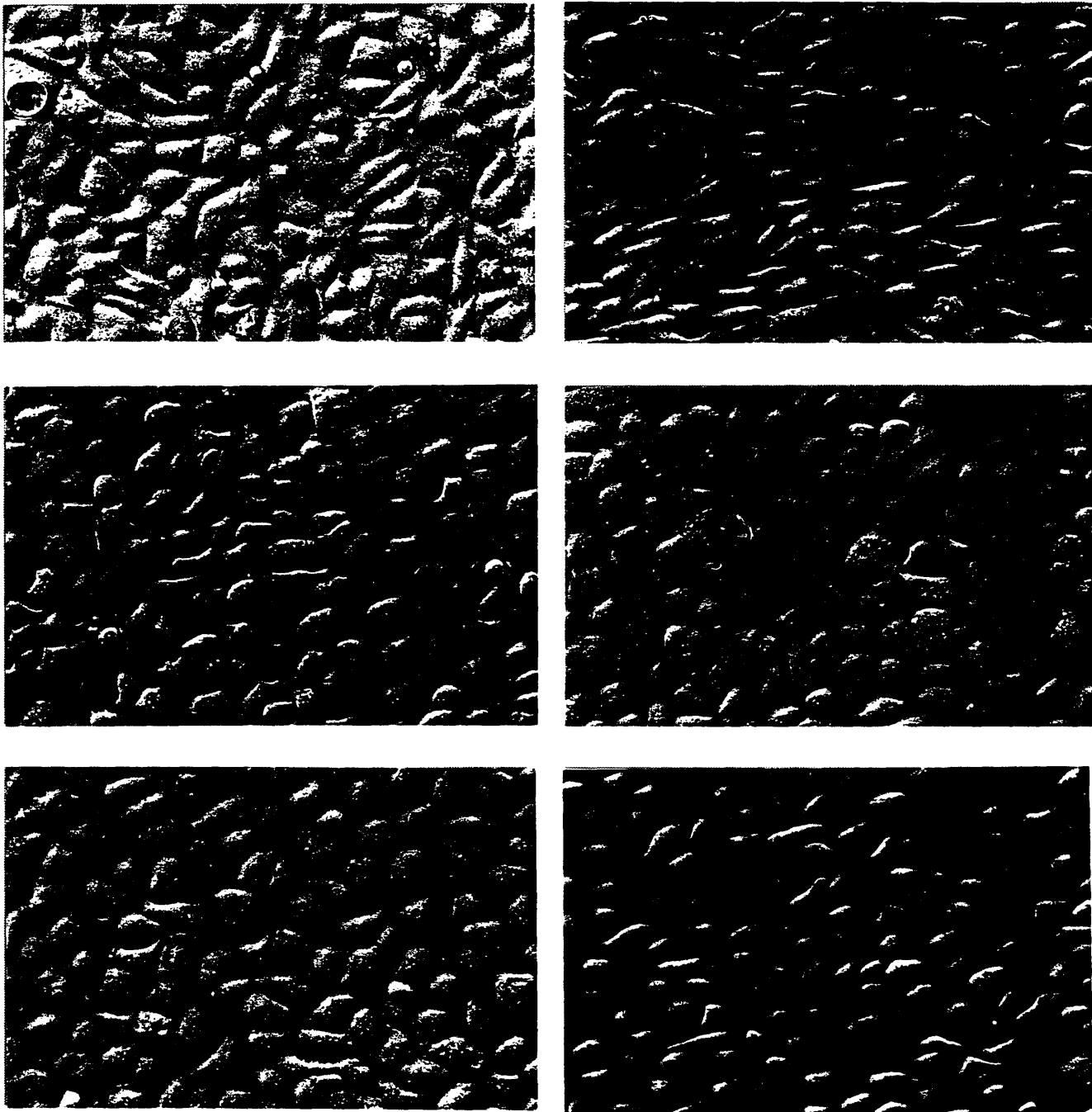


Figure 9.7 Hoffman phase-modulation micrographs of BAE cells treated with nocodazole and taxol under shear stress.

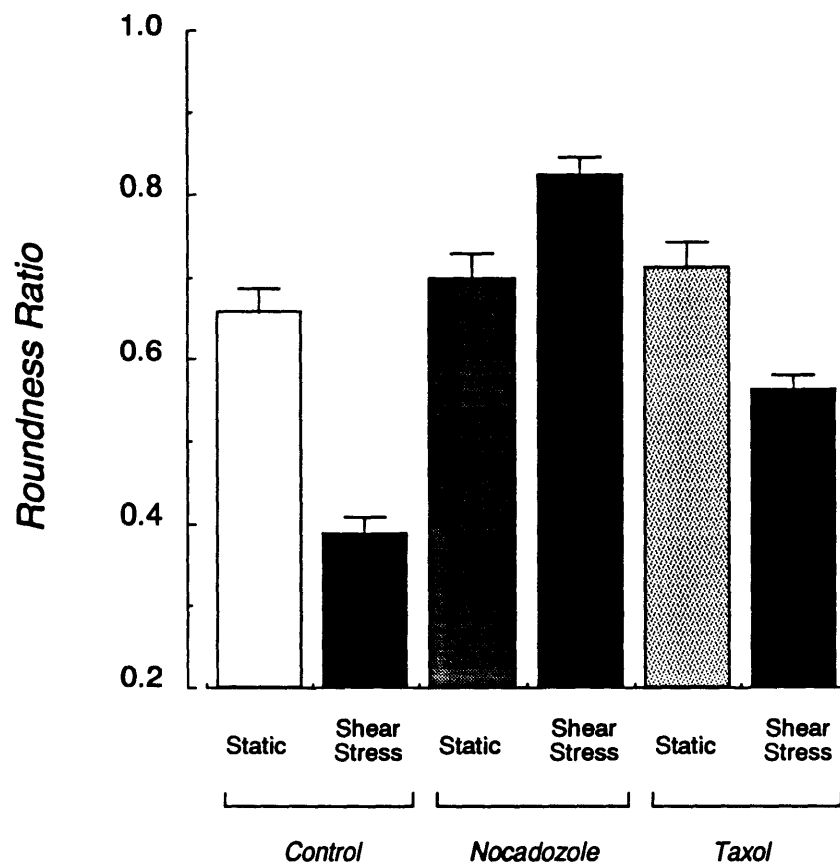


Figure 9.8 Cell shape analysis of BAEC treated with nocodazole and taxol.

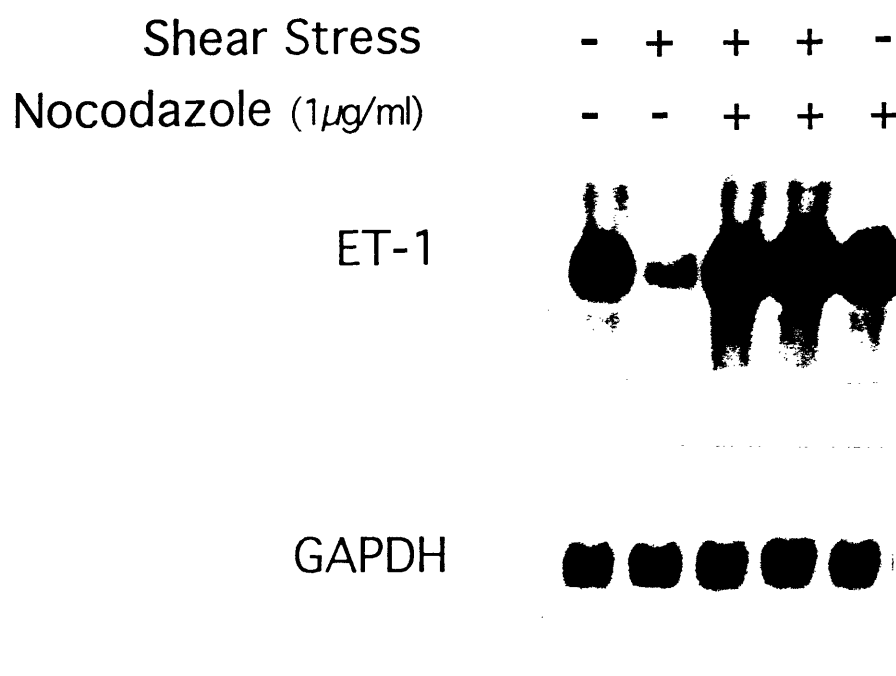


Figure 9.9 Nocodazole pretreatment inhibits shear-induced ET-1 mRNA downregulation.

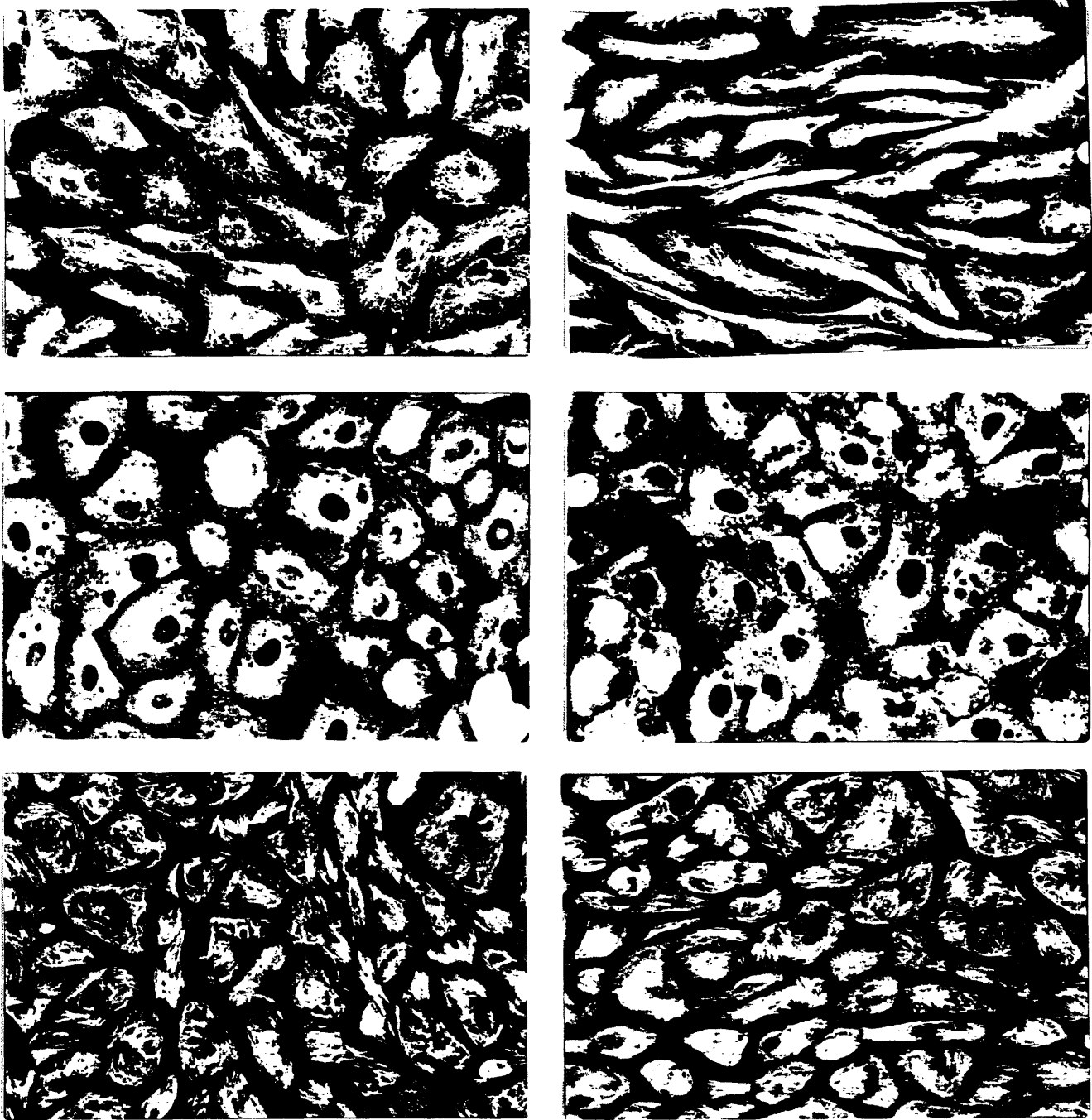


Figure 9.10 Tubulin staining of BAE cells exposed to shear stress.

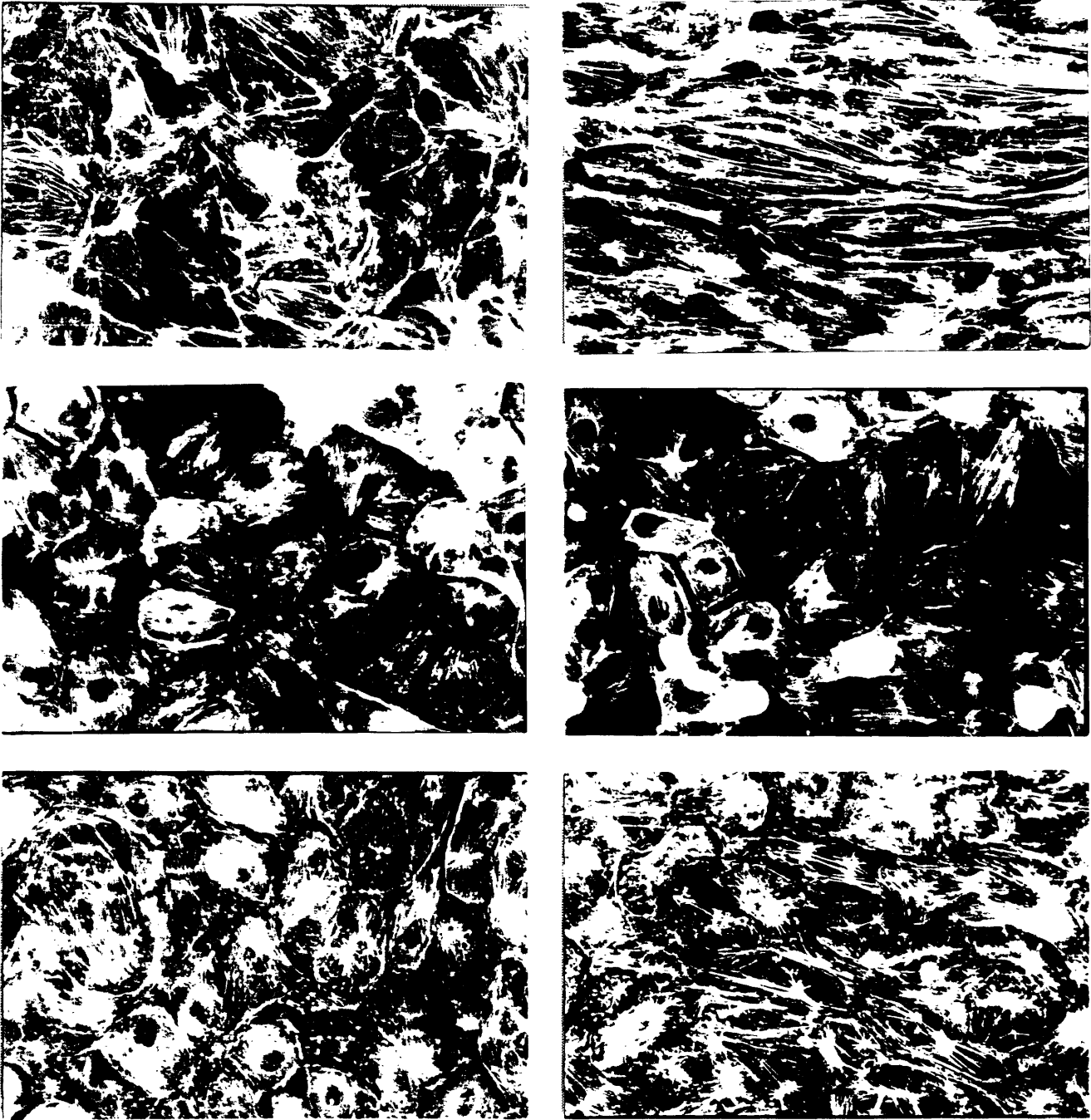


Figure 9.11 F-actin staining of BAE cells exposed to shear stress.

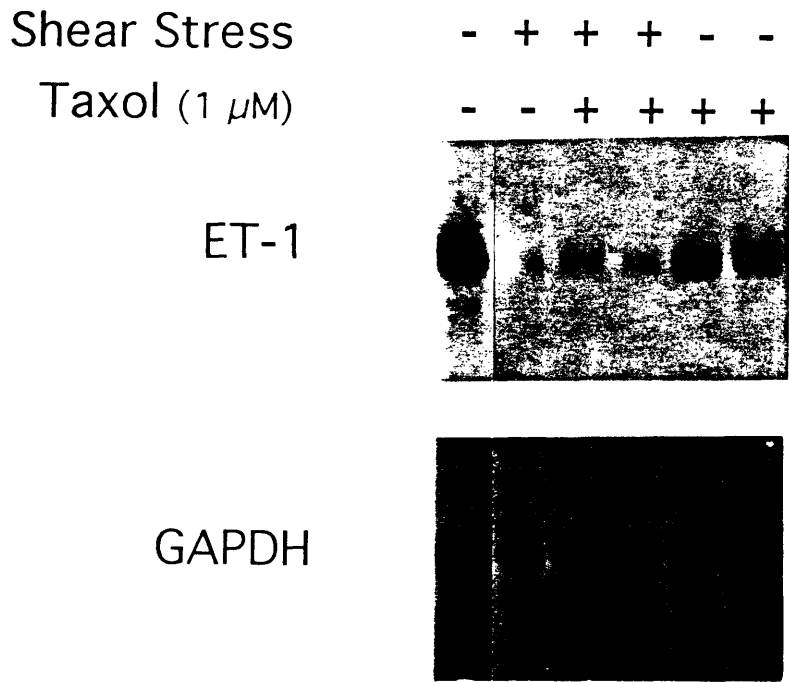


Figure 9.12 Taxol does not affect shear-induced ET-1 mRNA down-regulation.

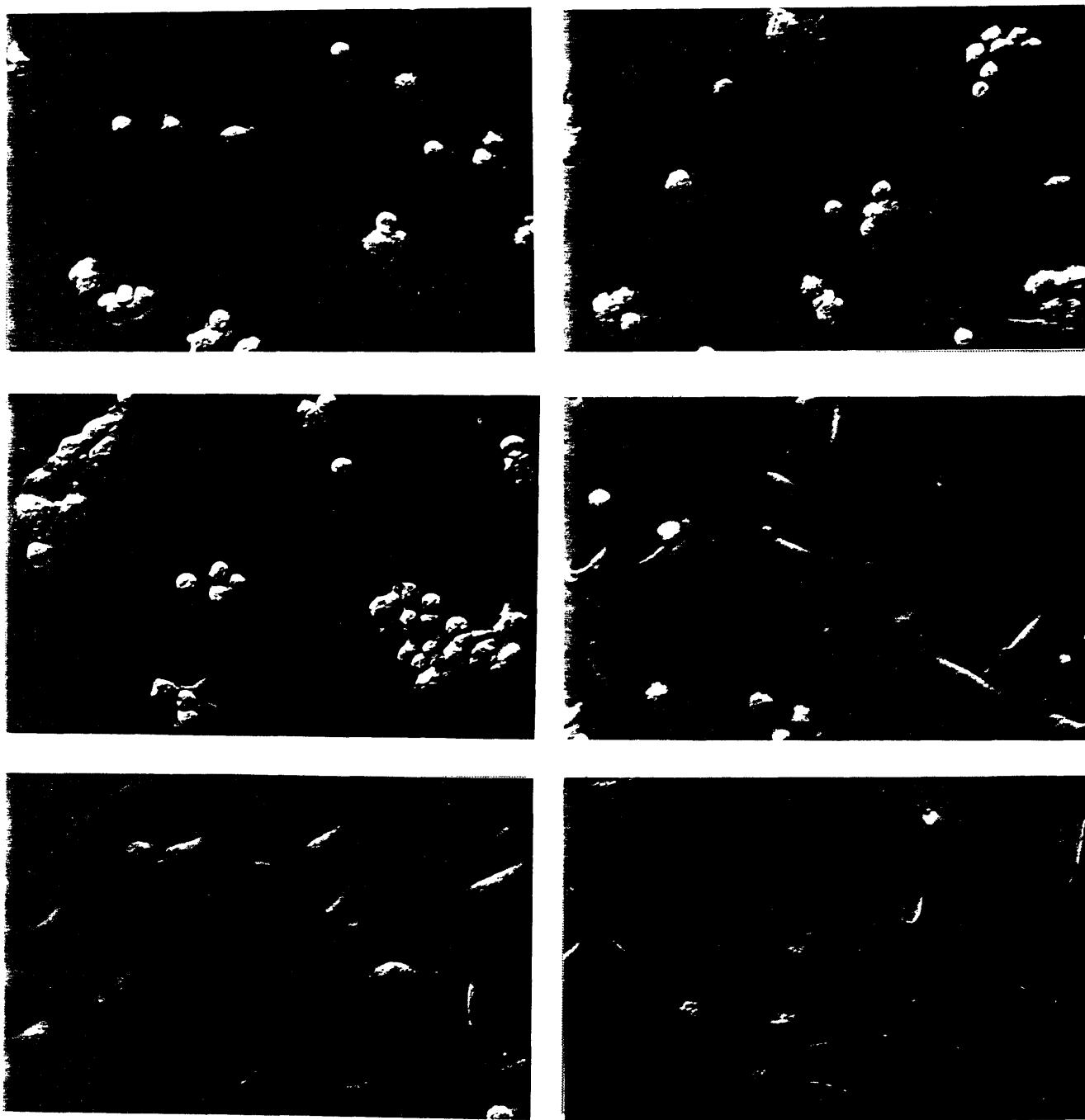


Figure 9.13 Hoffman phase modulation micrographs of BAE cells plated on Petri dish surfaces pre-coated with increasing concentrations of Pronectin F.

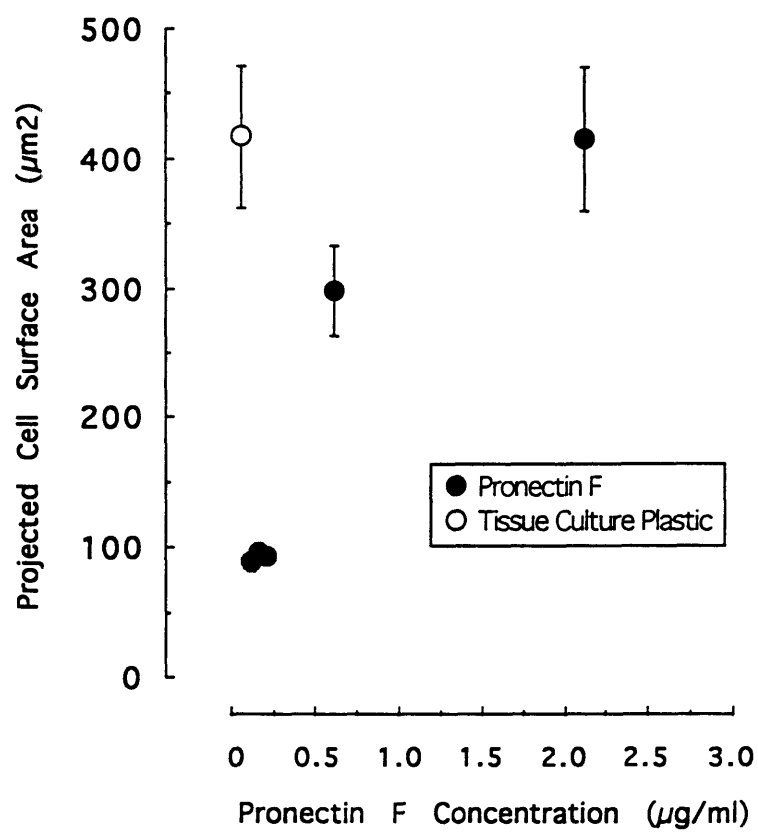


Figure 9.14 Morphologic analysis of BAE cells plated on Petri dish surfaces pre-coated with increasing concentrations of Pronectin F.

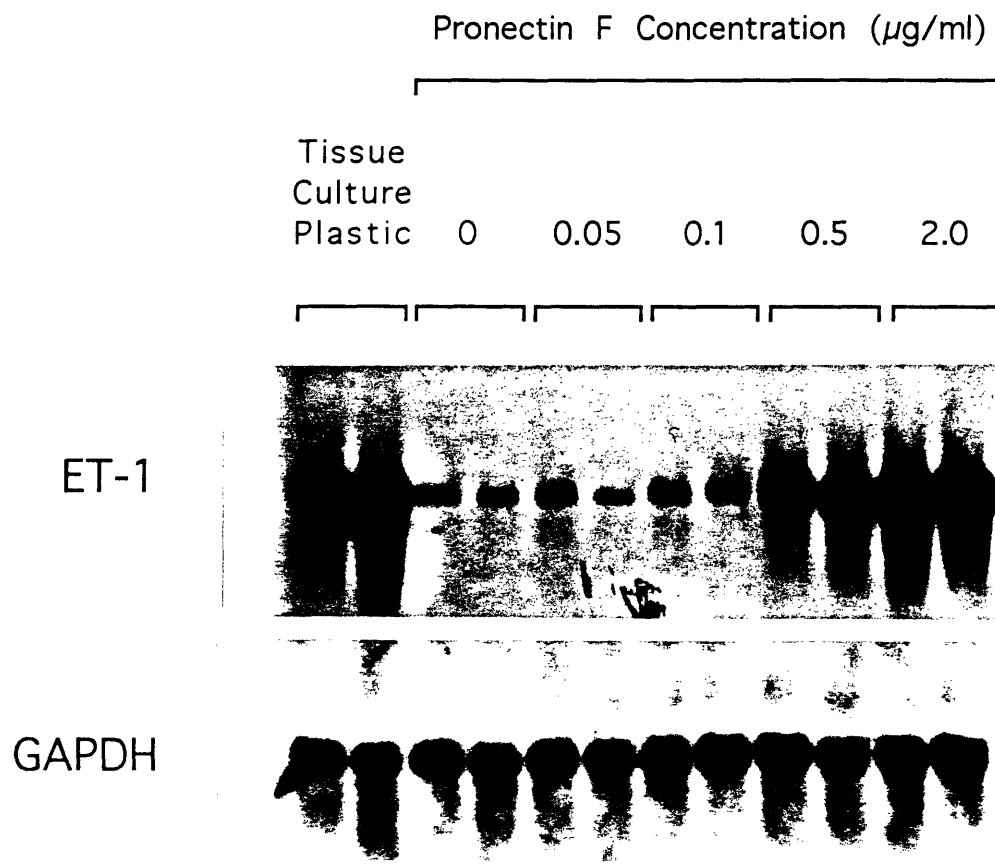


Figure 9.15 Northern blot analysis of BAE cells plated on increasing concentrations of Pronectin F.

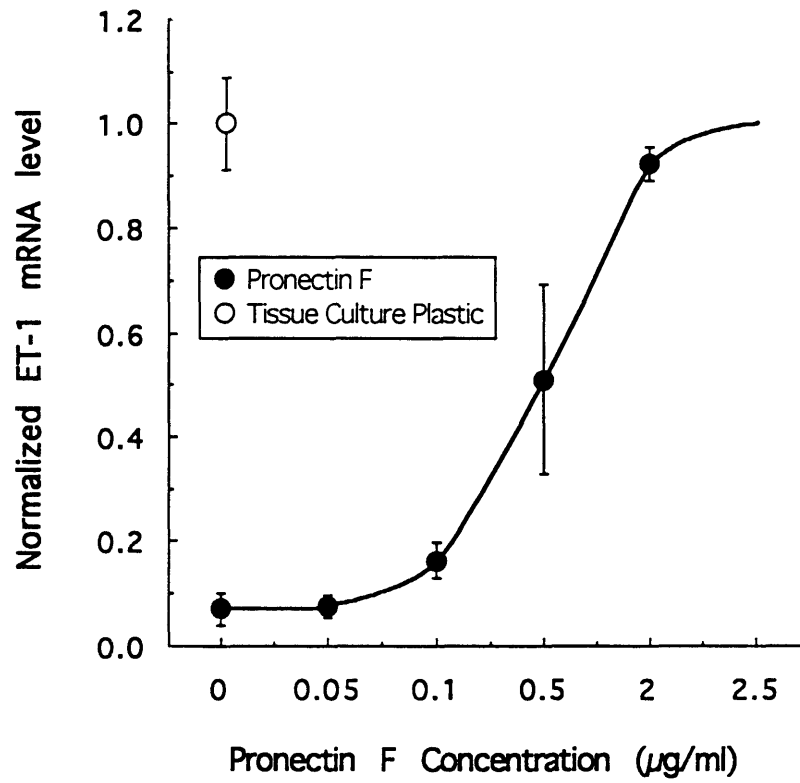


Figure 9.16 Normalized densitometric analysis of ET-1 mRNA from BAE monolayers plated on increasing concentrations of Pronectin F.

CHAPTER 10

Theoretical Models for Vascular Structure Regulation and for Endothelial Cell Transduction Process

10.1 The meaning of the gene regulatory changes with respect to previous work

The review of previous literature suggested indirectly a schematic model whereby the endothelial cell acting as a shear stress sensory element would play a role in the control loop of wall shear stress, in order to maintain it at the optimal level of 15 dyn/cm². In addition, numerous studies have shown a correlation between foci of initiation and development of atherosclerosis and local shear stress characteristics.

The results presented in this thesis and by others (reviewed by Davies P.F. et al., 1993) in the field suggest a possible model of gene regulation of the gene products studied that would correspond to the observations made *in vivo* (figure 10.1). The results presented in this thesis suggest that in response to decreased shear stress that is lower than the average level of 15-20 dyn/cm², the level of expression of both ET-1 and PDGF-B chain would be significantly increased. Given ET-1 and PDGF-B chain's vasoconstrictive and mitogenic properties to cells of the vessel wall, it is tempting to speculate that these increases may in the short term increase vessel tone, and in the longer term decrease internal caliber by thickening the vessel wall. Furthermore, the increased level of ET-1 and PDGF-B expression under conditions of low shear stress suggest their potential involvement in the underlying pathological processes seen in the focal development of

atherosclerosis. Conversely, elevated levels of shear stress appear to not only decrease expression of both ET-1 and PDGF-B chain, but also increase that of bFGF and t-PA; the first (bFGF) has been proposed to be an endothelial mitogen (Rifkin D.B., 1989) and the latter (t-PA) to be potentially involved in dissolution of vessel wall matrix (Mignatti P. et al., 1993), both essential processes for the increase in vessel caliber and expansion known to occur in response to elevated levels of shear stress (Masuda H. et al., 1989).

These findings allow us to propose that although Nature has evolved to optimize vascular structure via an exquisite regulation by shear stress of multiple potent endothelial products, it is these very processes that lead to vascular disease in focal areas. In these unfavorable local fluid mechanical conditions result, shear stress of low magnitude and time-varying character provokes increased expression of ET-1 and PDGF-B among others, substances which are otherwise essential in the homeostasis of vascular structure and function, but in this situation act as local stimulators of intimal hyperplasia.

Other findings presented here concern the differential regulation of TM and t-PA, the former which can be proposed to act as a protective anti-coagulant under conditions of low flow or shear stress such as occurs in stasis, and the latter being induced at high flow or shear to both maintain vessel patency and potentially assist in vascular remodeling.

10.2 Present model of endothelial response to shear stress

I will present here a hypothetical working model for the regulation of the ET-1 gene by fluid shear stress, given the available knowledge (figure 10.2). Shear stress is transmitted via the cytoskeleton, possibly the microfilament or the microtubule network to focal adhesion contacts (Morita T. et al., 1992; Wang N. et

al., 1993). The transmitted force also induces a release of intracellular calcium stores (Mo M. et al., 1991; Dull R.O. et al., 1991; Geiger R.V. et al., 1992; Shen J. et al., 1992), and, via intracellular tension changes, alters the activity of focal adhesion contact- or cytoskeleton-associated tyrosine kinases (Burrige K. et al., 1992; Lipfert L. et al., 1992; Davies P.F. et al., 1993; Malek A.M. et al., 1993c). The increased tyrosine kinase activity would initiate a cascade that could in the short-term activate cytoplasm-located nuclear binding proteins and induce them to translocate to the nucleus (Schindler C. et al., 1992) where they would alter the transcription of a specific set of genes (Resnick N. et al., 1993), and via one or more protein synthesis-dependent steps result in decreased ET-1 gene transcription (Malek A.M. et al., 1993b). In the longer term, the altered intracellular $[Ca^{2+}]_i$ and tyrosine kinase activity would result in a new set-point of dynamic equilibrium in cytoskeletal remodeling yielding altered cell morphology (Levesque et al., 1985; Malek A.M. et al., 1993a), and characterized finally by a streamlined shape and submembranous actin stress fibers (Barbee K.A. et al., 1994). This final steady state result would yield lower effective shear stress magnitude and gradients on the EC surface (Satcher R.L.J. et al., 1992; Barbee K.A. et al., 1994). The shear stress-activated potassium current (Nakache M. et al., 1988; Olesen S. et al., 1988) could possibly be the temporary effect of altered membrane permeability that would eventually desensitize as the viscoelasticity (Herman I.M. et al., 1987; Adams D.S., 1992) of the cellular cytoskeleton begins to respond to the altered hemodynamic conditions.

10.3 Future directions

A great deal has been achieved in the last five years in the quest to elucidate the molecular response of the endothelial cell to shear stress. A number of key

products have been found to respond to the ever-present fluid stimulus and pharmacological and biochemical analyses have been carried in an attempt to determine the key mechanotransducers and second messenger signals in the response to shear. The future activity in the field will likely be centered around the following three directions:

1) the further elucidation of endothelial products which are responsive to flow and shear stress, in a systematic and organized fashion, attempting to make a distinction between transient and sustained events, and between observations specific to certain tissue culture conditions or experimental apparatus from those that apply to all endothelial cells irrespective of animal origin or passage number. These studies will add new insight to the possible physiology and pathology observed in vascular remodeling in response to altered flow states as well as the pathogenesis of disease entities such as atherosclerosis, hypertension, vein graft deterioration, aneurysm formation, post-stenotic dilatation and arterio-venous malformation genesis and progression,

2) the determination of the key early events that lead to altered endothelial cell function in response to flow, including but not limited to increased $[Ca^{2+}]_i$, increased phosphoinositide turnover, NO release, decreased pH_i , increased tyrosine phosphorylation of specific proteins and the identification of the latter, the role of the cytoskeleton and of various key focal adhesion contact- and cytoskeleton-associated proteins, and the isolation of shear- and strain-activated mechanosensitive channels, and specific inhibitors of the latter, to accurately determine their respective roles in the transduction of shear stress.

3) the molecular characterization of the responsive regions of shear-regulated genes such as ET-1 and PDGF-B chain, and the identification and isolation of shear-activated binding proteins in the hope of determining the events leading to

shear transduction into second messenger signals, and eventually to altered gene regulation. This latter step will potentially pave the way to the engineering of shear-responsive gene constructs. Such constructs, introduced into endothelium by the appropriate somatic gene transfer methods, would enable the expression of anti-inflammatory, anti-proliferative, or anti-thrombotic proteins in regions of either decreased or elevated shear stress where vascular pathology is observed with a higher propensity.

The effect of naturally-occurring physiological mechanical forces has by now been shown to play a key role in controlling the phenotype and function of cells in the cardiovascular system. In the future, continued study of the mechanisms of transduction and signalling of strain, pressure, and shear stress at the cellular and molecular levels should hopefully provide new insights into vascular development and function, and disease.

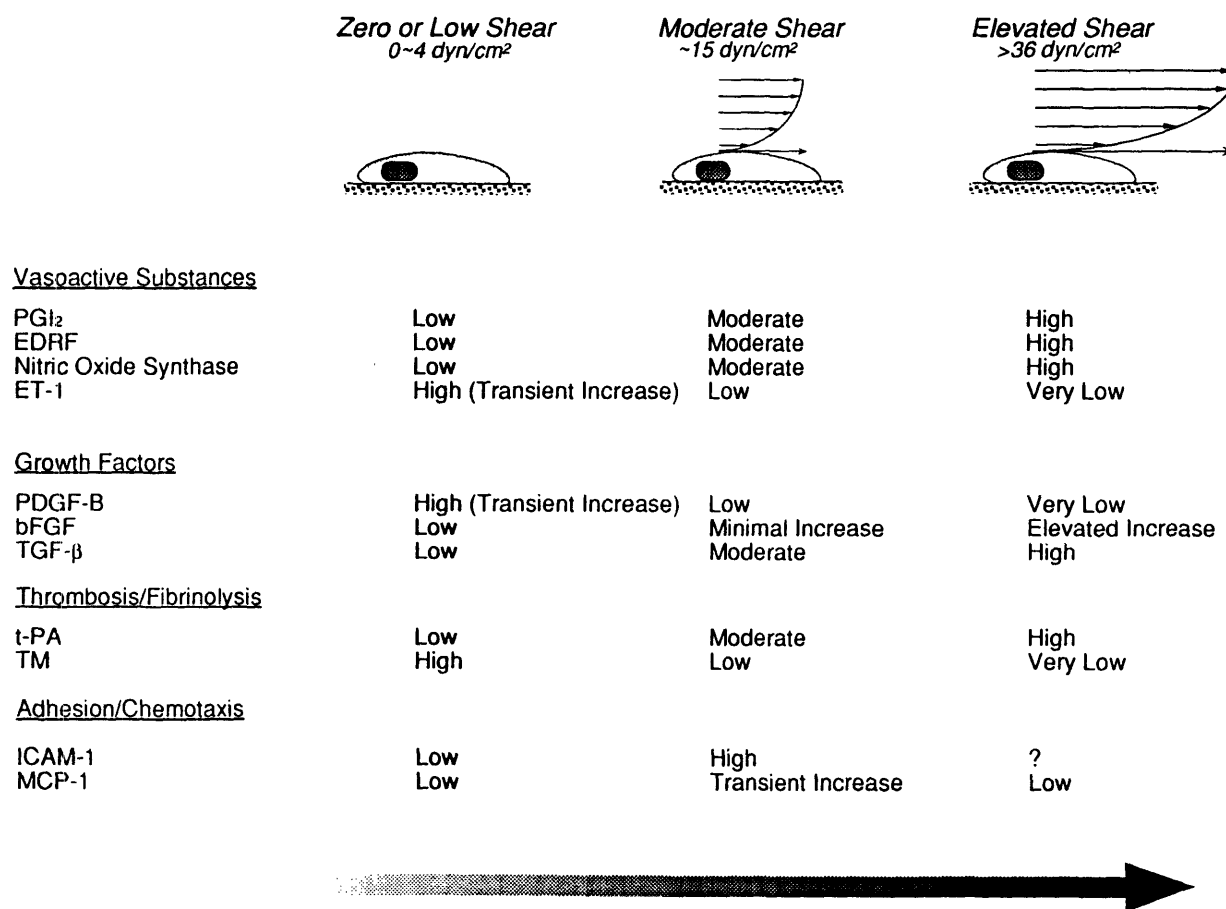


Figure 10.1 Hypothetical model of gene regulation by shear stress.

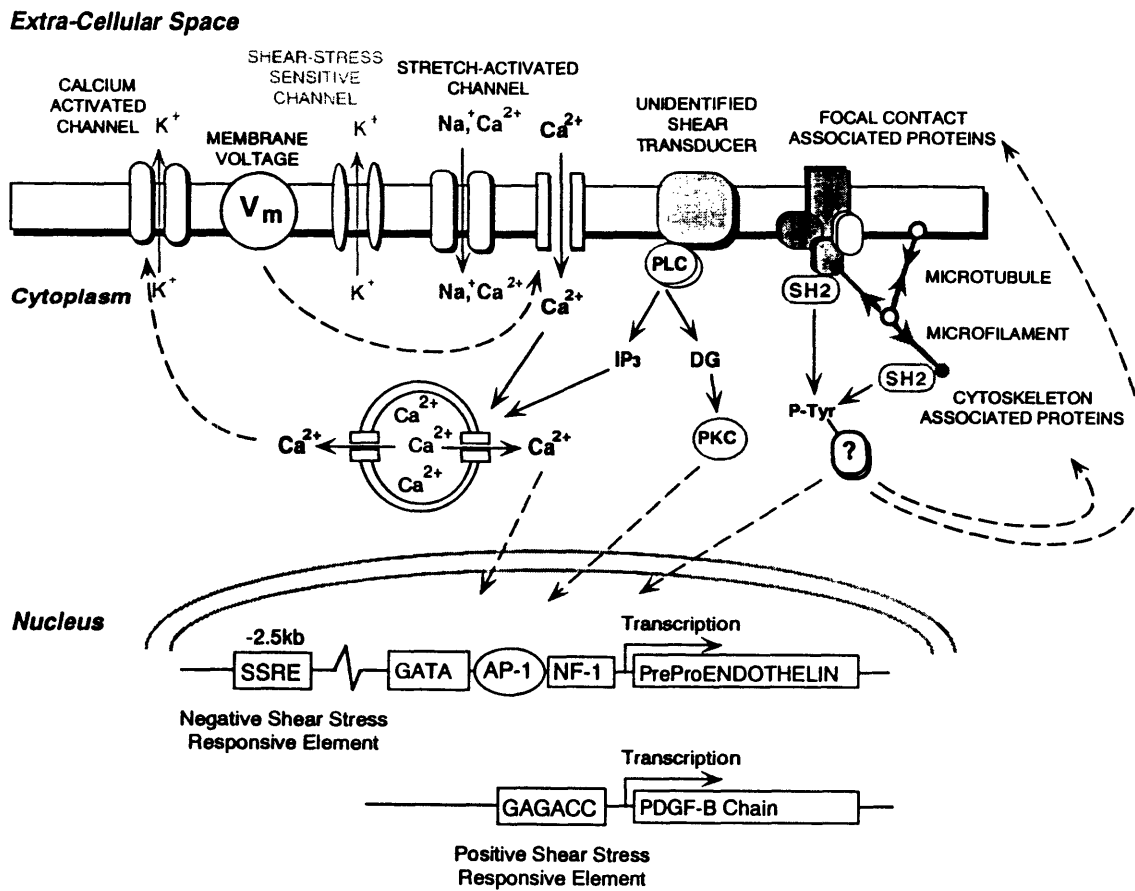


Figure 10.2 Hypothetical model of cellular transduction of shear stress.

APPENDIX

Cell culture

Bovine aortic endothelial (BAE) cells were isolated from freshly obtained aortae (Arena, Hopkinton, MA.) as previously described (Gimbrone M.A. Jr. et al., 1974) by using partial collagenase treatment. Endothelial purity of the cell population was assessed by using the acetylated-LDL (Biomedical Technologies, Stoughton, MA) uptake method (Netland P.A. et al., 1985) and was found to be greater than 98%. Cells were grown in Dulbecco's modified Eagle (DME) medium (Gibco, Grand Island, NY.) supplemented with 10% calf serum (Gibco), 4 mM L-glutamine, 25 mM HEPES pH 7.4, 10 units/ml of penicillin, and 10 µg/ml of streptomycin, at 37 °C, 5% CO₂ in a humidified incubator. Cells were passaged every 6-7 days by using 0.5% Trypsin-0.53mM EDTA·4Na for 2-3 min followed by dilution in the growth media and seeding in tissue culture plates (Falcon Labware, Oxnard, CA). Confluent cells were used from passage 6-15, and subjected to shear-stress 24-48 hr following the last change of culture medium. Where indicated, cells were cultured with media containing low serum (0.5% calf serum) or serum-free media (supplemented with insulin (5 µg/ml) transferrin (5 µg/ml) and ascorbic acid (100 µM)).

Dynamic stretch apparatus

Bovine aortic endothelial cells were grown to confluence on Silicone sheet (Dow Corning, NY) pre-coated with rat-tail type I collagen (Biomedical Technologies, Stoughton, MA). 36-48 hr following the last feeding with media containing 10% calf serum, confluent cells were mounted on a dynamic stretch

apparatus (courtesy of Dr. Thomas Kulik) and their substratum linearly stretched by 20% cyclically at a rate of 20/min. Cells were then lysed for RNA isolation.

RNA Isolation and Northern analysis

Total cellular RNA was obtained by using the acid guanidium thiocyanate phenol chloroform (AGPC) method (Chomczynski P. et al., 1987). RNA concentration and relative purity were quantified by measuring absorbance at 260 nm and the ratio of the absorbance at 260 nm relative to that at 280 nm. 25 µg of RNA were loaded per well and separated on 1.5% agarose gels containing 6% formaldehyde, 0.02 M morpholinopropanesulfonic acid (MOPS), 0.005 M sodium acetate, 0.001 M Na₂·EDTA. RNA was transferred onto GeneScreen membranes (New England Nuclear Products, Boston, MA.) by capillary blotting using 10X SSC (1.5 M sodium chloride, 0.15 M sodium citrate, pH 7), and immobilized by UV irradiation. The membranes were prehybridized at 42°C in 50% formamide, 0.2% polyvinyl-pyrrolidone, 0.2% bovine serum albumin, 0.2% ficoll, 0.05 M Tris-HCl (pH 7.5), 1.0 M NaCl, 0.1% sodium pyrophosphate, 1% SDS, 10% dextran sulfate, 100 µg/ml of denatured salmon sperm DNA and 1 µg/ml each of polyA and polyC. Hybridization was carried out in the same solution containing a ³²P-labelled 1.9Kb EcoRI cDNA specific for bovine preproendothelin-1 (pBET-1) (kind gift of Dr. Thomas Quertermous), 0.7Kb EcoRI of bovine thrombomodulin (TM) (kind gift of Dr. Robert Rosenberg), 1.77Kb EcoRI of human tissue-type plasminogen activator (t-PA) (ATCC No. 67585), 1.4Kb EcoRI of bovine basic fibroblast growth factor (bFGF) (kind gift of Dr. John Fiddes), 1.2Kb Sall-XbaI fragment of *c-sis* and 1.3Kb PstI cDNA fragment for glyceraldehyde phosphate dehydrogenase (GAPDH). Following overnight incubation, the membranes were washed in 2X SSC, 0.3% SDS at room temperature for 15 min, in 0.2X SSC, 0.3%

SDS for 30 min at room temperature, in 0.2X SSC, 0.3% SDS for 1 hr at 55°C, and then exposed to X-ray film (Kodak X-Omat-AR) at -80°C.

Densitometry

Autoradiograms exposed in the linear range of the X-ray films were scanned in two-dimensions. Densitometry of individual bands of interest was carried out on the stored digital image by subtraction of the local background and 2-D integration. To control for RNA loading and transfer to the filter, the hybridization signals of ET-1 mRNA were then normalized for each sample with respect to the density of the corresponding GAPDH mRNA signal. GAPDH was chosen as internal control because the concentration of GAPDH mRNA/ μ g of total RNA did not change significantly with or without shear stress (cf. chapter 5).

Radioimmunoassay for endothelin-1 peptide

A radioimmunoassay kit for bovine ET-1 peptide (RIK 6901, Peninsula Laboratories, Belmont, CA) was used. 5 μ l of supernatant were mixed with 45 μ l of assay buffer and the samples were processed according to the manufacturer's instructions. Cross-reactivity was 7% to ET-2 and ET-3 and 35% to Big ET-1. Samples were measured in triplicate, and the concentration obtained by reading off a cubic spline fit through the standard curve obtained from triplicate standard samples.

Isolation of nuclei & runoff transcription

Nuclear runoff experiments were performed according to the method of Greenberg and Ziff (Greenberg M.E. et al., 1984). The RNA transcripts were

hybridized to NaOH-denatured linearized cDNA plasmids (10 μ g) of ET-1, α -tubulin and pUC18, slot-blotted on Nytran membranes (Schleicher & Schuell, NH).

Transcription and protein synthesis inhibition

In order to assess the mRNA stability of endothelin-1, actinomycin D (5 μ g/ml), an inhibitor of transcription by RNA polymerase II, was added at the onset of the experiment, and cells lysed at various times following the start of fluid shear stress for RNA processing as described above. Protein synthesis was inhibited by 1 hour pre-treatment of the cells with 10 μ g/ml of cycloheximide.

Transfection experiments with ET-1 promoter constructs

To determine the transcriptional activity of the ET-1 promoter, four reporter construct plasmids were used: pET-1(-4.4CAT) (Lee M. et al., 1990) consisting of the proximal 4.4Kb of the ET-1 5'-flanking region inserted into the CAT reporter vector (kind gift of Dr. T. Quertermous, Vanderbilt University), pET-1(-157hGH) and pET-1(-1.4hGH) (Wilson D.B. et al., 1990) containing -157 bp and -1.4Kb of the 5' flanking sequence inserted into the hGH reporter vector (kind gift of Dr. D. Wilson, Children's Hospital, Boston). pSVGAL plasmid containing the SV40 enhancer fused to the β -galactosidase gene was used for normalization of transfection efficiency. 15 μ g of the reporter plasmid and 5 μ g of pSVGAL were used to transfect confluent BAE cell monolayers using the modified calcium phosphate method (Chen C. et al., 1987) for 9 hr. The cells were then fed with medium containing 10% calf serum for 9 hr, changed to serum-free medium for 6 hr, then exposed to shear stress or PMA for 18 hr. The activity of the promoters in the transfected cells were determined and normalized as previously described (Lee M. et al., 1990; Wilson D.B. et al., 1990).

Cell Lysis and immunoblotting of protein kinase C

BAEC cells were subjected to two cycles of freeze-thaw in lysis buffer (Trilivas I. et al., 1991) followed by centrifugation at 100,000 x g, 4°C for 60 min, to separate the cytosolic and particulate cellular fractions. Both fractions were electrophoresed on 10% SDS-polyacrylamide gels according to Laemmli. Following transfer on reinforced nitrocellulose membranes (Schleicher & Schuell, NH) using Towbin transfer buffer (4 °C), membranes were incubated overnight with antibody to either the α or β isoform of protein kinase C (PKC) (Seikagaku America, GA). The antibody was visualized with alkaline phosphatase conjugated anti-mouse secondary antibody using the ProtoBlot system (Promega, Madison, WI).

Protein kinase C activity assay

The soluble and particulate fractions of BAE cells exposed to either PMA or shear stress were partially purified using DE-52 column chromatography according to Thomas (Thomas T. P. et al., 1987; Presta M. et al., 1989). Fractions were assayed for PKC activity by measuring the calcium- and phosphatidylserine- and diolein-dependent transfer of radiolabel from [γ -³²P]-ATP to histone IIIs. PKC activity was computed by subtracting the corresponding values of control reactions in the absence of lipids and in the presence of 1 mM EGTA, and calibrated by dividing by the protein content of the partially-purified fraction by a Bradford Assay.

Determination of intracellular cAMP & cGMP content

Confluent monolayers of BAE cells were incubated in 100 μ M IBMX for 10 min prior to applying steady laminar shear stress of 20 dyn/cm² for 1, 3, 10, 30 and 60 min or 10 μ M forskolin for 3 min. Following stimulation, the cells were precipitated using 12% trichloroacetic acid at 4°C, and centrifuged for 10 min at 10,000 x g. The supernatant was extracted five times with water-saturated ether, lyophilized then resuspended in acetate buffer, and its cAMP content determined by radioimmunoassay (Biomedical Technologies, MA).

Image analysis

Image analysis was conducted on an Apple Macintosh II/fx running the Image Analyst™ program. Images were imported into the computer either by two-dimensional scanning of printed images or via a frame grabber (Data Translation, MA) connected to a Hitachi CCD camera (Hitachi, Japan, model KP-140) on an Olympus IMT-2 microscope. Cells were stained using coomassie blue in order to improve image contrast. Following image input, connectivity analysis was performed by edge detection of cell borders with user input when necessary. The program then performed best fitting of an ellipse through each contour and computed parameters such as the total area contained within the contour, the perimeter of the contour, as well as the roundness ratio (ratio of the major and minor radii, 1=circle, 0=line) of the ellipse fit through the contour.

Construction of apparatus

A plate of aluminum alloy is machined to serve as a base for the DC-motor and gearbox and accept a 10 or 15 cm dia. tissue culture plate (Falcon Labware, CA) in a rimmed depression. An oval-shaped opening is drilled flush with the surface of

the tissue culture plate base so as to permit the fitting of the apparatus on a microscope (Olympus IMT-2) stage and provide for the on-line visualization of the monolayer under shear. A 3/8 in. (for 10 cm tissue culture plate) and 3/4 in. (for 15 cm tissue culture plate) stainless steel shaft is connected to a block of transparent Plexiglas™ and machined to provide a conical surface of angle between 0.5° and 5°. A center plug of ultra-high-molecular-weight (UHMW) polyethylene is inserted and machined into the tip of the cone, which is then polished to optical clarity. The cone shaft is inserted by a slight friction fit into a pair of ultra high precision ball bearings (Barden, CT) housed in an aluminum alloy cylindrical block. A stainless steel spring is inserted around the cone shaft to act in compression against the inner race of the ball bearing and the shaft base. The bearing housing is permanently secured via 6 screws to a Plexiglas™ coverplate containing a groove designed to accept the lip of the tissue culture dish at 90° angle. The coverplate contains depressions to allow aeration of the sample and the device is used inside a standard tissue-culture incubator (37° C, 5% CO₂). The coverplate also incorporates two ports for sampling or recirculating flow medium during device operation; these can also be used to control the gas composition overlying the tissue culture medium by sealing the aeration holes. The cone shaft is then connected via a flexible coupling (Berg Inc., NY) to a DC-motor (Model E352, Robbins & Myers/Electrocraft, MN) with a feedback controller (Model Motomatic II, Robbins & Myers/Electrocraft, MN) that insures accurate speed control over long periods of time. The DC-motor controller also accepts inputs from an external signal generator or computer output via a digital to analog (D/A) board, thereby allowing for specific time profiles of cone velocity. When the coverplate is in position and is secured via the spring-loaded clamps, the device appears as shown in cross-section. A version of the device has been designed and

built to accommodate co-culture by using 10 cm tissue culture plates with filter inserts (Costar, MA). This device uses a thinner cone of smaller radius, which rests on the filter insert, and in order to maintain the filter surface flat, on a glass microscope slide cover (Fisher Scientific) secured on the center of the bottom plate with silicone glue (Dow Corning, NY).

Mode of operation of cone-plate apparatus

The coverplate, attached bearing housing, and the cone are washed in laboratory detergent, avoiding alcohol to prevent damage to the polished Plexiglas™ surface, then thoroughly rinsed with deionized water and exposed to 30 min. of UV-irradiation for sterilization. Under sterile conditions within a laminar air flow hood, confluent BAE cell monolayers, last fed with complete growth medium or serum-free DME 24-48 hr prior to onset of flow, and grown in 10- or 15-cm tissue culture dishes (Falcon Labware, CA) are mounted inside the pre-warmed cone and coverplate section of the apparatus. The coverplate, cone and underlying tissue culture plate are then transferred to the baseplate section housed inside the tissue culture incubator and secured in position with the clamps. The cone is then connected to the DC-motor via the flexible coupling following proper alignment of the motor and gearbox assembly with the cone shaft. The cells inside the viscometer were kept at a temperature of 37° C and a humidified atmosphere of 5% CO₂. Different combinations of cone angle (0.5-5°) and rotational velocities were chosen to achieve the different flow regimes described in the text. Kinematic viscosity of the medium was measured using a calibrated Canon-Fenske type viscometer (Fisher Scientific). Shear stress magnitude, τ_{ss} , and Reynolds number, R_e , were computed by using relations previously derived by Sdougos et al. (Sdougos H.P. et al., 1984; Malek A.M. et al., 1993a).

To determine the dynamic characteristics of the device, either a model FG-121B signal generator (NF Electronic, Japan) or a Model DT2901 D/A board (Data Translation, MA) connected to an IBM PS/2 55SX personal computer (IBM Corp, FL) was used to drive the motor controller, while the cone rotation velocity was obtained by measuring the DC motor tachometer output with a model VC6025 storage oscilloscope (Hitachi, Japan). Profiles and mean values of shear stress magnitude and Reynolds number were computed by numerical integration using MathCad (MathSoft Inc., MA) on a Macintosh computer (Apple Computer Inc., CA).

DNA and RNA synthesis rate measurement

Confluent BAE monolayers were incubated for 24 hr in serum-free DME medium, exposed to steady laminar fluid shear stress of either 20 or 36 dyn/cm² for 6 hr or 18 hr, then incubated with either 2 µCi/ml of either ³H-thymidine or ³H-uridine (New England Nuclear, MA) for 6 hr. Exposing BAE monolayers to either 6 or 18 hr of shear stress yielded similar results. The monolayers were then rinsed three times in ice-cold PBS, fixed with a 5:1:4 mixture (vol/vol) of methanol:acetic acid:water for 1 hr at 4°C, then air dried briefly according to the method of Simonson et al. (Simonson M.S. et al., 1989). The precipitates were then dissolved in 1% SDS at 37°C for 2 hr and aliquots in scintillation fluid counted using a liquid scintillation counter (Packard, IL). ANOVA was performed and the unpaired Student *t* test obtained for each category.

Immunostaining

BAE monolayers were washed three times with physiological buffered saline (PBS), fixed with 3.7% paraformaldehyde in PBS for 10 min, permeabilized with

0.1% triton X-100 for 10 min in PBS, washed in PBS, stained with TRITC-phalloidin for 10 min then washed three times in PBS (10 min), dried and fixed with M \ddot{o} wiol. For tubulin staining monolayers were fixed with methanol at -20°C for 15 min. The cells were then rinsed with PBS and incubated with monoclonal anti-tubulin antibody (Bohringer-Mannheim) for 10 min, washed three times with PBS, incubated with secondary anti-mouse Texas Red-cojugated antibody (Jackson Laboratories) for 10-15 min, washed three times 10 min with PBS, dehydrated with 100% ethanol and fixed in M \ddot{o} wiol. Stained cells at a radius of ~3 cm, corresponding to shear stress magnitude of 20 dyn/cm² were visualized an epifluorescence microscope (Olympus) and photographed with T-Max film (Kodak).

Western blotting with anti-Phosphotyrosine antibody

BAE monolayers were washed twice with ice-cold PBS, scraped in standard L \ddot{a} emmli lysis buffer (containing 1.25% β -mercaptoethanol, 1 mM sodium vanadate, 20 μ g/ml leupeptin and aprotinin, 50 mM PMSF, and 10 mg/ml p-nitrophenyl phosphate), solubilized by addition of 5x L \ddot{a} emmli SDS-PAGE buffer and immediately boiled for 5 min. Equal amounts of protein (100 μ g) were electrophoresed in 10% polyacrylamide gels and transferred onto nitrocellulose sheets (Schleicher & Schuell, NH) using the Transblot system (Bio-rad) at 15V/100mA for 12 hr at 4°C in Towbin buffer (25mM Tris•HCl, 192mM glycine, pH 8.3) containing 20% methanol and 1mM orthovanadate sodium. Following transfer, the membrane was washed twice in TBS (10mM Tris•HCl, pH 8.0, 150mM NaCl), blocked with 5% BSA (Sigma fraction V) for 1 hr, rinsed twice (10 min) in TBS, then twice in TBS with 0.5% Tween-20. Blots were probed sequentially with affinity-purified anti-phosphotyrosine antibody at a concentration

of 2 $\mu\text{g/ml}$ for 2 hr, and [^{125}I] protein A (100 $\mu\text{Ci}/\mu\text{g}$, ICN) followed by autoradiography according to Kamps (Kamps M.P. et al., 1988).

Western blotting with anti-thrombomodulin antibody

BAE monolayers were washed twice with ice-cold PBS, then scraped in standard Laemmli lysis buffer containing 1.25% β -mercaptoethanol and boiled for 5 min in Laemmli SDS-polyacrylamide gel electrophoresis (PAGE) sample buffer. Equal amounts of protein (100 μg) were loaded per lane and fractionated using SDS-PAGE electrophoresis in 10% acrylamide gels followed by transfer using the Transblot system (Bio-rad) at 15V/100mA for 12 hr at 4°C onto nitrocellulose sheets (Schleicher & Schuell) in Towbin transfer buffer (25mM Tris•HCl, 192mM glycine, pH 8.3) containing 20% methanol. Following transfer, the membrane was washed twice in TBS (10mM Tris•HCl, pH 8.0, 150mM NaCl), blocked with 5% BSA (Sigma fraction V) for 1 hr, rinsed twice (10 min) in TBS, then twice in TBS with 0.5% Tween-20 (TBST). The membrane was then incubated for 2 hr with affinity-purified rabbit polyclonal anti-bovine TM antibody (Jackman R.W. et al., 1986) in TBST then washed four times (10 min) in TBST. Signal was visualized using ^{125}I -protein A (ICN, 30mCi/mg) and autoradiography. Signal strength was compared by two-dimensional scanning and densitometry of TM band signal in X-rays exposed in the linear range of the autoradiography film.

REFERENCES

Adams D.S. (1992). Mechanisms of cell shape change: the cytomechanics of cellular response to chemical and mechanical loading. *J. Cell Biol.* **117**: 83-93.

Ando J., Komatsuda T. and Kamiya A. (1988). Cytoplasmic calcium response to fluid shear stress in cultured vascular endothelial cells. *In vitro & Cell. Dev. Biol.* **24**: 871-877.

Antonov A.S., Lukashev M., Romanov Y., et al. (1986). Morphological alterations in endothelial cells from human aorta and umbilical vein induced by forskolin and phorbol 12-myristate 13-acetate: a synergistic action of adenylate cyclase and protein kinase C activators. *Proc. Natl. Acad. Sci. USA* **83**: 9704-9708.

Asakura T. and Karino T. (1990). Flow patterns and spatial distribution of atherosclerotic lesions in human coronary arteries. *Circ. Res.* **66**: 1045-1066.

Bhagyalakshmi A. and Frangos J. (1989). Mechanism of shear-induced prostacyclin production in endothelial cells. *Biochem. Biophys. Res. Comm.* **158**: 31-37.

Barbee K.A., Davies P.F. and Lal R. (1994). Shear stress-induced reorganization of the surface topography of living endothelial cells imaged by atomic force microscopy. *Circ. Res.* **74**: 163-171.

Barrett T.B. and Benditt E.P. (1988). Platelet-derived growth factor gene expression in human atherosclerotic plaques and normal artery wall. *Proc. Natl. Acad. Sci. USA* **85**: 2810-2814.

Barrett T.B., Gajdusek C.M., Schwartz S.M., McDougall J.K. and Benditt E.P. (1984). Expression of the *sis* gene by endothelial cells in culture and *in vivo*. *Proc. Natl. Acad. Sci. USA* **81**: 6772-6774.

Battegay E.J., Raines E.W., Seifert R.A., Bowen-Pope D.F. and Ross R. (1990). TGF- β induces bimodal proliferation of connective tissue cells via complex control of an autocrine PDGF loop. *Cell* **63**: 515-524.

Ben-Ze'ev A. (1991). Animal cell shape changes and gene expression. *BioEssays* **13**: 207-212.

Berk B.C., Alexander R.W., Brock T.A., Gimbrone M.A. Jr. and Webb C.R. (1986). Vasoconstriction: a new activity for platelet-derived growth factor. *Science* **232**: 87-90.

Burridge K., Turner C.E. and Romer L.H. (1992). Tyrosine phosphorylation of paxillin and pp125^{FAK} accompanies cell adhesion to extracellular matrix: a role in cytoskeletal assembly. *J. Cell Biol.* **119**: 893-903.

Bussolari S.R., Dewey C.F. Jr. and Gimbrone M.A. Jr. (1982). Apparatus for subjecting living cells to fluid shear stress. *Rev. Sci. Instrum.* **53**: 1851-1854.

Caro C.G. (1977). Mechanical factors in atherogenesis. In: *Hwang Nh, Normann N., ed. Cardiovascular flow dynamics and measurements. Baltimore, Univ. Park Press* : 473-87.

Chen C. and Okayama H. (1987). High-efficiency transformation of mammalian cells by plasmid DNA. *Mol. Cel. Biol.* **7**: 2745-2752.

Chomczynski P. and Sacchi N. (1987). Single-step method of RNA isolation by acid guanidium thiocyanate-phenol-chloroform extraction. *Anal. Biochem.* **162**: 156-159.

Clowes A.W., Clowes M.M., Reidy M.A. and Belin D. (1990). Smooth muscle cells express urokinase during mitogenesis and tissue-type plasminogen activator during migration in injured rat carotid artery. *Circ. Res.* **67**: 61-67.

Collins T., Pober J.S., Gimbrone M.A. Jr., et al. (1987). Cultured human endothelial cells express platelet-derived growth factor A chain. *Am. J. Pathol.* **126**: 7-12.

Comp P.C. (1986). Hereditary disorders predisposing to thrombosis. *Progress in Hemostasis and Thrombosis, vol 8. Philadelphia. Grune&Stratton, 71.*

Conway E.M. and Rosenberg R.D. (1988). Tumor necrosis factor suppresses transcription of the thrombomodulin gene in endothelial cells. *Mol. Cell. Biol.* **8**: 5588-5592.

Conway E.M., Boffa M.C., Nowakowski B. and Steiner-Mosonyi M. (1992). An ultrastructural study of thrombomodulin endocytosis: internalization occurs in clathrin-coated and non-coated pits. *J. Cell. Physiol.* **151**: 604-612.

Cooke J.P., Rossitch E. Jr., Andon N.A., Loscalzo J. and Dzau V.J. (1991). Flow activates an endothelial potassium channel to release an endogenous nitrovasodilator. *J. Clin Invest.* **88**: 1663-1671.

Corrsin S. (1959). Outline of some topics in homogeneous turbulent flow. *J. Geophys. Res.* **64**: 2134-2150.

Davies P.F., Remuzzi A., Gordon E., Dewey F. Jr. and Gimbrone M.A. Jr. (1986). Turbulent fluid shear stress induces vascular endothelial cell turnover *in vitro*. *Proc. Natl. Acad. Sci. USA* **83**: 2114-2117.

Davies P.F., Dewey F.C. Jr., Bussolari S.R., Gordon E.J. and Gimbrone M.A. Jr. (1983). Influence of hemodynamic forces on vascular endothelial function, *in vitro* studies of shear stress and pinocytosis in bovine aortic cells. *J. Clin. Invest.* **73**: 1121-1129.

Davies P.F. and Tripathi S.C. (1993). Mechanical stress mechanisms and the cell, an endothelial paradigm. *Circ. Res.* **72**: 239-245.

Davis S., Lu M.L., Lo S.H., et al. (1991). Presence of an SH2 domain in the actin-binding protein tensin. *Science* **252**: 712-715.

DeForrest J.M. and Hollis T.M. (1978). Shear stress and aortic histamine synthesis. *Am. J. Physiol.* **246**: H701-H705.

Di Virgilio F., Lew D.P. and Pozzan T. (1984). Protein kinase C activation of physiological processes in human neutrophils at vanishingly small cytosolic Ca²⁺ levels. *Nature* **310**: 691-693.

Diamond S., Eskin S. and McIntire L. (1989). Fluid flow stimulates tissue plasminogen activator secretion by cultured human endothelial cells. *Science* **243**: 1483-1485.

Diamond S.L., Sharefkin J.B., Dieffenbach C., et al. (1990). Tissue plasminogen activator messenger RNA levels increase in cultured human endothelial cells exposed to laminar shear stress. *J. Cell. Physiol.* **143**: 364-371.

Dittman W.A., Kumada T., Sadler E.J. and Majerus P.W. (1988). The structure and function of mouse thrombomodulin. *J. Biol. Chem.* **263**: 15815-15822.

Dittman W.A., Kumada T. and Majerus P.W. (1989). Transcription of thrombomodulin mRNA in mouse hemangioma cells is increased by cycloheximide and thrombin. *Proc. Natl. Acad. Sci. USA* **86**: 7179-7182.

Dlugosz A.A. and Yuspa S. (1991). Staurosporine induces protein kinase C agonist effects and maturation of normal and neoplastic mouse keratinocytes *in vitro*. *Cancer Res.* **51**: 4677-4684.

Dorfman D.M., Wilson D.B., Bruns G.A.P. and Orkin S.H. (1992). Human transcription factor GATA-2, evidence for regulation of preproendothelin-1 gene expression in endothelial cells. *J. Biol. Chem.* **267**: 1279-1285.

Dull R.O. and Davies P.F. (1991). Flow modulation of agonist (ATP)-response (Ca^{2+}) coupling in vascular endothelial cells. *Am. J. Physiol.* **261**: H149-H154.

Dzau V.J. and Gibbons G.H. (1991). Endothelium and growth factors in vascular remodeling of hypertension. *Hypertension* **18**: III115-121.

Dzau V.J. (1989). Multiple pathways of angiotensin production in the blood vessel wall: evidence, possibilities and hypotheses. *J. Hypertension* **7**: 933-936.

Edelman E., Nugent M., Smith L. and Karnovsky M. (1992). Basic fibroblast growth factor enhances the coupling of intimal hyperplasia and proliferation of *Vasa vasorum* in injured rat arteries. *J. Clin. Invest.* **89**:465-473.

Esmon C.T. (1987). The regulation of natural anticoagulant pathways. *Science* **235**: 1348-1352.

Esmon C.T. (1989). The roles of protein C and thrombomodulin in the regulation of blood coagulation. *J. Biol. Chem.* **264**: 4743-4746.

Ford V.A., Stringer C. and Kennel S.J. (1992). Thrombomodulin is preferentially expressed in Balb/c lung microvessels. *J. Biol. Chem.* **267**: 5446-5450.

Frangos J.A., Eskin S.G., McIntire L.V. and Ives C.L. (1984). Flow effects on prostacyclin production by cultured human endothelial cells. *Science* **227**: 1477-1479.

Franke R., Gräfe M., Schnittler H., et al. (1984). Induction of human vascular endothelial stress fibers by fluid shear stress. *Nature* **307**: 648-649.

Fry D.L. (1968). Acute vascular endothelial changes associated with increased velocity gradients. *Circ. Res.* **22**: 165-200.

Furchgott R.F. and Zawadzki J.V. (1980). The obligatory role of endothelial cells in the relaxation of arterial smooth muscle by acetylcholine. *Nature* **288**: 373-376.

Garg U.C. and Hassid A. (1989). Nitric oxide-generating vasodilators and 8-bromo-cyclic guanosine monophosphate inhibit mitogenesis and proliferation of cultured rat vascular smooth cells. *J. Clin. Invest.* **83**: 1774-1777.

Geiger R.V., Berk B.C., Alexander R.W. and Nerem R.M. (1992). Flow-induced calcium transients in single endothelial cells: spatial and temporal analysis. *Am. J. Physiol.* **262**: C1411-C1417.

Gimbrone M.A. Jr., Cotran R., and Folkman J. (1974). Human vascular endothelial cells in culture. *J. Cell. Biol.* **60**: 673-684.

Glagov S., Zarins C., Giddens D.P.G. and Ku D.N. (1988). Hemodynamics and atherosclerosis, insights and perspectives gained from studies of human arteries. *Arch. Pathol. Lab. Med.* **112**: 1018-1031.

Goldsmith H.L. and Turitto V.T. (1986). Rheological aspects of thrombosis and haemostasis: basic principles and applications. *Thromb. and Haemost.* **55**: 415-435.

Gomi K., Zushi M., Honda G., et al. (1990). Antithrombotic effect of recombinant human thrombomodulin on thrombin-induced thromboembolism in mice. *Blood* **75**: 1396-1399.

Grabowski E.F., Jaffe E.A. and Weksler B.B. (1985). Prostacyclin production by cultured endothelial cell monolayers exposed to step increases in shear stress. *J. Lab. Clin. Med.* : 36-43.

Greenberg M.E. and Ziff E.B. (1984). Stimulation of 3T3 cells induces transcription of the *c-fos* protooncogene. *Nature* **311**: 433-438.

Guharay F. and Sachs F. (1984). Stretch-activated single ion channel currents in tissue-cultured embryonic chick skeletal muscle. *J. Physiol. (London)* **352**: 685-701.

Haegerstrand A., Hensen A., Gillis C. Larsson O., and Lundberg J., (1989). Endothelin: presence in human umbilical vessels, high levels in fetal blood and potent constrictor effect. *Acta Physiol. Scand.* **137**: 541-542.

Herman I.M., Brant A.M., Warty V.S., et al. (1987). Hemodynamics and the vascular endothelial cytoskeleton. *J. Cell Biol.* **105**: 291-302.

Hsieh H., Li N. and Frangos J. (1991). Shear stress increases endothelial platelet-derived growth factor mRNA levels. *Am. J. Physiol.* **260**: H642-H646.

Ingber D. (1990). Fibronectin controls capillary endothelial cell growth by modulating cell shape. *Proc. Natl. Acad. Sci. USA* **87**: 3579-3583.

Ingber D. (1991). Integrins as mechanochemical transducers. *Curr. Opin. Cell Biol.* **3**: 841-848.

Ingber D. (1993). Cellular tensegrity: defining new rules of biological design that govern the cytoskeleton. *J. Cell Sci.* **104**: 613-627.

Inoue A., Yanagisawa M., Takawa Y., et al. (1989). The human preproendothelin-1 gene: complete nucleotide sequence and regulation of expression. *J. Biol. Chem.* **264**: 14954-14959.

Ives C.L., Eskin S.G., McIntire L.V. and Debakey M.E. (1983). The importance of cell origin and substrate in the kinetics of endothelial cell alignment in response to steady flow. *Trans. Am. Soc. Artif. Organs* **29**: 269-274.

Jackman R.W., Beeler D.L., VanDeWater L. and Rosenberg R. (1986). Characterization of a thrombomodulin cDNA reveals structural similarity to the low density lipoprotein receptor. *Proc. Natl. Acad. Sci. USA* **83**: 8834-8838.

Janmey P., Enteneuer U., Traub P. and Schliwa M. (1991). Viscoelastic properties of vimentin compared with other filamentous biopolymer networks. *J. Cell Biol.* **113**: 155-160.

Jawien A., Bowen-Pope D.F., Lindner V., Schwartz S.M. and Clowes A.W. (1992). Platelet-derived growth factor promotes smooth muscle migration and intimal thickening in a rat model of balloon angioplasty. *J. Clin. Invest.* **89**: 507-511.

Kamiya A. and Togawa T. (1980). Adaptive regulation of wall shear stress to flow change in the canine carotid artery. *Am. J. Physiol.* **239**: H14-H21.

Kamps M.P. and Sefton B.M. (1988). Identification of multiple novel polypeptide substrates of the *v-src*, *v-yes*, *v-fps*, *v-ros*, and *v-erb-B* oncogenic tyrosine protein kinases utilizing antisera against phosphotyrosine. *Oncogene* **2**: 305-315.

Kandel J., Bossy-Wetzler E., Radvanyi F., et al. (1991). Neovascularization is associated with a switch to the export of bFGF in the multistep development of fibrosarcoma. *Cell* **66**: 1095-1104.

Kim D.W., Gottlieb A.I. and Langille B.L. (1989). *In vivo* modulation of endothelial F-actin microfilaments by experimental alterations in shear stress. *Arteriosclerosis* **9**: 439-445.

Klagsbrun M. and Baird A. (1991). A dual receptor system is required for basic fibroblast growth factor activity. *Cell* **67**: 229-231.

Kolodney M.S. and Wysolmerski R.B. (1992). Isometric contraction by fibroblasts and endothelial cells in tissue culture: a quantitative study. *J. Cell Biol.* **117**: 73-82.

Komuro I., Kaida T., Shibasaki Y., et al. (1990). Stretching cardiac myocytes stimulates protooncogene expression. *J. Biol. Chem.* **265**: 3595-3598.

Komuro I., Katoh Y., Kaida T., et al. (1991). Mechanical loading stimulates cell hypertrophy and specific gene expression in cultured rat cardiac myocytes, possible role of protein kinase C activation. *J. Biol. Chem.* **266**: 1265-1268.

Koyabashi E., Nakano H., Marimoto M. and Tamaoki T. (1989). Calphostin C (UCN-1028C), a novel microbial compound, is a highly potent and specific inhibitor of protein kinase C. *Biochem. Biophys. Res. Comm.* **159**: 548-553.

Kuchan M.J. and Frangos J.A. (1993). Shear stress regulates endothelin-1 via protein kinase C and cGMP in cultured endothelial cells. *Am. J. Physiol.* **264**: H150-H156.

Kraiss L.W., Kirkman T.R., Kohler T.R., Zierler B. and Clowes A.W. (1991). Shear stress regulates smooth muscle proliferation and neointimal thickening in porous polytetrafluoroethylene grafts. *Arteriosclerosis* **11**: 1844-1852.

Ku D.N., Giddens D.P., Zarins C.K. and Glagov S. (1985). Pulsatile flow and atherosclerosis in the human carotid bifurcation. *Arteriosclerosis* **5**: 293-302.

LaBarbera M. (1990). Principles of design of fluid transport systems in zoology. *Science* **249**: 992-1000.

Langille L. and O'Donnell F. (1986). Reductions in arterial diameter produced by chronic decreases in blood flow are endothelium-dependent. *Science* **231**: 405-407.

Lansman J.B., Hallam T.J. and Rink T.J. (1987). Single stretch-activated ion channels in vascular endothelial cells as mechanotransducers? *Nature* **325**: 811-813.

Lee M., Bloch K., Clifford J. and Quertermous T. (1990). Functional analysis of the Endothelin-1 gene promoter. *J. Biol. Chem.* **265**: 10446-10450.

Lee M., Dhahdly M.S., Temizer D., et al. (1991). Regulation of Endothelin-1 gene expression by *Fos* and *Jun*. *J. Biol. Chem.* **266**: 19034-19039.

Levesque M.J. and Nerem R.M. (1985). The elongation and orientation of cultured endothelial cells in response to shear stress. *J. Biomech. Eng.* **107**: 341-347.

Levesque M.J., Nerem R.M. and Sprague E.A. (1990). Vascular endothelial cell proliferation in culture and the influence of flow. *Biomaterials* **11**: 702-707.

Libby P., Warner S.J.C., Salomon R.N. and Birinyi L.K. (1988). Production of platelet-derived growth factor-like mitogen by smooth muscle cells from human atheroma. *N. Engl. J. Med.* **318**: 1493-1498.

Lipfert L., Haimovich B., Schaller M.D., et al. (1992). Integrin-dependent phosphorylation and activation of the protein tyrosine kinase pp125^{FAK} in platelets. *J. Cell Biol.* **119**: 905-912.

MacCumber M.W., Ross C.A., Glaser B.M. and Snyder S. (1989). Endothelin: visualization of mRNAs by *in situ* hybridization provides evidence for local action. *Proc. Natl. Acad. Sci. USA* **86**: 7285-7289.

MacCumber M.W., Ross C.A. and Snyder S. (1990). Endothelin in brain: receptors, mitogenesis, and biosynthesis in glial cells. *Proc. Natl. Acad. Sci. USA* **87**: 2359-2363.

Majerus P.W., De Munk G.A.W., Groeneveld E. and Rijken D.C. (1991). Acceleration of the thrombin inactivation of single chain urokinase-type plasminogen activator (pro-urokinase) by thrombomodulin. *J. Clin. Invest.* **88**: 1680-1684.

Malek A. and Izumo S. (1992). Physiological fluid shear stress causes down-regulation of Endothelin-1 mRNA in bovine aortic endothelium. *Am. J. Physiol.* **32**: C389-C396.

Malek A.M., Gibbons G.H., Dzau V.J. and Izumo S. (1993a). Fluid shear stress differentially modulates expression of genes encoding basic fibroblast growth

factor and platelet-derived growth factor B-chain in vascular endothelium. *J. Clin. Invest.* **92**: 2013-2021.

Malek A.M., Greene A.L. and Izumo S. (1993b). Regulation of endothelin-1 gene by fluid shear stress is transcriptionally mediated and independent of protein kinase C and cAMP. *Proc. Natl. Acad. Sci. USA* **90**: 5999-6003.

Malek A.M. and Izumo S. (1993c). Role of tyrosine kinase, intracellular calcium release, and mechanosensitive channels in endothelial shear stress transduction. (Abstract). *Circulation*. **88**: I-183, 976.

Malek A.M., Jackman R., Rosenberg R.D., and Izumo S. (1994). Endothelial expression of thrombomodulin is reversibly regulated by fluid shear stress. *Circ. Res.* **74**: 852-860.

Martin W., White D.G. and Anderson A.H. (1988). Endothelium-derived relaxing factor and atriopeptin II elevate cyclic GMP levels in pig aortic endothelial cells. *Br. J. Pharm.* **93**: 229-239.

Maruyama I. and Majerus P.W. (1985). The turnover of thrombin-thrombomodulin complex in cultured human umbilical vein endothelial cells and A549 lung cancer cells. Endocytosis and degradation of thrombin. *J. Biol. Chem.* **260**: 15432-15438.

Masuda H., Kawamura K., Tohda K., et al. (1989). Increase in endothelial cell density before enlargement in flow-loaded canine carotid artery. *Arteriosclerosis* **9**: 812-823.

Masuda H., Shozawa T., Kanda M. and Kamiya A. (1985). Endothelial surface of the blood flow loaded carotid artery, a scanning and transmission electron microscopical study. *Acta Pathol. Jpn.* **35**: 1037-1046.

Mattila P. (1991). Protein kinase C subtypes in endothelial cells. *FEBS*. **289**: 86-90.

McNeil P.L., Muthukrishnan L., Warder E. and D' Amore P. (1989). Growth factors are released by mechanically-wounded endothelial cells. *J. Cell Biol.* **109**: 811-822.

Mignatti P., Morimoto T. and Rifkin D. (1991). Basic fibroblast growth factor released by single, isolated cells stimulates their migration in an autocrine manner. *Proc. Natl. Acad. Sci. USA* **88**: 11007-11011.

Mignatti P. and Rifkin D.B. (1993). Biology and biochemistry of proteinases in tumor invasion. *Physiol. Rev.* **73**: 161-195.

Mo M., Eskin S. and Schilling W.P. (1991). Flow-induced changes in Ca²⁺ signalling in vascular endothelial cells: effect of shear stress and ATP. *Am. J. Physiol.* **260**: H1698-H1707.

Molinari A., Gorgietti C., Lansen J., et al. (1992). Thrombomodulin is a cofactor for thrombin degradation of recombinant single-chain urokinase plasminogen activator "in vitro" and in a perfused rabbit heart model. *Thromb. Haemost.* **67**: 226-232.

Moncada S. and Vane J.R. (1980). Prostacyclin in the cardiovascular system. *Adv. Prostaglandin Thromboxane Res.* **6**: 43-60.

Moore K. L., Esmon C.T. and Esmon N.L. (1989). Tumor necrosis factor leads to the internalization and degradation of thrombomodulin from the surface of bovine aortic endothelial cells in culture. *Blood.* **73**: 159-165.

Morita T., Kurihara H., Maemura K., Yoshizumi M. and Yazaki Y. (1992). Disruption of cytoskeletal structures mediates shear stress-induced endothelin mRNA synthesis in vascular endothelial cells. (Abstract). *Circulation.* **86**: I171, 683.

Muldoon L.L., Rodland K.D., Forsythe M.L. and Magun B.E. (1989). Stimulation of phosphoinositol hydrolysis, diacylglycerol release, and gene expression in

response to endothelin, a potent new agonist for fibroblasts and smooth muscle cells. *J. Biol. Chem.* **264**: 8529-8536.

Murray C.D. (1926). The physiological principle of minimum work. I. The vascular system and the cost of blood volume. *Proc. Natl. Acad. Sci. USA* **12**: 207-214.

Nakache M. and Gaub H.E. (1988). Hydrodynamic hyperpolarization of endothelial cells. *Proc. Natl. Acad. Sci. USA* **85**: 1841-1843.

Netland P.A., Zetter B.R., Via D.P. and Voyta J.C. (1985). *In situ* labeling of vascular endothelium with fluorescent acetylated low density lipoprotein. *Histochemical J.* **17**: 1309-1320.

Nollert M.U., Eskin S.G. and McIntire L.V. (1990). Shear stress increases inositol trisphosphate levels in human endothelial cells. *Biochem. Biophys. Res. Comm.* **170**: 281-287.

Nollert M.U., Hall E.R., Eskin S.G. and McIntire L.V. (1989). The effect of shear stress on the uptake and metabolism of arachidonic acid by human endothelial cells. *Biochem. Biophys. Acta* **1005**: 72-78.

Olesen S., D.E. Clapham and Davies P.F. (1988). Haemodynamic shear stress activates a K⁺ current in vascular endothelial cells. *Nature* **331**: 168-170.

Palmer R.M., Ferrige A.G. and Moncada S. (1987). Nitric oxide release accounts for the biological activity of endothelium-derived relaxing factor. *Nature* **327**: 524-526.

Prasad A.R.S., Logan S.A., Nerem R.M., Schwartz C.J. and Sprague E.A. (1993). Flow-related responses of intracellular inositol phosphate levels in cultured aortic endothelial cells. *Circ. Res.* **72**: 827-836.

Presta M., Maier J. and Ragnotti G. (1989). The mitogenic signaling pathway but not the plasminogen activator-inducing pathway of basic fibroblast growth factor is

mediated through protein kinase C in fetal bovine aortic endothelial cells. *J. Cell Biol.* **109**: 1877-1884.

Reich K., Gay C.V. and Frangos J.A. (1990). Fluid shear stress as a mediator of osteoblast cyclic adenosine monophosphate production. *J. Cell. Physiol.* **143**: 100-104.

Remuzzi A., Dewey F. Jr., Davies P., and Gimbrone M.A. Jr. (1984). Orientation of endothelial cells in shear fields *in vitro*. *Biorheology* **21**: 617-630.

Resnick N., Collins T., Atkinson W., et al. (1993). Platelet-derived growth factor B chain promoter contains a *cis*-acting fluid shear stress-responsive element. *Proc. Natl. Acad. Sci. USA* **90**:4591-4595.

Rifkin D.B. and Moscatelli D. (1989). Recent developments in the cell biology of basic fibroblast growth factor. *J. Cell Biol.* **109**: 1-6.

Robotewskyj A., Dull R.O., Griem M.L. and Davies P.F. (1991). (Abstr.). *FASEB J.* **5**: A527.

Rodbard S. (1975). Vascular caliber. *Cardiology* **60**: 4-49.

Ross R., Raines E.W. and Bowen-Pope D.F. (1986). The biology of platelet-derived growth factor. *Cell* **46**: 155-169.

Rubanyi G.M. and Botelho L.H.P. (1991). Endothelins. *FASEB J.* **5**: 2713-2720.

Rubanyi G.M., Romero J.C. and Vanhoutte P.M. (1986). Flow-induced release of endothelium derived relaxing factor. *Am. J. Physiol.* **250**: H1145-H1149.

Satcher R.L. Jr., Bussolari S.R., Gimbrone M.A. Jr. and Dewey C.F. Jr. (1992). The distribution of fluid forces on model arterial endothelium using computational fluid dynamics. *J. Biomech. Eng.* **114**:309-316.

Schilling W.P., Mo M. and Eskin S. (1992). Effect of shear stress on cytosolic Ca^{2+} of calf pulmonary artery endothelial cells. *Exp. Cell Res.* **198**: 31-35.

Schindler C., Shuai K., Prezioso V.R. and Darnell J.E. Jr. (1992). Interferon-dependent tyrosine phosphorylation of a latent cytoplasmic transcription factor. *Science* **257**: 809-813.

Schwartz M.A., Both G. and Lechene C. (1989). Effect of cell spreading on cytoplasmic pH in normal and transformed fibroblasts. *Proc. Natl Acad. Sci. USA* **86**: 4525-4529.

Schweigerer L., Neufeld G., Friedman J., et al. (1987). Capillary endothelial cells express basic fibroblast growth factor, a mitogen that promotes their own growth. *Nature* **325**: 257-259.

Sdougos H.P., Bussolari S.R. and Dewey C.F. Jr. (1984). Secondary flow and turbulence in a cone-plate device. *J. Fluid Mech.* **138**:379-404.

Shen J., Lusinskas F.W., Connolly A., Dewey F. Jr. and Gimbrone M. Jr. (1992). Fluid shear stress modulates cytosolic free calcium in vascular endothelial cells. *Am. J. Physiol.* **262**: C384-C390.

Sherman T. (1981). On connecting large vessels to small, the meaning of Murray's law. *J. Gen. Physiol.* **78**: 431-453.

Shirinsky V.P., Antonov A.S., Birukov K.G., et al. (1989). Mechano-chemical control of human endothelial orientation and size. *J. Cell Biol.* **109**:331-339.

Shubeita H.E., McDonough P.M., Harris A.N., Knowlton K.U., Glembotski C.C., Brown J.H., and Chien K. (1990). Endothelin induction of inositol phospholipid hydrolysis, sarcomere assembly, and cardiac gene expression in ventricular myocytes. *J. Biol. Chem.* **265**: 20555-20562.

Simonson M.S. and Dunn M.J. (1991). Endothelins: a family of regulatory peptides (State of the Art Lecture). *Hypertension*. **17**: 856-863.

Simonson M.S., Wann S., Mené P., et al. (1989). Endothelin stimulates phospholipase C, Na⁺/H⁺ exchange and *c-fos* expression and mitogenesis in rat mesangial cells. *J. Clin. Invest.* **83**: 708-712.

Smallwood J.I. and Malawista S.E. (1993). Colchicine, crystals, and neutrophil tyrosine phosphorylation. *J. Clin. Invest.* **92**: 1602-1603.

Soff G.A., Jackman R.W. and Rosenberg R.D. (1991). Expression of thrombomodulin by smooth muscle cells in culture: different effects of tumor necrosis factor and cyclic adenosine monophosphate on thrombomodulin expression by endothelial cells and smooth muscle cells in culture. *Blood* **77**: 515-518.

Sumpio B.E. and Widmann M.D. (1990). Enhanced production of endothelium-derived contracting factor by endothelial cells subjected to pulsatile stretch. *Surgery* **108**: 277-281.

Sutera S.P. and Nowak M.D. (1988). A programmable, computer-controlled cone-plate viscometer for the application of pulsatile shear stress to platelet suspensions. *Biorheology* **25**: 449-459.

Suwa N., Niwa T., Fukasuwa H. and Sasaki Y. (1963). Estimation of intravascular bed pressure gradient by mathematical analysis of arterial casts. *Tohoku J. Exp. Med.* **79**: 168-198.

Thoma R. (1893). Untersuchungen über die Histogenese und Histomechanik des Gefäßsystems. Enke, Stuttgart.

Thomas T. P., Gopalakrishna R. and Anderson W.B. (1987). Hormone- and tumor promoter-induced activation of membrane association of protein kinase C in intact cells. *Methods Enzymol.* **141**: 399-413.

Trilivas I., McDonough P. and Brown J.H. (1991). Dissociation of protein kinase C redistribution from the phosphorylation of its substrates. *J. Biol. Chem.* **266**: 8431-8438.

Turner C.E. (1991). Paxillin is a major phosphotyrosine-containing protein during embryonic development. *J. Cell Biol.* **115**: 201-207.

Uehara Y. and Fukazawa H. (1991). Use and selectivity of Herbimycin A as inhibitor of protein kinases. *Meth. Enzym.* **201**: 370-379.

Vlodavsky I., Fridman R., Sullivan R., Sasse J. and Klagsbrun M. (1987a). Aortic endothelial cells synthesize basic fibroblast growth factor which remains cell associated and platelet-derived growth factor which is secreted. *J. Cell. Physiol.* **131**: 402-408.

Vlodavsky I., Folkman J., Sullivan R., Fridman R., Ishai-Michaeli R., Sasse J. and Klagsbrun M. (1987b). Endothelial cell-derived basic fibroblast growth factor: synthesis and deposition into subendothelial extracellular matrix. *Proc. Natl. Acad. Sci. USA* **84**: 2292-2296.

Wang N., Butler J.P. and Ingber D.E. (1993). Mechanotransduction across the cell surface and through the cytoskeleton. *Science* **260**: 1124-1127.

Watson P.A. (1990). Direct stimulation of adenylate cyclase by mechanical forces in S49 mouse lymphoma cells during hyposmotic swelling. *J. Biol. Chem.* **265**: 6569-6575.

Watson P.A. (1991). Function follows form: generation of intracellular signals by cell deformation. *FASEB J.* **5**: 2013-2019.

Wechezak A.R., Viggers R.F. and Sauvage L.V. (1985). Fibronectin and F-actin redistribution in cultured endothelial cells exposed to shear stress. *Lab Invest.* **53**: 639-647.

Wechezak A.R., Wight T.N., Viggers R.F. and Sauvage L.R. (1989). Endothelial adherence under shear stress is dependent upon microfilament reorganization. *J. Cell. Physiol.* **139**: 136-146.

Weich H.A., Iberg N., Klagsbrun M. and Folkman J. (1991). Transcriptional regulation of basic fibroblast growth factor gene expression in capillary endothelial cells. *J. Cell. Biochem.* **47**: 158-164.

Weiler-Guettler H., Yu K., Soff G., Gudas L.J. and Rosenberg R. (1992). Thrombomodulin gene regulation by cAMP and retinoic acid in F9 embryonal carcinoma cells. *Proc. Natl. Acad. Sci. USA* **89**: 2155-2159.

Wilson D.B., Dorfman D.M. and Orkin S.H. (1990). A non-erythroid GATA-binding protein is required for function of the human preproendothelin-1 promoter in endothelial cells. *Mol. Cell. Biol.* **10**: 9854-9862.

Yanagisawa M., Kurihara H., Kimura S., et al. (1988). A novel potent vasoconstrictor peptide produced by vascular endothelial cell. *Nature* **332**: 411-415.

Yashimoto S., Ishizaki Y., Sasaki T. and Murota S. (1991). Effect of carbon dioxide and oxygen on endothelin production by cultured porcine cerebral endothelial cells. *Stroke* **22**: 378-83.

Young T. (1809). On the functions of the heart and arteries. *Philos. Trans. Royal Soc. Lond.*, 1-31.

Zamir M. (1977). Shear forces and blood vessel radii in the cardiovascular system. *J. Gen. Physiol.* **69**: 449-461.

Zarins C.K., Zatina M.A., Giddens D.P., Ku D.N. and Glagov S. (1987). Shear stress regulation of artery lumen diameter in experimental atherogenesis. *J. Vasc. Surg.* **5**: 413-420.

Zarins C.K., Giddens D.P., Bharadjav B.K., Sottiurai V.S., Mabon R.F., and Glagov S. (1983). Carotid bifurcation atherosclerosis, quantitative correlation of plaque localization with flow velocity profiles and wall shear stress. *Circ. Res.* **53**: 502-514.

Ziegelstein R.C., Cheng L. and Capogrossi M.C. (1992). Flow-dependent cytosolic acidification of vascular endothelial cells. *Science* **258**: 656-659.

PUBLICATION REPRINTS

1. Malek A. and Izumo S. (1992). Physiological fluid shear stress causes downregulation of endothelin-1 mRNA in bovine aortic endothelium. *Am. J. Physiol.* **32**: C389-C396.
2. Malek A.M., Gibbons G.H., Dzau V.J. and Izumo S. (1993). Fluid shear stress differentially modulates expression of genes encoding basic fibroblast growth factor and platelet-derived growth factor B-chain in vascular endothelium. *J. Clin. Invest.* **92**: 2013-2021.
3. Malek A.M., Greene A.L. and Izumo S. (1993). Regulation of endothelin-1 gene by fluid shear stress is transcriptionally mediated and independent of protein kinase C and cAMP. *Proc. Natl. Acad. Sci. USA* **90**: 5999-6003.
4. Malek A.M., Jackman R., Rosenberg R.D., and Izumo S. (1994). Endothelial expression of thrombomodulin is reversibly regulated by fluid shear stress. *Circ. Res.* **74**: 852-860.



Room 14-0551
77 Massachusetts Avenue
Cambridge, MA 02139
Ph: 617.253.5668 Fax: 617.253.1690
Email: docs@mit.edu
<http://libraries.mit.edu/docs>

DISCLAIMER OF QUALITY

Due to the condition of the original material, there are unavoidable flaws in this reproduction. We have made every effort possible to provide you with the best copy available. If you are dissatisfied with this product and find it unusable, please contact Document Services as soon as possible.

Thank you.

Some pages in the original document contain pictures, graphics, or text that is illegible.